HUMAN AIRWAY SMOOTH MUSCLE CELL Ca^{2+} DYNAMICS IN ASTHMA AND HEALTH

Thesis submitted for the degree of

Doctor of Philosophy

by

David Sweeney

July 2011

College of Medicine, Biological Sciences and Psychology

Department of Infection, Immunity and Inflammation

&

Department of Cell Physiology and Pharmacology

University of Leicester

ABSTRACT

Human airway smooth muscle cell Ca^{2+} dynamics in asthma and health

David Sweeney

Intracellular Ca^{2+} homeostasis and handling were investigated in passaged human airway smooth muscle, hASM, cells from asthma and normal donors.

Temporal changes in fluorescence of Ca^{2+}-sensitive indicator fura-2 loaded into quiescent sub-confluent hASM cells were monitored using epifluorescence video microscopy. Spontaneous amplitude changes in basal fluorescence of temporal waveforms, or Ca^{2+} oscillations, were measured. Also, spectral analysis using the FFT transform generated a Ca^{2+} oscillation dominant frequency (CODF) variable. Neither amplitude nor CODF were significantly different in asthma compared to normal hASM cell donors. However, there was a significant difference ($P<0.0001$) between CODF in airflow obstruction (AFO), defined as $FEV_1/FVC<70\%$ and $FEV_1< 80\%$, and non-AFO donors, making CODF a strong phenotypic predictor of AFO.

hASM cell Ca^{2+} handling was investigated by Ca^{2+} uncaging using confocal microscopy and by bradykinin stimulation using epifluorescence microscopy. Basal Ca^{2+} level, Ca^{2+} handling exponential decay rate constants (K), SERCA activity and expression, and SOCE after a SR Ca^{2+}-store depletion event, all demonstrated that Ca^{2+} handling was not significantly different between hASM cells from asthma or normal donors. There was no correlation between FEV_1 and K, however there was an emerging correlation between FEV_1/FVC and K for bradykinin.

The postulate that Ca^{2+} homeostasis and handling are intrinsically dysfunctional in hASM cells from asthma compared to normal donors is *ergo* not supported by these data.

Caffeine was found to decrease basal Ca^{2+} and inhibit Ca^{2+} oscillations in hASM cells.

Future work using freshly dispersed hASM cells is required to understand *in vivo* Ca^{2+} dynamics using the methods described in this thesis. Since CODF correlates with FEV_1, pattern recognition of Ca^{2+} oscillation frequency spectra has the potential to help define clinical asthma phenotypes. Inevitably, a post-genomic approach to comparative protein expression in asthma and normal hASM cell donors will accelerate understanding of Ca^{2+} dynamics.

PUBLICATIONS

Sweeney D., Challiss R.A.J., Brightling C.E.B. (2011) Calcium oscillation dominant frequency predicts airflow obstruction in passaged human airway smooth muscle cells in asthma.

Manuscript in preparation.

Sweeney D., Gomez E., Straatman K., Challiss R.A.J., Brightling C.E.B. (2011) Intracellular Ca^{2+} handling in human airway smooth muscle cells is not intrinsically different in asthma compared to health.

Manuscript in preparation.

ACKNOWLEDGEMENTS

Any project of this duration, four years, requires constant learning and empirical re-evaluation of one's field. To develop and grow, exposure to a team environment with specialists in their field is crucial. I chose this project because it mixes basic science with clinical realism. I have many people to thank for my safe passage throughout this voyage. However, I would like to particularly thank the beacons that have so graciously guided me.

First and foremost, I am grateful to Professor Chris Brightling for his advice and leadership throughout the project and for his impressive knowledge of clinical and statistical matters. Also, thanks to Professor John Challiss for his help and considerable expertise in assisting me to design experiments and use appropriate methods.

My thanks go to Dr Carl Nelson for his expert assistance with the epifluorescence microscope and for many useful discussions about interpretation of results. Also thanks to Dr Edith Gomez for her help and support throughout the latter stages of the project, particularly in performing real time PCR and western blotting. I gratefully acknowledge the help of Dr Kees Straatman for his expert assistance with the implementation of Ca^{2+} uncaging experiments using the Olympus FV 1000 confocal microscope. And thanks to Mr Raj Mistry for his assistance and skill in performing the IP_3 assay and of course for his uncanny ability to 'keep it real!' Finally, thanks to my fellow PhD students for their camaraderie and 'all in the same boat' sense of humour when things felt particularly bleak.

The funding for this research project was kindly provided by the Medical Research Council (MRC) and the British Thoracic Society (BTS).

David Sweeney, Leicester, July 2011

CONTENTS

Human airway smooth muscle cell Ca^{2+} dynamics in asthma and health i
Abstract ii
Publications iii
Acknowledgements iv
Contents v
Abbreviations viii

Chapter 1 Introduction 10
1.1 Epidemiology of asthma 10
1.2 Clinicopathology of asthma 10
1.2.1 Pathogenesis of asthma 10
1.2.2 Physiological regulation of airway smooth muscle 17
1.2.3 Underlying immunopathology of allergic asthma 21
1.2.4 Pulmonary function testing and asthma diagnosis 24
1.2.5 Therapeutic control of asthma 24
1.2.6 Pharmacological treatment of asthma 28
1.3 hASM cells and Ca^{2+} 35
1.4 Intracellular Ca^{2+} and Ca^{2+} oscillations 43
1.4.1 Understanding fluorescent Ca^{2+} sensitive indicators 46
1.5 $[Ca^{2+}]_i$ handling 51
1.5.1 Agonist induced intracellular $[Ca^{2+}]_i$ release 51
1.5.2 Store operated Ca^{2+} entry 56
1.5.3 Voltage operated Ca^{2+} ion channels 58
1.5.4 Excitation – contraction 58
1.6 Outline of project rationale 61
1.7 Hypothesis 65
1.7.1 Aims 65

Chapter 2 Materials and Methods 66
2.1 Materials 66
2.2 Primary hASM cell culture 66
2.3 Widefield epifluorescence microscopy 67
2.3.1 Spectral analysis of temporal fluorescence waveforms 68
2.4 Ca^{2+} uncaging 68
2.5 Bradykinin-stimulated $[Ca^{2+}]_i$ release 71
2.6 IP_3 mass assay 71

2.7 Store-operated Ca^{2+} entry (SOCE) ... 72
2.8 Real time PCR ... 72
2.9 Western blotting ... 75
2.10 Statistical analysis ... 75

Chapter 3 Investigation of $[Ca^{2+}]_i$ homeostasis ... 76
3.1 Introduction ... 76
3.1.1 Spectral analysis of hASM cell $[Ca^{2+}]_i$ changes ... 77
3.2 Results ... 84
3.2.1 Baseline $[Ca^{2+}]_i$ levels ... 84
3.2.2 $[Ca^{2+}]_i$ oscillations ... 87
3.2.3 Clinical Correlation ... 94
3.3 Discussion ... 104
3.3.1 Basal $[Ca^{2+}]_i$ ... 104
3.3.2 $[Ca^{2+}]_i$ oscillations ... 104
3.3.3 Correlation between lung physiology and $[Ca^{2+}]_i$ oscillations ... 105
3.4 Conclusion ... 107

Chapter 4 Investigation of $[Ca^{2+}]_i$ handling ... 108
4.1 Introduction ... 108
4.2 Results ... 112
4.2.1 Real time PCR ... 112
4.2.2 Western blotting ... 112
4.2.3 Ca^{2+} uncaging ... 112
4.2.4 Bradykinin induced $[Ca^{2+}]_i$ release ... 133
4.2.5 Caffeine ... 151
4.2.6 Store operated Ca^{2+} entry (SOCE) ... 155
4.3 Discussion ... 159
4.3.1 Ca^{2+} uncaging ... 159
4.3.2 Bradykinin ... 162
4.3.3 Ca^{2+} handling is not significantly altered in asthma ... 164
4.3.4 Caffeine, an anachronous case? ... 164
4.3.5 SOCE ... 165
4.4 Conclusion ... 167

Chapter 5 Discussion, conclusion and future 168
5.1 Summary of $[Ca^{2+}]_i$ homeostasis 168
5.2 Characterisation of hASM cell $[Ca^{2+}]_i$ at homeostasis 170
5.2.1 hASM cell Ca^{2+} handling after a disturbance to homeostasis 171
5.2.2 $[Ca^{2+}]_i$ homeostasis and handling conclusion 173
5.3 Clinical aspects 173
5.4 Limitations of using fluorophores to monitor live cell $[Ca^{2+}]_i$ 177
5.5 Reliability of results 181
5.6 Overall conclusion 185
5.7 Critique 186
5.8 Future research rationale 191
5.8.1 Respiratory drugs industry 191
5.8.2 $[Ca^{2+}]_i$, the elephant in the room 192
5.8.3 Inflammation 198

References 205

ABBREVIATIONS

$[Ca^{2+}]_i$	Intracellular Ca^{2+} concentration
ACh	Acetylcholine
ADAM-33	A Disintegrin And Metalloproteinase 33
AFO	Airflow obstruction
AHR	Airway hyperresponsiveness
APC	Antigen presenting cell
Ca^{2+}	Calcium ion
cAMP	Adenosine 3',5'-cyclic monophosphate
CDR	Complementarity determining region
CHF	Congestive heart failure
CICR	Calcium induced calcium release
CODF	Calcium oscillation dominant frequency
COPD	Chronic obstructive pulmonary disorder
CPA	Cyclopiazonic acid
DC	Dendritic cell
NP-EGTA	Nitrophenyl ethylene glycol-bis(2-aminoethylether)-N,N,N',N'-tetraacetic acid
FBS	Fetal bovine serum
FDS	Frequent discharge site
FEV_1	Forced expiratory volume in the first second
FEV_1/FVC	Forced expiratory ratio
FEV_1/FVC <70%	Airflow obstruction (AFO)
FEV_1<80%	Airflow impairment
FFT	Fast Fourier Transform
FITC	Fluorescein isothiocyanate
FVC	Forced vital capacity
GINA	Global initiative for asthma
GM-CSF	Granulocyte-macrophage colony stimulating factor
GPCR	G-protein coupled receptor
hASM	Human airway smooth muscle
Ig	Immunoglobulin

IL	Interleukin
INFγ	Interferon γ
IP_3	Inositol 1,4,5-trisphosphate
LABA	Long acting beta agonist
Ln or ln	Natural logarithm, $\log_e$
LT	Leukotriene
mHz	Millihertz
MMP	Matrix metalloproteinase
NANC	Non-adrenergic Non-cholinergic
NCX	Sodium-calcium ion exchanger
NHS	National Health Service
NSAID	Non-steroidal anti-inflammatory drug
PAF	Platelet-activating factor
PDGF	Platelet derived growth factor
PG	Prostaglandin
PMCA	Plasma membrane Ca^{2+}-ATPase
PSD	Power spectral density
RANTES	Regulated upon Activation, Normal T-cell Expressed and Secreted
RSV	Respiratory syncytial virus
ROI	Region of interest
ROS	Reactive oxygen species
SABA	Short acting beta agonist
SCF	Stem cell factor
SERCA	SR Ca^{2+}-ATPase
SOCE	Store operated calcium entry
SR	Sarco/endoplasmic reticulum
STIM1	Stromal interaction molecule 1
Th	T-helper lymphocyte
TNF-α	Tumour necrosis factor α
TRP	Transient receptor potential (ion channel)
TSLP	Thymic stromal lymphopoietin
WHO	World Health Organisation

CHAPTER 1

INTRODUCTION

1.1 Epidemiology of asthma

Asthma affects an estimated 300 million people of all ages and ethnicities and is the cause of around 250,000 deaths per year, worldwide. Most deaths are related to a lack of proper treatment. Over the past 40 years its prevalence has increased, by around 10% in Australia, New Zealand, North America, Brazil, Peru and UK as people live more modern urbanised lifestyles (WHO). In the UK, there are 1.1 million child (1 in 10) and 4.1 million adult (1 in 12) asthma sufferers costing the NHS over £996m annually (AsthmaUK, 2008).

1.2 Clinicopathology of asthma

1.2.1 Pathogenesis of asthma

The World Health Organisation's (WHO) definition of asthma is:

Asthma attacks all age groups but often starts in childhood. It is a disease characterized by recurrent attacks of breathlessness and wheezing, which vary in severity and frequency from person to person. In an individual, they may occur from hour to hour and day to day.

This condition is due to inflammation of the air passages in the lungs and affects the sensitivity of the nerve endings in the airways so they become easily irritated. In an attack, the lining of the passages swell causing the airways to narrow and reducing the flow of air in and out of the lungs.

[Source: http://www.who.int/respiratory/asthma/definition/en/]

Asthma is a chronic inflammatory disorder of the lungs causing episodic and paroxysmal obstruction to normal airflow. But there is no single pathognomonic sign that absolutely points to an asthma diagnosis. The WHO definition of asthma reflects this struggle to precisely identify what asthma actually is. Instead, it resorts to describing what its effects are. At a symptomatic level, as a working definition, it does however do a reasonably good job, because it is not actually known what asthma is. Fundamentally, there is only phenomenological evidence of a slowly progressing immunopathological degeneration of lung function, essentially pneumonitis, without a clear mechanistic cause. Hence, asthma remains an incurable disease with prognosis outcomes ranging from remission, stasis, or fatal. Therefore, in the absence of a distinct molecular aetiopathogenesis, asthma is best described in terms of a syndrome comprising an aggregate of signs and symptoms (Dolovich *et al.*, 1981).

The most striking pathohistological sign is a profound change to lung tissue whereby bronchiolar walls are thickened and lumen diameters are decreased, causing the classical symptom of pathological impairment to normal airflow associated with asthma and other obstructive respiratory diseases (Barnes, 2008a). This group of complex and dynamically interrelated lesions is called airway remodelling (Jeffery, 2001).

Bronchial walls are found to contain a marked infiltration of immune cells such as eosinophils, neutrophils, macrophages, T-lymphocytes particularly Th2 $CD4^+$ cells, activated mast cells and basophils. Histamine, leukotrienes (LT), TNF-α and INFγ promote the expression of endothelial vascular adhesion molecules, allowing diapedesis and migration of immune cells into the airways.

Asthma is associated with underlying chronic lower airways inflammation, supported by a raft of chemical mediators of inflammation. Mostly cytokines, soluble low

molecular weight proteins that regulate the immune response by mediating agonistic or antagonistic signaling between immune system cells. Of which, interleukins (IL) are a major subset that are secreted by leukocytes and act upon immune system cells. Cytokines that mediate leukocyte chemotaxis are called chemokines. And several other types of molecule also play a role.

Mediators of particular note in asthma are IL-4, IL-5, IL-6, IL-8, IL-9, IL-10, IL-12, IL-13, chemokines such as eotaxin and RANTES, prostaglandins (PG), LTs, histamine, kinins, ACh, nitric oxide, endothelins, adenosine, PAF, GM-CSF, proteases, peroxidases and ROS (Barnes *et al.*, 1998). Hence the biochemical participants of inflammation are diverse. Under normal circumstances they act exquisitely to promote healing and defend against infection but in pathology they cause damage to otherwise healthy tissue. As a simple illustration, IL-5 and IL-9 act to attract and activate eosinophils and PGI_2 or prostacyclin is a vasodilator.

IL-4 and IL-13 promote production of IgE isotype antibodies from activated B-cells in lymphoid tissue, which play a major role in mast cell, eosinophil and basophil activation. IgE molecules bind by their F_c regions to these cells via specific receptors (FcεRI). Subsequent cross-linking of IgE CDRs by usually harmless antigens, in association with SCF, IL-4 and IL-6 leads to synthesis and secretion of inflammatory mediators (Hart, 2001). These include cysteinyl leukotrienes such as LTC_4, LTD_4, and LTE_4, prostaglandins such as PGD_2, histamine, serotonin and bradykinin all of which are bronchoconstrictors.

Mast cell PDGF and proteases promote hyperplasia of airway smooth muscle cells and the latter secrete SCF which is a growth factor and chemoattractant for the former (Brightling *et al.*, 2002; Hollins *et al.*, 2008). Increased mass of airway smooth muscle

cells generated by hyperplasia and hypertrophy (Ebina *et al.*, 1993; Woodruff *et al.*, 2004) has recently been linked to increased numbers of mitochondria (Trian *et al.*, 2007). Subepithelial collagen deposition (Carroll *et al.*, 2000) and fibrosis thickens the lamina propria (Roche *et al.*, 1989), aided by hypertrophy and hyperplasia of airway smooth muscle cells (Hassan *et al.*, 2010). ADAM-33 is a matrix metalloproteinase (MMP) similar to collagenase, which is expressed by smooth muscle cells and fibroblasts. It functions to facilitate proliferation of these cell types, similar to the role of MMPs in neoplastic metastasis, and hence contributes to the evolution of AHR and subepithelial fibrosis (Van Eerdewegh *et al.*, 2002).

Pathological angiogenesis occurs and the bronchial wall is swollen by oedema due to leakage of plasma from vasodilated submucosal vasculature (Carroll *et al.*, 1997; Ribatti *et al.*, 2009). Mucosal goblet cell hyperplasia by epithelial cell metaplasia and submucosal hypertrophy of mucus glands produces abnormally thick luminal mucus that is not completely cleared by muco-ciliary transport or cough, causing plugging and occlusion of small airways (Aikawa *et al.*, 1992). Sputum is often yellow coloured due to the presence of eosinophils and contains crystallised eosinophil membrane proteins called Charcot-Leyden crystals. A useful non-invasive assessment of underlying inflammation is measurement of induced sputum eosinophilia (Chakir *et al.*, 2010). Mucus can also become purulent in cases of concurrent respiratory infection.

Chemical secretions from non-inflammatory or structural cells such as NANC innervation, secreting neuropeptides, gives rise to neuropathic inflammation (Kraneveld *et al.*, 2000). Airway epithelium secretes eotaxin (Kumar *et al.*, 2002) and a paracrine interplay with airway smooth muscle cells (Takeda *et al.*, 2009) also plays a part in mounting inflammation. Airway smooth muscle cells do not passively manifest airway hyperresponsiveness in asthma but also express an inflammatory phenotype and secrete

mediators that effect airway remodelling and immune cell chemotaxis (Damera *et al.*, 2011). Other powerful inflammatory mediators, primarily eosinophil major basic protein (MBP), cause areas of mucosa denuded of epithelial lining, giving rise to shedding of epithelial cells into the mucus called Curshmann spirals (Jeffery *et al.*, 1989). There may also be irreversible destruction of parenchyma, namely alveolar walls (Mauad *et al.*, 2004).

This histopathophysiology manifests symptoms of airway hyperresponsiveness or smooth muscle bronchospasm in response to various stimuli (Lotvall *et al.*, 1998), causing extensive non-specific narrowing of the airways exacerbated by airway remodelling (Siddiqui *et al.*, 2009).

Asthma is categorised as extrinsic if dependent upon external antigens causing a genetically predisposed type I (IgE) hypersensitivity reaction called atopy (Teerlink *et al.*, 2007). Also called atopic asthma, triggers include common allergens such as house dust mite or cockroach shell proteins and faeces, pet dander/dried saliva, fungal spores, seasonal pollens particularly from trees and grasses, foods such as nuts, dairy products which may not just cause asthma but a systemic release of histamine leading to the cardiovascular collapse of anaphylaxis. But potentially any antigen can become an allergen, even self-antigens.

The second category is intrinsic or non-atopic asthma which is dependent upon various diverse non-immune mediated triggers including exercise, cold air, NSAID drugs such as aspirin, tartrazine dyes, β-blockers, histamine, methacholine, N-acetylcysteine, aerosolised pentamidine, any nebulised drug, upper respiratory tract infections such as rhinitis, sinusitis, or common cold; post nasal drip, aspiration, gastroesophageal reflux, occupational factors – workplace exposure and sensitisation to fumes, seasonal changes

in weather, predictable perimenstrual or catamenial asthma associated with hormonal changes of the menstrual cycle, psychological stress, cardiac-asthma caused by uncompensated CHF, smoking and passive smoking, noxious chemical dusts and gases such as particulate and gaseous atmospheric pollutants from car exhaust fumes, O_3, SO_2, NO_2.

Atopic asthma is the most common form and usually first manifests in children but can occur *de novo* from any age. It is usually familial and asthma inevitably progresses from allergic chronic rhinitis, nasal polyps, urticaria, atopic dermatitis or eczema. That is, chronic development of immunogenic sensitivity and non-tolerance of epithelial surfaces to environmental 'danger' signals (Matzinger, 2002). The genetic basis for this progression into asthma is unclear but it is known through linkage analysis of various chromosomal loci that susceptibility to asthma is polygenic and includes an environmental element that often acts to trigger the disease (Kumar *et al.*, 2009). Hence a simple skin test using a panel of antigens can identify a reactive or trigger compound group through a classic weal-and-flare type 1 (IgE) mediated hypersensitivity reaction. Serum IgE titres may also be taken to gauge the progression of underlying sensitisation and airway inflammation. But these of themselves are not diagnostic of asthma.

The immune reaction to antigen is characterised by an initial primary sensitisation phase that sets the stage for a more amplified secondary reaction upon re-exposure to the same antigen or epitope. In atopy initial sensitisation stimulates production of Th2 cells that secrete IL-4 and IL-5 among other cytokines to stimulate IgE production, mast cell growth and eosinophil activation. Then first re-exposure to the antigen elicits an early or acute phase reaction that is followed some hours later by a late phase reaction that may last 12 to 24 hours. The latter is characterised by the swarming migration of

leukocytes to the lungs recruited by chemotactic cytokines secreted by mast cells and others, such as eotaxin from epithelial cells which is an eosinophil chemoattractant and activator, during the acute reaction some 4 to 8 hours earlier.

Although obesity is a rising risk factor in westernised cultures, respiratory viral infection, for example by parainfluenza virus, RSV or rhinovirus, is the most common cause of inflammation in non-atopic asthma, possibly leading to an increased firing rate of submucosal vagal afferents, exacerbated by inhalation of environmental particulates. A family history is rare and the condition mainly involves recruitment of neutrophils and production of IgG antibodies but does not involve increased levels of eosinophils or IgE.

One of the inflammatory consequences of tissue injury is an increase in plasma membrane arachidonic acid metabolism to promote healing and stave off infection. It is thought that a disturbance in arachidonic acid metabolism caused by taking aspirin in some individuals causes drug induced asthma by inhibiting cycloxygenase and hence prostaglandin synthesis, whilst leaving the products of the lipoxygenase pathway, leukotrienes, unimpeded to cause bronchoconstriction.

Whatever the trigger, the resulting resistance to airflow in hyperresponsive airways is episodic, reversing fully or partially either spontaneously or as a result of bronchodilator treatment. During an asthma exacerbation, acute bronchospasm results in orthopneic dyspnoea and clinical respiratory symptoms of wheeze, breathlessness, chest tightness, cough and excess sputum production. As breathing becomes more difficult, there will be a transition from normal diaphragmatic breathing to use of respiratory accessory muscles to draw air into the lungs. Chest X-rays will show lung hyperinflation. Respiratory auscultation reveals musical sounding crackles or rhonchi

throughout the lungs. There is a marked fall in systolic blood pressure and pulse pressure during inspiration called pulsus paradoxus. Exhaustion, tachycardia, tussive syncope, infection and dehydration are common, pneumothorax and lung collapse are rare but serious sequelae.

Bronchomotor tone is subject to circadian biorhythmic cycles which are maximal around 3 to 4am and indeed bronchoconstriction symptoms are commonly found to be worse at night than during the day. During a severe asthma exacerbation airflow may be so attenuated that wheezing cannot be heard and diagnosis is then based upon reduced breath sounds and prolonged expiration. In patients with a long history of asthma, uncontrolled episodes of recurrent severe exacerbation and compromised ventilation over several days can lead to a state called status asthmaticus which often proves fatal. The chest becomes silent with acute hypercapnic and hypoxic respiratory failure, effectively asphyxiation, despite emergency medical intervention (Coleman *et al.*, 2009).

1.2.2 Physiological regulation of airway smooth muscle

Normal regulation of hASM basal tone is achieved through physiological antagonism. The bronchconstrictor side includes efferent cholinergic innervation from the vagus nerve which synapse at ganglia in the lung tissue itself. Then short postganglionic parasympathetic muscarinic innervation releases the neurotransmitter, bronchoconstricting agonist, acetylcholine at M_3-cholinoceptors.

In asthma, chemical products of inflammation such as histamine, bradykinin and serotonin (5-hydroxytryptamine, 5-HT), and a whole raft of differentially expressed cytokines such as TNF-α, IL-1, IL-4, and prostaglandin LTs etc. shift the normal

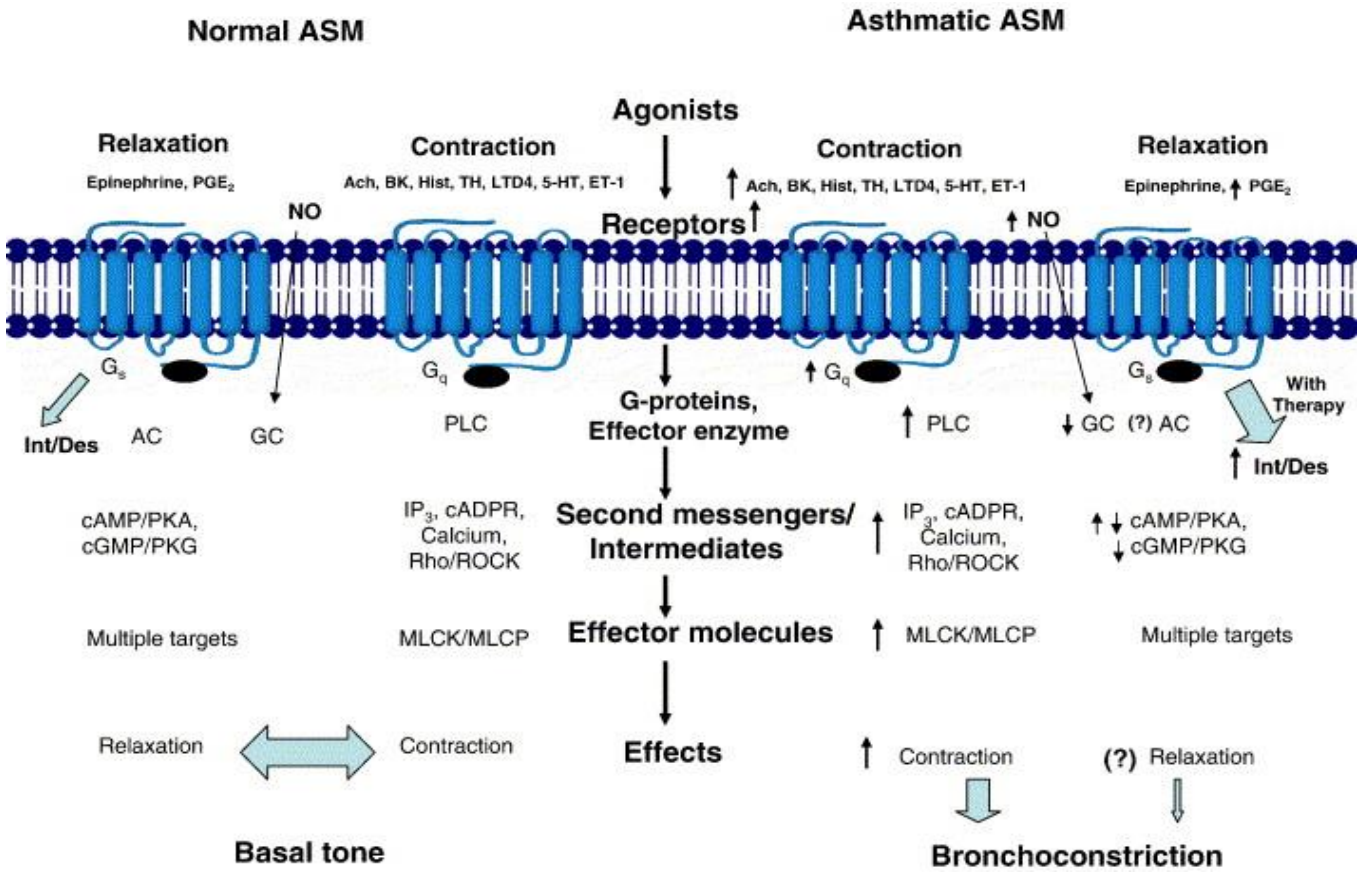

Figure 1.1 GPCR agonist induced hASM cell contraction has a physiological function to maintain basal tone of bronchial airway smooth muscle. In pathological states, such as asthma, where airflow is variably restricted due to bronchoconstriction, several downstream mechanisms may be unregulated or increased in function leading to an increased calcium release and hypercontraction of hASM cells. Reprinted with permission,

Deshpande A., Penn R.B. (2006) Targeting G protein-coupled receptor signaling in asthma, Cellular Signaling, 18(12), pp. 2105-2120.

Table 1.1 Some $G\alpha_q$ coupled GPCR agonists commonly found in asthma.

Reprinted with permission,

Deshpande A., Penn R.B. (2006) Targeting G protein-coupled receptor signaling in asthma, Cellular Signaling, 18(12), pp. 2105-2120.

Table 1. Agonists of GPCRs relevant to the asthmatic condition

Agonist	Receptor	Features in asthma
	G_q-coupled receptors	
Acetylcholine	M_3 muscarinic	Increased acetylcholine release, receptors are maintained well
Bradykinin	BK_1	Increased release and decreased degradation of bradykinin
Thrombin	PAR1, 2, 3	Increased thrombin levels cause bronchoconstriction, mucus secretion, airway remodeling
Histamine	H_1	Increased release of histamine both at rest and upon allergen challenge, promoting bronchoconstriction, plasma exudation and mucus secretion
LTD4, LTC4	CysLT1R	Increased levels of LTD4 and LTC4 in plasma, BAL fluid and sputum of asthmatics. Increased receptor expression in the lungs and ASM under inflammatory conditions
Serotonin	$5\text{-}HT_{2a}$,$5\text{-}HT_{2c}$	Levels of serotonin correlated with the severity of asthma
Thromboxane	TP	Increased levels of thromboxane in asthmatic airways
Neurokinin	NK_1 and NK_2	Increased levels of neurokinin after nasal allergen challenge. Receptor expression is increased in asthmatics. Neurokinins cause mucus secretion, plasma exudation and bronchoconstriction
Endothelin-1	ETA and ETB	Increased levels of ET-1 in BAL fluid, plasma. ET-1 increases mucus secretion, airway remodeling
ATP, UTP	P_2Y_2, P_2Y_4, P_2Y_6	Increased levels of ATP in the airways during inflammatory conditions
$PGF_{2\alpha}$	FP	Bronchoconstriction, mild airway secretion
	G_i-coupled receptors	
Acetylcholine	M_2 muscarinic	Prejunctional M_2 receptors lose responsiveness
Thrombin	PAR1	See above
Thromboxane	TP	Increased levels of thromboxane during airway diseases
Adenosine	A_1	Increased levels of adenosine in plasma and BAL, receptors in the lungs are increased in asthma.
PGD2	DP2	Increased levels in BAL fluid
	G_s-coupled receptors	
Adrenaline	β_2 adrenergic	Receptor desensitization and loss of responsiveness with therapy
Prostaglandin E2	EP_2	Increased PGE_2 levels with airway inflammation
Prostacyclin (PGI_2)	IP	Increased PGI_2 levels with airway inflammation
VIP	$VPAC_1$,$VPAC_2$	Increased VIP levels with airway inflammation
Adenosine	A2b adenosine	Increased ATP metabolites including adenosine increased with airway inflammation

physiological balance towards hASM contraction and hence increase the probability of AHR (Figure 1.1). This is counterbalanced by antagonist, bronchodilator, actions of NANC (non-adrenergic non-cholinergic) nerves that secrete a variety of neurotransmitters. Namely, vasoactive intestinal polypeptide (VIP), nitric oxide (NO) and the neurokinins: Substance P and neurokinin A and B. Also, circulating adrenal hormones epinephrine and norepinephrine acting at β_2-adrenoceptors.

The latter are all drug targets, β_2-adrenoceptor agonists have been successfully exploited with the result that analogues such as salbutamol are now first line anti-asthma therapeutics. Table 1.1 lists some commonly found GPCR agonists important in asthma.

There is no sympathetic innervation of lung tissue, but evolutionary conservation of β_2-adrenoceptors in hASM is clearly important. Thus, in terms of the evolutionary survival of the species, it is clear that in times of attack, reflexive secretion of epinephrine and norepinephrine prepares the body for the oft quoted 'fight or flight' condition. This includes increased pulmonary airflow, vasodilation and hence delivery of higher oxygen partial pressure, PaO_2, to muscles. β_2-adrenoceptor stimulation here tipping the hASM tonal balance into relaxation and hence bronchodilation. It is not therefore surprising that inhaled β_2-adrenergic agonists, such as the prototypical salbutamol, are so successful in ameliorating the effects of an asthma exacerbation.

Unfortunately, it is possible that adrenoceptor sensitivity is decreased in some cases of asthma treatment, probably an iatrogenic effect of β_2-adrenoceptor agonists, thus requiring higher doses to produce the same clinical efficacy (Lipworth *et al.*, 1989). Such that in cases of tachyphylaxis, or receptor desensitisation and internalisation, the

bronchoconstrictor nature of parasympathetic muscarinic innervation and/or inflammatory mediators on hASM cells goes unchallenged.

Salbutamol first appeared on the market in the late 1960s and to date there hasn't been anything else that even comes near to its phenomenal clinical success. Hence, balance of probability suggests that a new drug that will surpass the β_2 agonist class is overdue. Recent advances in genomics have identified the expression of 'bitter' receptors, TAS2Rs, on hASM cells whose ligands produce a more potent bronchodilator effect than β_2 agonists (Deshpande *et al.*). Perhaps this high profile finding published in the journal *Nature Medicine* will have kick-started the race for patent conscious drug companies worldwide to be first to get a new product to market.

1.2.3 Underlying immunopathology of allergic asthma

In terms of underlying immunopathology, allergic asthma is a disease whereby there is an imbalance between Th1 and Th2 cells, favouring Th2 cells and an allergic phenotype. Under normal conditions Th1 cells predominate in airways and this is a state of immunological tolerance to allergens. The two sets of Th $CD4^+$ cells form an immunoregulatory loop, whereby cytokines from each cell type act to modulate the activities of the other (Figure 1.2).

This is another example of physiological antagonism. This mechanism is nicely reviewed in (Barnes, 2008a).

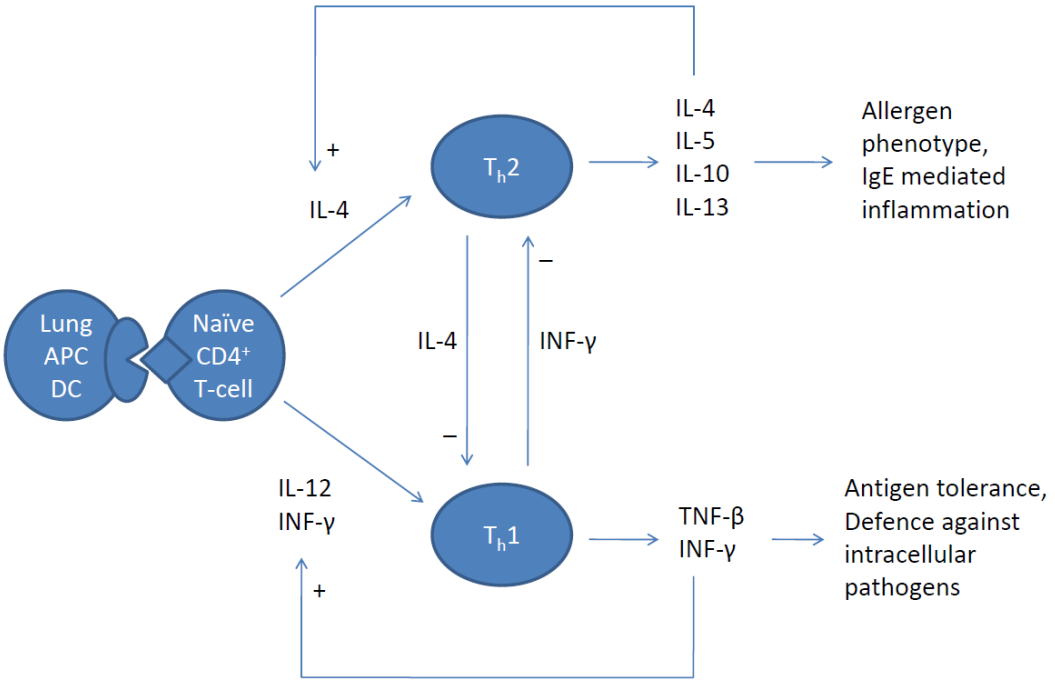

Figure 1.2 Mutual immunoregulatory negative feedback loops modulate the activation of Th1 and Th2 cells. In allergic asthma there is an imbalance favouring Th2 cells and an allergen phenotype with reduced antigen tolerance. Self-enhancing positive feedback loops amplify the proliferation and commitment of Th1 and Th2 cells. (APC = Antigen Presenting Cell, DC = Dendritic Cell).

Naïve Th cells are activated and become committed in response to particular immunogenic stimuli and cytokines, with Th2 cells fostering allergic inflammation and production of IgE via B-lymphocytes, and Th1 cells attacking intracellular microbes particularly viruses by secreting INFγ and IL-2 which activates macrophages and cytotoxic T_c $CD8^+$ lymphocytes. Differentiation of Th2 cells requires transcription factor GATA3. Hence in allergic asthma there is an increase in $GATA3^+$ Th2 cells. Stimulation of the IL-4 receptor activates transcription factor STAT6 which increases expression of GATA3. Interestingly, IL-4 is currently a favoured drug target, with an antibody IL-4 receptor antagonist, anti-IL4Rα (Corren *et al.*, 2010) and a recombinant IL-4 variant that inhibits IL-4 and IL-13 binding at the IL-4Rα (Wenzel *et al.*, 2007), both of which are undergoing clinical trials in the USA.

However, in terms of the Th1 story, the balance is further disturbed. The transcription factor T-bet regulates Th1 lymphocyte differentiation and this is known to be down regulated in lung Th1 lymphocytes. T-bet inhibits GATA3 DNA binding. Hence in allergic asthma the cytokines produced by Th2 lymphocytes are free to act unimpaired by the restraining influence of the Th1 set of cytokines. However, the molecular basis for this imbalance is not clear.

One interesting possibility that explains the commitment of Th2 cells came from work on the pathogenesis of atopic dermatitis. Lung APCs such as dendritic cells initiate a Th2 type inflammation after stimulation by a cytokine 'master switch' called thymic stromal lymphopoietin (TSLP) secreted by epithelial and mast cells. The key point is that there is evidence that links TSLP expression with allergic inflammation in *in vivo* atopic dermatitis and asthma (Liu, 2006). Interestingly, TSLP also inhibits T_{reg} cells which regulate tolerance and act to suppress Th2 allergic immune response (Nguyen *et al.*, 2010). By inhibiting T_{reg}, TSLP further acts to allow Th2 mediated allergy to

predominate. And Th2 GATA3 acts to inhibit STAT4 and therefore Th1 T-bet thus inhibiting production of Th1 cytokines (Barnes, 2008b).

1.2.4 Pulmonary function testing and asthma diagnosis

In order to assess adult airflow limitation and identify airflow obstruction, pulmonary lung function testing is undertaken using spirometry. Measurements of FEV_1, FVC and hence FEV_1/FVC are taken. Airflow limitation (AFL) is taken to be significant when FEV_1<80% predicted and airflow obstruction (AFO) when FEV_1/FVC<70%. In order to test for AFO reversibility, the hallmark of asthma, spirometry is usually performed before and after administration of an inhaled short acting β_2-agonist (ISABA) bronchodilator such as salbutamol. AFO is significantly reversed if FEV_1 is increased by >12% or FVC is increased by >15% post-bronchodilator. If the outcome of these tests is positive then a diagnosis of asthma can be made.

If the bronchodilator test proves non-diagnostic but asthma is still suspected, then a test for AHR is undertaken in patients whose FEV_1>65% predicted using an inhaled bronchoconstrictor such as histamine or more commonly muscarinic agonist methacholine. A decrease in FEV_1 of >20% to a methacholine concentration ≤8 mg/ml, known as the provocative concentration or PC_{20}, confirms AHR and an asthma diagnosis can then be made. If a decrease in FEV_1 is not observed under these conditions, then it can be said with 95% confidence that the patient is not asthmatic.

1.2.5 Therapeutic control of asthma

Currently, there is no cure for asthma but fortunately, for most sufferers, disease progression is slow or spontaneously abates. However, there are comprehensive management guidelines and the lead has been taken by the USA. A panel of scientists and clinicians from the National Heart Lung and Blood Institute (NHLBI), part of the

National Institutes of Health (NIH) of the USA and the World Health Organisation (WHO), have come together to form a collaboration called the Global Initiative for Asthma (GINA). GINA guidelines are further peer reviewed by suitably qualified external reviewers. The guidelines describe current best clinical practice for the diagnosis, management and control of asthma to meet the needs of most patients under most circumstances (Global Initiative for Asthma, 2010).

The emphasis is upon control of asthma through judicious treatment rather than assessment of its severity. This is because the intrinsic intensity of the disease, or severity, is harder to assess and manage than day-to-day symptom control. However, upon initial presentation it is useful to be able to assess severity and use this as a starting point for rational treatment. Asthma exacerbation severity is classified as mild, moderate or severe. These classes are decided on an individual basis by giving careful weight to asthma signs and symptoms and functional assessments including spirometry and arterial blood gases.

Control decisions are composed of two distinct processes. Firstly, the degree of impairment measured by assessing functional FEV_1 limitation and intensity of exacerbations. Secondly, risk:- assessment of acute exacerbation probability and the expected rate of decline in lung function over time. These two clinical decision factors act independently. For example, there may be a low degree of impairment in FEV_1 but the risk of a severe exacerbation may be great. In that case the need for adequate control would be more critical than in the case where impairment was high but the risk of exacerbation was low. The GINA control guidelines define 5 treatment management steps (Figure 1.3). GINA 1 defines well controlled asthma with only the occasional use of a 'reliever' ISABA as required. The subsequent four steps prescribe progressively more complex pharmacological strategies for regular inhaled, oral or hospitalised

parenteral drug delivery in order to maintain control, with the use of an ISABA as required at all steps. Maintenance of control is achieved by following an iterative feedback cycle of assessment, treatment and monitoring. At each step checks are made for treatment adherence, avoidance of environmental triggers, and the progression of comorbidities. The aim is, for the same level of control, to step down if possible. In the UK general practitioners usually refer patients to an asthma specialist at GINA 3.

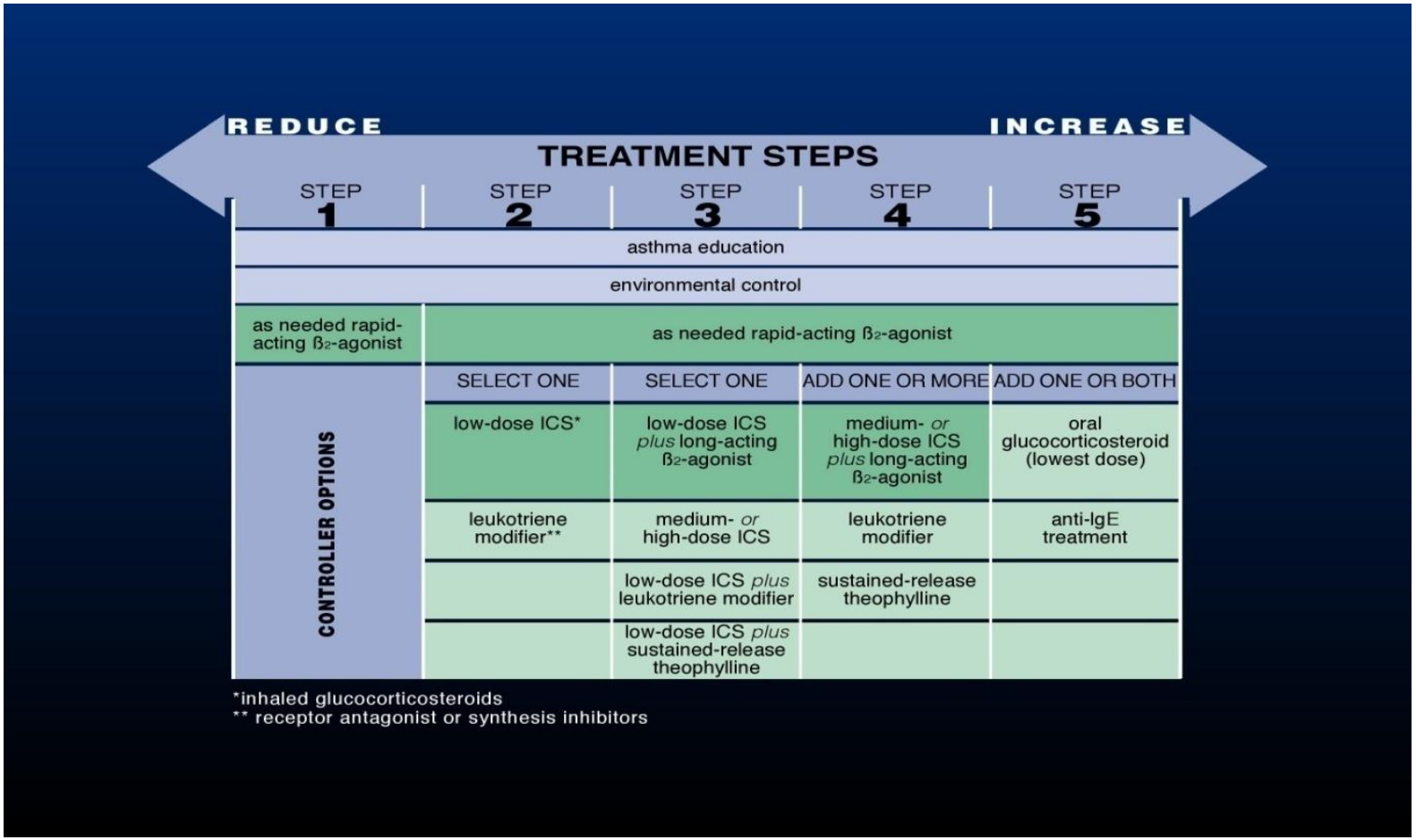

Figure 1.3 Therapeutic control of asthma is achieved in steps, with patients categorized into GINA steps 1 to 5.

Public domain source: GINASlideSet2006_Final.pptx.

http://www.ginasthma.com/OtherResourcesItem.asp?l1=2&l2=3&intId=842

1.2.6 Pharmacological treatment of asthma

Management of asthma is achieved by combining pharmacotherapy with lifestyle changes to control impairment and risk. Drug treatment to combat AFO has two aims, treatment of bronchoconstriction and of airway inflammation. The former is a 'reliever', an hASM relaxant, for fast relief of acute AFO. The latter is a 'preventer', taken regularly and independent of symptoms to control inflammation in persistent asthma. Also, several second line treatments are available as control becomes more fractious. They are usually delivered directly to the lungs by metered-dose aerosol or dry power inhalation, and have rapid pulmonary onset with minimal systemic effects. However, as the disease progresses systemic oral or parenteral administration may be required.

β_2-Adrenoceptor agonists

hASM cell β_2-adrenoceptor stimulation by selective sympathomimetic agents activates adenylyl cyclase, increases intracellular cAMP and effects muscle relaxation. They also inhibit release of certain bronchoconstrictors from mast cells, slow capillary leakage and increase mucociliary clearance by increasing activity of cilia or affecting mucus composition. Any of the short acting β_2-adrenoceptor agonists (SABA), salbutamol, terbutaline or fenoterol, are currently the most effective and most widely used bronchodilators for mild to moderate asthma exacerbations. After inhalation SABA effects begin within 5 minutes producing bronchodilation for around 3 to 5 hours.

Use of more than one aerosol per month suggests that asthma is not controlled at this therapeutic level. Long acting β_2-adrenoceptor agonists (LABA), such as salmeterol or formoterol, are bronchodilators lasting up to 12 hours. Compared to SABAs they have

a long lipophilic organic side chain that is thought to prolong the effect of the drug by dissolving in the lipid bilayer plasma membrane, increasing the number of drug molecules in a 'slow release' fashion that can stimulate the receptor over a longer time. They are used for long term control of asthma, useful nocturnally and for exercise induced asthma. LABAs are added to corticosteroids if the latter in standard dose has failed to adequately control asthma. The addition of a LABA to a standard corticosteroid is equivalent to doubling the inhaled corticosteroid dose in terms of control. For example combination inhalers containing formoterol and budesonide are now common. LABAs are not recommended as single therapy as they can cause severe or fatal asthma exacerbations which may be related to β-adrenoceptor polymorphism.

SABAs and LABAs all have a longer duration of action than corresponding endogenous agonists epinephrine and norepinephrine. SABAs are not subject to cellular uptake and are low affinity substrates in catecholamine metabolism by catechol-O-methyl transferase (COMT). LABA action is enhanced by COMT inhibitors. Both are metabolised by monoamine oxidase but MAOIs and tricyclic antidepressents enhance their effects. Converesly, β-blockers such as propranolol will decrease their effectiveness.

β_2-adrenoceptor selectivity is dose dependent, the dose response relationship is log-linear such that a ten-fold increase in dose is needed for a doubling in bronchodilation. At low dose, selectivity of agonists for the β_2- over the β_1-adrenoceptor limits side effects of tachychardia, arrhythmia and myocardial ischaemia. However, at higher inhaled doses or systemic administration these cardiac side effects begin to appear together with β_2 mediated hypokalaemia, hypomagnesia, hyperglycaemia, ketoacidosis and pharmacological tolerance can occur. Other side effects include fine skeletal

muscle tremor, muscle cramps, paradoxical bronchospasm, urticaria, peripheral vasodilation, angioedema, hypotension, and headache.

Antimuscarinics

All three types of muscarinic cholinoceptor are found in lung tissue. M_1 mediate cholinergic signaling in parasympathetic ganglia. M_2 are presynaptic autoreceptors that modulate ACh release from vagal nerve terminals. M_3 are in postsynaptic parasympathetic effectors and effect bronchoconstriction and a reduction in mucus secretion by the production of intracellular cGMP. The antimuscarinic agents used clinically, ipratropium and tiotropium, are receptor non-selective but do block vagal ACh mediated bronchospasm and may reduce mucus hypersecretion. They do not treat allergy or exercise induced bronchoconstriction. They are N-quaternary derivatives of atropine without the side effects of atropine, arrhythmia, blurred vision, dry mouth, hallucination. They are not as effective as β_2-adrenoceptor agonists but are an alternative in cases of tolerance and concurrent use of cardiac β-blockers. An antimuscarinic may be added to a SABA to control moderate to severe asthma. Antimuscarinics are taken by inhalation only and have a slow onset time of between 30 to 60 minutes. Ipratropium rapidly dissociates from M_3 receptors and has a rapid duration of action at the receptor with a half life of 16 mins. Tiotropium has a longer duration of action due to its higher affinity for M_1 and M_3 (half life 35 hours) receptors than for M_2 (half life 3.5 hours) receptors.

Methylxanthines

Major compounds in this group include theophylline, theobromine and caffeine, all are found naturally in tea, cocoa and coffee. Only theophylline (1,3-dimethylxanthine) and its ester derivative aminophylline are used clinically. They are not useful for asthma

exacerbations but may be added to a SABA. As adjuvant therapy in moderate to severe asthma, they may be given orally or by slow (over 20 minutes) iv injection with plasma drug concentration pharmacokinetic monitoring, because the therapeutic dose is close to the toxic dose. Side effects include arrhythmia, tachycardia, GI disturbance, hypokalaemia, insomnia, convulsions together with a variable but generally short plasma half life and potential for drug-drug interaction as it is metabolised by P450 liver enzymes. Slow release preparations are useful for nocturnal asthma control. Theophylline is a mild bronchodilator with mild anti-inflammatory actions and it increases mucociliary clearance and diaphragmatic contractility. As a PDE inhibitor it causes bronchodilation by reducing cAMP metabolism allowing cAMP and cGMP levels to increase. Adenosine present in asthmatic BAL fluid causes degranulation of mast cells and hence bronchoconstriction, theophylline combats this effect since it is an A_1 and A_2 receptor antagonist. NF-κB is a pro-inflammatory transcription factor activated when core chromatin histones are acetylated. Theophylline activates histone deacetylases causing an anti-inflammatory effect that can potentiate the effects of corticosteroids, since histone deaceylases are recruited to inflammation sites by activated glucocorticoid receptors.

Corticosteroids

For asthma that is not adequately controlled by SABAs, corticosteroids are the most potent and effective primary 'preventer' anti-inflammatory therapy available for moderate to severe asthma (Suissa *et al.*, 2000). Drug choices include equally effective beclometasone dipropionate, budesonide, fluticasone propionate, mometasone furate. Corticosteroid is a term that includes glucocorticoids and mineralocorticoids both secreted by the adrenal cortex. However, the drugs are traditionally referred to as

‘corticosteroids’ even though the actual drug is a glucocorticoid or glucocorticosteroid. The tradition will be preserved here for the sake of consistency with other sources. Mineralocorticoids control water and electrolyte homeostasis and are not useful in asthma. Glucocorticoids however have pleiotropic immunosuppressive and anti-inflammatory activity and analogues of the endogenous corticosterone, itself synthesised from cholesterol, are used in asthma therapy.

In the cytoplasm glucocorticoids (G) bind with their cognate receptors (R) to form a GR complex which translocates to the nucleus where it denies pro-inflammatory transcription factors access to DNA. Glucocorticoids also recruit histone deacetylases to transcription sites where they act to silence cytokine directed inflammatory gene transcription in a process called transrepression. The GR complex also promotes the transcription and hence expression of anti-inflammatory proteins such as lipocortin-1 and annexin-A1, called transactivation. Corticosteroids are used to treat acute and chronic inflammation and hence decrease AFO and AHR. Inhaler treatment is preferred. Prescribing one or two doses daily yields improvement after 24 hours. Maximal protection is achieved after 1 to 2 weeks that can significantly attenuate the late phase allergen response.

Treatment is chronic, does not reverse airway structural remodelling, and withdrawal leads to relapse into worsening chronic asthma symptoms. Oral or parenteral systemic corticosteroids enable control of acute severe exacerbations or are used when inhaled therapy does not provide adequate control in patients with difficult to treat refractory asthma. Concurrent vitamin D and calcium supplementation will stave off osteoporosis. Oral corticosteroid dose is 30-60mg per day, until control is achieved and then dose is backed off to achieve a minimum dose that still controls asthma.

Standard inhaled doses are unlikely to have systemic effects although higher inhaled and oral doses will. Side effects of taking inhaled corticosteroids are dysphonia and oral candidiasis. But more seriously, systemic effects are essentially that of Cushing's Syndrome, *viz.* hyperglycaemia, osteoporosis, weight gain, muscle proteolysis, dilation of skin capillaries, stunted growth, negative calcium and nitrogen balance, glaucoma, cataracts. In refractory cases of severe asthma large doses of oral or inhaled corticosteroids often do not control exacerbations (Holgate *et al.*, 2006). Then alternative personalised multi-drug strategies are devised (Chanez *et al.*, 2007). Interestingly, at high dose it is suggested that the mechanism of action is not just mediated by glucocorticosteroid receptors but rather biophysical changes to membrane fluidity become more predominant (Lamche *et al.*, 1990), which may not be advantageous to the patient.

Cromoglycate and Nedocromil

For mild persistent or exercise induced asthma, sodium cromoglycate and nedocromil can control asthma over the long term as a 'preventer'. They are useful in the prophylaxis of bronchoconstriction caused by respiratory mastocytosis rather than during acute exacerbations. Both drugs are inhaled. They are hydrophilic and pass through plasma membranes relatively easily. They have their main action in the respiratory mucosa. They reduce the release of bronchoconstricting mediators by degranulation from mast cells, and are said to stabilise the mast cell membrane. They also decrease activation of eosinophils, neutrophils and macrophages. A definitive mechanism of action that explains their usefulness in asthma has not yet been worked out for these drugs. Recent work has suggested that they enhance release of glucocorticoid stimulated annexin-A1 (Yazid *et al.*, 2009).

Leukotriene modifiers

Leukotrienes are powerful inflammatory mediators generated by the action of 5-lipoxygenase on arachidonic acid after tissue injury, including allergen challenge. They are synthesised in activated eosinophils, mast cells, macrophages and basophils. LTC_4 and D_4 are bronchoconstrictors that increase AHR, mucosal oedema and mucus secretion. LTB_4 is a neutrophil chemoattractant. Zileuton decreases leukotriene production by inhibiting 5-lipoxygenase. Zafirlukast and montelukast are cysteinyl leukotriene receptor antagonists. These types of drug are given orally which can assist adherence over inhalers especially in children. They can be used instead of inhaled corticosteroid with less symptom reduction but with near equal exacerbation frequency in mild to moderate asthma. They are also useful in exercise induced asthma and in aspirin (or other NSAID) induced asthma. Side effects are less than corticosteroids, namely headache, GI upset, insomnia and malaise.

Anti-IgE

A molecular biology approach has produced a humanised recombinant monoclonal IgG_1 anti-human IgE antibody, omalizumab, raised in mice that is not immunogenic in humans. It is genetically humanised preserving the important CDR regions. It is used as an additional therapy that binds IgE but does not activate mast cell degranulation. It is useful in allergic IgE mediated severe persistent asthma that is not controlled adequately by oral or inhaled corticosteroids or LABA polypharmacy.

TNF-α

TNF-α (tumour necrosis factor) is an acute phase inflammatory cytokine that can be inhibited using a soluble TNF receptor antagonist, etanercept. It is used to help control

inflammation in rheumatoid arthritis but it is not currently licensed for use in asthma in the UK.

1.3 hASM cells and Ca^{2+}

The increase in breathing effort required to transport air in and out of the lungs, marks a shift from quiescent diaphragmatic breathing to the involvement of voluntary intercostal muscles often causing patient fatigue and psychological distress, ultimately requiring oxygen therapy. hASM tissue is central to the clinical manifestation of asthma as it is the direct effector of acute bronchoconstriction and reduced pulmonary airflow. During an asthma exacerbation, extra mechanical stresses act upon hASM tissue which may affect the hASM cell contractile protein phenotype and state of differentiation (Low *et al.*, 1998; Trepat *et al.*, 2007). Whilst it is commonly believed that airway inflammation is the root cause of airway hyperresponsiveness, there is also a possibility that airway smooth muscle cells might be intrinisically abnormal, specifically in terms of Ca^{2+} homeostasis and handling. There have been several papers that make a pro-calcium dysregulation argument (Table 1.2). Therefore, based upon the fact that bronchoconstriction is clearly central to asthma, it is reasonable to suspect that there is an intrinsic *in situ* abnormality in hASM cells from asthmatics (Borger *et al.*, 2006).

Since hASM cell contraction is initiated by the action of Ca^{2+} dependent proteins, molecular pathological changes present in the hASM cell in asthma may involve changes to the cell's Ca^{2+} signaling system, or signalsome. The Ca^{2+} signalsome includes all the components of the Ca^{2+} signaling system generated by the transcriptome of a particular cell type, this has been described as the calcium signaling 'toolkit' (Berridge *et al.*, 2003). A change in Ca^{2+} signaling may be genetically intrinsic to hASM cells from birth or acquired by changes in airway mechanical force,

environmental triggers, or inflammatory products or a combination of these factors. It is possible that the epigenome can be affected by these acquired change agents, effecting changes in hASM cell gene expression.

The goal of this project is determine whether Ca^{2+} homeostasis and handling in human airway smooth muscle cells is intrinsically different in asthma compared to normal donors. The molecular triggering event that precedes activation of the sliding filament actinomyosin mechanism of myocyte contraction is an increase in intracellular calcium ion concentration, $[Ca^{2+}]_i$. Therefore, characterisation of Ca^{2+} dynamics in isolated cells is essential to achieving this goal.

hASM cells have an elongated spindle-like or fusiform appearance (Ma *et al.*, 2002) *in-vivo* and this morphology is generally preserved *in-vitro* by low passage cells as seen by light microscopy (Figure 1.4). Furthermore, these cells contain abundant amounts of α-smooth muscle actin (α-SMA) filaments (Figure 1.5), a smooth muscle cell differentiation biomarker, which is essential to the molecular mechanism of smooth muscle cell contraction.

A disturbance to the homeostatically regulated $[Ca^{2+}]_i$ heralds the generation of signaling events and therefore information transfer in most cell types including smooth muscle cells (Hofer *et al.*, 2003). However, Ca^{2+} signaling is more sophisticated than a simple bulk increase in $[Ca^{2+}]_i$. Physiologically, it is the sub-cellular spatio-temporal profile of Ca^{2+} oscillations, in particular the frequency, which is important (Parekh, 2011). At the level of individual Ca^{2+} release channels there is a constant basal 'chatter' of stochastic opening and closing giving rise to small elementary Ca^{2+} releases, called puffs if from IP_3Rs and sparks if from RyRs. The analysis of this behaviour is

comprehensively covered in a paper published from a group at St George's Medical School, London (Gordienko *et al.*, 2002).

Hence, the hASM cell cytoplasm has been termed an 'excitable medium' with respect to Ca^{2+} release (Berridge *et al.*, 1994). During a signaling event, this pseudorandom 'chatter' background is disturbed by concerted rises in $[Ca^{2+}]_i$ of higher signal to noise ratio. This signaling may be confined to a region of the cell or extend globally throughout the cell. Hence, regional time varying spikes or transients that occur in a defined region of the cell give rise to $[Ca^{2+}]_i$ oscillations. Furthermore, such oscillations can give rise to a global $[Ca^{2+}]_i$ disturbance or wave that propagates throughout the cell. Logically, a $[Ca^{2+}]_i$ wave must have a single origin, and this has been called a frequent discharge site, FDS, (Gordienko *et al.*, 2002). Otherwise, multiple FDSs would lead to the generation of more complex waveforms by superposition. It could be that the organisation of Ca^{2+} release in hASM cells from asthma donors makes $[Ca^{2+}]_i$ oscillations more likely.

Global changes occur when repetitive local time varying $[Ca^{2+}]_i$ oscillations in a defined region of the cell give rise to a saltatory coupling between Ca^{2+} release channels leading to a propagated wave. Probably the most striking example comes from *Xenopus*, or common frog, oocytes where waves of $[Ca^{2+}]_i$ having a single origin can be monitored spiralling throughout the cell. Whereas oscillations are spatially confined and time varying, waves are described by changes in time and space dimensions, giving rise to spatio-temporal fluctuations in the $[Ca^{2+}]_i$ background.

It is thought that $[Ca^{2+}]_i$ waves begin when local $[Ca^{2+}]_i$ release from a SR cluster or microdomain of $[Ca^{2+}]_i$ release channels (IP_3R and RyRs) discharges enough $[Ca^{2+}]_i$ to

Table 1.2 Literature evidence suggesting that Ca^{2+} homeostasis and handling is altered in asthma compared to normal hASM cells.		
Title	**Extract from abstract**	**Author, year**
Calcium, the control of smooth muscle function and bronchial hyperreactivity	It is suggested that a defect in Ca^{2+} mobilization or in the receptor - Ca^{2+} mobilization coupling process at the level of the smooth muscle may constitute an important underlying cause of bronchial hyperreactivity.	(Triggle, 1983)
Airway smooth muscle, asthma, and calcium ions.	All of the pathogenetic processes in asthmatic airways are Ca^{2+}-dependent phenomena: excitation-contraction coupling in smooth muscle, stimulus-secretion coupling in mast cells and mucous glands, nerve impulse initiation and conduction, and the development of inflammatory infiltration.	(Middleton, 1984)
Toxic oxygen products alter calcium homeostasis in an asthma model	The data support the hypothesis that toxic oxygen products generated with SRS-A and/or LTC_4 induce an alteration in Ca^{++} homeostasis in airway smooth muscle.	(Weiss, 1985)
Sensitization alters contractile responses and calcium influx in human airway smooth muscle	These results suggest that airway hyperresponsiveness may be associated with altered calcium mobilization in airway smooth muscle.	(Black *et al.*, 1989)
Calcium regulation and contractile dysfunction of smooth muscle	Chronic asthmatic disease seems to be associated with altered Ca^{2+} handling via changes in gene coding for receptors, enzymes and regulatory proteins, thus contributing to abnormal responsiveness and cell growth.	(Sakai *et al.*, 1993)
Cytosolic Calcium Oscillations in Smooth Muscle Cells	There is evidence that alterations in Ca^{2+} oscillations modulate smooth muscle responsiveness.	(Savineau *et al.*, 2000)
Modulation of calcium homeostasis as a mechanism for altering smooth muscle responsiveness in asthma	Studies using isolated bronchial preparations or cultured cells show that inflammatory mediators and cytokines may alter calcium homeostasis in airway smooth muscle and render the cells nonspecifically hyperreactive to agonists.	(Amrani *et al.*, 2002)

Title	Extract from abstract	Author, year
Airway hyperresponsiveness and calcium handling by smooth muscle: a "deeper look"	We propose that abnormal calcium handling by the airway smooth muscle may be an important determinant of airway hyperresponsiveness. The amplitude, frequency, or localization of Ca^{2+} oscillations in the smooth muscle may determine the degree of airway sensitivity and reactivity, which are characteristic features of asthma.	(Parameswaran *et al.*, 2002)
CD38/cyclic ADP-ribose signaling: role in the regulation of calcium homeostasis in airway smooth muscle.	Recent studies have identified cyclic ADP-ribose as a calcium-mobilizing second messenger in airway smooth muscle cells, and modulation of the pathway involved in its metabolism results in altered calcium homeostasis and may contribute to airway hyperresponsiveness.	(Deshpande *et al.*, 2005)
Bronchial smooth muscle remodeling involves calcium-dependent enhanced mitochondrial biogenesis in asthma	BSM in asthmatic patients is characterized by an altered calcium homeostasis that increases mitochondrial biogenesis, which, in turn, enhances cell proliferation, leading to airway remodelling.	(Trian *et al.*, 2007)
Mechanisms altering airway smooth muscle cell Ca^{2+} homeostasis in two asthma models	In the human asthma model the expression of SR Ca^{2+} channels is altered. The investigation of the Ca^{2+} homeostasis of ASMC has the potential to provide new therapeutical options in asthma.	(Kellner *et al.*, 2008)
Effect of proinflammatory cytokines on regulation of sarcoplasmic reticulum Ca^{2+} reuptake in human airway smooth muscle	In human ASM, SERCA is regulated by mechanisms such As CaMKII and that airway inflammation maintains $[Ca^{2+}]_i$ levels by decreasing SERCA expression and slowing Ca^{2+} reuptake.	(Sathish *et al.*, 2009)

Title	Extract from abstract	Author, year
Diminished sarco/endoplasmic reticulum Ca^{2+}-ATPase (SERCA) expression contributes to airway remodelling in bronchial asthma	Rises in $[Ca^{2+}]_i$ following cell surface receptor-induced SR activation, or inhibition of SERCA-mediated Ca^{2+} re-uptake, were attenuated in ASM cells from asthmatics. Likewise, the return to baseline of $[Ca^{2+}]_i$ after stimulation by bradykinin was delayed by approximately 50% in ASM cells from asthmatics.	(Mahn *et al.*, 2009)
Ca^{2+} homeostasis and structural and functional remodelling of airway smooth muscle in asthma	It is proposed that a unifying mechanism for the abnormal asthmatic phenotype is dysregulation of Ca^{2+} homeostasis caused at least in part by a downregulation in expression and function of sarcoendoplasmic Ca^{2+}-ATPases (SERCAs).	(Mahn *et al.*)

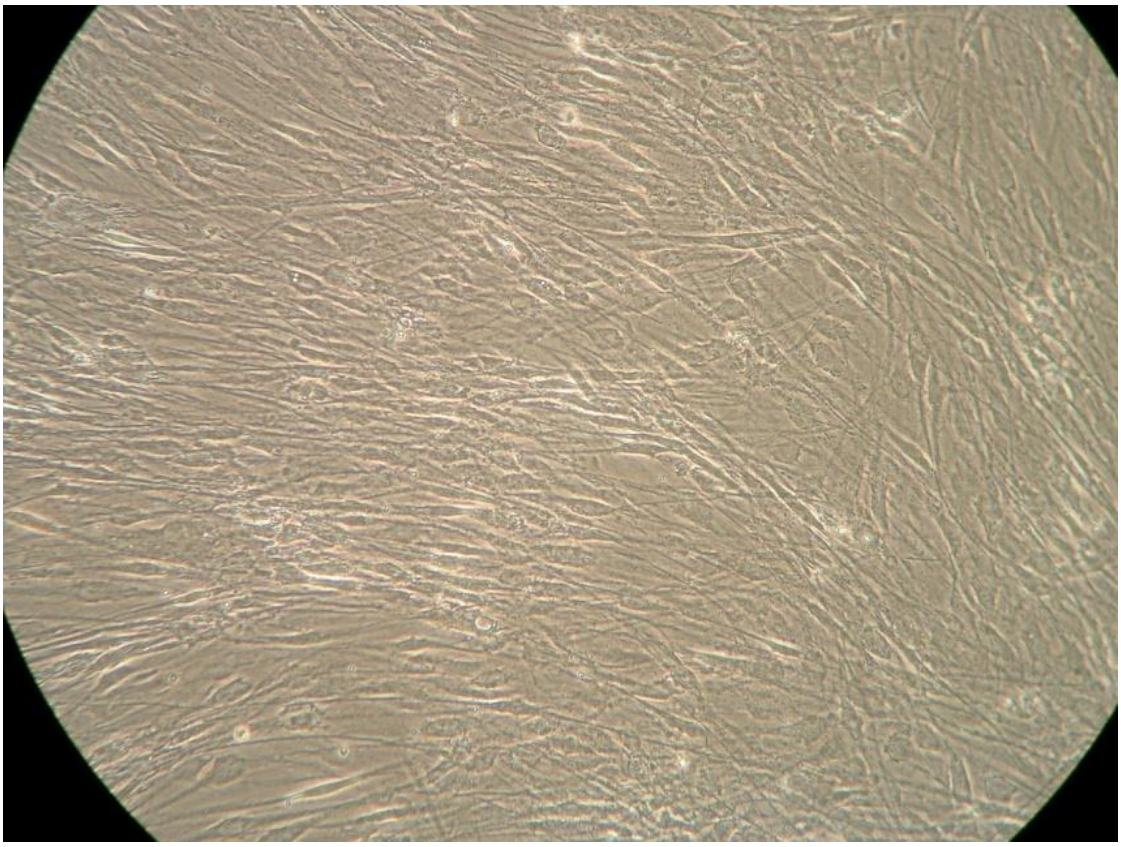

Figure 1.4 Human airway smooth muscle (hASM) cells grown in culture show a characteristic fusiform morphology as shown in this light microscopy image of approx. 90% confluent ASM cells (x40 magnification).

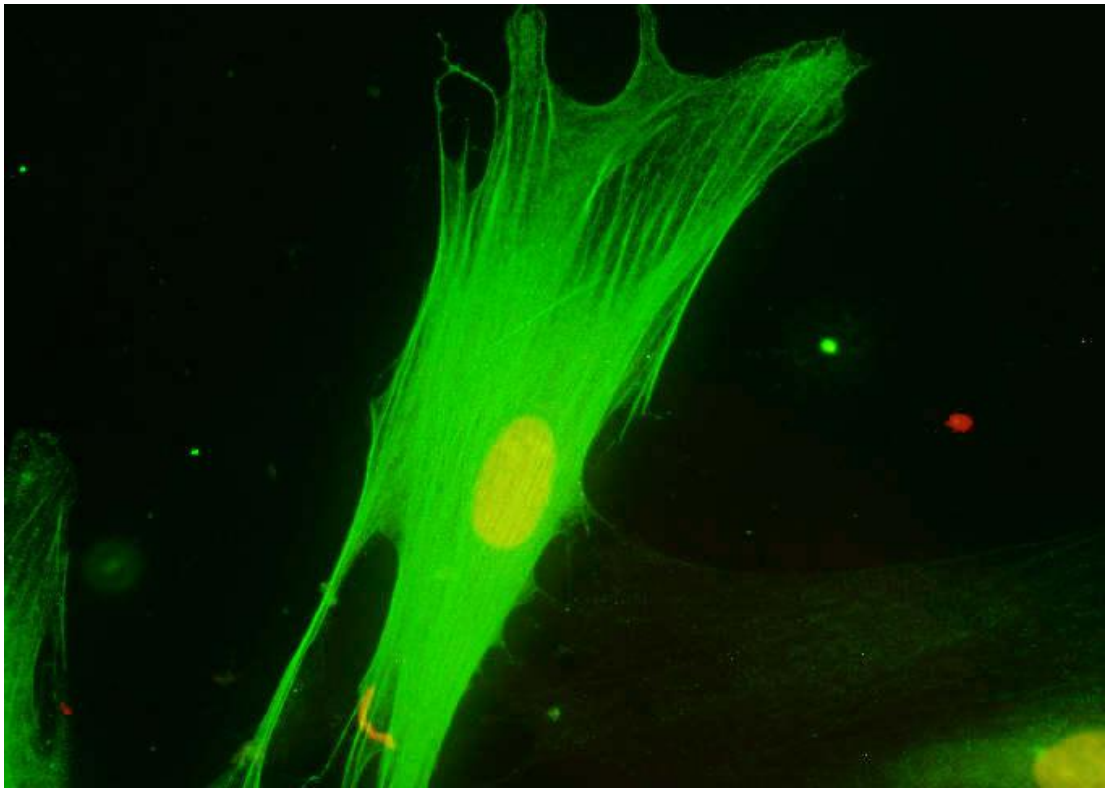

Figure 1.5 An airway smooth muscle cell showing filaments of α-smooth muscle actin (green stain: FITC-conjugated anti-αSMA antibody) using a fluorescence microscope (x40 objective). The location of the nucleus is identified using a yellow stain (propidium iodide).

open adjacent Ca^{2+} ion release channels, which in turn opens more distant channels. Thus this is a regenerative system of repeaters.

A travelling wave of $[Ca^{2+}]_i$ is created by this regenerative reaction-diffusion process called 'Calcium Induced Calcium Release' (CICR). As the wave passes, individual $[Ca^{2+}]_i$ release channels are inhibited by the high local $[Ca^{2+}]$, and $[Ca^{2+}]_i$ is transported out of the cytoplasm, creating the falling edge of the wave.

1.4 Intracellular Ca^{2+} and Ca^{2+} oscillations

It was over one hundred years ago that a technician in Sydney Ringer's lab used tap water in place of distilled water for a series of physiological experiments on isolated frog hearts. Ringer was initially perplexed because his physiological buffer, which should have been made up using distilled water, should not have allowed spontaneous contractions. Eventually Ringer spotted the error, it was the Ca^{2+} ions in the London tap water that were responsible. And this was confirmed when adding Ca^{2+} to his physiological buffer, which was carefully made with distilled water, caused the hearts to contract. This marked the discovery of the now famous Ringer's solution, a serendipitous discovery one might say! This is probably the earliest recorded scientific account linking Ca^{2+} ions to muscle contraction (Ringer, 1883).

The next major breakthrough didn't come until 1970 when Endo working at the University of Tokyo found that he could repeatedly release SR stored Ca^{2+} from skinned skeletal muscle fibres with caffeine. And that the Ca^{2+} release could itself regenerate a further Ca^{2+} release. Hence he concluded 'calcium induces its own release of calcium from the reticulum' (Endo *et al.*, 1970). This process is of course well known today as calcium induced calcium release (CICR) and is a fundamental concept for explaining the generation of $[Ca^{2+}]_i$ waves.

In 1976 work on sympathetic ganglion cells showed that rhythmically induced hyperpolarisation and depolarisation is due to increased membrane permeability to Ca^{2+} and Na^{+} ions (Kuba *et al.*, 1976). Hence the idea that oscillations in membrane potential could be driven by the movement of ions and that Ca^{2+} ions are a player in this system was established. Also in the same year $[Ca^{2+}]_i$ oscillations were first described (Ridgway *et al.*, 1976), by using a luminescent Ca^{2+} ion sensitive photoprotein indicator called aequorin derived from the sponge *Aequorea sp.* It is now known of course that $[Ca^{2+}]_i$ oscillations play a physiological role in most cells (Berridge, 1990).

All modern fluorescent Ca^{2+} sensitive fluorophores are chemically based upon the Ca^{2+} chelating molecule BAPTA, a tetracarboxylic acid (1,2-bis(o-aminophenoxy)ethane-N,N,N',N'-tetraacetic acid). The first of which was the non-ratiometric quin-2, a quinoline substituted tetracarboxylate BAPTA derivative. One of its earliest uses was to reveal Ca^{2+} oscillations in agonist stimulated hepatocytes (Woods *et al.*, 1986). By 1985 a new generation of fluorescent Ca^{2+} sensitive dyes, notably the ratiometric pentacarboxylate fura-2, were introduced with brighter fluorescence intensity, greater Ca^{2+} ion selectivity and greater photochemical stability than anything else available before (Grynkiewicz *et al.*, 1985). This greatly accelerated the field of $[Ca^{2+}]_i$ imaging. Since 1985 around 2,600 papers have been published that mention calcium oscillations using fura-2.

In 1983 Berridge described the agonist induced phosphoinositide cascade and the all important IP_3 came to the fore as a non-mitochondrial Ca^{2+} ion mobilising agent (Streb *et al.*, 1983). Indeed, perhaps the most renowned researcher in this field of recent times was Professor Michael J. Berridge of Cambridge University. He has published many definitive papers that have advanced our understanding of calcium homeostasis (Berridge *et al.*, 2003) and calcium oscillations (Berridge *et al.*, 1988) in general, and in

particular the importance of IP_3-mediated $[Ca^{2+}]_i$ release (Berridge, 1993). However, today the likes of Professor Anant Parekh at Oxford University and other excellent researchers worldwide have accepted the baton and are increasing our understanding even further. The literature now expounds upon how biological information is encoded into $[Ca^{2+}]_i$ oscillations and waves, in terms of frequency and amplitude, and how Ca^{2+} ion sensitive proteins act as the biological tranducers for that information.

Today of course $[Ca^{2+}]_i$ oscillations are known to be a normal physiological phenomenon that occurs across a whole spectrum of both excitable and non-excitable cells (Berridge *et al.*, 1988; Berridge, 1990). $[Ca^{2+}]_i$ oscillations may occur in certain cells spontaneously, notably rhythmic pacemakers such as cardiac myocytes, gastrointestinal interstitial cells of Cajal, pancreatic β-cells or GnRH hypothalamic neurons. Or they can be induced by the action of endogenous chemicals acting at cell surface GPCRs coupled to phosphoinositide downstream signaling. Such $[Ca^{2+}]_i$ signaling throughout the hASM cell initiates many biological processes for example, contraction, regulation of gene transcription, cell differentiation (Dolmetsch *et al.*, 1998) and actin remodelling to name a few processes. $[Ca^{2+}]_i$ oscillations also maintain the normal physiological Ca^{2+} signalsome by a process of Ca^{2+} ion induced transcription of Ca^{2+} signaling components (Dolmetsch *et al.*, 1998; Isenberg, 2004; Morales *et al.*, 2007). Furthermore, it is emerging that specificity of effect is achieved not only through frequency and amplitude modulation (Berridge, 1997a) but by restriction of $[Ca^{2+}]_i$ oscillations, generated by a local summation of Ca^{2+} sparks, to particular spatio-temporal patterns. Hence, most cellular processes are regulated on a local or regional basis by $[Ca^{2+}]_i$ oscillations, whilst larger cell wide changes are regulated by cell wide global $[Ca^{2+}]_i$ waves, but in both cases effector proteins are sensitive to frequency encoded Ca^{2+} oscillations (Pucovsky *et al.*, 2006; Parekh, 2011).

If it is found that $[Ca^{2+}]_i$ handling in hASM cells in asthma is dysregulated and spontaneous $[Ca^{2+}]_i$ waves emerge as a result of it, then this would form a strong mechanistic basis for AHR in asthma (Savineau *et al.*, 2000). Hence, $[Ca^{2+}]_i$ oscillations may be an intrinsic property of asthma hASM cells due to an acquired or heritable developmental fault. Moreover, irrespective of cause, spectral analysis (Uhlen, 2004) of baseline $[Ca^{2+}]_i$ oscillations in hASM cells from asthma and normal donors will address this question and the question of mechanistic cause will follow.

1.4.1 Understanding fluorescent Ca^{2+} sensitive indicators

Bright fluorescent Ca^{2+}-sensitive dyes have been available for over twenty five years and have allowed dynamic Ca^{2+} signaling in living cells to be assessed (Knot *et al.*, 2005; Giepmans *et al.*, 2006), through the concurrent development of the necessary microscope hardware and software, and image acquisition systems. Thus the fluorescence microscope (Lichtman *et al.*, 2005) and its associated light sources, spectral filters, electro-optical detectors, amplifiers and software controllers are at the heart of this method. But when investigating fast localised Ca^{2+} events at a fundamental sub-cellular level, the confocal microscope in particular is a formidable tool (Conchello *et al.*, 2005).

Fluorescent indicators are of two basic types, single wavelength (SW) intensity modulating dyes or dual wavelength ratiometric dyes. An example of a commonly used SW Ca^{2+} sensitive indicator is fluo-4 and a commonly used ratiometric indicator is fura-2.

SW dyes are the simpler fluorescence Ca^{2+} indicators. Fluo-4 functions as an indicator essentially because an increase in $[Ca^{2+}]$ increases the intensity of the emitted

fluorescence at a wavelength close to and just above the excitation wavelength (Figure 1.6).

Fura-2 is a ratiometric indicator that employs a shift in the excitation wavelengths and a common emission wavelength. Under low [Ca^{2+}] conditions its excitation maximum is around 380nm and as the [Ca^{2+}] increases and binds to the fura-2 its excitation maximum shifts to 340nm. The emission spectrum at each excitation wavelength does not shift but remains around 510nm (Figure 1.7). By alternating the excitation wavelengths between 340 and 380nm and measuring the emitted fluorescence (F) intensity at 510nm, a ratio of fluorescence intensities can be derived. In this form, F_{340}/F_{380} or R, is a direct measure of $[Ca^{2+}]_i$. Since F_{340} increases as fura-2 binds Ca^{2+} ions and F_{380} decreases, a net increase in the ratio, $R = F_{340}/F_{380}$, indicates that $[Ca^{2+}]_i$ is rising and vice versa.

For SW indicators because fluorescence intensity is measured at a single wavelength, other factors can change intensity in addition to changes in $[Ca^{2+}]_i$; these artefacts might include changes in cell thickness and density, photo-bleaching or loss of indicator due to leakage from the cell.

The problems seen with SW indicators are somewhat offset by using a ratiometric indicator because dye leakage or cell thickness variation is effectively cancelled by measuring relative fluorescence ratios. However, the equipment needed to use ratiometric dyes is more complex then with non-ratiometric SW dyes.

Fura-2 is excitable in the UV spectrum range and this is not always advantageous particularly if the cells are known to autofluoresce, or if one is performing UV photoactivated Ca^{2+} uncaging experiments (cf. section 2.4) in which case SW fluo-4 would be a better choice. Also, using fura-2 involves an extra complication because the

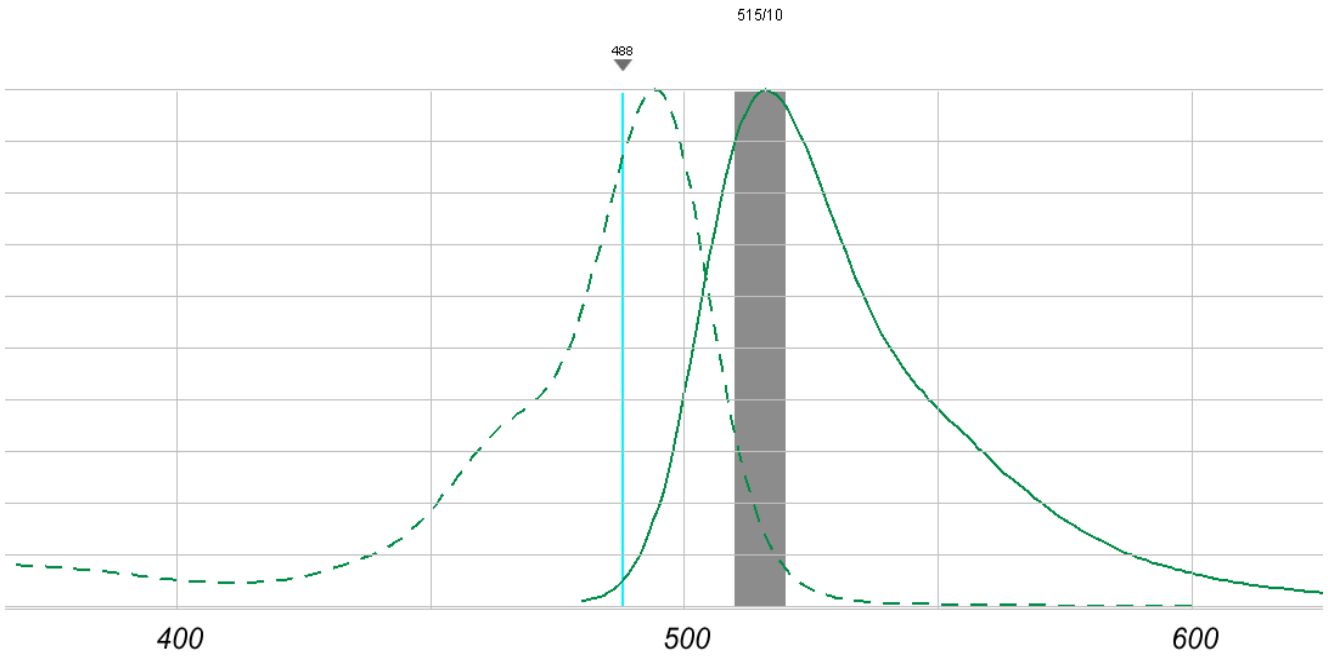

Figure 1.6 Excitation (dotted line) and emission (solid line) spectra of fluo-4. Fluo-4 is a single wavelength Ca^{2+} ion sensitive fluorescent indicator. Excitation can be performed using a 488nm argon laser and emission can be detected around 510-520nm. As Ca^{2+} ions bind to the dye it increases fluorescence intensity in both excitation and emission spectra.

Source:

http://www.invitrogen.com/site/us/en/home/support/Research-Tools/Fluorescence-SpectraViewer.html

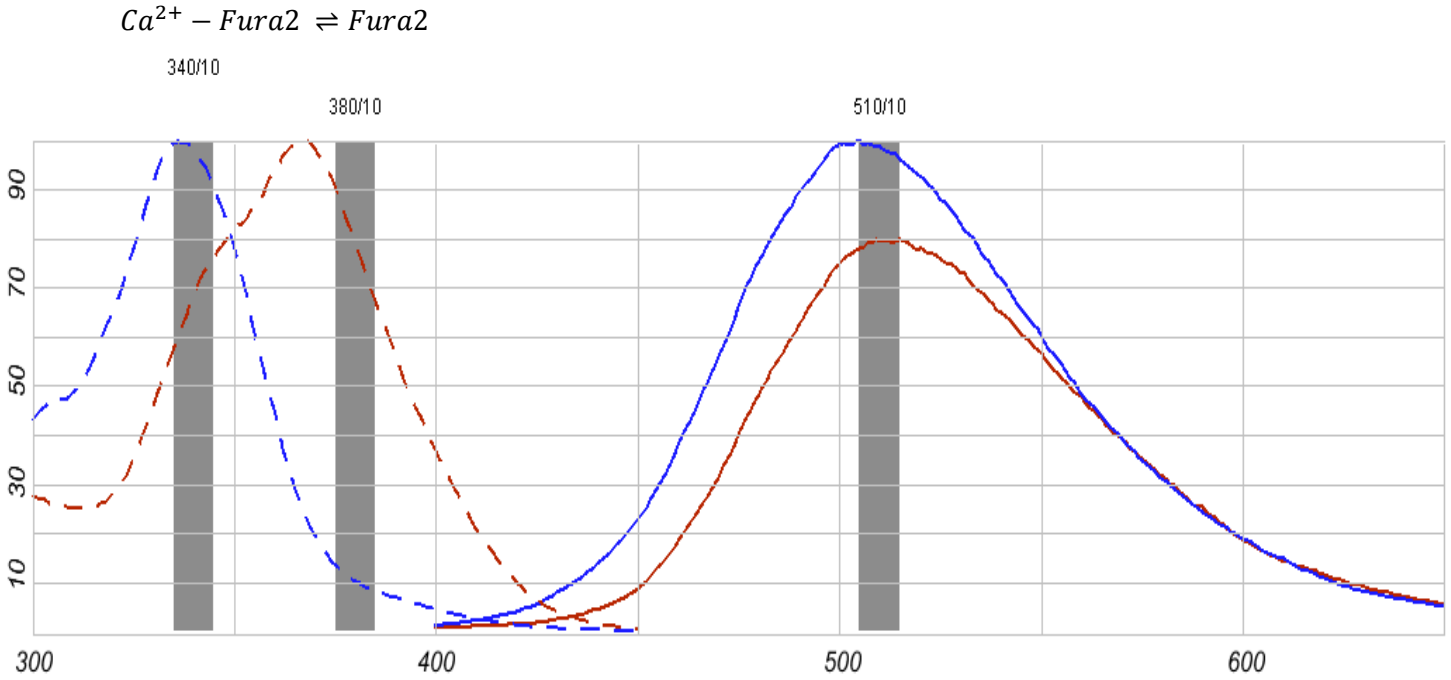

Figure 1.7 Excitation (dotted lines) and emission (solid lines) spectra of fura-2. When few Ca^{2+} ions bind to fura-2 excitation the maximum is around 380nm and when $[Ca^{2+}]$ increases the excitation maximum shifts to around 340nm. Emission spectrum is around 520nm for Ca^{2+} ion unbound and bound fura-2. The ratio F_{340}/F_{380} is a direct measure of $[Ca^{2+}]$, it increases when $[Ca^{2+}]_i$ increases and decreases when $[Ca^{2+}]_i$ decreases.

Source:

http://www.invitrogen.com/site/us/en/home/support/Research-Tools/Fluorescence-SpectraViewer.html

equipment needs to regularly switch wavelengths. However, these two are probably the most popular fluorescent Ca^{2+} indicators today.

A calibration of the indicator can be performed and this allows estimates of $[Ca^{2+}]_i$ to be made, however, the fluorescence ratio (R) and intensity values (F) are perfectly acceptable where an absolute $[Ca^{2+}]$ value is not required. For example, where disease versus control relative comparisons are being made.

Leakage of fura-2 from the cell during the course of an experiment is still a problem just as with SW indicators. However, clever chemistry has resulted in a molecule with the same spectral characteristics as fura-2 but with much reduced leakage properties such that monitoring can proceed for up to one hour or more, this compound is called fura-PE3 and an AM ester is available for ease of loading. Fura-PE3 still retains the same BAPTA backbone just like fura-2 but rather than being a polycarboxylate molecule it is a zwitterionic molecule having substituted amine piperazineoacetic acid groups (Vorndran *et al.*, 1995).

Both fura-2 and fluo-4 are polycarboxylate anion molecules that have low lipophilicity. Hence acetoxymethyl ester (AM) groups are used to 'mask' the carboxylate anions generating an uncharged lipophilic and cell-permeant molecule. Once in the cell, the AM ester bonds are hydrolysed by endogenous cellular esterases and the indicator's negative charges re-appear and it is then a Ca^{2+} sensitive indicator. Being a polyanion it cannot pass back through the plasma membrane so is trapped inside the cell, although there are anion transporters in the plasma membrane that can permit it to leak from the cell. Addition of pluronic F127 (0.04%w/v) a non-ionic polyol surfactant assists dye loading by making the plasma membrane lipid bilayer and fluophore-pluronic F127 micelle interaction less hydrophobic. Probenecid (2.5μM) inhibits uric acid

transporters which are responsible for anion transport out of the cell. This also assists in the dye-loading process since the dye can be transported from the cell while it is still in the non-hydrolysed AM form, hydrolysis taking around 15-20min. The dye is now loaded ready to make measurements in a living cell. An alternative to probenecid is sulphinpyrazone but at higher concentration usually around 100µM. Probenecid is not used in the perfusion buffer since it can cause cellular stress and consequent membrane blebbing.

1.5 $[Ca^{2+}]_i$ handling

The reaction of hASM cells to a deliberate increase in $[Ca^{2+}]_i$ level can be used as a measure of the cell's kinetic ability to restore changes in $[Ca^{2+}]_i$ to basal levels. Also the amount of $[Ca^{2+}]_i$ released by such a $[Ca^{2+}]_i$ increase can be measured. Then a comparison of $[Ca^{2+}]_i$ handling parameters in hASM cells can be made between asthma and normal.

1.5.1 Agonist induced intracellular $[Ca^{2+}]_i$ release

A major mechanism by which hASM cell $[Ca^{2+}]_i$ levels are altered *in vivo* is by the action of various chemical agents, circulating hormones and local mediators of inflammation. The neurotransmitter acetylcholine (ACh) or other endogenous first messengers produced by local immune reactions such as histamine, bradykinin or serotonin (5-HT) are examples. Commonly, these ligands are complementary to hASM cell surface receptors of the type 7-transmembrane G-protein coupled receptors (7TM-GPCR, commonly abbreviated to GPCR).

For example, bradykinin stimulates increases in $[Ca^{2+}]_i$ via the small water soluble second messenger molecule inositol 1,4,5-trisphosphate (IP_3). The systematic chemical name for inositol is cyclohexane-1,2,3,4,5,6-hexol and the biologically active

stereoisomer is *cis*-1,2,3,5-*trans*-4,6-cyclohexanehexol commonly called *myo*-inositol. In inositol 1,4,5-trisphosphate, the *myo*-inositol ring has phosphate groups $-PO_4^{2-}$ substituted for hydroxyl groups at positions C1, C4 and C5 giving the molecule an overall negative charge at physiological pH. As IP_3 is an integral part of the agonist mediated $[Ca^{2+}]_i$ release pathway, I wanted to test the hypothesis that the amount of IP_3 generated by hASM cells in asthma compared to normal donors is different.

IP_3 is generated as a result of bradykinin binding to its cognate plasma membrane 7TM-GPCR receptor. There are two recognised forms B_1 and B_2 both of which mediate $[Ca^{2+}]_i$ release via $G\alpha_q$ coupling. B_2 receptors predominate in hASM cells (Marsh *et al.*, 1992). Bradykinin induces a conformational change in the B-receptor upon binding. Since GPCRs act as guanosine nucleotide exchange factors (GEF), the $G\alpha_q\beta\gamma$ heterotrimer exchanges GDP for GTP, whereupon $G\alpha_q$ dissociates from $\beta\gamma$. $G\alpha_q$ then activates plasma membrane bound phospholipase C (PLC) which cleaves phosphatidylinositol 4,5-bisphosphate (PIP_2) into IP_3 and diacylglycerol (DAG). DAG is lipophilic and remains mobile within the plasma membrane whilst IP_3 is hydrophilic and can freely diffuse throughout the cytoplasm. IP_3 binds to sarco/endoplasmic recticulum IP_3 receptors (IP_3R) and promotes the release of $[Ca^{2+}]_i$ from the SR Ca^{2+} store, into the cytoplasm through this receptor operated Ca^{2+} ion release channel. This leads to hASM cell contraction or other signaling functions (Figure 1.8). Intrinsic GTP-ase activity returns $G\alpha_q$ back to its inactive GDP $G\alpha_q\beta\gamma$ bound state.

Similarly, methacholine, a more stable analogue of ACh, acts via M_3 cholinoceptors which also couple to $G\alpha_q$, to release $[Ca^{2+}]_i$. Inhaled methacholine is used to assess patients' bronchoconstrictor responses when asthma is suspected.

Several G-protein types exist and have different downstream signaling functions. We have seen that $G\alpha_q$ acts to increase IP_3 and $[Ca^{2+}]_i$. But another important G-protein is $G\alpha_s$, this increases cAMP, and acts as a physiological antagonist to the actions of $G\alpha_q$. $G\alpha_s$ stimulates adenylyl cyclase which hydrolyses two phosphoanhydride bonds of ATP thus increasing cytoplasmic levels of second messenger cAMP. cAMP increases the catalytic activity of protein kinase A (PKA). PKA then phosphorylates IP_3Rs, decreasing their opening probability, thus reducing $[Ca^{2+}]_i$ and causing hASM cell relaxation. A reduction in the frequency of IP_3-dependent $[Ca^{2+}]_i$ oscillations caused by inhibition of IP_3Rs by cAMP also contributes to hASM relaxation (Bai *et al.*, 2006). β_2-adrenoceptors are $G\alpha_s$ coupled GPCRs and are the target of anti-asthma drugs salbutamol and salmeterol for example.

$[Ca^{2+}]_i$ release from the IP_3R is transient and the receptor is rapidly inhibited, entering a refractory period, caused by the rising levels of $[Ca^{2+}]_i$. This is a negative feedback property of the IP_3R with bell-shaped characteristic (Figure 1.9), conferring the potential for producing calcium oscillations (Bezprozvanny *et al.*, 1991; Brandman *et al.*, 2008). A similar bell-shaped characteristic also exists for the other major receptor operated Ca^{2+} ion channel on the SR, the ryanodine receptor (RyR). The RyR endogenous ligand is cADPR (cyclic adenosine diphosphate ribose, or cyclic ADP-ribose) generated by the ectoenzyme CD38.

Some agonists such as ACh (Dai *et al.*, 2006) and serotonin are able to generate $[Ca^{2+}]_i$ oscillations with frequency dependent upon agonist concentration (Perez *et al.*, 2005). Whereas other agonists such as bradykinin produce a sharp increase followed by a smooth decrease back to baseline $[Ca^{2+}]_i$ levels. Bradykinin stimulates a reproducible monophasic $[Ca^{2+}]_i$ response in hASM cells from which the restorative kinetics of the cell can be conveniently measured.

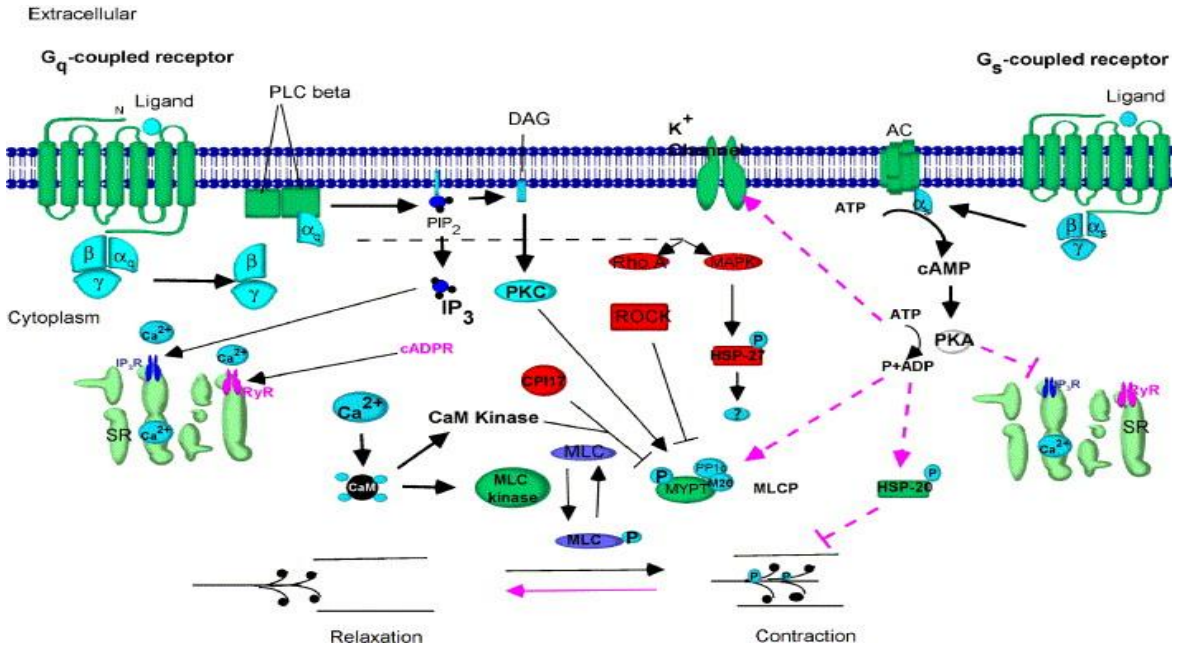

Figure 1.8 Binding of a ligand such as bradykinin to a $G\alpha_q$ coupled GPCR causes hydrolysis of membrane phospholipid PIP_2 by $G\alpha_q$ sensitive PLC, generating IP_3 which causes release of free Ca^{2+} from SR stores at IP_3Rs. Ca^{2+} then binds to CaM activating MLCK which phosphorylates MLC initiating the hASM actin-myosin sliding filament contraction mechanism. An inhibitory counterbalance pathway also exists, whereby a ligand such as epinephrine binds to a $G\alpha_s$ coupled GPCR , which activates adenylyl cyclase to dephosphorylate ATP to cAMP whence cAMP sensitive PKA blocks IP_3Rs by phosphorylation and phosphorylates other targets, thus relaxing the hASM actin-myosin apparatus. Reprinted with permission,

Deshpande A., Penn R.B. (2006) Targeting G protein-coupled receptor signaling in asthma, Cellular Signaling, 18(12), pp. 2105-2120.

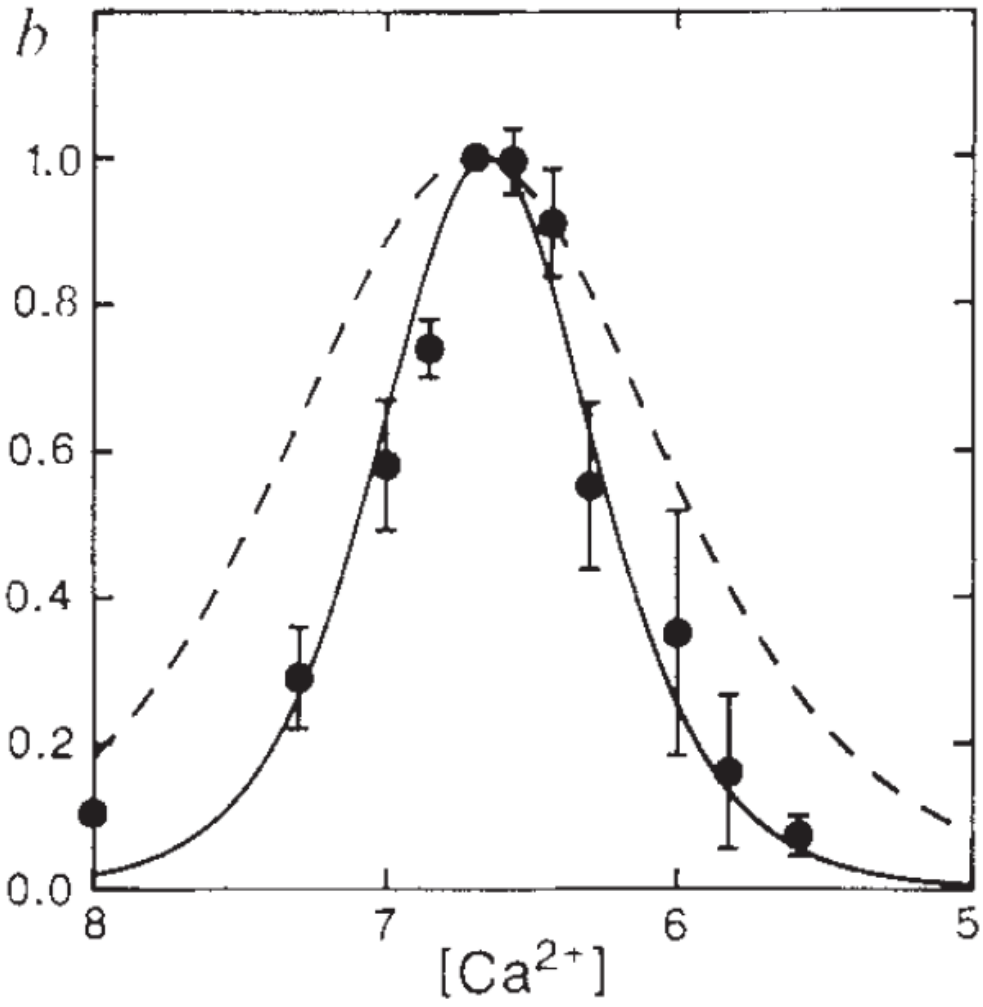

Figure 1.9 The probability of IP_3-induced IP_3R calcium ion channel opening (normalised y-axis) varies with free [Ca^{2+}] following a bell-shaped characteristic. At rest, i.e. low [Ca^{2+}], the IP_3R calcium ion channel is essentially closed, maximal release occurs between 0.01 and 0.3μM free [Ca^{2+}], and is inhibited by higher [Ca^{2+}]. This is a leveraged system because a low [Ca^{2+}] can control a much larger [Ca^{2+}] change by a feed-forward type mechanism. Reprinted with permission,

Bezprozvanny, I, Watras, J, Ehrlich, BE (1991) Bell-shaped calcium-response curves of Ins(1,4,5)P3- and calcium-gated channels from endoplasmic reticulum of cerebellum. Nature 351(6329): 751-754.

IP_3Rs are not only regulated by Ca^{2+} ions and IP_3 but a raft of accessory proteins that modulate $[Ca^{2+}]_i$ release. In pathological states IP_3R dysregulation can give rise to spontaneous $[Ca^{2+}]_i$ oscillations (Choe *et al.*, 2006). Furthermore, the nature of IP_3-dependent $[Ca^{2+}]_i$ oscillations depends upon the relative proportions of the three IP_3R subtypes present and their functional interactions (Ramos-Franco *et al.*, 1998; Miyakawa *et al.*, 1999). Spontaneous $[Ca^{2+}]_i$ oscillations are not just IP_3 dependent but can be generated by other mechanisms that have oscillatory characteristics, such as the RyR (Prakash *et al.*, 1997) and in particular subtype 3 (Dabertrand *et al.*, 2008).

1.5.2 Store operated Ca^{2+} entry

Ca^{2+} entry upon SR Ca^{2+}-store depletion is called capacitative or store operated calcium entry (SOCE). It is also referred to as I_{CRAC} (CRAC = calcium release activated current), a highly specific inward Ca^{2+} current. As the SR Ca^{2+}-store becomes depleted, the $[Ca^{2+}]$ decrease is sensed by the EF-hand domain of STIM1. This protein then translocates through the SR membrane until it is near the plasma membrane. It then stimulates, via mechanical coiled-coil interactions (Figure 1.10), formation of a highly Ca^{2+} selective plasma membrane Ca^{2+} channel composed of ORAI1 tetramers. It may act in association with other ion channel proteins such as transient receptor potential (TRP) channels, with subsequent influx of Ca^{2+} ions into the cytoplasm (Marthan, 2004; Putney *et al.*, 2008). Ca^{2+} fluxes into the cell and fills the SR Ca^{2+}-store via the action of SERCA active transport pumps.

It should be noted that STIM1 is a single transmembrane protein that does not form a channel, in this scenario it acts as a low $[Ca^{2+}]$ sensor in the SR lumen. It is thought that the repetitive nature of $[Ca^{2+}]_i$ oscillations is based upon the SOCE mechanism. Whereby Ca^{2+} release and re-uptake into the SR occurs and SOCE induced Ca^{2+} entry

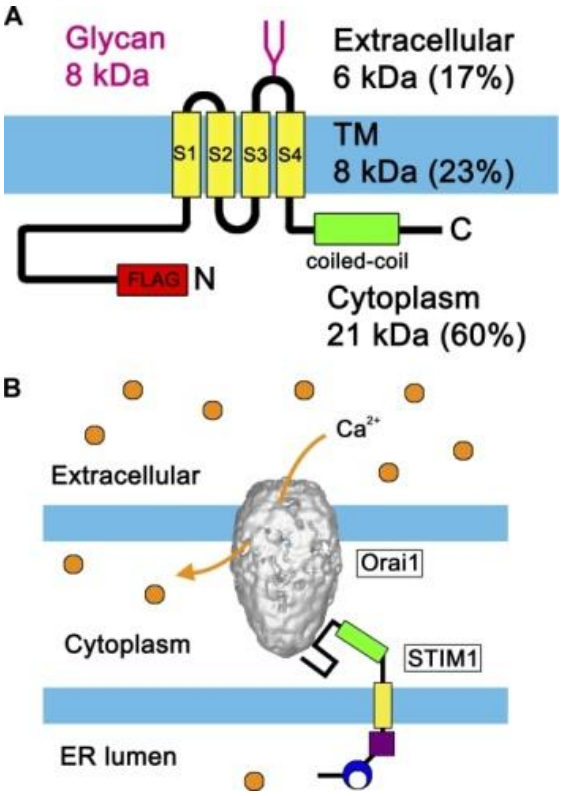

Figure 1.10 a) Tetrameric structure of the plasma membrane bound ORAI1 selective Ca^{2+} ion channel showing a coiled-coil coupling domain in green.

b) Coupling between single transmembrane protein STIM1 (stromal interaction molecule 1) in the ER/SR membrane and the extended 'teardrop shaped' cytoplasmic region of ORAI1, induces an inward selective Ca^{2+} ion current via a conformational change in ORAI1. Protein-protein interaction is believed to be via mechanical coupling between the two coiled–coil domains.

Reprinted with permission,

Maruyama Y., Ogura T., Mio K., Kato K., Kaneko T., Kiyonaka S., Mori Y., Sato C. (2009) Tetrameric Orai1 Is a Teardrop-shaped Molecule with a Long, Tapered Cytoplasmic Domain, J Biol Chem., vol. 284(20), pp. 13676–1368

across the plasma membrane tops up the SR ensuring the maintenance of the $[Ca^{2+}]_i$ oscillations (Sneyd *et al.*, 2004; Putney *et al.*, 2008). Interestingly, Ca^{2+} influx need not be dependent upon the STIM1/ORAI1 SOCE paradigm but Ca^{2+} ion selective TRP channels can also regulate IP_3R dependent $[Ca^{2+}]_i$ oscillations (Bradley *et al.*, 2005; Xing *et al.*, 2008).

1.5.3 Voltage operated Ca^{2+} ion channels

Other Ca^{2+} entry pathways present particularly in vascular and cardiac smooth muscle cell types depend upon Ca^{2+} channel depolarisation. Thus vasoconstrictors act to depolarise L-type voltage operated calcium channels (VOCC). Via a generated action potential (AP) in cardiac cells but by a graded non-AP mediated process allowing a slower, hence graded, Ca^{2+} influx into vascular cells. Also, plasma membrane second messenger operated channels, which can be activated by DAG and pass Ca^{2+} and Na^{+} ions, may contribute to depolarisation in cardiovascular smooth muscle cells. However, these pathways of Ca^{2+} entry appear not to be of primary importance in non-excitable hASM cells. Indeed VOCC antagonists verapamil or nifedipine whilst being efficacious vasodilators and antiarrhythmics in cardiac medicine have no reported clinical efficacy in respiratory conditions such as asthma.

1.5.4 Excitation – contraction

It is the variable properties of $[Ca^{2+}]_i$ oscillations and waves that are the prime movers driving the cause-effect mechanisms of hASM cell excitation-contraction (Sanderson *et al.*, 2008) and excitation-transcription (Morales *et al.*, 2007) coupling in hASM cells. Clearly, the information carried by a single $[Ca^{2+}]_i$ spike or transient will be different to that of a series of transients. And the subsequent effects on Ca^{2+} signalsome proteins such as the calcium-dependent proteins calmodulin (CaM) and myosin light-chain

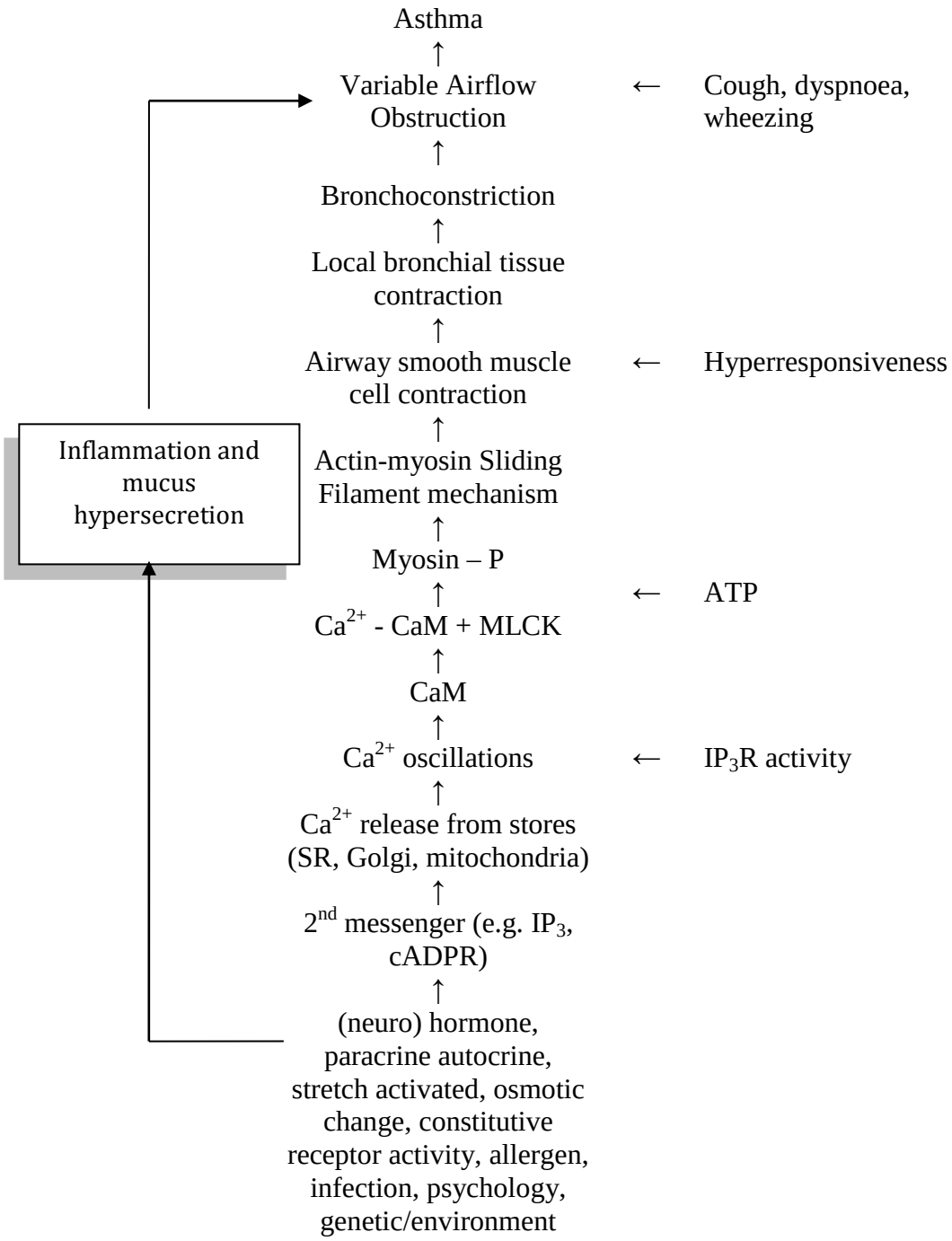

Figure 1.11 Pathway to asthma emphasising the events that lead to bronchonconstriction.

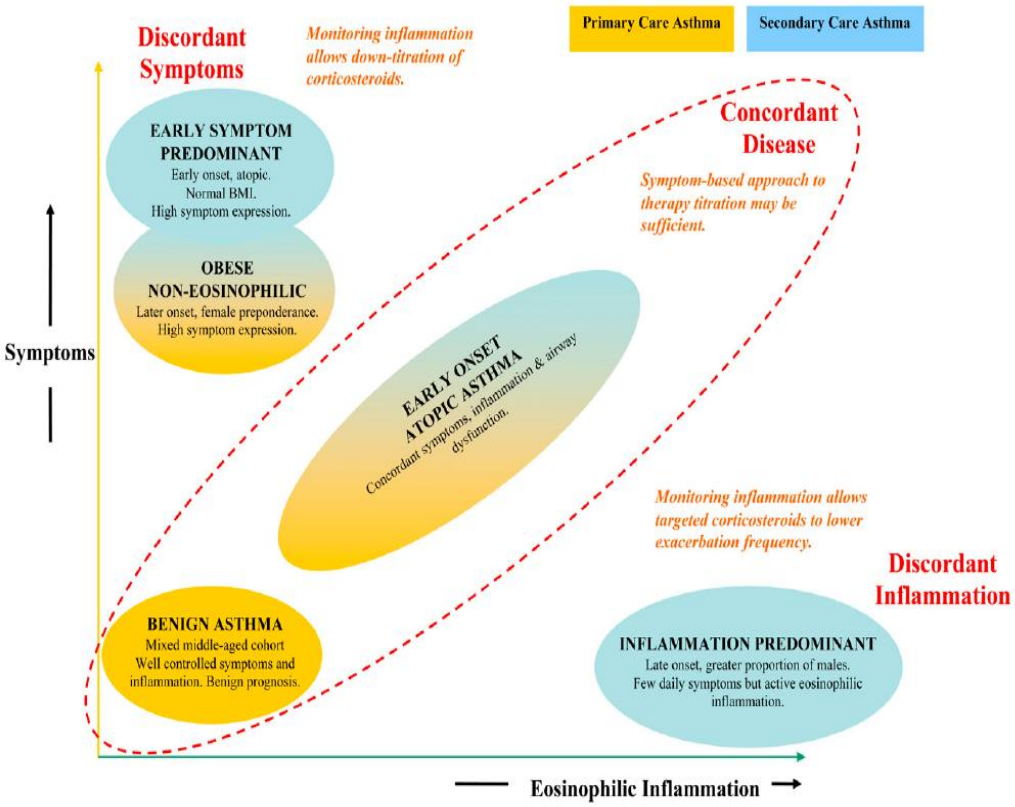

Figure 1.12 By plotting symptoms as a function of eosinophilic inflammation in relative terms, cluster analysis of primary and secondary care asthma cohorts highlight the heterogeneity of the asthma syndrome and identifies particular multidimensional clinical phenotypes. Some clusters show symptom and inflammation dependence (concordant disease) whereas others are relatively independent of eosinophilic inflammation or symptoms (discordant disease) and are more difficult to treat. The pathophysiological basis of this heterogeneity is currently not fully understood.

Reprinted with permission,

Haldar, P., et al. (2008). Cluster analysis and clinical asthma phenotypes. Am J Respir Crit Care Med 178(3): 218-24.

kinase (MLCK) will, in a cause-effect fashion, affect the degree of contraction of the hASM cell. For example the frequency of agonist induced $[Ca^{2+}]_i$ oscillations increases in a concentration dependent fashion (Perez *et al.*, 2005). The chain of effects set off by molecular changes external to the cell through second messenger mediated release of $[Ca^{2+}]_i$, actinomyosin sliding filament mechanism, finally giving rise to bronchoconstriction and asthma are shown in Figure 1.11. A further pathway which enhances bronchoconstriction is mediated by the small G-protein Rho kinase. It is thought to increase the Ca^{2+} sensitivity of the actin-myosin contractile apparatus, thus increasing the force of contraction for the same increase in $[Ca^{2+}]_i$.

Therefore, it is necessary to characterise the nature of basal $[Ca^{2+}]_i$ oscillations in asthma and normal hASM cells to determine whether there is a difference. If there is a significant difference, then what are the underlying structural and functional changes in the Ca^{2+} handling protein(s) that give rise to the differing calcium waveforms? Hence, answering this question logically, by applying molecular biology techniques of qPCR, western blotting, siRNA knockdown, protein over-expression and pharmacological inhibition, will identify what part of the $[Ca^{2+}]_i$ handling system that is causing the cellular pathology, in this case hyperreactive asthma hASM cell contraction. Ultimately, directed protein engineering by gene therapy vectors could be devised to correct the pathophysiology of bronchoconstriction in asthma.

1.6 Outline of project rationale

To recap, $[Ca^{2+}]_i$ oscillations are controlled by Ca^{2+} influx through the plasma membrane, a process called store operated calcium entry (SOCE), although the precise mechanisms involved are not fully known (Sneyd *et al.*, 2004). And it is thought that $[Ca^{2+}]_i$ oscillations are generated and further regulated by a process of calcium induced

calcium release (CICR) via inositol 1,4,5-trisphosphate receptors (IP_3R) and ryanodine receptors (RyR) in the membrane of the sarcoplasmic reticulum (SR) Ca^{2+} store (Berridge, 1993). An example of feedback regulation that takes the form of a bell-shaped response: released Ca^{2+} ions causing an additional release which in turn leads to negative feedback whence the oscillation resets to basal $[Ca^{2+}]_i$ (Bezprozvanny *et al.*, 1991). Hence, the encoding of signaling information carried by the $[Ca^{2+}]_i$ waveform may be related to the relative expression and/or sub-cellular organisation of these receptor operated Ca^{2+} ion channels (Miyakawa *et al.*, 1999). Interestingly, $[Ca^{2+}]_i$ oscillations with different characteristics from normal would be expected to change $[Ca^{2+}]_i$ oscillation driven gene transcription, generating a different expression set of Ca^{2+} handling proteins, thereby sustaining the abnormal $[Ca^{2+}]_i$ oscillations. The result gives rise to pathopysiological properties such as hASM bronchoconstriction, hypertrophy and hyperplasia and/or a reduced apoptosis rate.

With reference to hASM cells, the molecular basis of agonist/inflammatory mediator induced bronchoconstriction essentially pivots around increases in $[Ca^{2+}]_i$ initiated by increases in activity of the downstream set of molecular events that lead to contraction. Upregulation or increased activity of any of these downstream molecular players would turn normal physiological basal hASM tone into pathological bronchoconstriction (Figure 1.1). Indeed even GPCR splice variants exist in hASM cells (Einstein *et al.*, 2008) that may give rise to abnormal responses in asthmatics after ligand binding. Hence, assessment of the second messenger IP_3 generation and $[Ca^{2+}]_i$ release and recovery by an agonist, such as bradykinin, would show if there is a difference in $[Ca^{2+}]_i$ handling between asthma and normal hASM cells.

Local acute attacks of bronchoconstriction can in most cases be successfully treated, however if untreated or treatment is ineffective, after a certain point it becomes an

irreversible chronic condition exacerbated by progressive inflammation. Inflammation and bronchoconstriction are the major stalwarts of asthma and, in a 'chicken and egg scenario,' it is not clear which came first. Therefore, the focus is upon isolated *passaged* hASM cells from asthma and normal donors. A hypothesis can then be raised to ask whether, 'hASM cell $[Ca^{2+}]_i$ homeostasis and handling is intrinsically different in asthma compared to normal donors?' Hence, in this scenario, a pathological change to Ca^{2+} signaling, such as spontaneous $[Ca^{2+}]_i$ oscillations, would suggest a *non-inflammation* based link between hASM cell Ca^{2+} dynamics and AHR in asthma. It is therefore important to characterise the nature of the hASM cell $[Ca^{2+}]_i$ waveforms in order to understand the nature of $[Ca^{2+}]_i$ dynamics in health and disease.

There are many upstream aetiologies that may singly or acting synergistically trigger an asthmatic response. This is consistent with the definition of a syndrome. It is important to realise that clinical characteristics of obstructive respiratory diseases, labelled as asthma or COPD etc., are not single isolated entities but form a continuous spectrum. Figure 1.12 shows how multidimensional clinical phenotypes of asthma can be resolved when symptoms are plotted as a function of eosinophilic inflammation (Haldar *et al.*, 2008). This graphically shows for both atopic and non-atopic forms how different and sometimes overlapping clinical phenotypes contribute to the heterogeneity of the term 'asthma'. With some phenotypes characteristic of mild to moderate asthma that have traditionally been recognised and treated by symptom led titration of corticosteroid dose, showing a direct dependence of symptoms with eosinophilic inflammation. Whereas other less well controlled phenotypes characteristic of severe asthma are relatively independent of either symptoms or eosinophilic inflammation. In these, careful monitoring of eosinophilic inflammation is required to make sure corticosteroids are not over-prescribed in symptom predominant phenotypes and under-prescribed in

inflammation predominant phenotypes. Also individuals can move from one cluster or phenotype to another over time as the progression of the disease and its treatment changes.

So in a complex multidimensional system which has multiple interacting causes and complex cumulative immunologically driven effector responses, it would seem sensible to remove one of the major components of the disease manifestation, hASM cells. Then to investigate whether they are intrinsically altered in terms of $[Ca^{2+}]_i$ homeostasis and handling in asthma compared normal donors. Or, indeed whether changes to $[Ca^{2+}]_i$ are a phenotypic consequence of the inflammatory environment of the asthmatic lung, which is not included in the terms of reference of this project.

Fundamentally, at the end of the day, the common downstream link which allows hASM cells to become pathological effectors in terms of bronchoconstriction would be reflected in altered $[Ca^{2+}]_i$ regulation. This then is the focus of my PhD project and of this thesis.

1.7 Hypothesis

The dynamics of $[Ca^{2+}]_i$ homeostasis and handling is intrinsically altered in passaged hASM cells from asthma compared to normal donors.

1.7.1 Aims

1) To characterize $[Ca^{2+}]_i$ homeostasis by determination of the frequency and amplitude of $[Ca^{2+}]_i$ oscillations in quiescent isolated hASM cells from asthma and normal donors.
2) To characterize $[Ca^{2+}]_i$ handling by monitoring exponential decay rate kinetics after receptor dependent (agonist) and receptor-independent (Ca^{2+} uncaging) mechanisms to rapidly increase $[Ca^{2+}]_i$, in hASM cells from asthma and normal donors.
3) To determine if agonist generated second messenger, IP_3, is altered in asthma compared to normal hASM cells.
4) To establish if $[Ca^{2+}]_i$ homeostasis and handling is altered in asthma and normal hASM cells and whether there is a correlation with clinical biomarkers of lung function, principally FEV_1 and FEV_1/FVC.
5) If $[Ca^{2+}]_i$ homeostasis and handling is functionally dysregulated in asthma hASM cells, to identify the structural basis (gene and protein) for this change.

CHAPTER 2

MATERIALS AND METHODS

2.1 Materials

From Sigma-Aldrich, Poole, UK: Bradykinin acetate, Probenecid, Pluronic F-127, Cyclopiazonic acid, Caffeine. From Invitrogen, UK: Gibco cell culture medium and chemicals, Fura-2 AM, Fluo-4 AM, NP-EGTA AM. *Myo*-[^{3}H]-inositol 1,4,5-trisphosphate (20Ci/mol) Amersham Pharmacia, Bucks, UK. SERCA2 mouse monoclonal antibody, Abcam, UK. Real time PCR primers, Eurofins, UK.

2.2 Primary hASM cell culture

Human airway smooth muscle (hASM) bundles were isolated by microscopic dissection from bronchial biopsies and large airway tissue from surgical resections, with NHS Regional Ethics Committee approval. Explants were attached and grown in 6-well plates for up to 1 month. Primary hASM cells were sub-cultured *in vitro* using 75cm^2 flasks at 37°C in 5% CO_2-humidified air and characterised by flow cytometry as smooth muscle if >90% α-smooth muscle actin (α-SMA) was present. Cells were passaged a maximum of 4 times. Cell culture medium contained:- Dulbecco's modified Eagle's medium (DMEM) Glutamax-1 supplemented with 10% FBS, 100U/ml penicillin, 100µg/ml streptomycin, 0.25µg/ml amphotericin B, 100µM non-essential amino acids, and 1mM sodium pyruvate (Gibco, Invitrogen, UK).

2.3 Widefield epifluorescence microscopy

hASM cells sparsely grown for at least 48h on 25mm diameter borosilicate glass coverslips with thickness no. 1.5 (VWR international, UK) were loaded with 2μM of the cell permeant Ca^{2+}-sensitive fluorophore fura-2AM in the presence of 2.5mM probenecid and 0.04% w/v pluronic F127, at room temperature for 50min in HEPES-saline buffer solution containing: (in mM) 118.4 NaCl, 4.7 KCl, 2.0 $CaCl_2$, 1.2 $MgCl_2$, 11.1 glucose, 10 HEPES, pH 7.4. hASM cells were then washed in HEPES-saline buffer and left at room temperature for 20min for de-esterification of the AM ester bonds. The hASM cells were visualised on an inverted epifluorescence microscope (Nikon Diaphot 200) using a 40x oil immersion objective lens. The cells were alternately excited at 5Hz by monochromatic UV light at 340nm or 380nm generated by a SpectraMaster (Olympus, UK) fluorescence source with xenon lamp and filter system, switched electronically by computer controlled software (UltraView Imaging Suite version 4.0, Perkin Elmer, UK). Green fluorescence emission was collected at 525nm. The excitation light (340 and 380nm) was directed through the fluorescent objective onto the cells. The emitted fluorescence was transmitted back through the objective lens, through a dichroic mirror, captured and digitized using a charge coupled device (CCD) camera and displayed and analysed in the UltraView software. Changes in fura-2 fluorescence (F) intensity were measured as a ratio, R, where $R = F_{340}/F_{380}$ such that R increases as the $[Ca^{2+}]_i$ increases according to the equation first described by Grynkiewicz and colleagues (Grynkiewicz *et al.*, 1985). For each coverslip 5-10 cells, superfused with warmed HEPES-saline buffer at 37˚C, were monitored simultaneously and a fluorescence region of interest (ROI) area subsequently defined for each cell within the cytoplasm avoiding the nucleus.

2.3.1 Spectral analysis of temporal fluorescence waveforms

Briefly, fluorescence ratio, R, data taken from the Perkin-Elmer UltraView software for several cells was saved as an ascii text file. This was then imported into the main analysis program, *SpectralAnalysis.m*, which is a Matlab executable file. The program then displayed the first fluorescence waveform and its FFT from which the CODF is highlighted. The user can then step through each subsequent waveform, or cell, by pressing the 'next' button. Finally, the program stores the CODF data in an output text file which can be used to transfer data into Excel or Prism. Full instructions are presented in a file called *readme.txt* downloadable together with the Matlab spectral analysis program and a technical article describing the FFT method (Uhlen, 2004).

2.4 Ca^{2+} uncaging

hASM cells (approx. 10,000 cells) sparsely grown for at least 48h on 25mm diameter borosilicate glass coverslips (thickness No. 1.5; VWR international, UK) were co-loaded with 2μM fluo-4 AM and 2.5μM nitrophenyl-EGTA AM (NP-EGTA AM) (Invitrogen, UK) in the presence of 2.5mM probenecid and 0.04% pluronic F127, at room temperature for 50min in HEPES-saline buffer solution containing: (in mM) 118.4 NaCl, 4.7 KCl, 2.0 $CaCl_2$, 1.2 $MgCl_2$, 11.1 glucose, 10 HEPES, pH 7.4. Cells were then washed in HEPES-saline buffer and left at room temperature for 20min to allow de-esterification to occur.

Ca^{2+} transients were monitored using an Olympus confocal scanning laser inverted microscope (FV1000, Olympus, UK). A single scan head was used to monitor changes in $[Ca^{2+}]_i$ by detecting fluo-4 fluorescence with the 488nm line of a multi-line argon laser (~2% laser intensity) using "round-trip" mode, with emission occurring at around 512nm and a wide confocal aperture setting of 374μm. Near-instantaneous switching

allows uncaging, or photo-activation, with a 405nm laser flash without bleaching or response saturation, then automatic switch back to 488nm laser scanning to capture the subsequent $[Ca^{2+}]_i$ cellular recovery event. Intensity-time traces, with an image scan time interval of 32.77ms, extending over 26s were acquired with X60/1.2 NA oil-immersion objective with 6X optical zoom. Uncaging pulses of the same intensity were delivered with the 405nm laser (100% laser intensity) for 300ms in "tornado" mode in a region of interest of diameter 15 pixels or 2µm, selected in the cytoplasm away from the nucleus. Each cell tested was only flashed once. On the microscope stage, coverslips were placed into a 1ml cell chamber of an open perfusion microincubator (PDMI-2, Harvard Apparatus, UK) where the temperature of the inflowing perfusate was maintained at 37°C by a temperature-regulated Peltier heat pump driven plate. Cells were perfused at a rate of 1.55ml/min with HEPES-saline and then HEPES-saline containing 10µM cyclopiazonic acid (CPA, Sigma-Aldrich, UK). Fluorescence intensity-time curves were analysed by non-linear exponential curve fitting, using GraphPad Prism 5.0 software, and a recovery rate K (s^{-1}) was determined for each trace. Figure 2.1 shows an uncaging event for a hASM cell and outlines the chemistry of Ca^{2+} ion uncaging. Mean K values were calculated for each donor/subject and comparison made between asthma and normal. Control experiments were performed with cells loaded with fluo-4 AM only (no NP-EGTA AM), to confirm that the 405nm flash *per se* does not cause an increase in $[Ca^{2+}]_i$.

a)

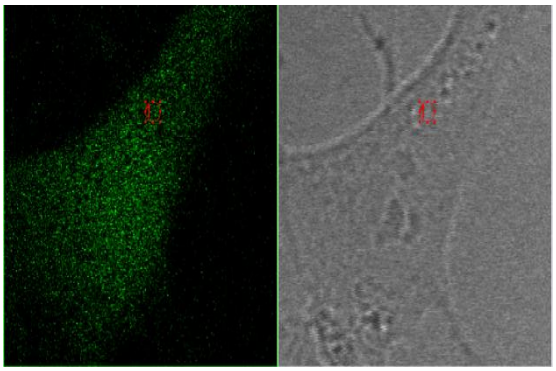

b)

Chemistry of Ca^{2+} uncaging by flash photolysis

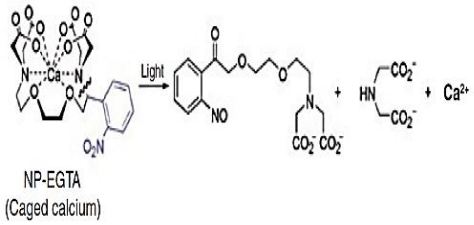

NP-EGTA
(Caged calcium)

c)

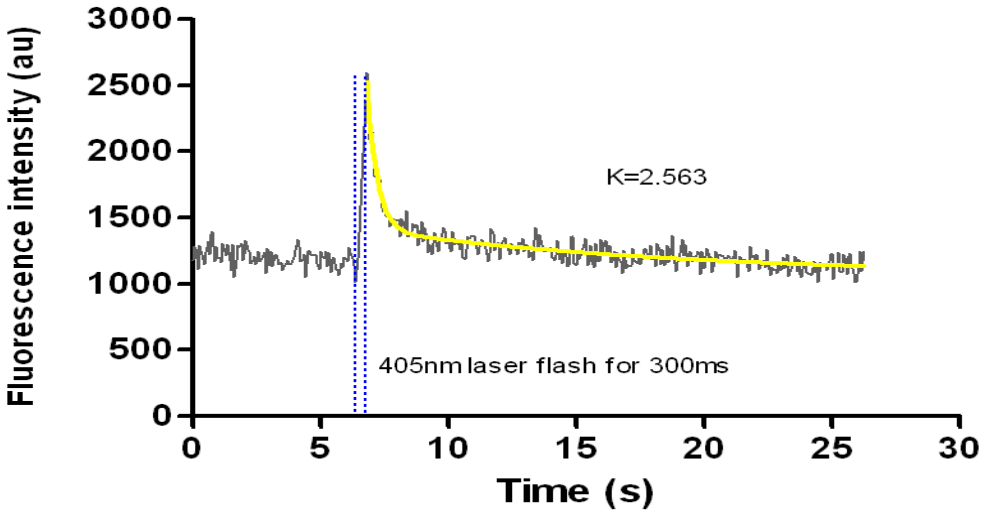

Figure 2.1 a) Confocal image (left) of a fluo-4AM loaded hASM cell and corresponding white light image (right) showing the circular region of interest (red) where laser uncaging was focused; b) Ca^{2+} ions are selectively sequestered in a NP-EGTA molecular 'cage', upon exposure to UV light the structure breaks up and releases its Ca^{2+} ion. A 12,500 fold decrease in affinity for Ca^{2+} (K_d increases from 80nM to >1mM) occurs with high photochemical quantum yield of approx 0.2; c) To determine if there is a difference in Ca^{2+} handling in hASM cells from asthmatic compared to normal donors, cytoplasmic Ca^{2+} uncaging was performed and the rate of Ca^{2+} recovery was monitored and a Ca^{2+} recovery rate constant (K [s^{-1}]) was obtained. The intensity-time graph (grey line) shows the cellular recovery after Ca^{2+} ion uncaging with 405nm laser light (within the blue dotted lines). The yellow line shows the exponential curve fit and thence the overall recovery rate constant, K, is obtained.

2.5 Bradykinin-stimulated $[Ca^{2+}]_i$ release

The nonapeptide bradykinin was chosen as it generates a reliable and robust $[Ca^{2+}]_i$ response in >95% of low passage asthma and normal hASM cells and is present in asthma as an inflammatory mediator. I chose a concentration of bradykinin (1μM) to robustly increase cytoplasmic $[Ca^{2+}]_i$ and challenge the cellular homeostatic system to accentuate any Ca^{2+} restorative differences between asthmatic and normal hASM cells. A lower agonist concentration would have yielded smaller cellular $[Ca^{2+}]_i$ responses thereby biasing response variability and potentially confounding the results. The aim is to create conditions whereby there is a high probability of uncovering an abnormality in the handling of a reproducible $[Ca^{2+}]_i$ release. Changes in $[Ca^{2+}]_i$ were monitored via changes in fluorescence ratio, R ($R = F_{340}/F_{380}$), of fura-2AM loaded hASM cells. An epifluorescence wide-field inverted microscope and digital recording software were used to capture the changes in R as per section 2.3. The displacement from baseline to peak fluorescence ratio value (ΔR), the area under the curve (AUC) during the 60s drug application window, and the $[Ca^{2+}]_i$ exponential decay rate (K) using non-linear exponential decay curve fitting, were all computed starting at the peak of the $[Ca^{2+}]_i$ response using Graphpad Prism 5.0.

2.6 IP_3 mass assay

IP_3 generated in hASM cells by agonists, such as bradykinin, can be measured using a competitive radioligand binding assay (Challiss *et al.*, 1988). Briefly, a standard curve is generated of $[^3H]IP_3$ bound to a bovine adrenal gland-derived IP_3 binding protein (primarily IP_3R2) in the presence of increasing concentrations of unlabelled IP_3. The IP_3 that is bound to IP_3Rs on the adrenal binding protein, whether it be unlabelled or labelled, is separated from the free, unbound, IP_3 by filtration through Whatman GF/B filters, which retain the bound IP_3 fraction (Challiss *et al.*, 1988). The filters are then

transferred into scintillation vials containing scintillation fluid. The vials are vortexed and the radioactivity counted (d.p.m.) in a scintillation counter. A protein assay is also performed to permit IP_3 levels to be expressed as pmol mg^{-1} of protein.

2.7 Store-operated Ca^{2+} entry (SOCE)

Widefield epifluorescence microscopy (section 2.3) was used to assess SOCE. A pictorial representation of the protocol is shown in Figure 4.30 derived from a published protocol (Bird *et al.*, 2008). After 60s in low-Ca^{2+} HEPES-saline buffer to decrease $[Ca^{2+}]_i$ levels with a presumed negligible effect on SR $[Ca^{2+}]$ levels, 10μM cyclopiazonic acid (CPA) in low Ca^{2+} HEPES-saline buffer was perfused over the cells for 8min. Over this time, SERCA had been inhibited and Ca^{2+} released from the SR Ca^{2+} stores via Ca^{2+} 'leak' channels and removed from the cell by various efflux mechanisms, such as the plasma membrane Ca^{2+} ATPase (PMCA), Na^+/Ca^{2+}-exchangers (NCX), etc. The peak-to-trough release, ΔR, value for Ca^{2+} store-emptying was noted. Then, 2mM Ca^{2+}-containing HEPES-saline buffer was re-perfused over the cells. Similarly, the store refilling peak-to-trough, ΔR, or SOCE value was noted.

2.8 Real time PCR

Reverse transcription real time PCR was used for relative quantification of mRNA expression of SERCA2abc in hASM cells from normal and asthma donors. Total cellular RNA was isolated from cultured hASM cells using Peq Gold total RNA kit (Peq Lab) and optional DNaseI treatment used according to manufacturer's instructions. RNA quality and quantity were assessed using a TECAN infinite NANO-QUANT plate reader (Tecan) and 1μg of total RNA from each hASM cell culture were reverse transcribed using SuperScript Vilo cDNA synthesis kit (Invitrogen). Amplification of 1ng of cDNA per reaction in a final volume of 20μl was performed using the Express

SYBR GreenER qPCR SuperMix Universal (Invitrogen) in a Chromo4 Real-Time Detector (Bio-Rad). After an initial incubation for 2 min at 50°C followed by 5 min at 95°C, the conditions of amplification were: denaturation at 95°C, annealing at 59°C, extension at 72°C for 37 cycles. All samples were tested in triplicate and 18S rRNA was used for normalisation. 18S rRNA was chosen for normalisation because it showed a very low variability of expression among the different donors and showed no significant difference of expression between asthma (average C_t value for all asthma donors was 10.44 ± SD 0.46) and normal (average C_t value for all normal donors was 10.40 ± SD 0.65) hASM cells. However, in general the choice of control gene can lead to uncertainty in results if it is not transcribed at constant levels. In such cases, it is common to choose up to six control genes for normalization. The sequences of the primers were as follows: for serca2abc, serca2abc7608F: CCTGTGCATGACTGATGTTG and serca2abc7808R: CAGAGCCTCATTCCTCTTGC; for the reference gene 18S rRNA, h18SRNA.891F: GTTGGTTTTCGGAACTGAGG and h18SRNA.1090R: GCATCGTTTATGGTCGGAAC. PCR efficiency was very close to the ideal 100% (Figure 2.2). The relative quantification was done using the comparative $2^{-\Delta\Delta Ct}$ method and expressed in arbitrary units.

a)

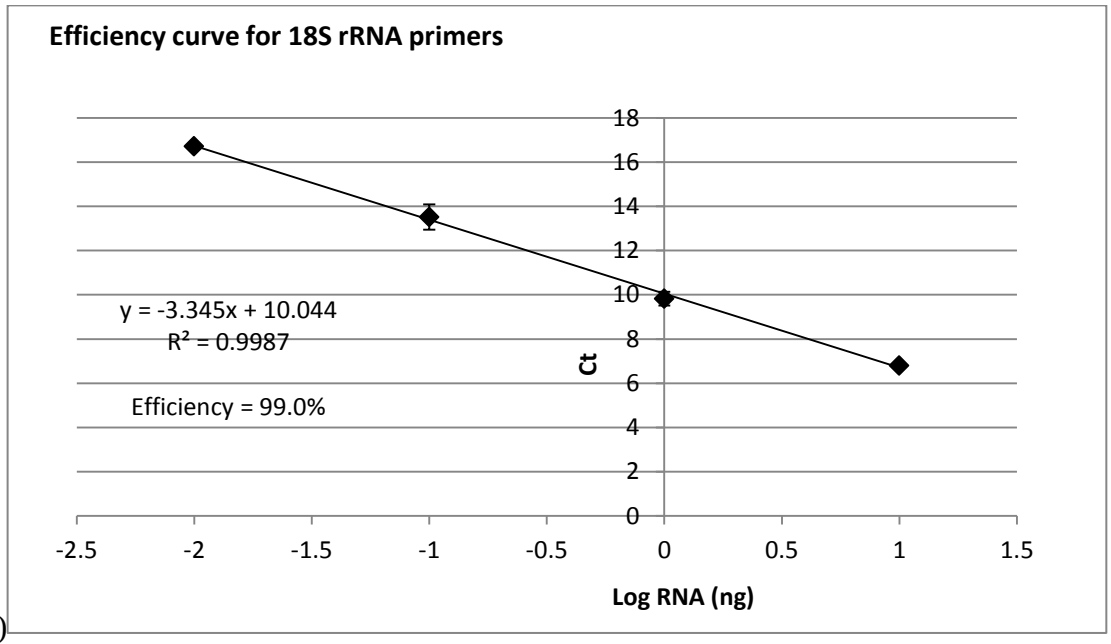

b)

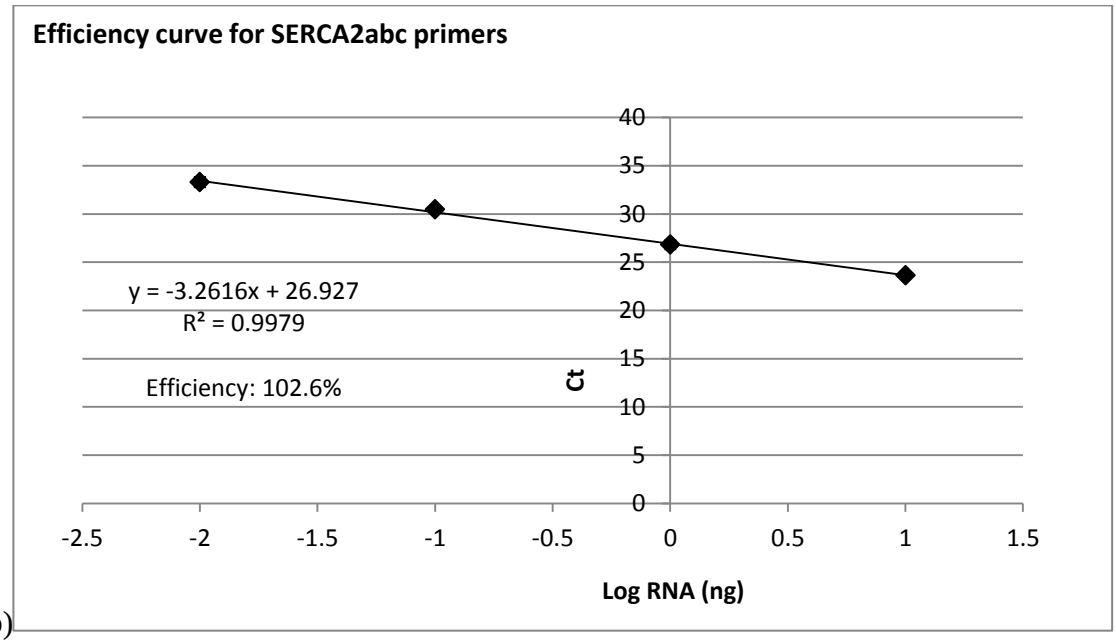

Figure 2.2 Standard curves obtained using a) 18S rRNA primers and b) SERCA2abc primers. For ten-fold dilutions in hASM cell RNA concentration, C_t decreases linearly, a) for 18S rRNA primers, PCR efficiency was 99% and, b) for SERCA2abc primers, PCR efficiency was 102.6%.

2.9 Western blotting

hASM cells from normal and asthma donors were grown to about 90% confluence. The cells were washed once with ice-cold PBS and then scraped into ice-cold lysis buffer containing 50mM Tris-HCl (pH 7.5), 1% Triton X-100, 10mM β-glycerophosphate, 1mM EDTA, 1mM EGTA, 1mM sodium orthovanadate, 1mM benzamidine HCl, 0.2mM phenylmethylsulfonyl fluoride, 1μg/ml each of leupeptin and pepstatin, 0.1% β-mercaptoethanol and 50mM sodium fluoride (Gomez *et al.*, 2008). The lysates were then centrifuged for 10min at 16000 x *g*. The supernatants were kept and total protein concentrations were determined by the Bradford assay (Bio-Rad) using bovine serum albumin to generate standard curves. SDS-PAGE and western blotting were performed; briefly, samples were subjected to electrophoresis on SDS polyacrylamide gels and gels were transferred to polyvinylidene fluoride membranes (Millipore). Mouse anti-SERCA2 (ab2817) antibody was purchased from Abcam and was detected using a horse anti-mouse IgG HRP-conjugated secondary antibody (Cell Signaling Technology). Mouse anti-actin antibody was purchased from Santa Cruz as a HRP conjugate. Detection was by enhanced chemiluminescence reagent (GE healthcare).

2.10 Statistical analysis

Raw data from hASM cells are expressed as mean ± s.d. and mean hASM cell donor values are expressed as mean ± s.e.m. Data were compared using Student's unpaired *t*-test, where the criterion for a significant difference was $P \leq 0.05$. The Pearson product-moment correlation coefficient, r, was used to test for correlation between two variables. Ca^{2+} handling decay rate constants, K, were derived by exponential non-linear regression. GraphPad Prism 5.0 was used throughout.

CHAPTER 3

INVESTIGATION OF $[Ca^{2+}]_i$ HOMEOSTASIS

3.1 Introduction

It is known that $[Ca^{2+}]_i$ signaling functions not merely by bulk increases and decreases in basal $[Ca^{2+}]_i$ but by repetitive or periodic $[Ca^{2+}]_i$ transients (Berridge *et al.*, 2003; Hirota *et al.*, 2007; Salazar *et al.*, 2008). If the transient generates a propagated disturbance starting from one particular point or region of the cell, a spatio-temporal disturbance or wave ensues. If the disturbance is fixed to a particular region of the cell, it is a temporal non-propagated disturbance called an oscillation. Hence, it is possible for a local oscillation, time varying, to give rise to a global wave, varying in time and space. Oscillations are akin to a ball bouncing on a spot, but when the player runs with the bouncing ball it describes a wave motion. To avoid confusion between these two terms I will henceforth refer simply to *oscillations* when discussing quiescent changes in basal $[Ca^{2+}]_i$, only referring specifically to a wave when regular distinct peaks are observed on a time varying fluorescence intensity waveform.

Moreover, these disturbances in $[Ca^{2+}]_i$ represent an amplitude and frequency encoded signal, transducing information that carries specific biological meaning (Dolmetsch *et al.*, 1997). Instructions conveyed by changes in $[Ca^{2+}]_i$ may lead to, for example, regulation of gene transcription, cytokinesis, secretion or contraction. It is the central hypothesis of this project that $[Ca^{2+}]_i$ homeostasis is intrinsically different in hASM cells from asthma sufferers compared to those from healthy or normal control donors. It would therefore seem sensible to begin by monitoring $[Ca^{2+}]_i$ changes in single quiescent live hASM cells from asthma and normal donors. Hence in the first instance,

whether there is a difference in the mean baseline or basal $[Ca^{2+}]_i$ level of hASM cells from asthmatic and normal donors must be determined, and then examination of $[Ca^{2+}]_i$ oscillation and wave phenomena will be investigated.

3.1.1 Spectral analysis of hASM cell $[Ca^{2+}]_i$ changes

An objective analysis of $[Ca^{2+}]_i$ waveforms from single hASM cells from asthma and normal donors was performed to capture essential characteristics for comparison. Since the pattern of any periodic waveform essentially consists of a series of spikes repeated over time, the most obvious characteristics to measure and compare are the frequency and amplitude. However, even if a biological system is generating regular $[Ca^{2+}]_i$ spontaneous waves with high signal to noise ratio, the inter-peak repetition time will not always be constant, and under most circumstances such waveforms are not seen. More commonly, monitoring will produce waveforms that are complex summations of individual cellular Ca^{2+} oscillation phenomena, a process called superposition. Indeed, it is thought that Ca^{2+} oscillations are generated by what is essentially stochastic single channel noise, where clusters of channels or microdomains form, they can generate deterministic Ca^{2+} signaling behaviour (Skupin *et al.*, 2010). Hence 'by eye' manual measurements made on a temporal waveform can only ever be erroneous and subjective. Therefore, analysis requires the convergence of biology with an objective mathematical modelling approach. In this case, a standard spectral analysis approach was adopted from the field of engineering.

In order to measure frequency it was recognised that each waveform is not a pure sinusoid with a single frequency, but a complex signal made up of many different frequencies. The Fast Fourier Transform (FFT) converts time domain signals into frequency domain spectra. It essentially resolves the component frequencies of the time

domain waveform. This technique was appropriate and public domain software and instructions had already been developed for use with $[Ca^{2+}]_i$ oscillation data using a Matlab platform (Uhlen, 2004). Analysis of $[Ca^{2+}]_i$ oscillation amplitude directly from the time domain waveforms was a simpler task that was accelerated using software in the public domain, another program written for Matlab called *Findpeaksliders* (O'Haver, 2009).

Figure 3.1 shows a $[Ca^{2+}]_i$ oscillation waveform obtained from an asthma hASM cell and shows how frequency and amplitude are defined. The change in amplitude is the difference between peak R and basal R values, i.e. ΔR. Frequency, with dimension s^{-1} and SI unit Hertz or Hz, is approximated by the reciprocal of the time between consecutive peaks and is of course precise for a pure sinusoid. Clearly, in the case of $[Ca^{2+}]_i$ oscillations from hASM cells an estimate of frequency using this technique would involve a significant degree of subjective error, and in many cases where repeated peaks are not obvious it would be entirely inappropriate.

Hence, in these waveforms the time between $[Ca^{2+}]_i$ peaks is not always consistent and in a complex waveform such as Figure 3.1 this is certainly the case.

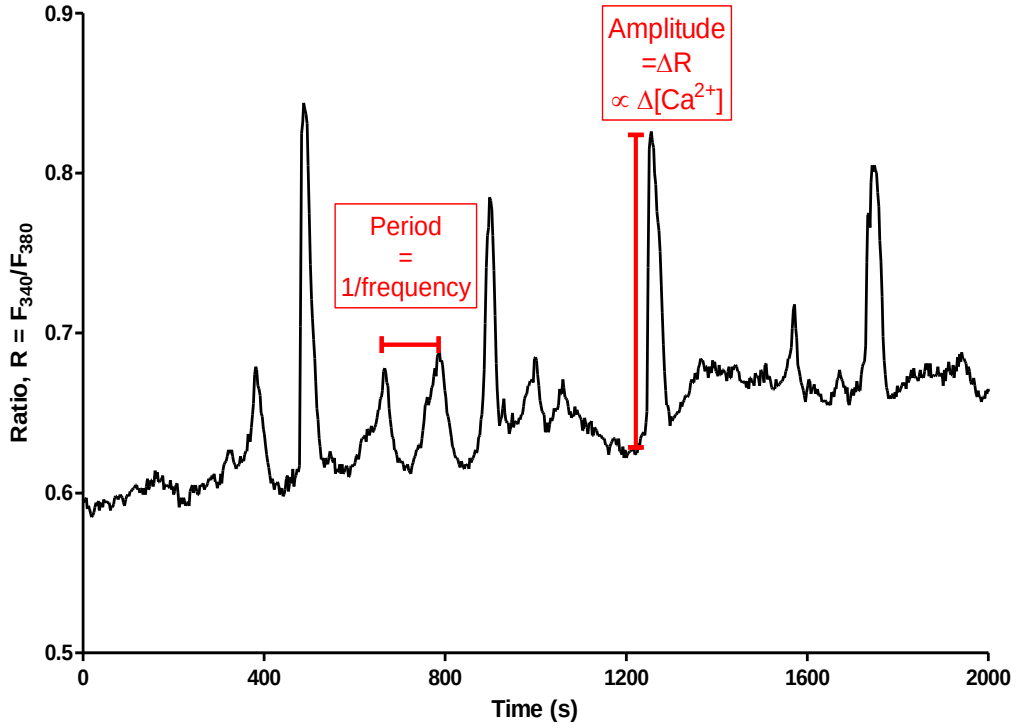

Figure 3.1 Both frequency and amplitude are parameters that can be measured from analysis of a time varying $[Ca^{2+}]_i$ oscillation waveform. For the monitoring system used, changes in fluorescence intensity, R, are proportional to changes in $[Ca^{2+}]_i$.

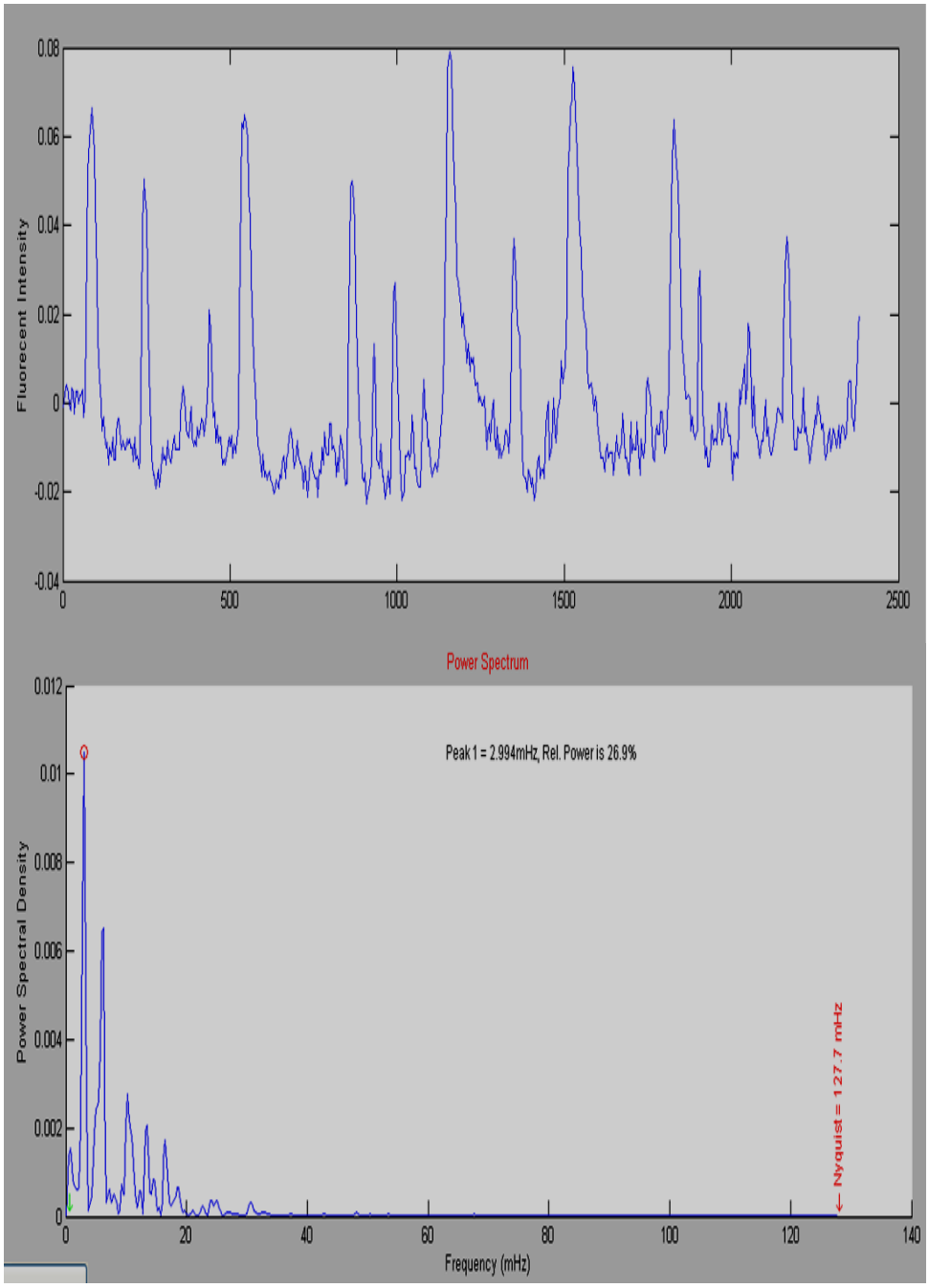

$[Ca^{2+}]_i$ oscillations, time series

FFT frequency spectrum

Figure 3.2 Frequency can be measured by transforming the time series fluorescence intensity data (upper graph) into a frequency spectrum (lower graph) using the FFT algorithm and noting the highest peak or calcium oscillation dominant frequency, CODF (mHz), identified here as the peak topped with a red circle. Source for public domain software and full operational instructions: *Uhlen, P (2004) Spectral analysis of calcium oscillations. Sci STKE, (258)**:** pl15.*

However, if a time domain waveform is transformed into a frequency domain spectrum, Figure 3.2, then it can be seen that the waveform consists of more than one frequency. The frequency spectrum clearly shows a frequency with the highest peak. I have called this the calcium oscillation dominant frequency, or CODF. CODF can be taken as a defining characteristic of the original time domain $[Ca^{2+}]_i$ waveform. The other frequency components in the FFT spectrum represent harmonics associated with the original waveform. Indeed the entire FFT frequency spectrum contains enough information to reconstruct the original time domain waveform. Interestingly, whole FFT spectra are used by intelligence agencies in computationally intensive comparative analysis routines to 'finger-print' waveforms from clandestine radio transmitters. However, it is sufficient to take the dominant frequency of each waveform as an accurate descriptor of $[Ca^{2+}]_i$ oscillation behaviour. Not surprisingly this type of analysis is called dominant frequency analysis. A good non-mathematical introduction is given in (Ng *et al.*, 2007) where the technique is applied to electrocardiogram waveforms derived from the electrical events of atrial fibrillation. The principle applies equally to $[Ca^{2+}]_i$ oscillation waveforms, indeed practically any time varying waveform could be analysed using this technique.

The Fourier transform is a mathematical modelling technique that takes a real world signal or waveform, such as a $[Ca^{2+}]_i$ oscillation time series, and transforms that waveform into a series of, theoretically infinite, sinusoidal functions that when added together reconstruct an accurate description of the original. Indeed the inverse FFT or IFFT transforms frequency spectra back to time domain waveforms. Of course the most accurate model would be obtained by using an infinite number of sinusoids, but that would be time consuming and is not necessary. The Fast Fourier Transform (FFT) can be limited to analyse the sinusoidal components of an input waveform by sampling

it at a set rate. Then, in near real time it displays the set of frequencies of those sinusoids on a plot of the power spectral density (PSD) against frequency, called a frequency power spectrum, or just power spectrum. This process is fast because it samples at a rate of twice the highest frequency of the bandwidth limited input waveform, a task suited to most modern personal computers. Therefore the problem of infinite series does not arise.

From this FFT derived power spectrum, it is readily possible to determine a dominant frequency based upon peak height. The classical basis of this technique was presented to the French Academy of Sciences by Joseph Fourier in 1822, and the FFT algorithm itself was published by J. W. Cooley and J. W. Tukey in a paper in 1965.

Essentially, the Fourier series combines a summation of cosine and sine functions in order to mathematically model a complex waveform, from this a spectrum of individual frequency components can be derived. The Fourier equation is a function of a single variable, x, which could be time or space. It is indeed a summation of sine and cosine functions with various constants as the following FFT equation shows,

$$f(x) = a_0 + \sum_{n=1}^{\infty} \left(a_n \cos \frac{n\pi x}{L} + b_n \sin \frac{n\pi x}{L} \right)$$

For illustrative purposes, Figure 3.3 shows how dominant frequency is visualized for regular and irregular ECG waveforms. For each of the time series waveforms in the top panels, below is the corresponding FFT power spectrum, the highest peak represents the dominant frequency. By analogy to $[Ca^{2+}]_i$ waveforms, sometimes a cell will display a fairly regular set of peaks, perhaps from a single FDS, whilst other cells will display a more complex less regular temporal waveform, with the complexity logically reflected in the corresponding FFT spectrum.

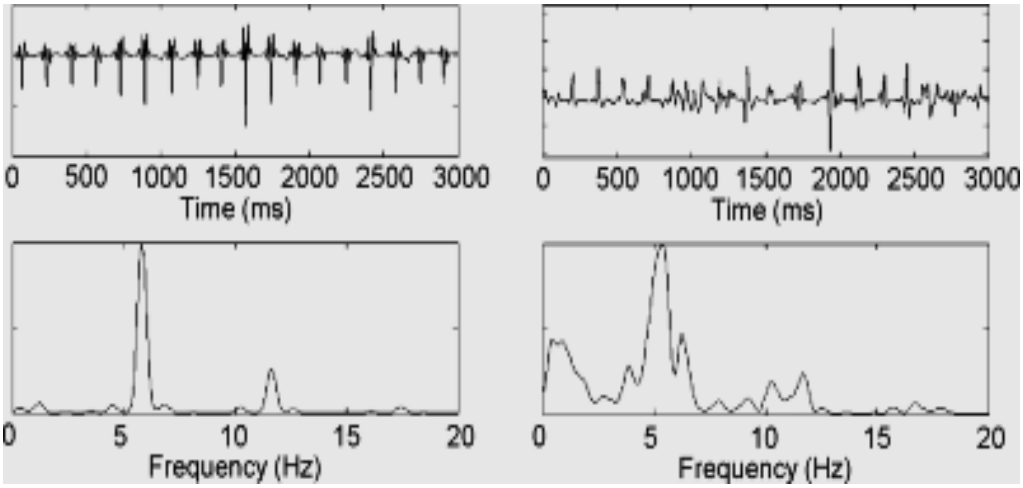

Figure 3.3 Two examples of cardiac electrograms and their corresponding power spectrum: one with very regular intervals and morphology and one with more irregular intervals and morphology. The signal on the left has 83% of the area of the power spectrum under the dominant frequency and its harmonics, whereas the signal on the right only has 49% of the area under the dominant frequency and its harmonics.

Reprinted with permission,

Ng J., Goldberger J,J. (2007) Understanding and Interpreting Dominant Frequency Analysis of AF Electrograms, Journal of Cardiovascular Electrophysiology, 18(6), pp.680-685.

Therefore, the CODF, which is the frequency with the highest peak PSD in the power spectrum, of each $[Ca^{2+}]_i$ waveform from each hASM cell, was recorded for hASM cells from normal and asthma donors.

3.2 Results

3.2.1 Baseline $[Ca^{2+}]_i$ levels

The ratio, R, of fura-2 fluorescence emission at 510nm when excited alternately at 340 and 380nm (F_{340}/F_{380}) at each sampling or exposure time of 200ms is proportional to $[Ca^{2+}]_i$. Without external drug stimulation, the resultant time dependent waveforms (Figure 3.4) are therefore a record of the quiescent basal changes in $[Ca^{2+}]_i$. Mean baseline R values for asthma and normal hASM cell donors were compared (Figure 3.5). This shows that under quiescent or homeostatic conditions, basal R-values and hence basal $[Ca^{2+}]_i$ were not significantly different in hASM cells from asthma compared to normal donors. Similarly, mean donor baseline R values did not correlate with airway physiology.

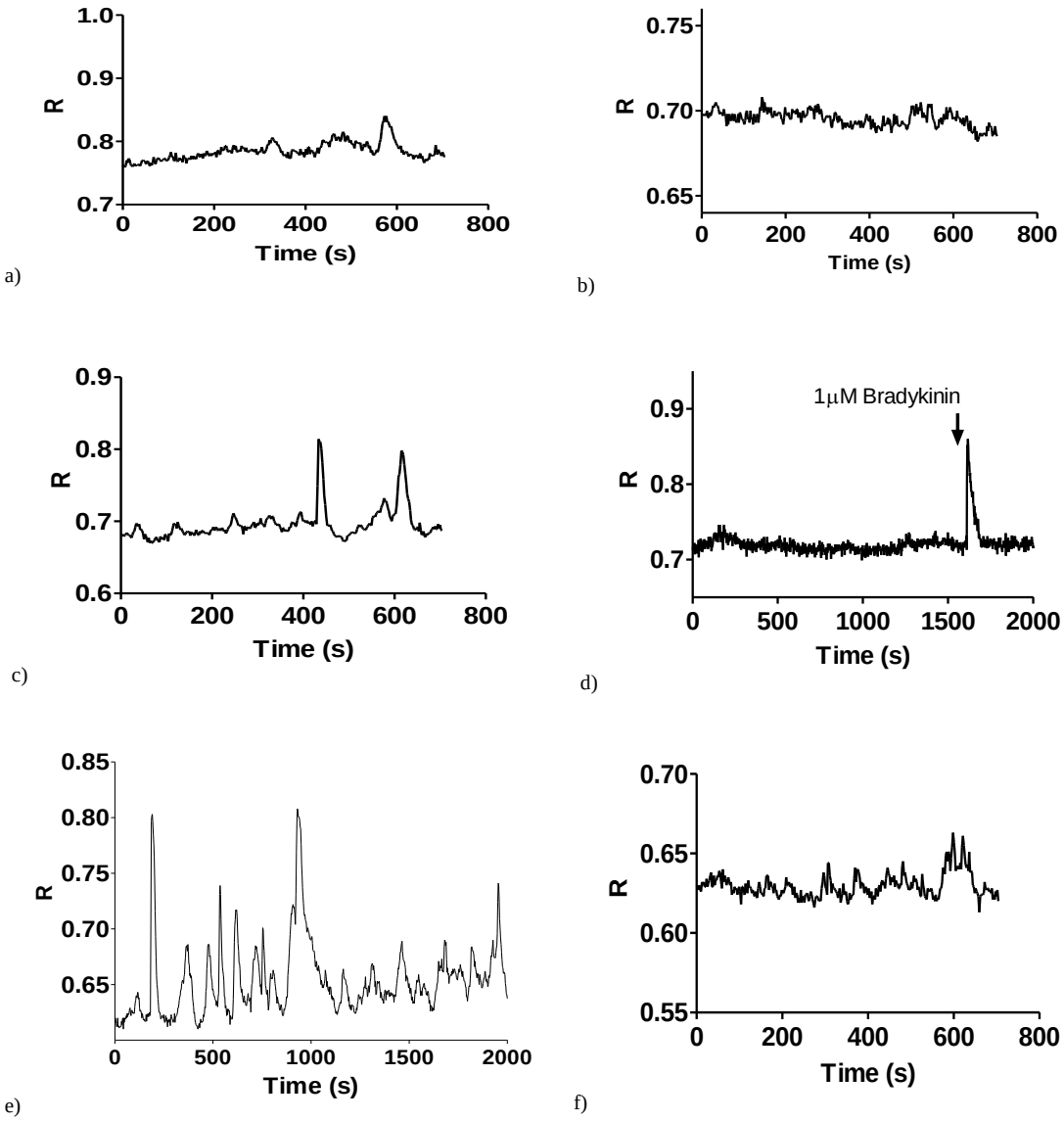

Figure 3.4 Examples of changes in fluorescence ratio ($R = F_{340}/F_{380}$) of fura-2 loaded hASM cells as a function of time. The ratio, R, is proportional to the change in intracellular calcium ion concentration, $[Ca^{2+}]_{i}$. Some cells display large repetitive spikes (for example waveform e), that are called call waves, whilst others are comparatively quiet and display occasional bursts of complex activity that are called oscillations (waveforms a, b, c, f). hASM cells that display $[Ca^{2+}]_i$ waves are considerably more rare than those that are quiet or show bursts of complex oscillations. Image d) shows a deliberate increase in $[Ca^{2+}]_i$, a positive control to demonstrate the ability of the cells to release Ca^{2+} ions, caused by application of agonist bradykinin.

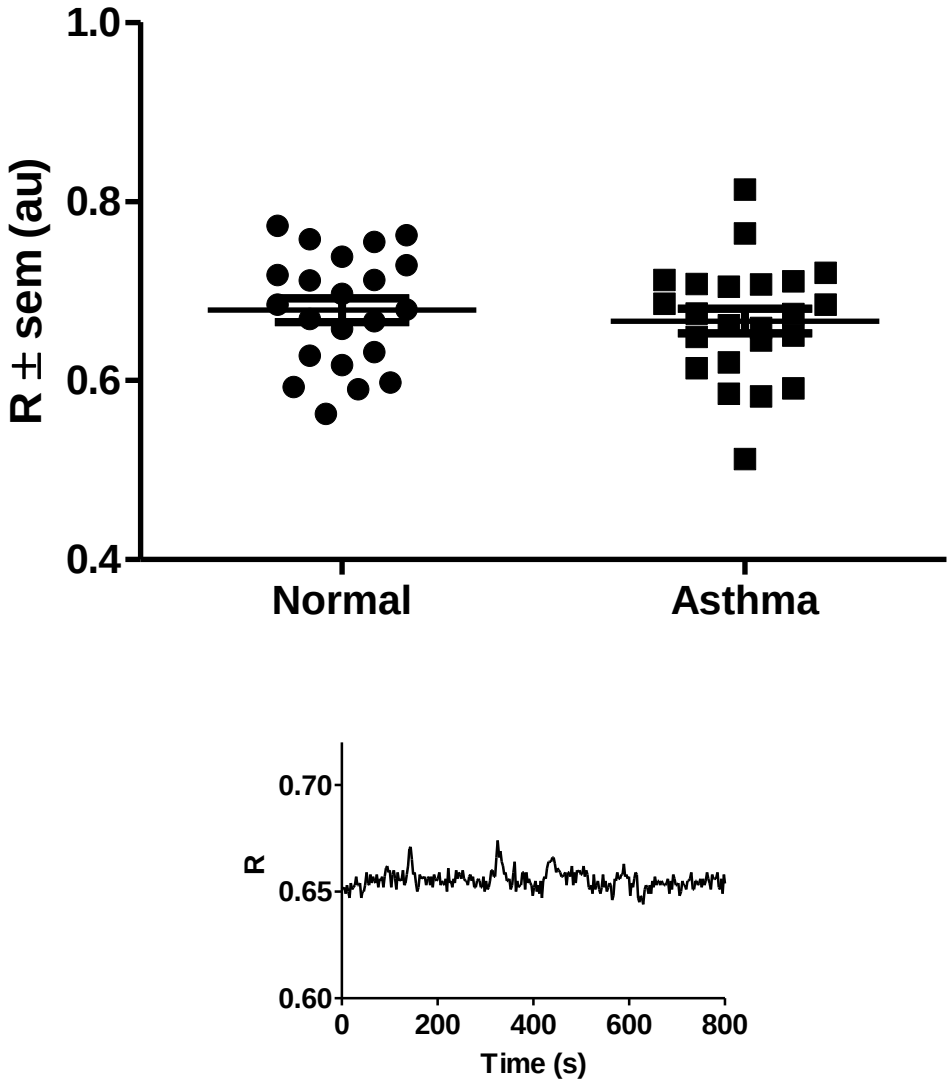

Figure 3.5 Comparison of basal or baseline mean R ± sem values for asthma (n=23) and normal (n=22) hASM cell donors show that there was no significant difference (Student's t-test) in basal $[Ca^{2+}]_i$. The lower pane shows a representative basal Ca^{2+} waveform.

3.2.2 $[Ca^{2+}]_i$ oscillations

The distribution of $[Ca^{2+}]_i$ oscillation frequency values based on dominant frequency analysis of $[Ca^{2+}]_i$ waveforms from single hASM cells was determined. Figure 3.6 shows that the distribution of calcium oscillation dominant frequency, CODF, for hASM cells is right skewed. This can be normalised by logarithmic transformation of CODF. Figure 3.7 shows that the normalised distribution of ln CODF is not significantly different between asthma and normal hASM cells. In addition to assessing the range of cellular CODFs, it is useful to group data from individual patients or donors to assess the variation of mean ln CODF with disease characteristics or phenotypes in individual asthma compared to normal hASM cell donors. Therefore, the mean ln CODF of hASM cells from asthma and normal donors was compared, and Figure 3.8 shows that there was no significant difference.

The distribution of $[Ca^{2+}]_i$ oscillation amplitudes, ΔR, for individual asthma and normal hASM cells similarly has a right skewed distribution (Figure 3.9) that can be normalised by logarithmic transformation (Figure 3.10). Again, there was no significant difference in mean ln $[Ca^{2+}]_i$ oscillation amplitude between asthma and normal hASM cell donors (Figure 3.11). Thus, as with the distributions of amplitude and frequency for individual cells, there was no significant difference between individual asthma and normal donors.

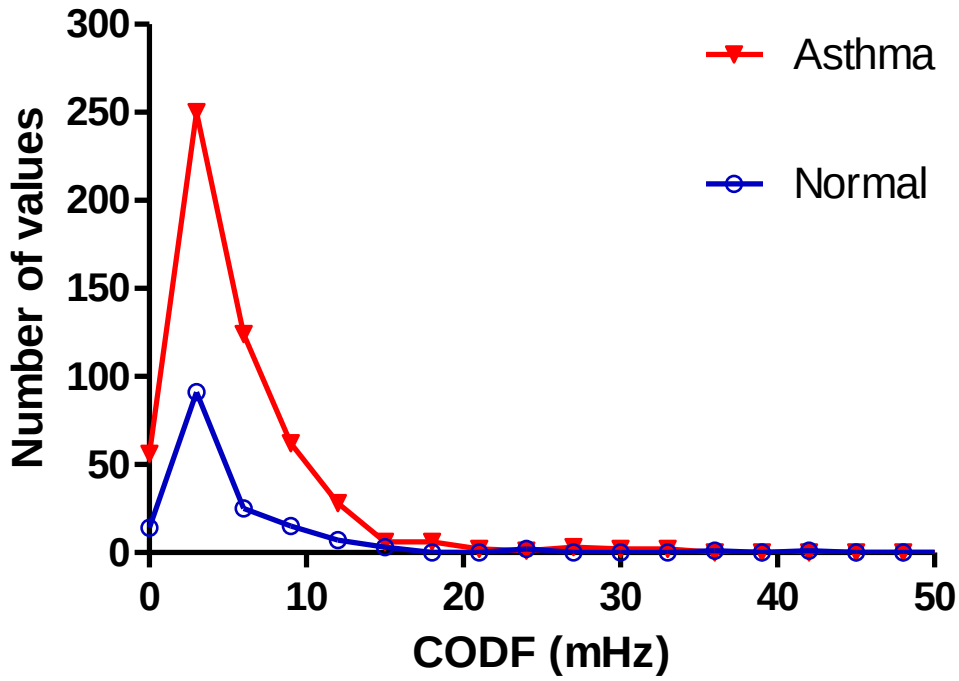

Figure 3.6 CODF for individual asthma (n = 708) and normal (n = 492) hASM cells belong to a right skewed distribution.

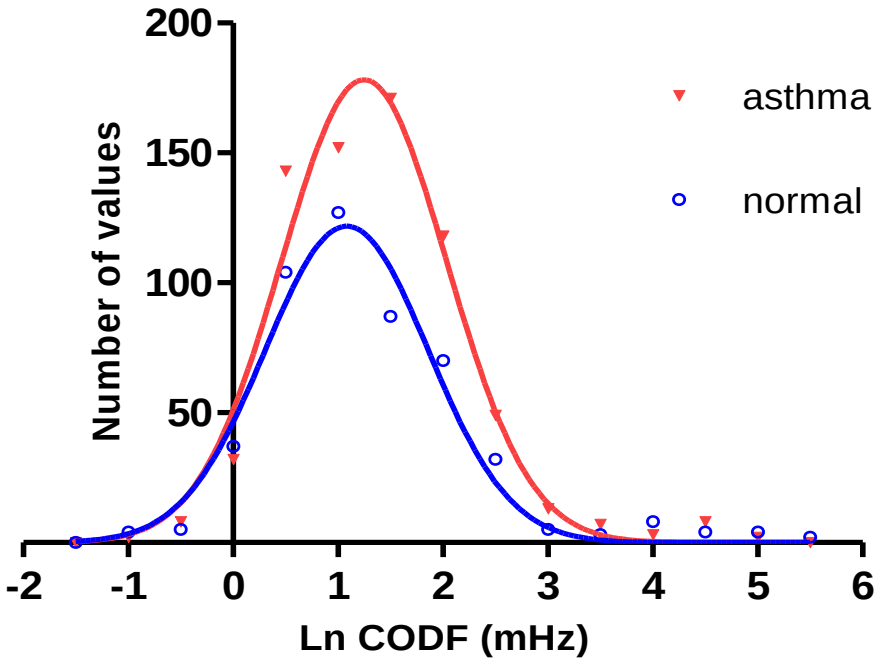

Figure 3.7 Distribution of dominant $[Ca^{2+}]_i$ oscillation frequency, CODF, for hASM cell temporal waveforms. Both asthma and normal populations have right skewed overlapping distributions that are normalized by logarithmic transformation, demonstrating that there was no significant difference (Student's t-test) between disease and health. Asthma n=708, normal n = 492 hASM cells analysed.

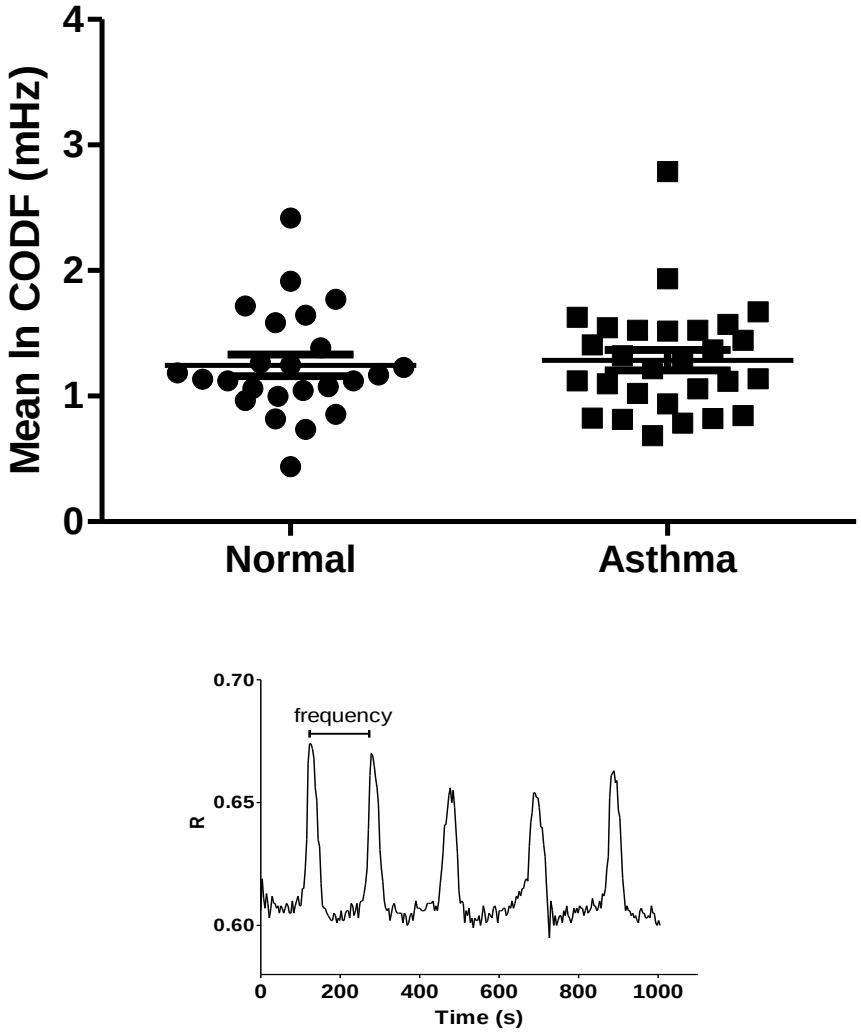

Figure 3.8 The mean dominant $[Ca^{2+}]_i$ oscillation frequency, mean ln CODF ± sem, was not significantly different (Student's t-test) in hASM cells from asthma (n=28) compared to normal (n=24) donors. The lower pane shows a representative Ca^{2+} waveform from which CODF was derived.

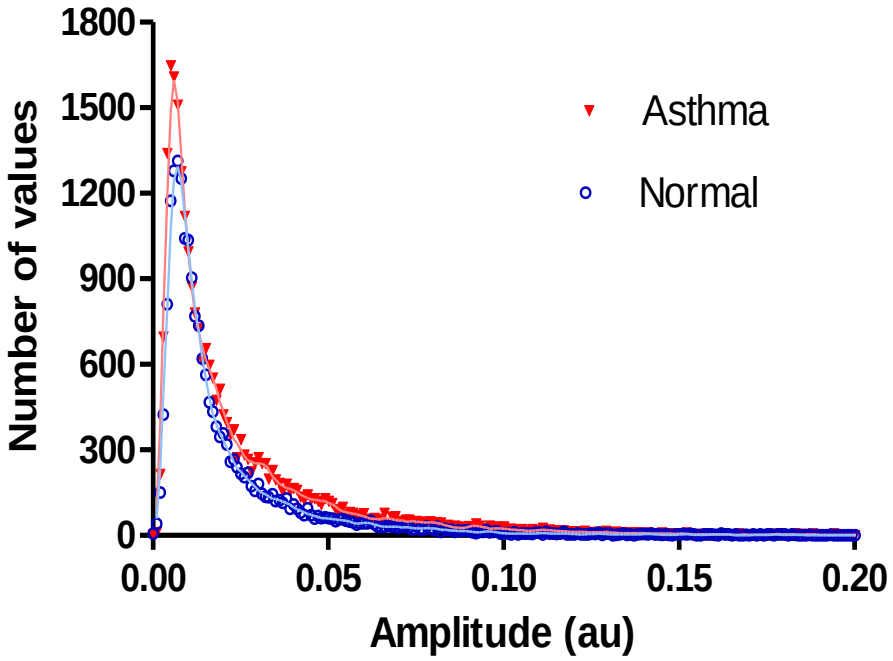

Figure 3.9 $[Ca^{2+}]_i$ oscillation amplitudes, ΔR, for individual asthma and normal hASM cells also belong to a right skewed distribution. Asthma n = 26338 Normal n = 20101.

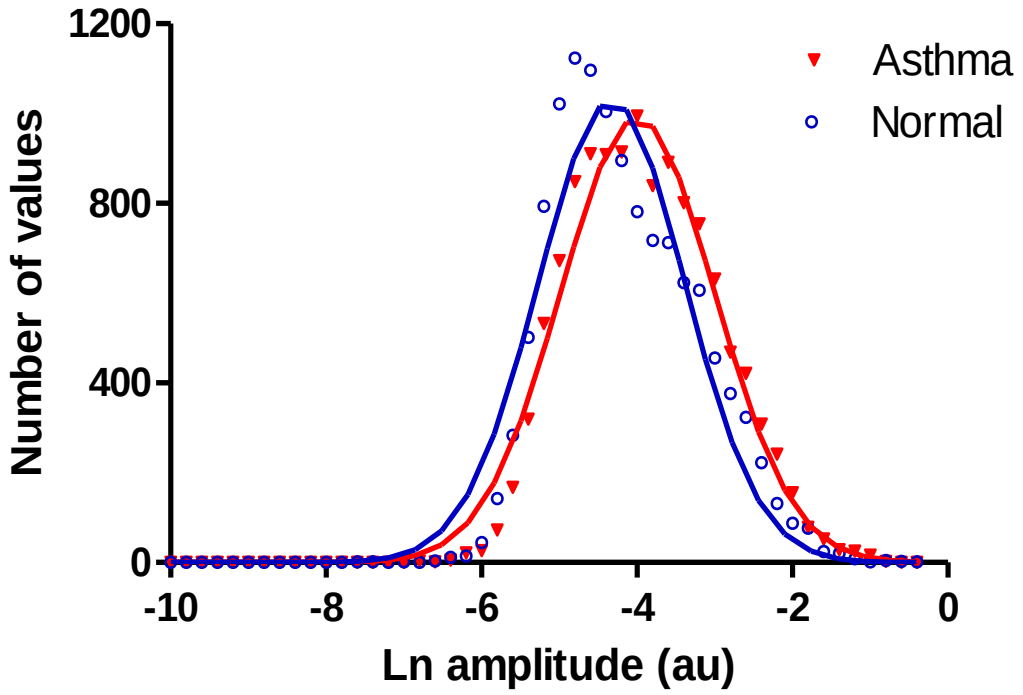

Figure 3.10 Logarithmic transformation of the $[Ca^{2+}]_i$ oscillation amplitude, ΔR, produces a more symmetric normal distribution. Nevertheless, there was no significant difference (Student's t-test) between asthma and normal hASM cells. Asthma n =26338, Normal n = 20101.

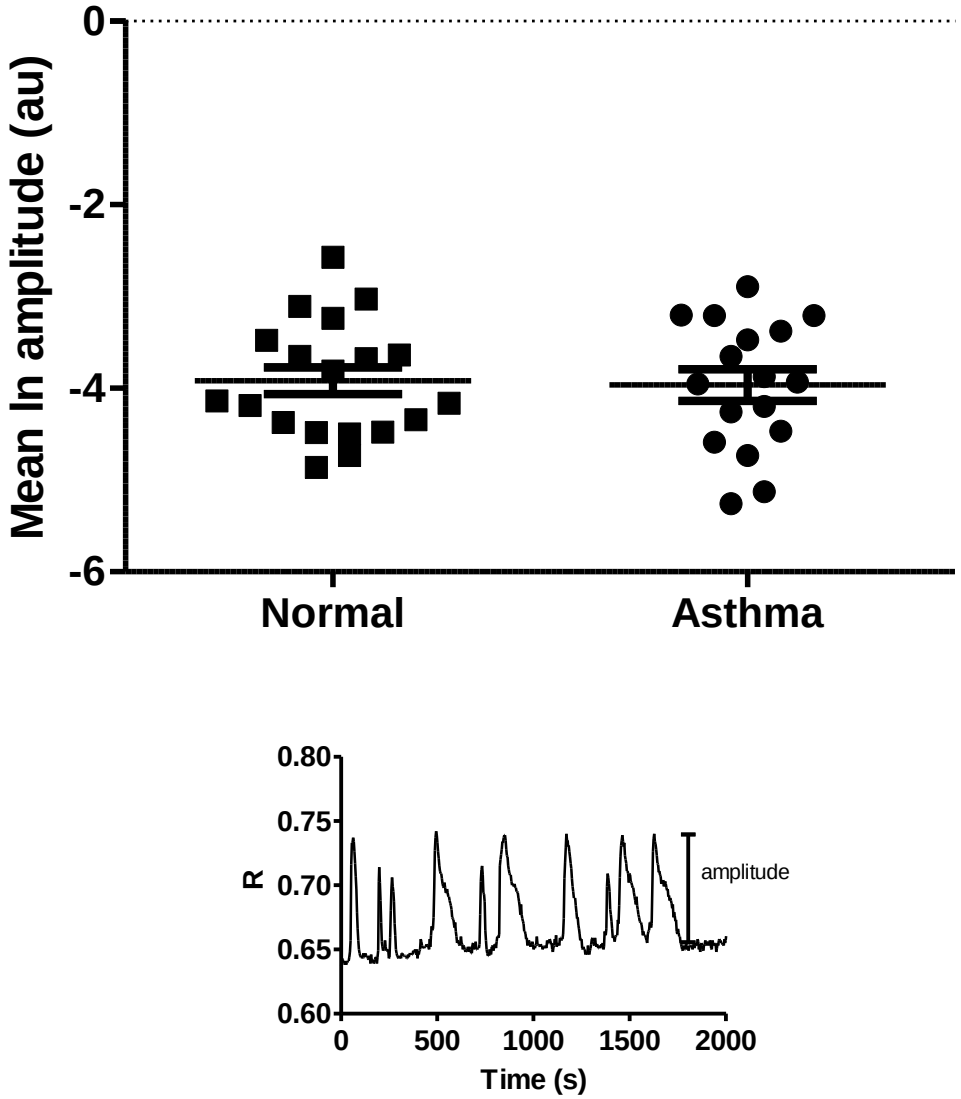

Figure 3.11 There was no significant difference (Student's t-test) in $[Ca^{2+}]_i$ oscillation mean ln amplitude (i.e. mean ln $\Delta R \pm$ sem) between asthma (n=17) and normal (n=19) hASM cell donors. The lower pane shows a representative Ca^{2+} waveform.

3.2.3 Clinical Correlation

Figure 3.12 shows that there is a significant inverse correlation between FEV_1 and mean ln (ie natural logarithm) of the donor $[Ca^{2+}]_i$ oscillation dominant frequency, CODF, such that r = -0.42, P = 0.0036. That is, there is a non-disease specific inverse correlation between FEV_1 (% of predicted) and mean ln CODF in asthma and normal hASM cell donors. Figure 3.13 shows that this significant inverse relationship is not preserved when FEV_1/FVC is plotted as a function of mean ln CODF for all donors. However, with P=0.064 this could become significant when more donors are added.

Normal donors were then excluded, in order to test for a correlation between airway physiology and CODF for asthma donors only. Under these conditions, there is still a significant correlation (Figure 3.14a) between FEV_1 and mean ln CODF (r = -0.48, P = 0.016), but correlation with FEV_1/FVC remains non-significant (Figure 3.14b) with mean ln CODF (r = -0.32, P = 0.11).

Since there was a correlation between CODF and FEV_1 but not FEV_1/FVC for asthma hASM cell donors, the next step was to determine if there was a significant phenotypic difference between CODF in donors with and without disordered airway physiology. Donors whose lung function indicated airflow obstruction (AFO), defined as FEV_1/FVC<70%, and airflow impairment, defined as FEV_1<80%, were therefore compared to those donors without such disordered airway physiology. Firstly, there was a significant difference (P =0.032) in mean ln CODF for AFO and non-AFO hASM cell donors (Figure 3.15a) where AFO is defined as FEV_1/FVC<70%. Secondly, mean ln CODF for donors with AFO and airflow impairment (defined as FEV_1/FVC<70% and FEV_1<80%), showed a strongly significant difference at P<0.0001 (Figure 3.15b).

Hence, mean ln CODF can be considered to be a strong correlator for hASM cell donors with airflow obstruction and impairment.

In order to determine if the differences shown in Figure 3.15 can be reliably used to predict AFO in asthma characterised by $FEV_1/FVC<70\%$ and $FEV_1<80$, a ROC (Receiver Operator Curve) was constructed to determine the sensitivity and specificity of using CODF as a predictor of AFO. In Figure 3.16 the axes of sensitivity and 100%-Specificity% dictate that the further the curve is toward the upper left-hand half of the graph the greater is the sensitivity and specificity of the test. This is directly assessed by calculating the area under the curve (AUC). An AUC>0.8 is considered to be clinically relevant for any test being considered. In this case the AUC was 0.91. That is, CODF identifies AFO with specificity and sensitivity of at least 91%, indicating that the use of CODF as a test for AFO in asthma ($FEV_1<80\%$ and $FEV_1/FVC<70\%$) is highly significant ($P<0.0001$) and unlikely to be due to chance alone. Table 3.1 summaries the available clinical characteristics.

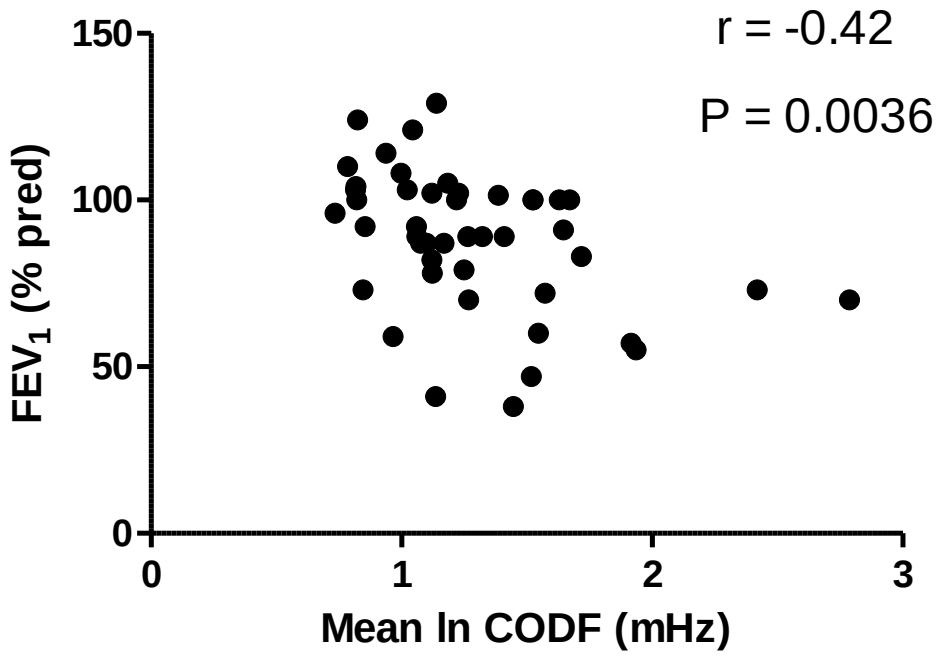

Figure 3.12 Pearson correlation between FEV_1 (% predicted) and mean ln CODF for all donors (n=46).

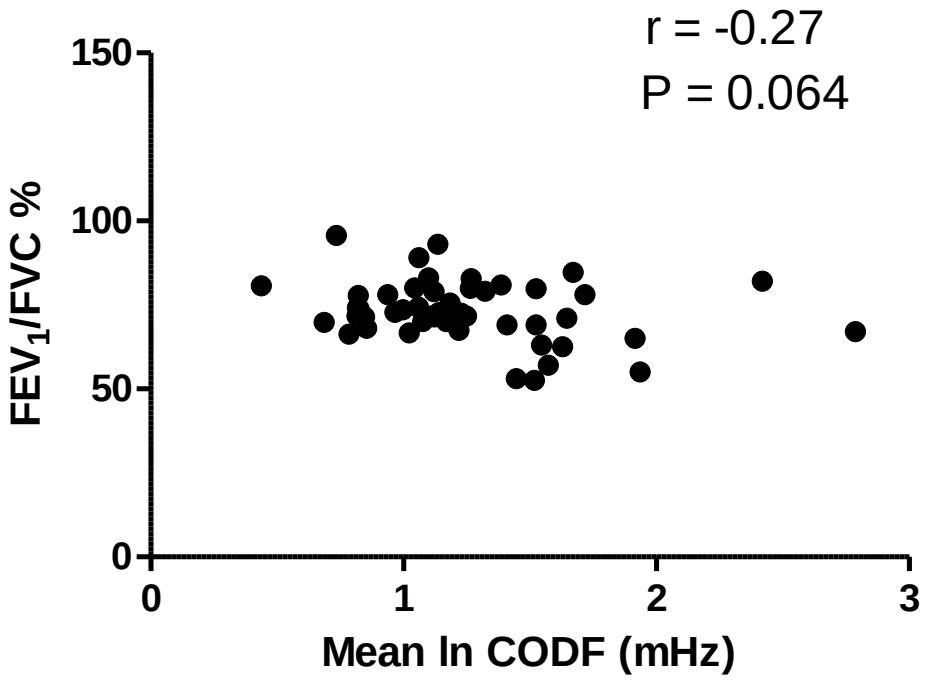

Figure 3.13 Pearson correlation between FEV_1/FVC % and mean ln CODF for all donors (n=46).

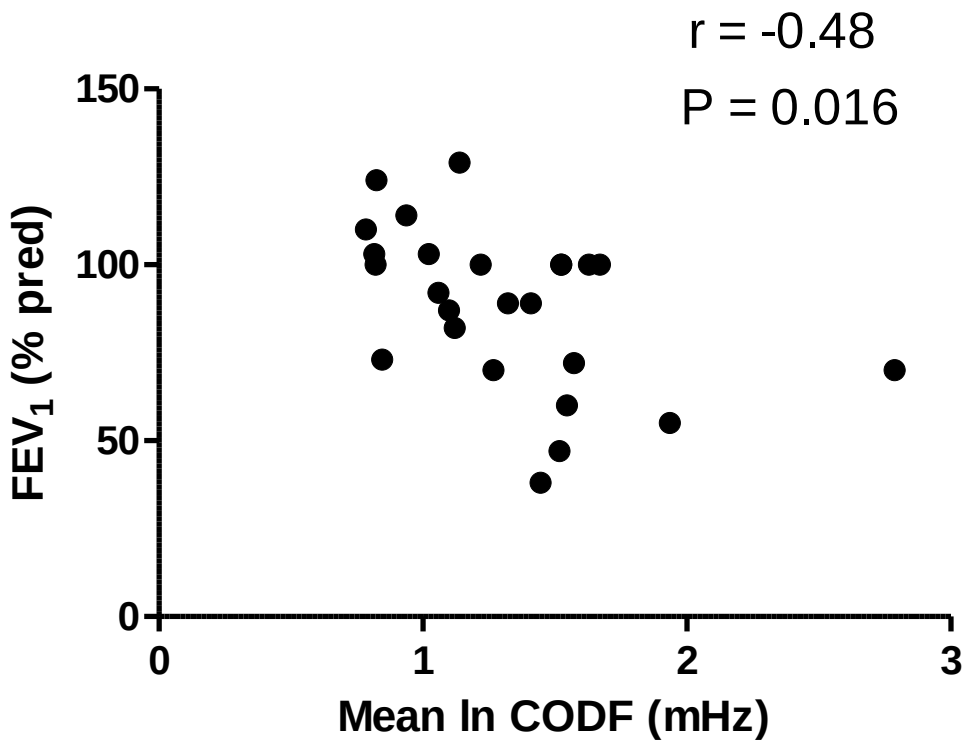

Figure 3.14a) After removal of normal donors, a Pearson correlation between FEV_1 and mean ln CODF persisted for asthma donors only (n=25).

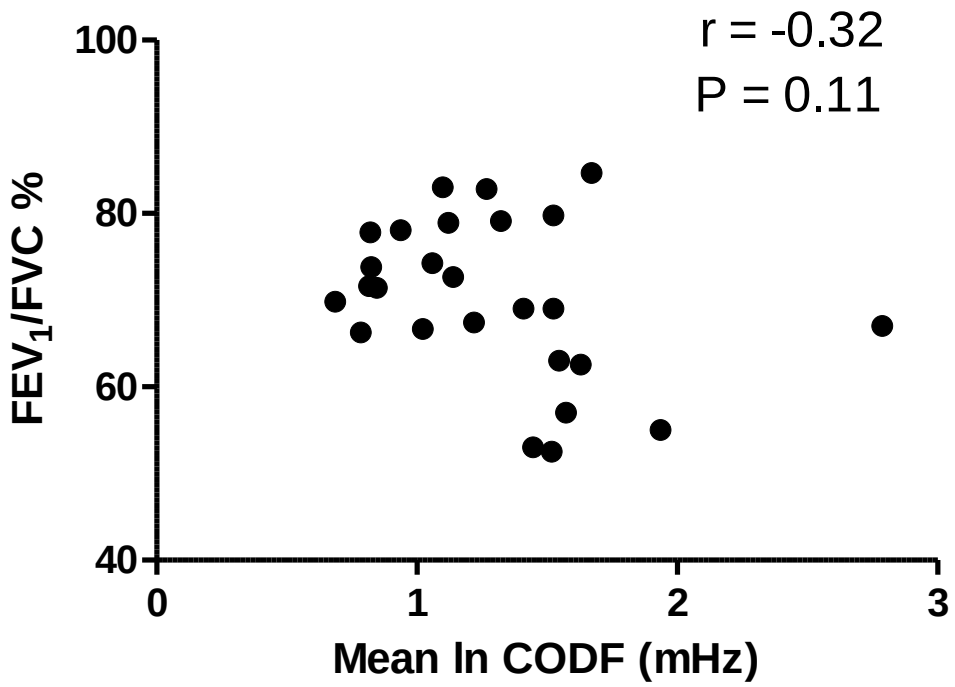

Figure 3.14b) After removal of normal donors, there was no significant Pearson correlation between FEV_1/FVC % and mean ln CODF for the remaining asthma donors (n=26).

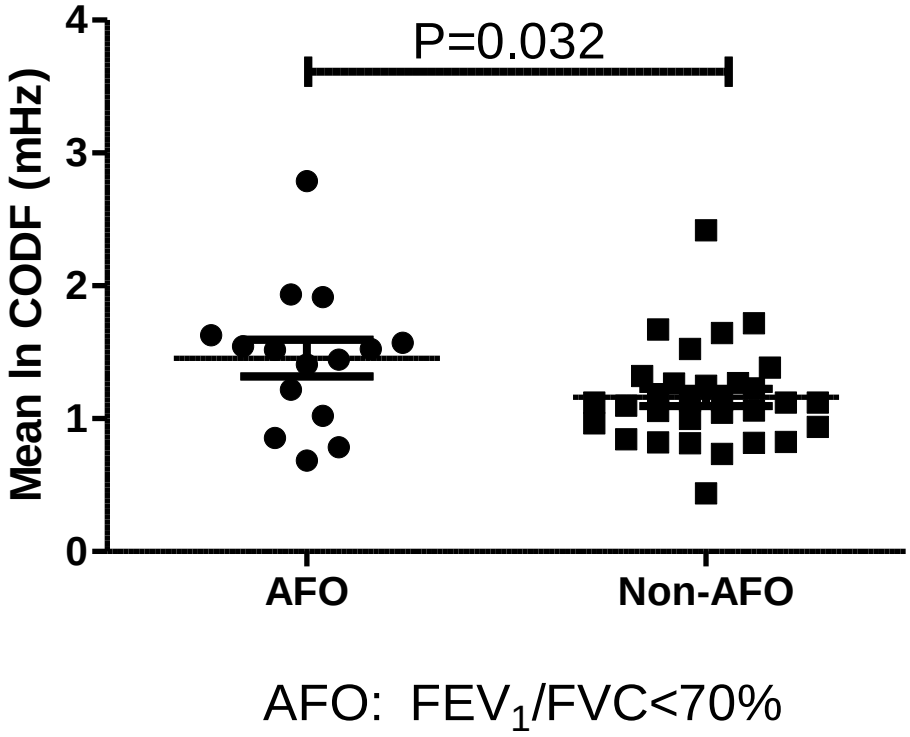

Figure 3.15a Donors with disordered lung function physiology $FEV_1/FVC<70\%$ belong to an airflow obstruction group (AFO, n=15) and their mean ln CODF was significantly different (Student's t-test) from the remaining non-AFO hASM cell donor group (i.e. $FEV_1/FVC>70\%$, n=31).

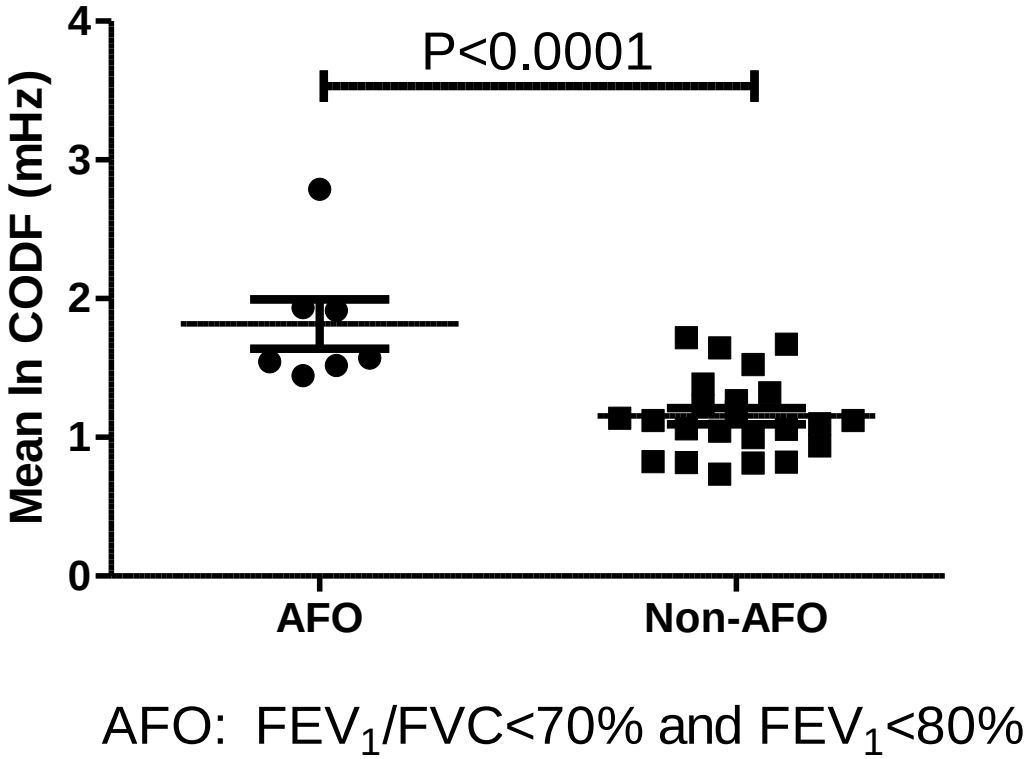

Figure 3.15b A strong significant difference (Student's t-test) was found when mean ln CODF was compared from donors (n=7) with AFO and lung function impairment, i.e. $FEV_1/FVC < 70\%$, $FEV_1 < 80\%$, termed the 'AFO' group, and the remaining donors (n=23) that form a non-AFO group.

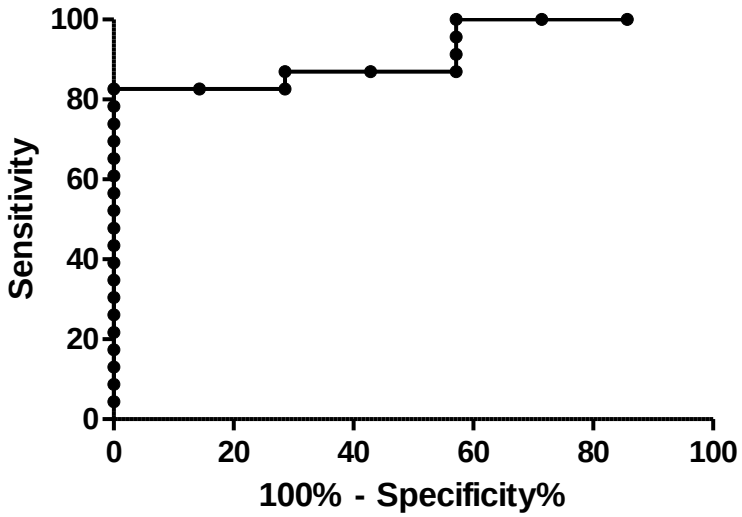

Figure 3.16 Receiver-operator curve (ROC) for mean ln CODF in donors (n=7) with airflow obstruction, AFO, defined as $FEV_1/FVC<70\%$ and $FEV_1<80\%$ versus non-AFO donors (n=23). Since AUC is 91% the use of mean ln CODF as a predictor of AFO is statistically significant at the level of $P<0.001$.

Table 3.1 Clinical characteristics (A = Asthma , N = Normal)					
Age	**Gender**	**Diagnosis**	**Mean Ln CODF**	**FEV_1 (% predicted)**	**FEV_1 / FVC (%)**
69		A	1.5462	60	63
37		A	1.9354	55	55
33	M	A	1.5731	72	57
68		A	1.5245	100	69
60		A	1.0991	87	83
60	M	A	1.4466	38	53
60	F	A	2.7874	70	67
35	F	A	1.4089	89	69
23	M	A	1.0589	92	74
32	M	A	1.1213	82	79
57	M	A	1.6288	100	63
40	M	A	1.2667	70	83
73	F	A	1.1394	129	73
34	M	A	1.3221	89	79
52	M	A	0.8461	73	71
63	M	A	0.8202	100	78
63	M	A	1.2186	100	67
61	M	A	0.8154	103	72
28	F	A	1.5175	47	53
19	M	A	1.6715	100	85
42	F	A	0.9382	114	78
57	F	A	1.0232	103	67
50	F	A	0.7840	110	66
51	M	A	0.8244	124	74
33	F	A	1.5247	100	80
61	F	N	1.2491	79	72
74		N	1.9151	57	65
63		N	2.4189	73	82
69		N	1.7176	83	78
61		N	1.1688	87	70
25		N	1.1365	41	93
74		N	0.8538	92	68
83		N	1.0447	121	80
63	M	N	0.9650	59	73
63	M	N	0.9967	108	74
27	F	N	0.7337	96	96
36	M	N	1.3853	101.4	81
52	M	N	1.1840	105	76
57	F	N	1.2640	89	80
57	F	N	1.1205	102	72
20	M	N	1.1217	78	71
52	M	N	1.0760	87	70
77	M	N	1.2277	102	73
24	M	N	1.0605	89	89

3.3 Discussion

3.3.1 Basal $[Ca^{2+}]_i$

Under quiescent conditions basal R-values, and hence $[Ca^{2+}]_i$, were not significantly different in hASM cells from asthma or normal donors. This is important because it demonstrates that the position of the dynamic $[Ca^{2+}]_i$ equilibrium in asthma and normal hASM cells is not different. It also shows that $[Ca^{2+}]_i$ homeostasis is being maintained to the same extent in cells from asthma and normal. Therefore, even if there was a structural difference, the functional outcome is unaffected in the quiescent hASM cell.

3.3.2 $[Ca^{2+}]_i$ oscillations

The distribution of both CODF and amplitude (ΔR) values based on the analysis of basal $[Ca^{2+}]_i$ waveforms from single hASM cells is right or positive skewed. This is a common finding generally in nature, examples include concentration and human height, indicating that the data are in fact log-normally distributed (Limpert *et al.*, 2001). Therefore, upon logarithmic transformation of these data, parametric statistical analysis can be performed. It was found that asthma and normal hASM cells share common CODF and $[Ca^{2+}]_i$ amplitude values. That is, the two sets of distributions were overlapping and are not significantly different (Figures 3.7 and 3.10).

By grouping hASM cell data by donor there was no significant difference in CODF and amplitude for asthma compared to normal hASM cell donors, just as for hASM cells.

3.3.3 Correlation between lung physiology and $[Ca^{2+}]_i$ oscillations

Since clinical data for each donor was readily available to this project, then the CODF and amplitude data were tested for a correlation with FEV_1 and FEV_1/FVC. If a correlation was found to exist then those two parameters are associated, although not necessarily by causal determinism. Also, whether there was a significant difference between donors with disordered airway physiology and donors with normal airway physiology was tested.

The analysis showed that there was no correlation between lung function and amplitude but there was a significant correlation with CODF. It was found that for asthma and normal hASM cell donors, there was a significant inverse correlation between FEV_1 (% predicted) and mean ln CODF (Figure 3.13). But this inverse relationship was not preserved when FEV_1/FVC was compared against mean ln CODF for asthma and normal hASM cell donors (Figure 3.14). However this might become significant if more donors are added since P was near significance (0.064) but r was fairly low (-0.27). These tests, performed on asthma and normal donors, where non-disease specific.

Tests where then performed to test for disease dependent relationships. Figure 3.15a showed that a significant correlation persists between asthma hASM cell donor FEV_1 values and mean ln CODF, after normal lung function donors had been removed. Similarly, there was no significant correlation between asthma hASM cell donor FEV_1/FVC and mean ln CODF (Figure 3.15b).

Then the effect that a clinically defined disease phenotype, *viz.* AFO, had upon CODF, relative to non-AFO hASM cell donors was investigated. For those hASM cell donors with airflow obstruction (AFO), based on the criterion $FEV_1/FVC<70\%$, mean ln

CODF was significantly different to that of the remaining donors in the non-AFO group (Figure 3.16a). The disease correlation can be further tested by considering AFO and airflow impairment together, such that the criterion of both $FEV_1/FVC<70\%$ and $FEV_1<80\%$ must be satisfied.

With this new AFO criterion, a highly significant difference was found between the mean ln CODF of the AFO group and the remaining non-AFO donors (Figure 3.16b). Indeed, a receiver-operator curve (ROC) shows that mean ln CODF is an excellent predictor of AFO, with AUC = 91% and $P<0.001$ (Figure 3.17).

The finding that CODF is significantly raised in hASM cell donors with AFO lends support to the hypothesis that hASM cell cytoplasm is inherently more excitable (Berridge *et al.*, 1994) in terms of $[Ca^{2+}]_i$ oscillations than that of non-AFO hASM cell donors. This suggests the presence of an organised Ca^{2+} oscillator in AFO donors. One suggestion is that there is a different pattern of Ca^{2+} release channel organisation or microdomain (Berridge, 2006) involvement in specific asthma hASM cell phenotypes, in this case an AFO phenotype. Since this Ca^{2+} oscillator exists in passaged hASM cells, independent of external influence from inflammatory mediators, it follows that it must be a heritable trait, determined genetically or epigenetically.

High $[Ca^{2+}]$ microdomains have also been shown to exist in the wrinkled surface topologies of cells (Brasen *et al.*, 2010) often in juxtaposition with the SR (Poburko *et al.*, 2004). Indeed, small invaginations in cell membranes called caveolae function as distinct local signaling entities that are enriched by the structural protein caveolin. Caveolae have also been shown to play a role in $[Ca^{2+}]_i$ handling (Darby *et al.*, 2000) and have a lipid raft structure. They have been shown to contain SOCE, TRPC, RyR and IP_3R channels and SERCA, PMCA and NCX transporters (Floyd *et al.*, 2007;

Prakash *et al.*, 2007; Pani *et al.*, 2009). Caveolae for example are known to provide a structural support for $[Ca^{2+}]_i$ release mediated by muscarinic M_3-receptor stimulation in hASM cells (Gosens *et al.*, 2007). And it is known that as muscarinic stimulation increases, so does $[Ca^{2+}]_i$ release via RyR subtypes 1 and 3 pursuant to bronchoconstriction (Du *et al.*, 2005).

3.4 Conclusion

Basal R-values and hence basal $[Ca^{2+}]_i$ levels were found not to be different in asthma compared to normal hASM cell donors. This suggests that $[Ca^{2+}]_i$ homeostasis is not different in asthma compared to normal hASM cell donors. There was no significant difference between either CODF or Ca^{2+} oscillation amplitude in asthma or normal hASM cell donors. There was however a significant non-disease specific inverse correlation between mean ln CODF and FEV_1 but not FEV_1/FVC in normal and asthma donors, which is reflected in asthma donors alone. Furthermore, there was a significant difference in mean ln CODF when an asthma phenotype was considered. Hence, there was a significant difference between AFO and non-AFO hASM cell donors ($P<0.0001$), where AFO was defined as $FEV_1/FVC<70\%$ and $FEV_1<80\%$, to such an extent that a ROC demonstrates that mean ln CODF is an excellent predictor of AFO (AUC=91%, $P<0.001$). This appears to lend support to the hypothesis that the cytoplasm of AFO hASM cell donors is more excitable in terms of Ca^{2+} oscillation dominant frequency than non-AFO donors.

CHAPTER 4

INVESTIGATION OF $[Ca^{2+}]_i$ HANDLING

4.1 Introduction

Asthma is a chronic airway inflammation characterised by bronchial oedema, mucus hypersecretion and hASM contraction. These changes give rise to an increased paroxysmal probability of airway narrowing called airway hyperresponsiveness (AHR), which leads to variable airflow obstruction. The significant contribution to AHR made by hASM cell contraction may simply be a consequence of the inflammatory environment, a point that I will return to in Chapter 5. However, an alternative explanation for the increased likelihood of hASM cell contraction is that there is an intrinsic abnormality in the regulation of excitation-contraction coupling. A proposed mechanistic basis for this effect is that $[Ca^{2+}]_i$ handling and homeostasis are intrinsically dysregulated in hASM cells from asthma compared to normal donors (Triggle, 1983; Parameswaran *et al.*, 2002; Trian *et al.*, 2007; Perez-Zoghbi *et al.*, 2009).

Recently, sarco/endoplasmic reticulum Ca^{2+}-ATPase (SERCA) has been identified as a significant determinant of $[Ca^{2+}]_i$ dysregulation in hASM cells (Mahn *et al.*, 2009; Prakash *et al.*, 2009; Sathish *et al.*, 2009; Mahn *et al.*, 2010). In particular, it is suggested that diminished expression of SERCA2 leads to increased $[Ca^{2+}]_i$ levels and therefore an increased likelihood of hASM cell contraction. This is a credible mechanism which can explain how altered properties of hASM cells can contribute to the pathology of AHR and the manifestation of the signs and symptoms of asthma.

It has already been shown in Chapter 3 that there is no significant difference in hASM cell basal $[Ca^{2+}]_i$ levels in asthma compared to normal donors. In this chapter the hypothesis that $[Ca^{2+}]_i$ homeostasis is dysregulated is further tested by considering the dynamics of $[Ca^{2+}]_i$ handling. This dynamic approach to the assessment of Ca^{2+} handling in hASM cells also allows investigation of SERCA activity. SERCA activity could be dysregulated in asthma not just because of diminished expression, but through the effect of other protein regulators of SERCA. For example, *ORMDL3* has been found to be associated with asthma through a genome-wide study (Galanter *et al.*, 2008). The protein product of *ORMDL3* is located at the SR membrane and has been linked to SERCA inhibition, the subsequent decrease in SR $[Ca^{2+}]$ leads to an unfolded protein response (UPR) and inflammation (Cantero-Recasens *et al.*, 2010). Hence ORMDL3 inhibition of SERCA could contribute to the inflammatory process observed in asthma. Therefore, a change to SERCA activity in asthma could affect Ca^{2+} handling and recovery rates following changes in $[Ca^{2+}]$. Thus, a dynamic approach to Ca^{2+} handling can demonstrate whether SERCA activity is dysfunctional in asthma compared to normal hASM cell donors.

It is important to make a distinction between $[Ca^{2+}]_i$ handling and $[Ca^{2+}]_i$ homeostasis. They are different but related concepts. When a system is at equilibrium it will act to oppose an applied constraint. That is, there is a tendency or driving force for the system to return to equilibrium. In this case, equilibrium is synonymous with homeostasis. And the measure of this tendency or drive toward maintenance of homeostasis is termed $[Ca^{2+}]_i$ handling. In fact, $[Ca^{2+}]_i$ handling is a description of pre-equilibrium kinetics. Therefore, after a disturbance to homeostasis, subsequent $[Ca^{2+}]_i$ handling can be defined as those set of dynamic processes by which the cell returns to homeostatically controlled basal $[Ca^{2+}]_i$ levels. Incidentally, Ca^{2+} homeostasis can also be considered to

be a dynamic equilibrium process whereby small efflux changes are balanced by small influx changes.

Hence, $[Ca^{2+}]_i$ handling was then investigated to determine whether cellular recovery after a deliberately provoked $[Ca^{2+}]_i$ response is different in asthma compared to normal hASM cell donors. Specifically, single $[Ca^{2+}]_i$ responses were provoked in hASM cells by UV photo-release of caged Ca^{2+} into a small region of the cytoplasm (Kao, 2006), or by addition of the Ca^{2+} mobilising GPCR agonist bradykinin. Bradykinin generates a reliable monophasic cell-wide $[Ca^{2+}]_i$ response in hASM cells that is clinically relevant to asthma. In each case the cellular response was monitored in real time as the raised $[Ca^{2+}]_i$ level returned to a stable baseline value. The recovery follows an exponential decay process that was quantified by estimating the rate of decay or recovery (K $[s^{-1}]$) by exponential curve fitting. Since exponential decay is essentially asymptotic, measuring K values gives the most precise measure of recovery rate. Other measurements of recovery such as AUC and time to return to baseline are subjective and lead to large percentage errors because the precise time at which $[Ca^{2+}]_i$ returns to basal is uncertain. This becomes especially important if there is fluorophore bleaching and leakage from the cell. As a consequence, the cell appears to take longer to recover due to a rising baseline (Amrani *et al.*, 1994).

In order to determine if SERCA function is diminished, the effect of pharmacologically inhibiting SERCA upon $[Ca^{2+}]_i$ recovery rate (K) was also investigated using the Ca^{2+} uncaging technique. This will give an indication of whether there is any difference in hASM cell SERCA activity between asthma and normal donors.

Biological function depends upon underlying structure. Hence, a structural approach, including assessment of SERCA2 gene transcription, using real time PCR, and

SERCA2 protein expression using western blotting was also taken to complement the functional results.

After investigating the effect of disturbing $[Ca^{2+}]_i$ homeostasis and the subsequent reaction of the cell, attention turned to another cornerstone of $[Ca^{2+}]_i$ homeostasis, that of store operated Ca^{2+} entry (SOCE). For this, a protocol was developed to assess emptying and refilling of the SR Ca^{2+} store. The hypothesis was, 'Is there a difference between SOCE in hASM cells from asthma and normal donors?'

SERCA, amongst other mechanisms, contributes to the maintenance of the low cytoplasmic $[Ca^{2+}]$. The protocol design enabled measurement of the amount of Ca^{2+} released from the SR store when SERCA is inhibited under conditions of low extracellular Ca^{2+}. Also, when extracellular Ca^{2+} is restored the effect of SR Ca^{2+} store refilling, i.e. SOCE, was also assessed. This was achieved using epifluorescence video microscopy of fura-2 loaded hASM cells.

4.2 Results

4.2.1 Real time PCR

There was no significant difference in the relative quantity of SERCA2abc mRNA normalised to a constitutively transcribed 'house keeping' gene 18S rRNA (Figure 4.1) between asthma and normal donors.

4.2.2 Western blotting

There was no significant difference in the expression of SERCA2 protein in asthma compared to normal donors. Visual inspection of western blotting bands (Figure 4.2) immediately suggests that there is no difference. This visual result was confirmed by densitometry analysis of band intensity (Figure 4.3), relative to the constitutively expressed 'house keeping' protein β-actin.

4.2.3 Ca^{2+} uncaging

Ca^{2+} uncaging was employed to investigate hASM cell $[Ca^{2+}]_i$ handling, or homeostatic drive, after $[Ca^{2+}]_i$ had been deliberately increased. The role played by SERCA activity in this system was also investigated. The method involves loading a caged form of Ca^{2+} (see Methods) into hASM cells and applying a short burst of focused laser illumination to release the Ca^{2+}. The short burst of uncaged $[Ca^{2+}]_i$ released into the cytoplasm was monitored using a confocal microscope. Initially, $[Ca^{2+}]_i$ increases rapidly and then decays exponentially back to a baseline level. The rate of decay or recovery is denoted by K (s^{-1}). This represents the sum of recovery rates for the Ca^{2+} efflux and sequestration mechanisms activated in the cell. Thus, this method was used to investigate $[Ca^{2+}]_i$ handling, the tendency of hASM cells to return to $[Ca^{2+}]_i$ homeostasis, in asthma compared to normal donors.

In addition, cyclopiazonic acid (CPA) was used to inhibit pharmacologically SERCA activity. Thus, K_{-CPA} denotes a K value in the absence of SERCA inhibition and K_{+CPA} denotes a K value when SERCA is inhibited. These would be equivalent to K_{+SERCA} (SERCA is present) and K_{-SERCA} (SERCA is inhibited) respectively. K_{-CPA} and K_{+CPA} values were obtained in hASM cells from asthma and normal donors to determine if there is a significant difference in $[Ca^{2+}]_i$ handling after homeostasis had been deliberately disturbed by uncaging Ca^{2+}. The difference, $\Delta K = K_{-CPA} - K_{+CPA}$, is a measure of SERCA activity. ΔK values obtained in hASM cells from asthma and normal donors were compared to assess whether there is a significant difference in SERCA activity or function.

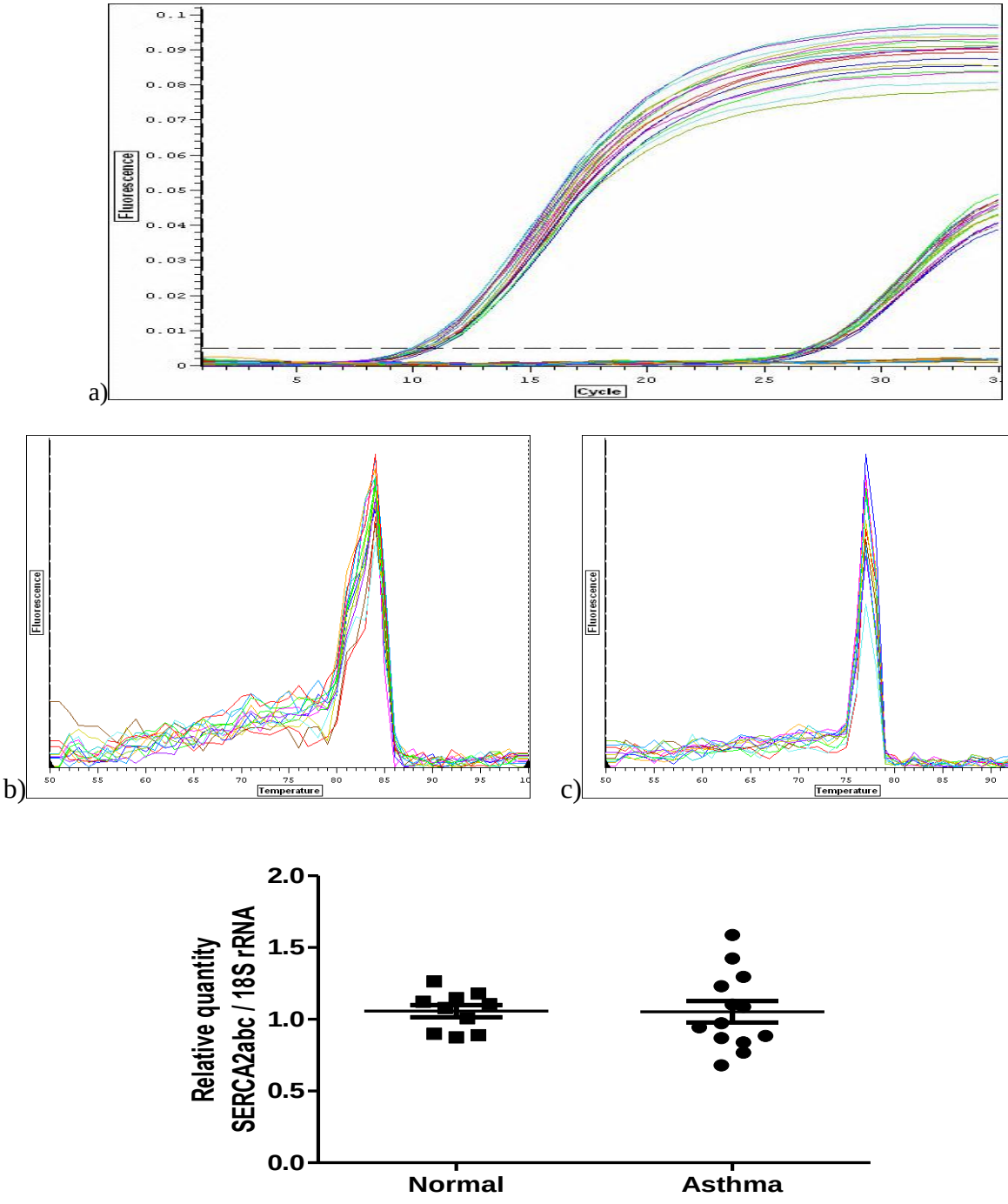

Figure 4.1 a) Using a threshold of 0.005 and 1ng of input cDNA, C_t values were consistently found at around 10 for 18S rRNA and 27 for SERCA2abc.
b,c) Specific PCR product melting curves were obtained using both pairs of primers, 18S rRNA and SERCA2abc, respectively. d) The relative expression of SERCA2abc mRNA normalised to 18S rRNA was not significantly different (Student's t-test) in asthma (n=13) compared to normal (n=10) hASM donors.

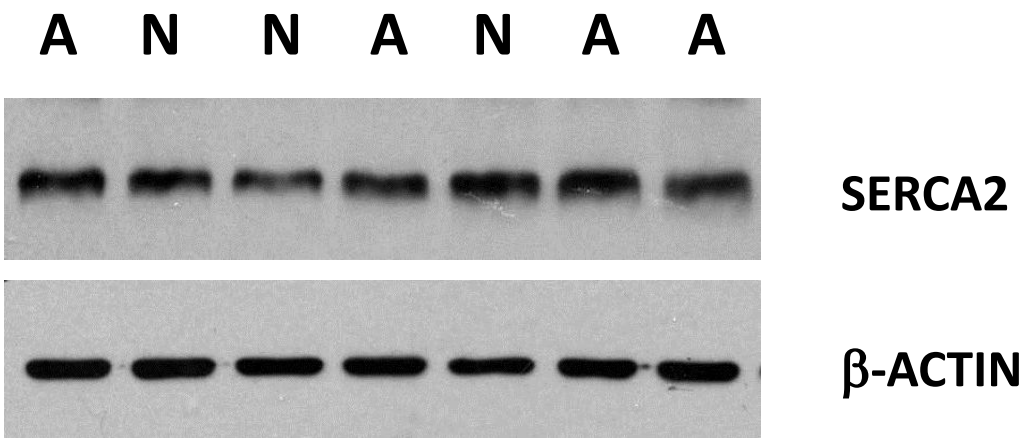

Figure 4.2 Example western blot showing total SERCA2 protein and β-actin immunoreactivities in hASM cells from four asthma (A) and three normal (N) donors. There is no difference in expression by visual inspection. The consistency of the β-actin band intensities indicates uniform sample loading.

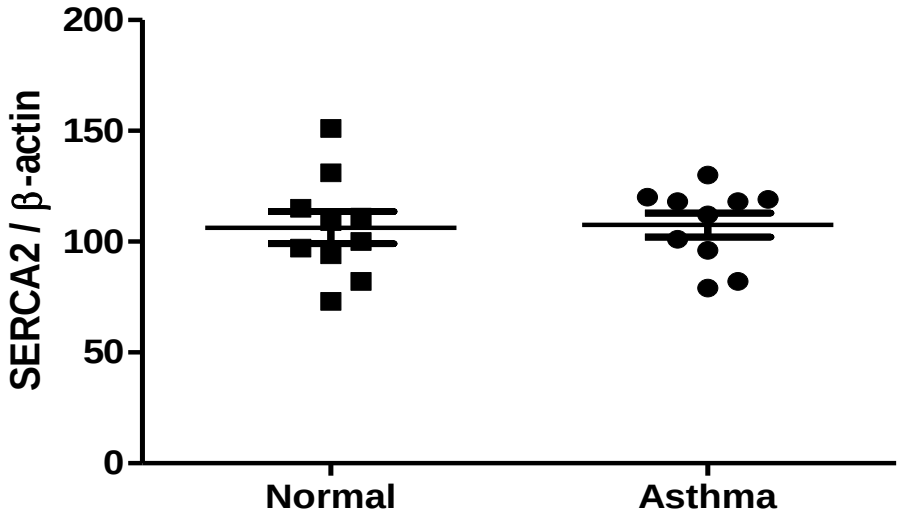

Figure 4.3 Densitometry of total SERCA2 immunoreactivity from western blots shows that there is no significant difference (Student's t-test) in SERCA2 protein expression compared to β-actin control in asthma (n=10) compared to normal (n=10) hASM cell donors.

4.2.3.1 Theoretical focus: If SERCA is inhibited by CPA then K increases

Clearly, the Ca^{2+} recovery rate constant (K) when SERCA is inhibited (K_{+CPA}) is smaller, since a burst of $[Ca^{2+}]_i$ is removed from the cytoplasm at a slower rate, than when SERCA is not inhibited (K_{-CPA}). Hence it would be expected that $K_{-CPA} > K_{+CPA}$. The difference between the K values, $\Delta K = K_{-CPA} - K_{+CPA}$, when SERCA isn't and is inhibited is a measure of cellular SERCA activity. If SERCA is diminished in hASM cells from asthma donors then one would expect $\Delta K_{asthma} < \Delta K_{normal}$. This is because K_{-CPA} for asthma would be less (i.e. slower recovery rate) than the K_{-CPA} for normal, with K_{+CPA} essentially remaining constant assuming all other mechanisms are equal (Figure 4.4).

4.2.3.2 Experimental evidence

Confirmation of the theoretical prediction in section 4.2.3.1 is provided by Figure 4.5. It shows that the cellular response to a $[Ca^{2+}]_i$ uncaging event when SERCA is not inhibited, denoted by -CPA, and when it is inhibited, denoted by +CPA. In the case of –CPA, peak to baseline decay rate is clearly faster, simply by visual inspection, than in the case of the +CPA condition, consistent with the expectation that $K_{-CPA} > K_{+CPA}$.

These results can be presented in another way (Figure 4.6), whereby the K value for each cellular Ca^{2+} recovery event is plotted as a columnar dot plot. Again, it can be seen that the rate of recovery with SERCA (-CPA) is faster than when SERCA is inhibited (+CPA).

The mean donor Ca^{2+} uncaging recovery rates (K_{-CPA}) for asthma and normal donors showed no disease specific difference in the ability of the hASM cells to recover from the burst of $[Ca^{2+}]_i$ of an uncaging event (Figure 4.7). This is strong evidence that

$[Ca^{2+}]_i$ handling is not significantly different in hASM cells from asthma compared to normal donors.

When one of the cytoplasmic $[Ca^{2+}]_i$ efflux mechanisms, *viz.* SERCA, was inhibited, again there was no disease specific difference in mean Ca^{2+} uncaging recovery rates (K_{+CPA}) for asthmatic and normal donors. Hence, with SERCA effectively removed from the system, Ca^{2+} handling is not altered in hASM cells from asthma compared to normal donors. Predictably, the K values decreased because the SERCA efflux mechanism has been inhibited and hence it takes longer for the cell to clear the rapid $[Ca^{2+}]_i$ increase (Figure 4.8).

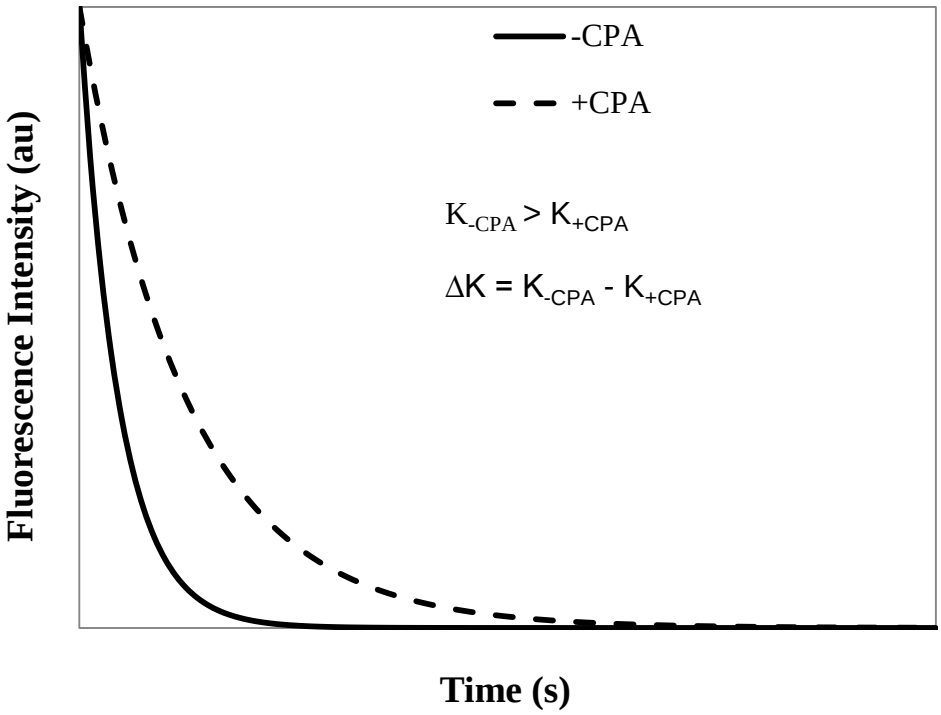

Figure 4.4 The rate of cellular recovery is expected to be faster for cells where SERCA is not inhibited (solid line) than when it is inhibited (dotted line).

a)

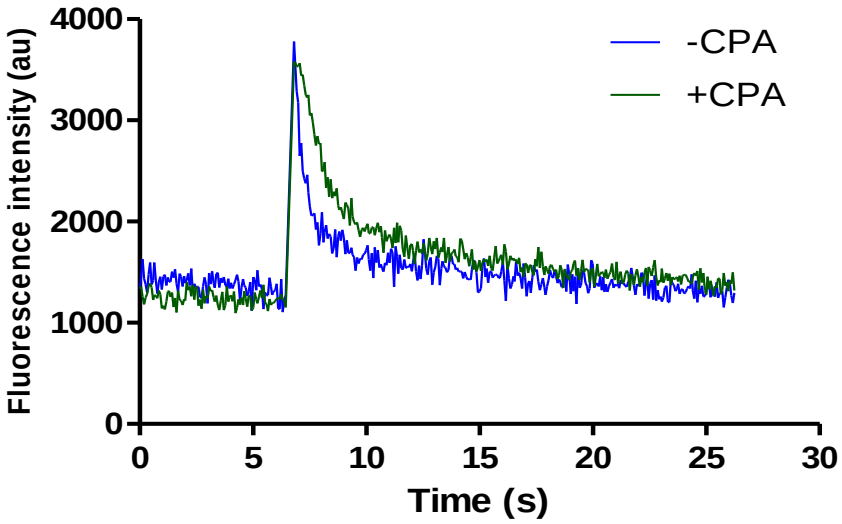

b) c) d)

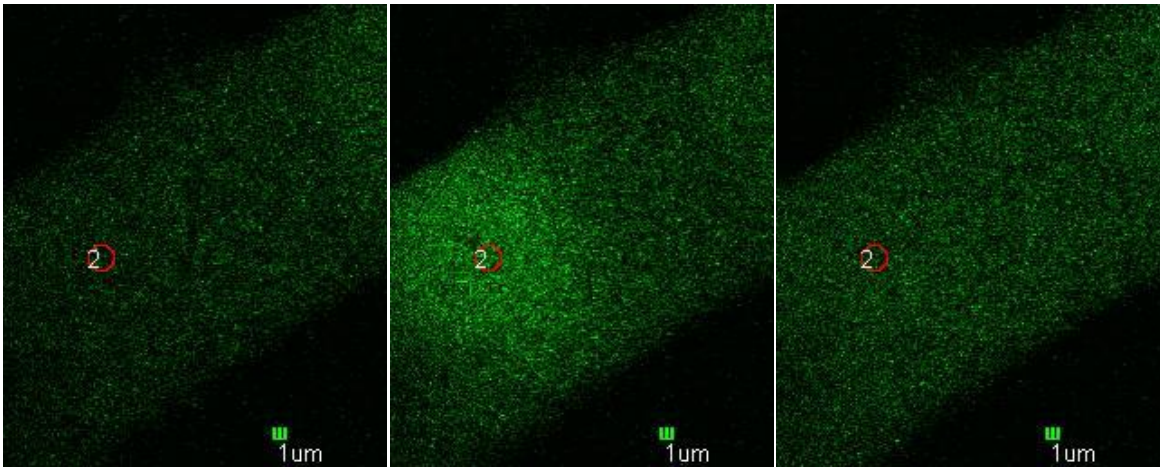

Figure 4.5 Local Ca^{2+} uncaging into a region of hASM cell cytoplasm, from the same donor, when SERCA is not (-CPA) and is (+CPA) inhibited. For any hASM cell the relationship $K_{-CPA} > K_{+CPA}$ is expected to be valid. Visual inspection of the two graphs confirms this (a); in the case of -CPA the peak to baseline rate of decay is more rapid than that of +CPA (separate cells). The lower three images are examples of Ca^{2+} uncaging as seen by the confocal microscope. The middle image (c), flanked by before (b) and after shots (d), shows an increase in fluo-4 fluorescence intensity at the moment the 405nm laser uncages Ca^{2+}, within the red circular ROI, labeled 2.

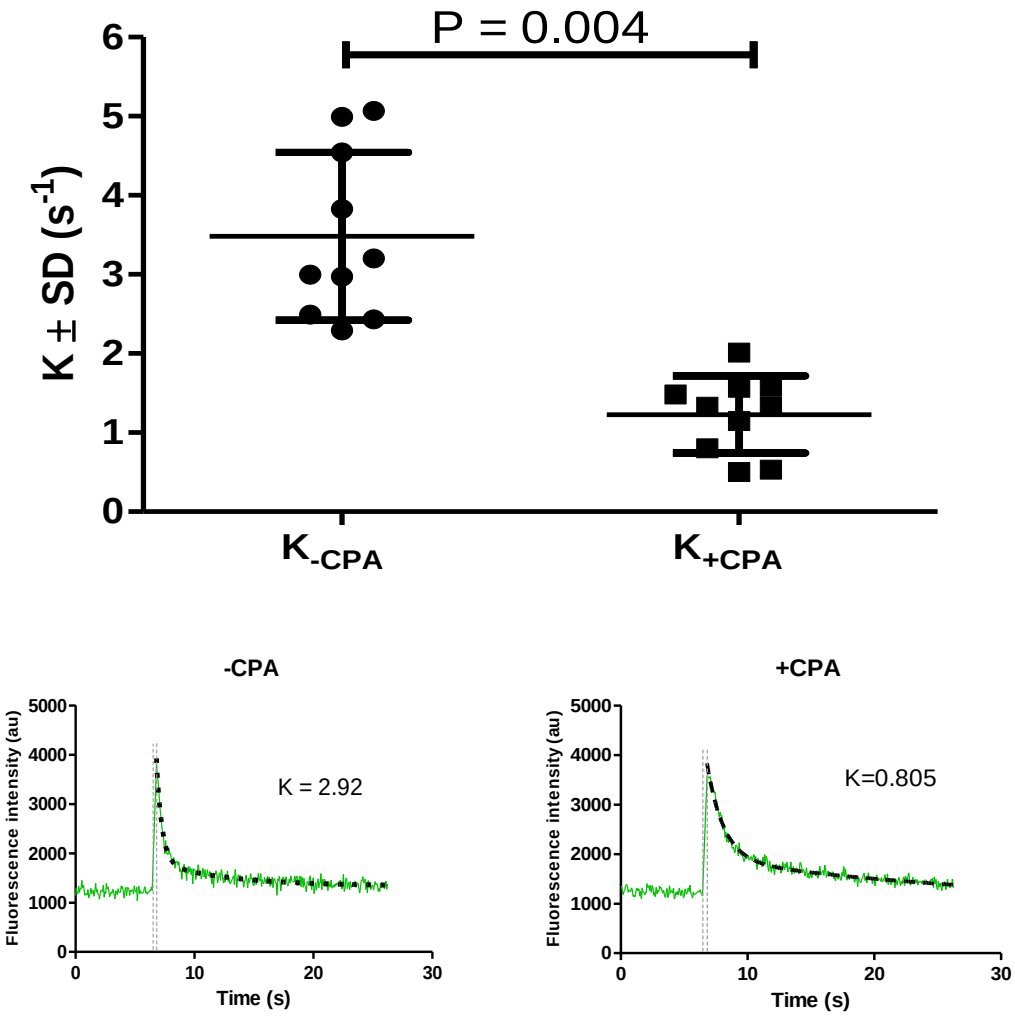

Figure 4.6 For one donor (n=10 cells), the recovery rate (K) of hASM cells from a Ca^{2+} uncaging event is faster when SERCA is not inhibited (-CPA) compared to when it is inhibited (+CPA), Student's t-test P=0.004. The lower panes show Ca^{2+} waveforms (green line) with 300ms photo-activation of caged Ca^{2+} (grey line) and superimposed non-linear regression analysis (black dotted line) to determine rate of decay, K_{-CPA} and K_{+CPA}.

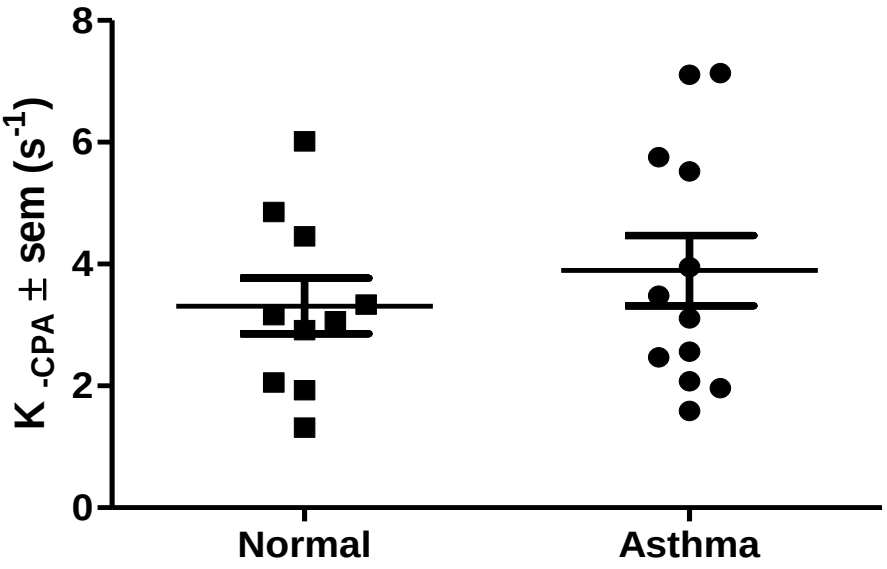

Figure 4.7 Comparison of mean Ca^{2+} uncaging recovery rates without SERCA inhibition (K_{-CPA}) in hASM cells from asthma (n=10) and normal (n=10) donors. There is no significant difference (Student's t-test) in the mean Ca^{2+} uncaging recovery rate between asthma and normal hASM cell donors.

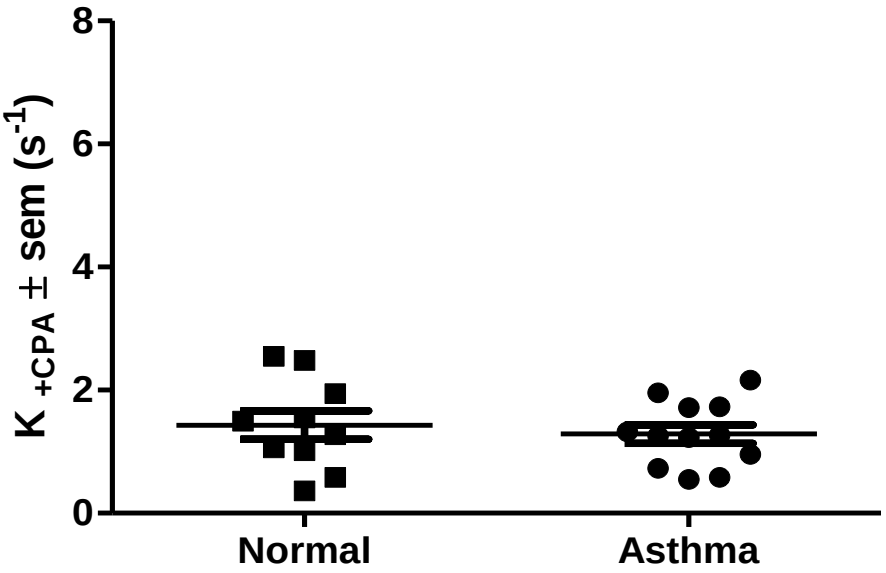

Figure 4.8 Comparison of mean Ca^{2+} uncaging recovery rates with SERCA inhibition (K_{+CPA}) in hASM cells from asthma (n=12) and normal (n=10) donors. When SERCA is inhibited by 10µM CPA, K values decrease but there is no significant difference (Student's t-test) between asthma and normal hASM cell donors which suggests all other efflux mechanisms are acting equally.

Figure 4.9 shows the variation in K across asthma and normal hASM cell donors and compares it to those same donors when SERCA is inhibited. It is clear that when SERCA is not inhibited the range of K is far wider than when SERCA is inhibited, but this variation applies equally to asthma and normal donors. It appears that some donors have a considerably higher level of SERCA function than others whose K values are comparable to those of donors whose SERCA function is inhibited. When SERCA is inhibited the variation in K is much smaller.

There is a significant ($P<0.0001$), but non-disease specific difference in the Ca^{2+} uncaging recovery rate (K) when SERCA is not inhibited (K_{-CPA}) and when it is inhibited (K_{+CPA}) as would be expected. However, what is noteworthy is the variation of K for hASM cell donors across the spectrum of asthmatics and normals. With some hASM cell donors having values for K_{-CPA} and K_{+CPA} approximately equal. This demonstrates that a) SERCA is important in $[Ca^{2+}]_i$ homeostasis of hASM donors, b) normal and asthmatic hASM cell donors belong to a heterogeneous group in terms of SERCA function, and c) that this heterogeneity is a composite of *in vivo* and *in vitro* variability.

In section 4.2.3.1 it was predicted that if there is a difference in SERCA function in asthma then the difference between the -CPA and +CPA recovery rates would demonstrate this. More formally, the relationship that has to be satisfied is:

$$\Delta K_{asthma} < \Delta K_{normal}$$

Where $\Delta K = K_{-CPA} - K_{+CPA}$

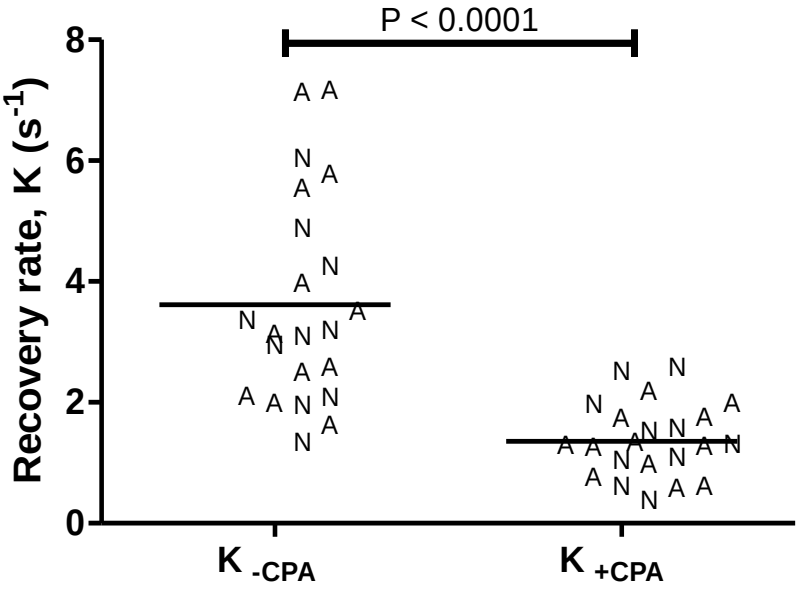

Figure 4.9 Comparison of mean Ca^{2+} uncaging recovery rates (K) of hASM cell asthma (n=12) and normal (n=10) donors ± CPA. There is a wider range of K_{-CPA} values for asthma (A) and normal (N) donors compared to K_{+CPA}. Whilst some donors have hASM cells that have a high K_{-CPA} value others appear to hardly have any SERCA function at all. When SERCA is inhibited the variation in K values is much smaller. (Student's t-test P<0.0001).

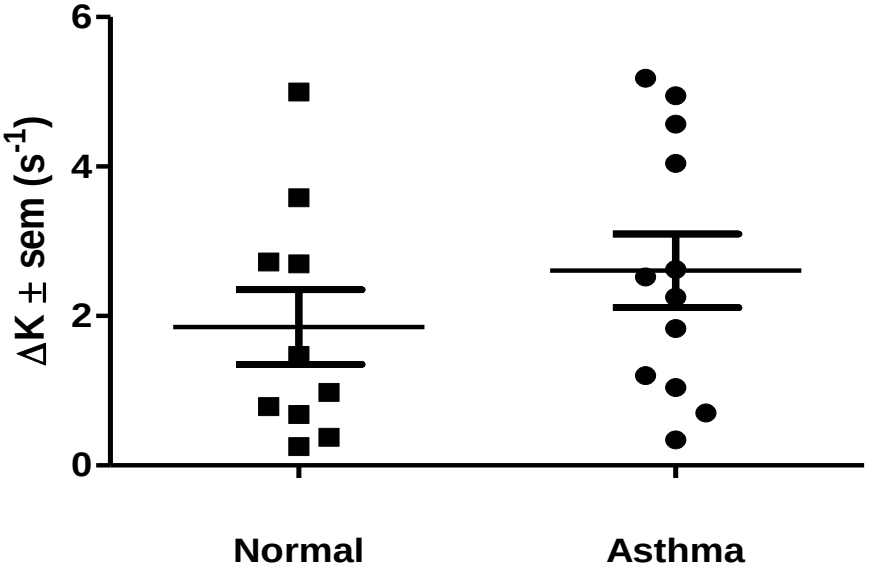

Figure 4.10 Difference between mean K_{-CPA} and mean K_{+CPA} (ΔK) in hASM cells from asthma (n=12) and normal (n=10) donors. There is no significant difference (Student's t-test) in ΔK between asthmatic and normal donors. That is, $\Delta K_{asthma} \approx \Delta K_{normal}$

The result is shown in Figure 4.10. ΔK for asthma and normal hASM cell donors is not significantly different. Hence, there does not appear to be a difference in SERCA function in asthma compared to normal and actually, $\Delta K_{asthma} \approx \Delta K_{normal}$.

4.2.3.3 Clinical aspects

In order to determine whether K may be used as a clinical predictor of lung dysfunction, I looked for a correlation between FEV_1 and K in asthma and normal donors. Hence, FEV_1 (% of predicted adult value) was plotted as a function of mean donor $[Ca^{2+}]_i$ recovery rate (K). Figure 4.11 is a plot of FEV_1 as a function of K_{-CPA} (without SERCA inhibition) for (a) normal and (b) asthma donors. Similarly, Figure 4.12 is a plot of FEV_1 as a function of K_{+CPA} (when SERCA is inhibited). For both, there was no significant correlation. Figure 4.13 is a plot of FEV_1 as a function of ΔK, a relative measure of SERCA function, which also shows a non-significant correlation for (a) normal and (b) asthma donors. Table 4.1 lists the clinical characteristics of the hASM cell donors used.

a) Normal

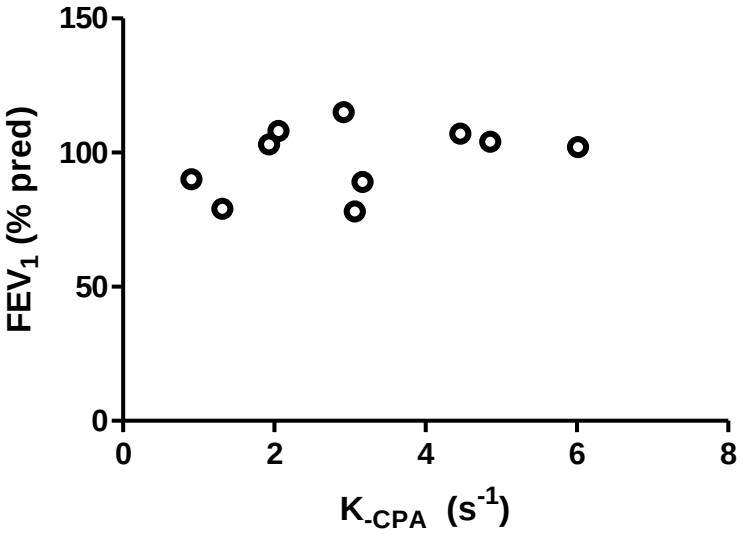

b) Asthma

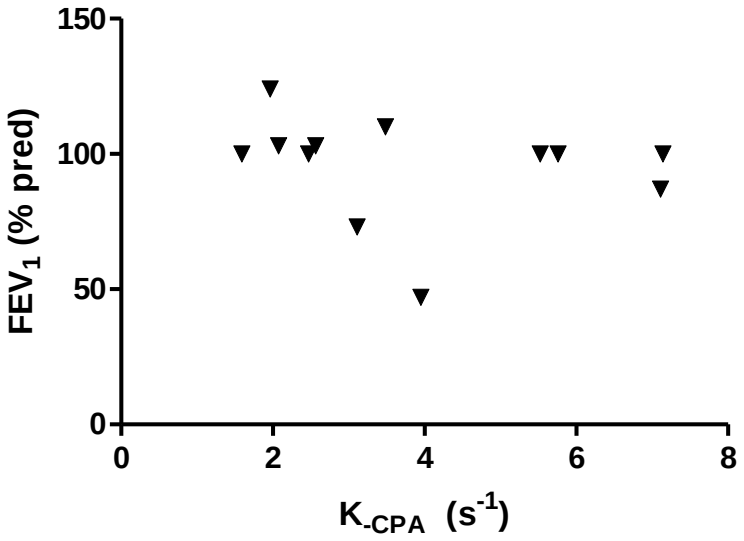

Figure 4.11 FEV_1 as a function of K_{-CPA}. There is no significant Pearson correlation between FEV_1 and mean donor K when SERCA is not inhibited for (a) normal (n=10) or, (b) asthma (n=12) donors.

a) Normal

b) Asthma

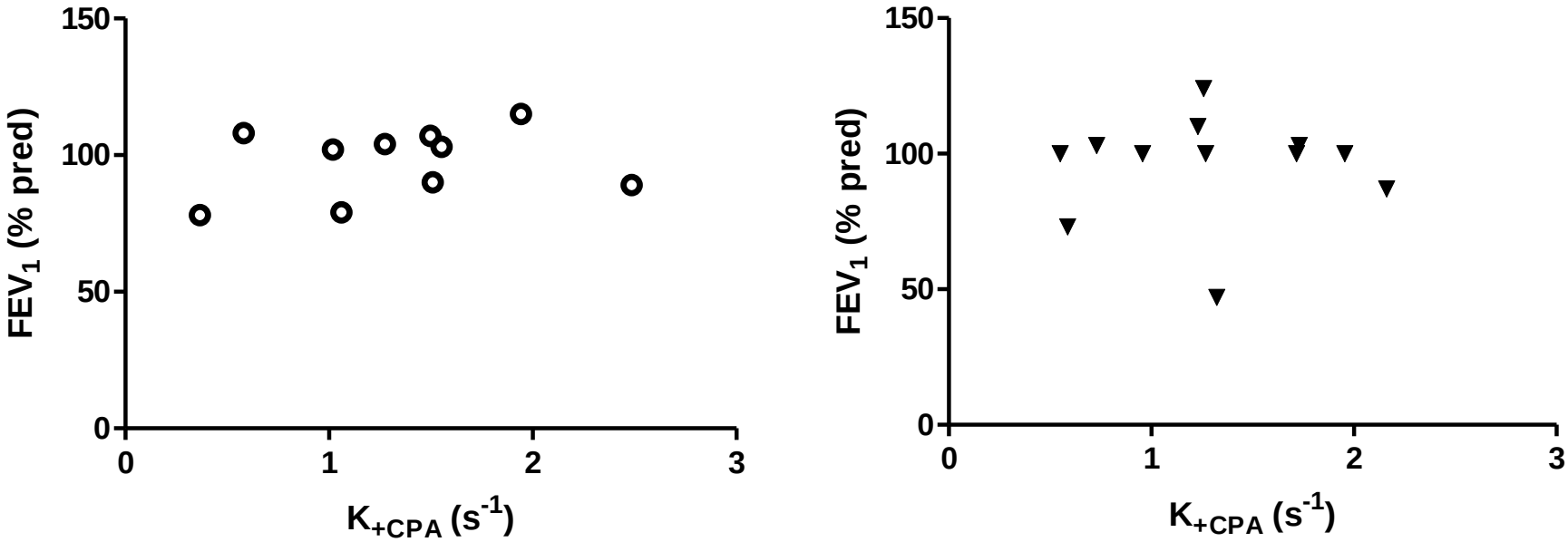

Figure 4.12 FEV_1 as a function of K_{+CPA}. There is no significant Pearson correlation between FEV_1 and mean donor K when SERCA is not inhibited for (a) normal (n=10) or, (b) asthma (n=12) donors.

a) Normal

b) Asthma

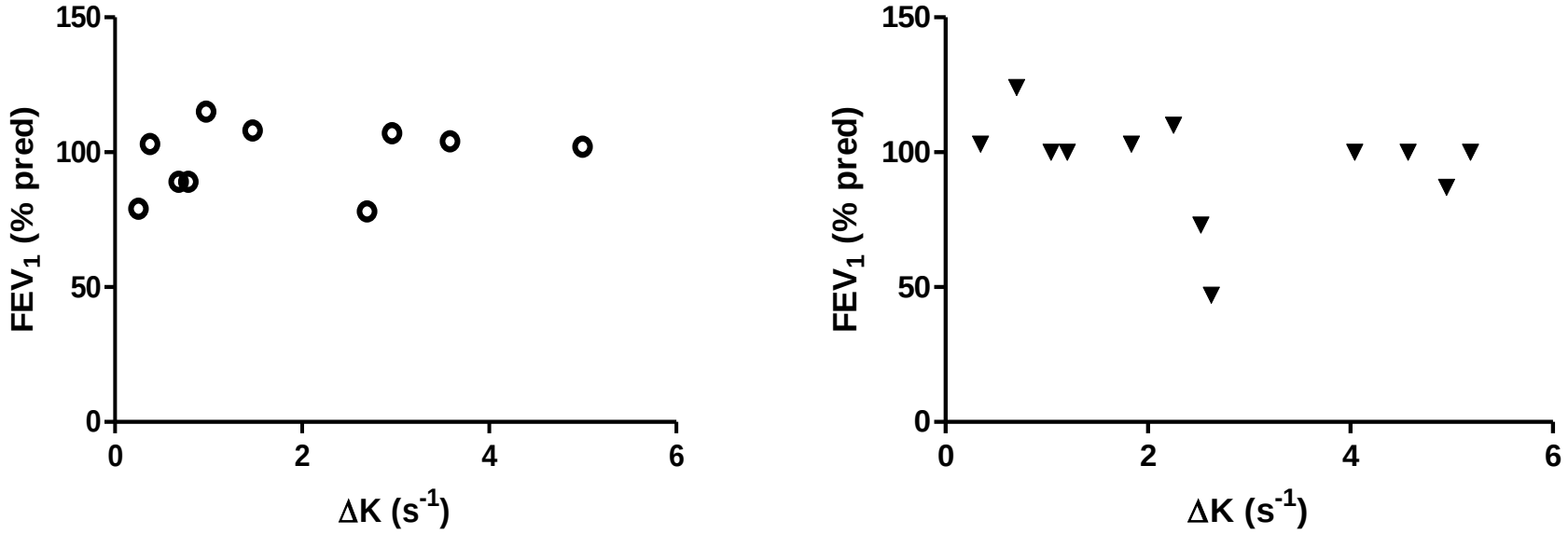

Figure 4.13 FEV_1 as a function of ΔK. There is no significant Pearson correlation between FEV_1 and mean donor ΔK for (a) normal (n=10) or, (b) asthma (n=12) donors.

Table 4.1 Clinical characteristics (A = Asthma, N = Normal)						
Age	**Sex**	**FEV_1 (% pred)**	**Diagnosis**	**K_{-CPA}**	**K_{+CPA}**	**ΔK**
57	M	100	A	2.468	1.267	1.201
52	M	73	A	3.107	0.586	2.521
33	F	100	A	5.524	0.956	4.568
63	M	100	A	7.139	1.954	5.185
63	M	100	A	5.759	1.716	4.043
61	M	103	A	2.563	0.730	1.833
28	F	47	A	3.947	1.323	2.624
52	M	87	A	7.109	2.160	4.949
19	F	100	A	1.590	0.549	1.041
57	F	103	A	2.074	1.729	0.345
50	F	110	A	3.482	1.229	2.253
		124	A	1.961	1.258	0.703
63	M	108	N	2.054	0.581	1.473
59	M	115	N	2.918	1.942	0.976
57	F	89	N	3.335	2.550	0.785
		104	N	4.855	1.274	3.581
36	M	79	N	1.314	1.061	0.253
54	M	103	N	1.929	1.553	0.376
20		78	N	3.063	0.367	2.697
77	M	102	N	6.016	1.019	4.997
25	F	107	N	4.458	1.498	2.960
24	M	89	N	3.166	2.486	0.680

a)

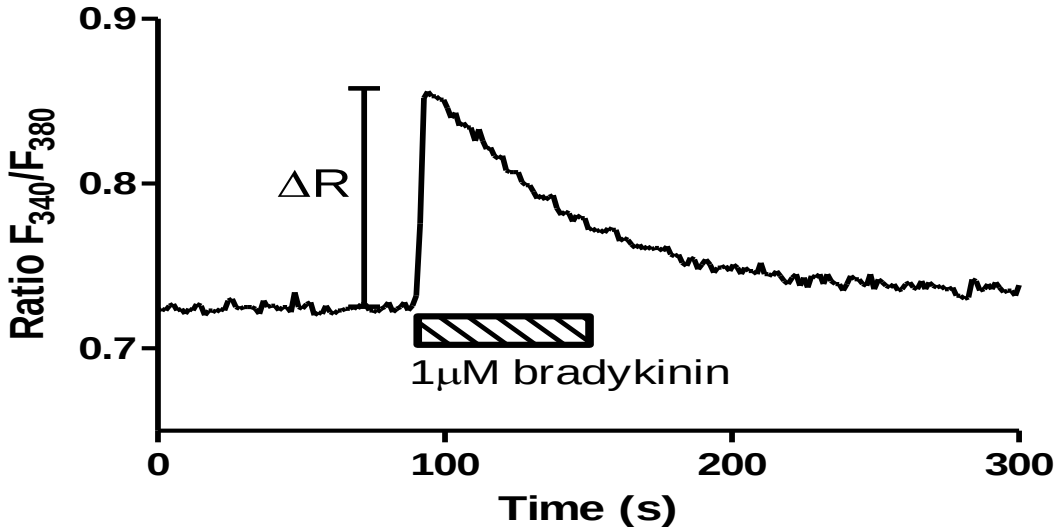

b) 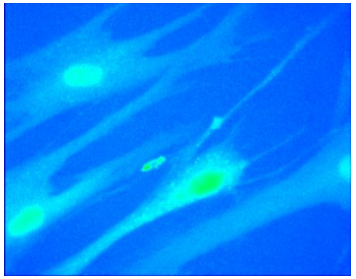

c) 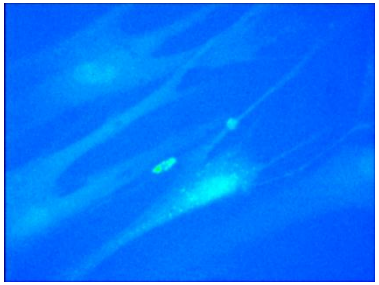

d) 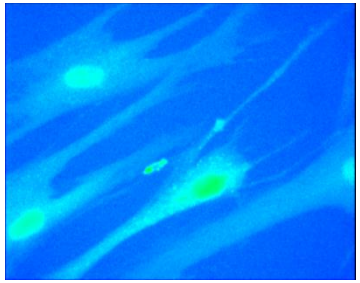

Figure 4.14 The effect of bradykinin (1μM) addition to a single representative hASM cell. Before bradykinin addition, the fura-2 loaded hASM cells appear bright (b). During a 60s perfusion of bradykinin, $[Ca^{2+}]_i$ increases from a basal to a peak fluorescence ratio and the cells appear less bright (c). Homeostatic mechanisms then act to remove the released $[Ca^{2+}]_i$ from the cytoplasm in an exponential decay process (a), returning the cell back to a quiescent state (d). All images excited at λ = 380nm @ x40 magnification.

4.2.4 Bradykinin induced $[Ca^{2+}]_i$ release

Increasing $[Ca^{2+}]_i$ using the agonist bradykinin represents a more complex system than $[Ca^{2+}]_i$ uncaging, since it involves ligand activation of a signaling cascade. Bradykinin binds to cell surface B_2 bradykinin receptors leading to $G\alpha_q$-dependent activation of phospholipase C and the generation of the second messenger IP_3. IP_3 in turn binds to IP_3Rs, which are Ca^{2+} channels within the sarcoplasmic reticulum, thus increasing $[Ca^{2+}]_i$ (Marsh *et al.*, 1992). Whereas Ca^{2+} uncaging is a conceptually simpler, receptor independent, demonstration of a cellular homeostatic (efflux) response to a local burst of $[Ca^{2+}]_i$ (Kao, 2006), bradykinin stimulation on the other hand can be viewed as demonstrating receptor-dependent $[Ca^{2+}]_i$ handling involving the whole cell. The latter is also clinically relevant to asthma since bradykinin is present in the inflammatory milieu (Barnes, 1992). Thus, for the agonist addition method of investigating $[Ca^{2+}]_i$ handling, both the amount of IP_3 generated and the rate kinetics of $[Ca^{2+}]_i$ decay were investigated.

Application of bradykinin to hASM cells causes a rapid increase in $[Ca^{2+}]_i$ (Figure 4.14). This was monitored using the fluorescence ratio, $R = F_{340}/F_{380}$, of fura-2. Hence, the fluorescence change (ΔR) is calculated because it is proportional to the increase in $[Ca^{2+}]_i$. Bradykinin was applied for 60s and the subsequent peak to baseline decay process represents the $[Ca^{2+}]_i$ recovery response of the cell. It gives a useful functional indication of how living hASM cells handle an agonist driven increase in $[Ca^{2+}]_i$. That is, the overall rate process (K) describes the dynamic changes that act to drive the cell back to basal $[Ca^{2+}]_i$ homeostasis during exposure to 1µM bradykinin for 60s. As with Ca^{2+} uncaging responses, this process can be readily modelled by exponential decay kinetics.

Measurements of the subsequent $[Ca^{2+}]_i$ response will be presented. This includes basic metrics, including baseline to peak fluorescence ratio change (ΔR) and area under the curve (AUC) over a time window of 60s corresponding to the duration of bradykinin application. These measurements give an indication of the amount of agonist stimulated $[Ca^{2+}]_i$ release. Also, the rate at which $[Ca^{2+}]_i$ declines from peak to baseline (K) was determined to give an indication of the kinetics of $[Ca^{2+}]_i$ efflux and/or sequestration to restore resting $[Ca^{2+}]_i$, driving the cell back to homeostasis. The amount of IP_3 generated was also measured.

4.2.4.1 Inositol 1,4,5-trisphosphate (IP_3)

No significant differences were observed in bradykinin-IP_3 concentration-responses in hASM cells from asthma or normal donors (figure 4.15a and b). Figure 4.15c shows representative examples of concentration-response curves obtained in hASM cells obtained from asthma and normal donors. In these examples, bradykinin stimulated approx. 8-10 fold increases in IP_3 accumulation over basal levels with EC_{50} values of approx. 100 nM.

When assessing hASM data from all normal (n=8) and asthma (n=11) donors no significant differences in bradykinin EC_{50} values or basal-to-peak IP_3 increases were seen after stimulation with bradykinin (Figure 4.16a, b). Mean increases in $[IP_3]$ (595 ± 45 versus 607 ± 54 pmol mg^{-1} protein) and EC_{50} values (74 versus 67 nM: pEC_{50} (M) values: 7.133 ± 0.083 versus 7.122 ± 0.075) were nearly identical between normal and asthma groups. In addition, for normal and asthma donors, there was no significant clinical correlation when FEV_1 was plotted as a function of either bradykinin pEC_{50} (Figure 4.17) or $[\Delta IP_3]$ (Figure 4.18). Table 4.2 lists the clinical characteristics of the asthma and normal donors used.

a) b)

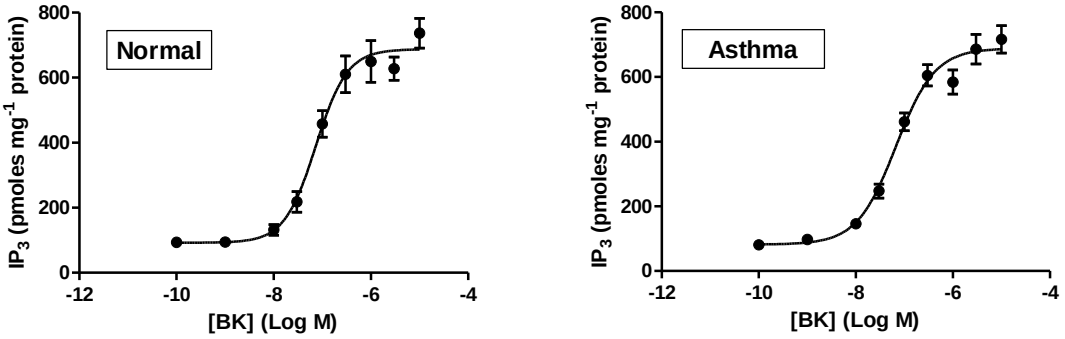

c)

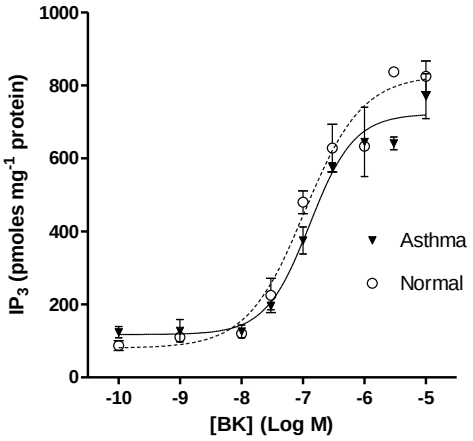

Figure 4.15 Concentration-dependent IP_3 responses to bradykinin in hASM derived from normal and asthmatic donors. There was no significant difference (Student's t-test) in cumulative bradykinin-IP_3 concentration response curves for (a) normal (n=8), and (b) asthma (n=11) hASM cell donors. (c) Representative examples of concentration-response curves in one asthma and one normal hASM cell donor. The amount of IP_3 (in pmol mg^{-1} protein) was measured after exposure to bradykinin concentrations ranging from 1 nM to 10 µM for 15 sec.

a)

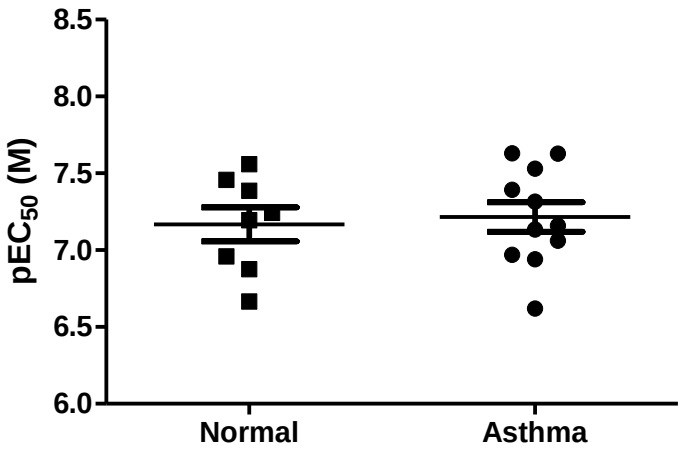

b)

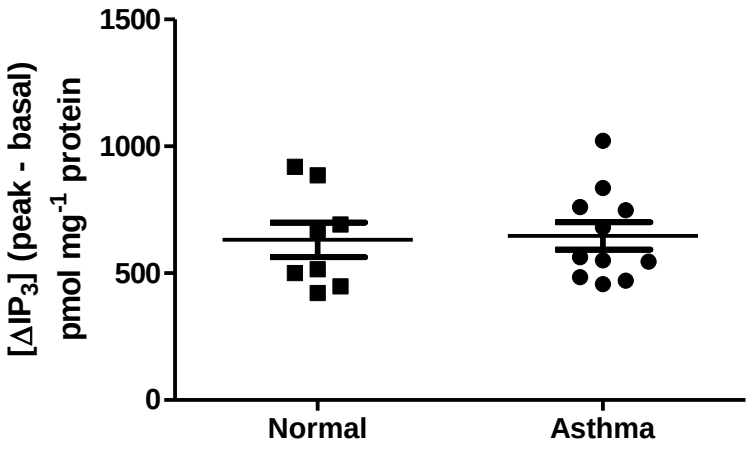

Figure 4.16 a) Graph showing the bradykinin pEC_{50} (M) (-log [bradykinin] (mean±sem) causing an IP_3 accumulation that is 50% of the maximal value) in asthma (n=11) and normal (n=8) hASM cell donors. b) The change in IP_3 accumulation basal-to-peak (i.e. ΔIP_3) after stimulation by 10µM bradykinin for asthma (n=11) and normal (n=8) hASM cell donors. For both responses no significant differences (Student's t-test) between asthma and normal donors were observed.

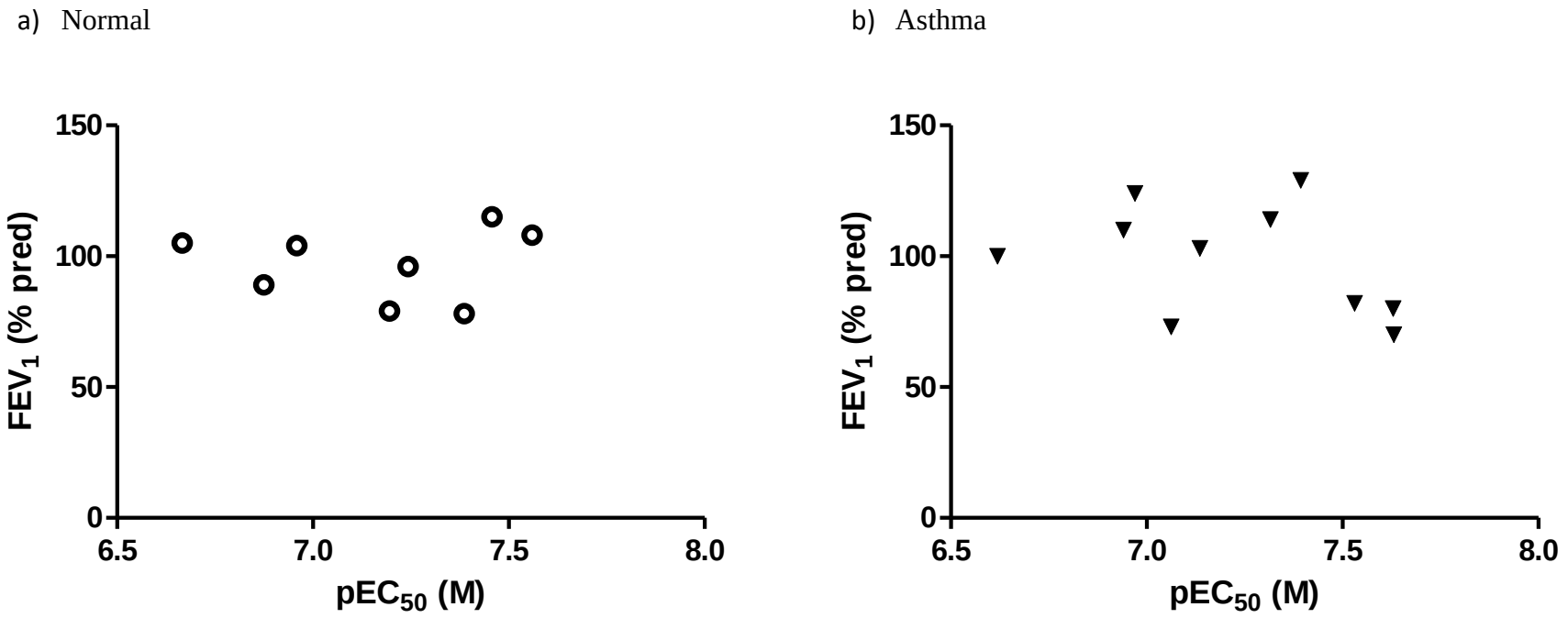

Figure 4.17 Graph showing that there is no significant Pearson correlation between FEV_1 plotted as a function of pEC_{50} (M) in either (a) normal (n=8) or, (b) asthma donors (n=10).

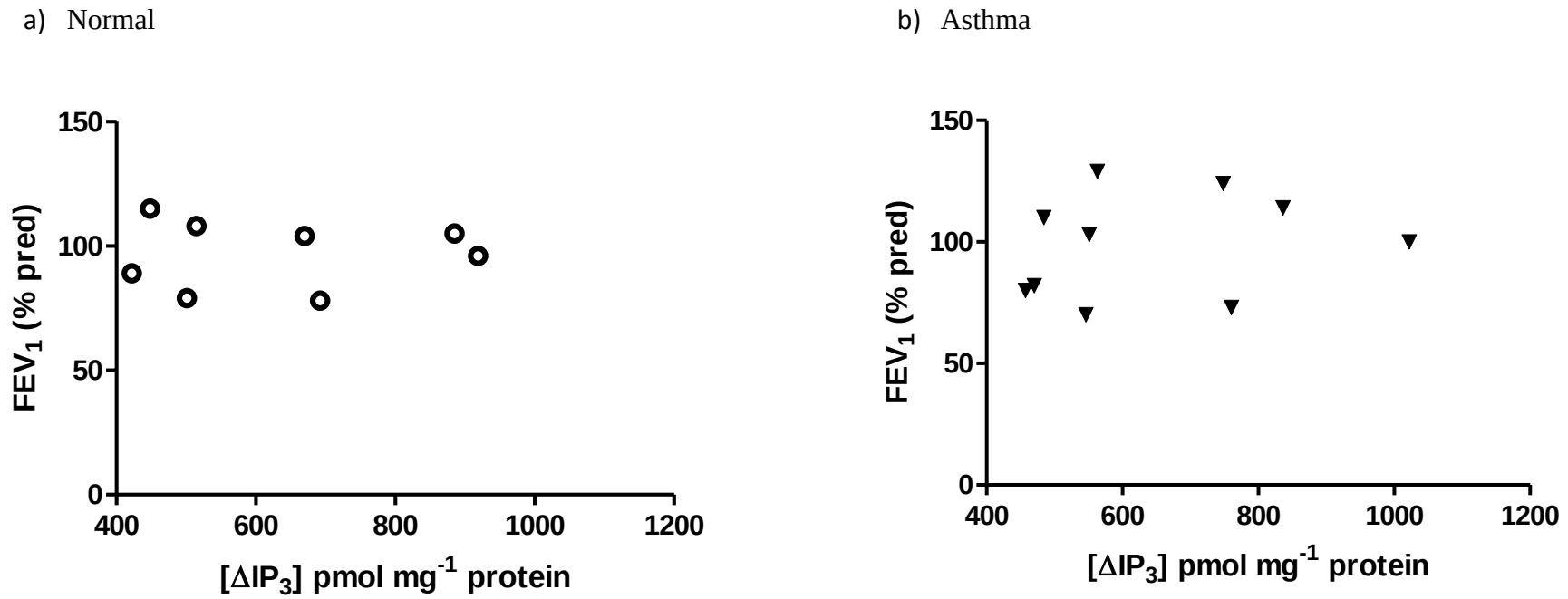

Figure 4.18 Graph showing that there is no significant Pearson correlation between FEV_1 plotted as a function of $[\Delta IP_3]$ (peak – basal) for (a) normal (n=8) or, (b) asthma donors(n=10).

Table 4.2 **Clinical characteristics** (A = Asthma, N = Normal)					
Age	**Sex**	**FEV_1 (% predicted)**	**Diagnosis**	**pEC_{50} (M)**	**Increase over basal ([ΔIP_3])**
32	M	82	A	7.530	470
57	M	100	A	6.619	1022
40	M	70	A	7.630	546
48	F	80	A	7.629	457
73	F	129	A	7.393	563
52	M	73	A	7.062	760
42	F	114	A	7.315	836
57	F	103	A	7.135	551
50	F	110	A	6.940	484
39	F		A	7.159	681
		124	A	6.970	748
63	M	108	N	7.560	515
59	M	115	N	7.457	448
27	F	96	N	7.243	919
52	M	105	N	6.666	885
		104	N	6.959	670
20	M	78	N	7.386	692
61	F	79	N	7.195	501
24	M	89	N	6.875	422

4.2.4.2 ΔR for hASM cells and donors

A comparison of single cell baseline-to-peak $[Ca^{2+}]_i$ responses (ΔR) to bradykinin is presented for normal and asthma hASM cells (Figure 4.19). $[Ca^{2+}]_i$ responses were not significantly different between asthma and normal hASM cells and the distribution appears normal or Gaussian in shape. The basal-to-peak average $[Ca^{2+}]_i$ responses (ΔR) of cells from individual donors to bradykinin is shown in Figure 4.20. As for the cell data in Figure 4.19, individual donors show no statistically significant difference between $[Ca^{2+}]_i$ responses in normal and asthma hASM cells.

4.2.4.3 Area under the curve, AUC

Area under the bradykinin mediated $[Ca^{2+}]_i$ response curve gives an indication of the cytoplasmic $[Ca^{2+}]$ increase during the 60 second stimulation period. That is, AUC from peak response at t=0s to t=60s, or $AUC_{t=0\rightarrow 60s}$. Figure 4.21 shows the distribution of cellular AUC $[Ca^{2+}]_i$ responses and Figure 4.22 shows the mean AUC per donor. In Figure 4.21, the distribution of cellular AUC appears to be right skewed. In both cases, the AUC distribution of cells and donors shows a non-significant difference between normal and asthma.

4.2.4.4 Rate of bradykinin mediated $[Ca^{2+}]_i$ decline (K)

Decay or decline rate constant, K, values were determined for each $[Ca^{2+}]_i$ response by non-linear regression. Figure 4.23 shows the rate of decline after stimulation with bradykinin (1μM). There was no statistical difference between K values for normal and asthma hASM cells. The rate of donor recovery is shown in Figure 4.24. Similarly, there was no statistical difference between K values for hASM cells from normal and asthma donors.

There was also no significant correlation of FEV_1 as a function of $[Ca^{2+}]_i$ decline rate K (Figure 4.25) for normal and asthma donors. However, there was a significant correlation of FEV_1/FVC as a function of log K for normal and asthma donors, which was preserved in the asthma-only group (Figure 4.26). Hence, there appears to be a correlation of AFO (FEV_1/FVC) with log K but this is not reflected in airflow impairment (i.e. FEV_1) and log K. Table 4.3 gives clinical details of the normal and asthma donors used.

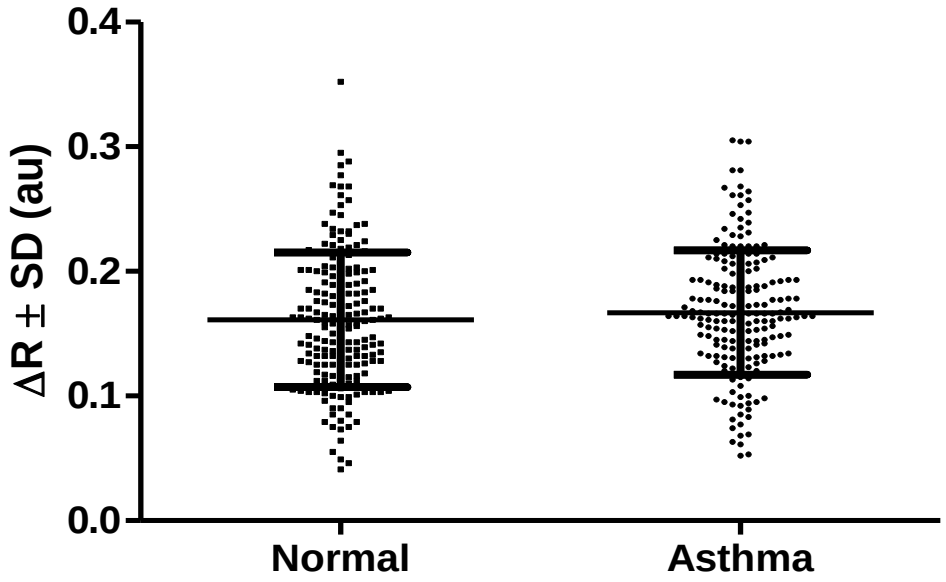

Figure 4.19 Peak change in fluorescence ratio, ΔR, relative to basal in hASM cells stimulated by bradykinin (1μM). There is no significant difference (Student's t-test) in the release of $[Ca^{2+}]_i$ from asthma (n=193) or normal (n=186) hASM cells.

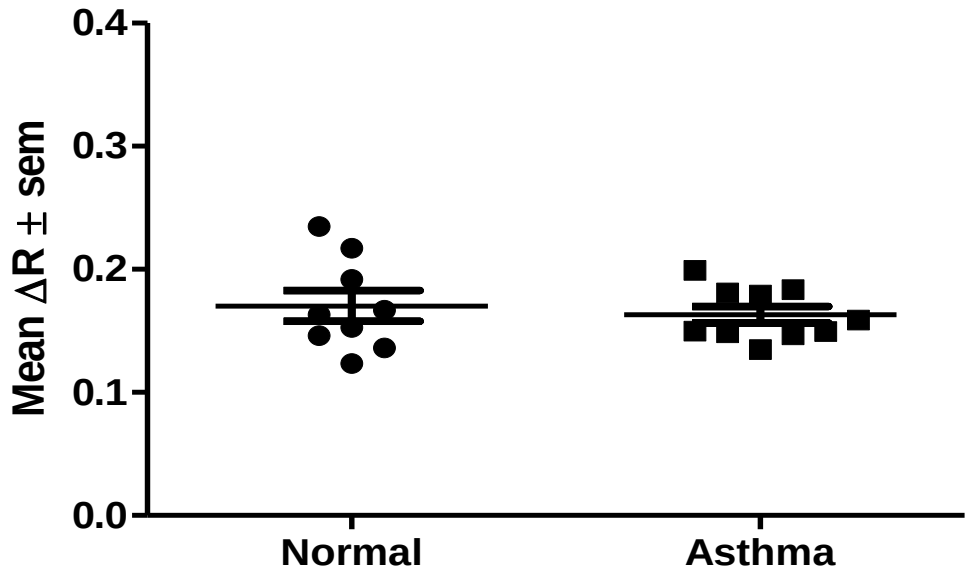

Figure 4.20 Mean change in R (ΔR), peak relative to basal in hASM cells from asthma (n=10) and normal (n=9) donors in response to bradykinin (1μM). There is no significant difference (Student's t-test) in the reaction of hASM cells from asthma or normal donors to Ca^{2+} mobilization by bradykinin.

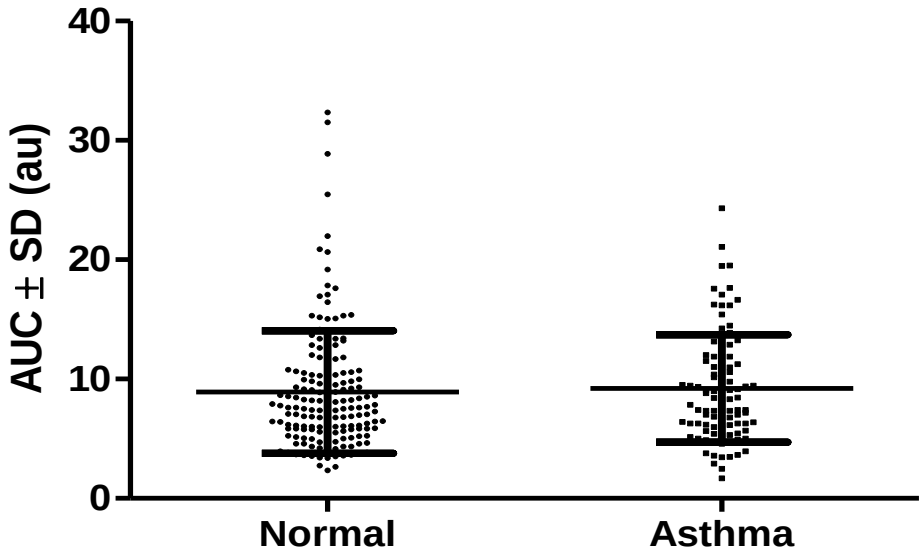

Figure 4.21 AUC (area under curve) for $[Ca^{2+}]_i$ responses of hASM cells after application of bradykinin (1μM). There is no significant difference (Student's t-test) in the reaction of hASM cells from asthma (n=98) or normal (n=165) to Ca^{2+} mobilization by bradykinin.

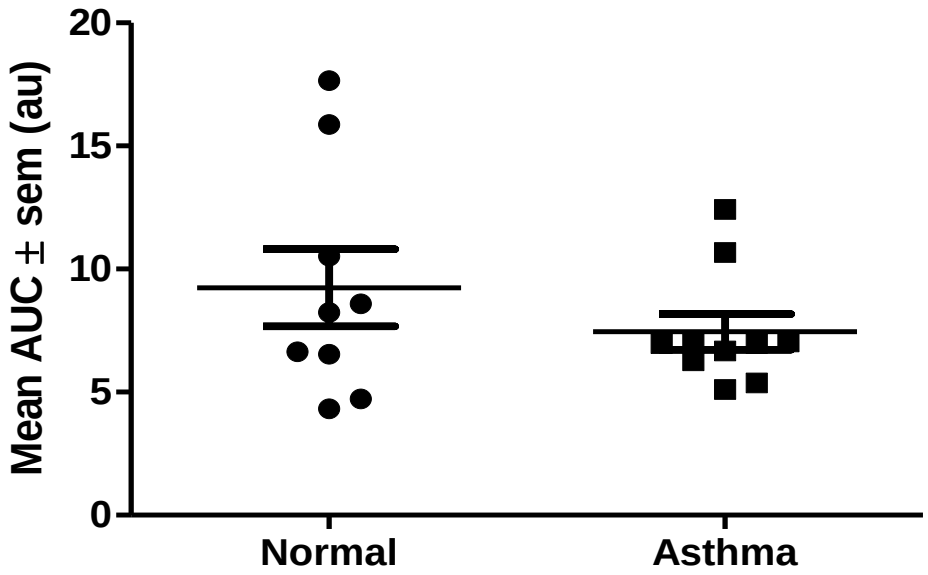

Figure 4.22 Mean AUC (area under curve) for $[Ca^{2+}]_i$ responses of asthma and normal donors to bradykinin (1μM). There is no significant difference (Student's t-test) in the reaction of hASM cells from asthma (n=10) or normal (n=9) donors to Ca^{2+} mobilization by bradykinin.

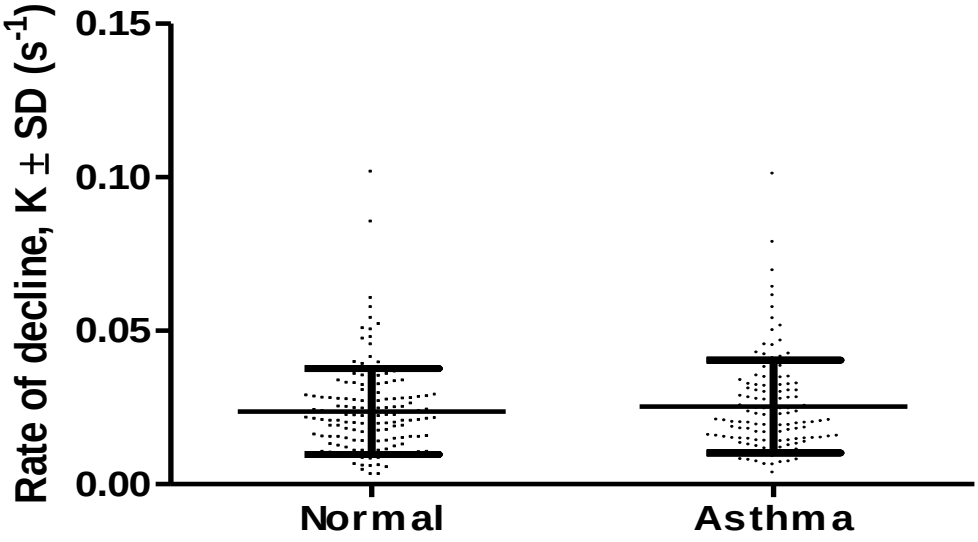

Figure 4.23 Rate of decline (K) from bradykinin-mediated $[Ca^{2+}]_i$ release in single hASM cells. There is no significant difference (Student's t-test) in the reaction of hASM cells from asthma (n=133) or normal (n=151) to Ca^{2+} mobilization by bradykinin.

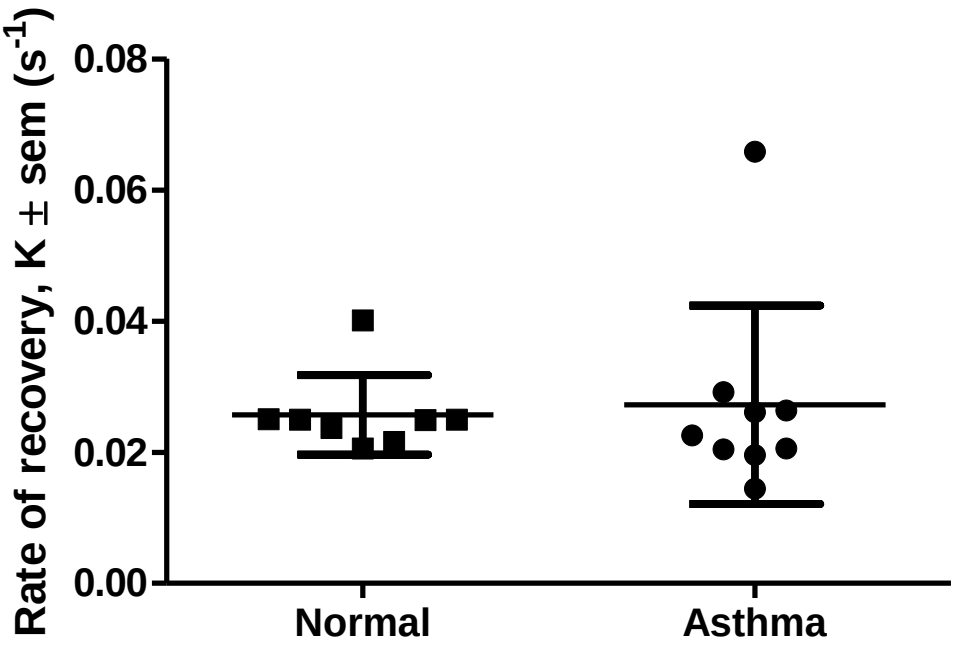

Figure 4.24 Rate of decline from bradykinin mediated Ca^{2+} release in hASM cells from normal and asthma donors. There is no significant difference (Student's t-test) in the reaction of hASM cells from asthma (n=8) or normal (n=9) donors to Ca^{2+} mobilization by bradykinin.

a) Normal

b) Asthma

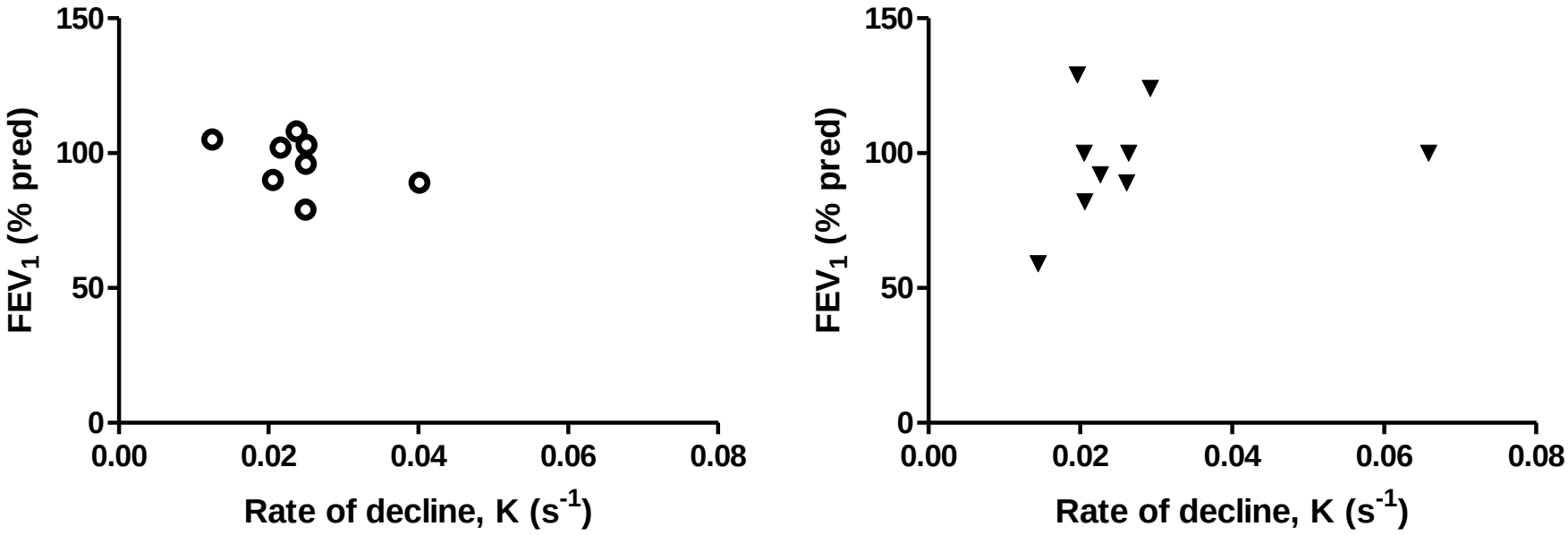

Figure 4.25 There is no significant Pearson correlation of FEV_1 as a function of rate of decline of bradykinin-stimulated $[Ca^{2+}]_i$ release for (a) normal (n=8) or, (b) asthma (n=9) donors.

a) Normal and asthma

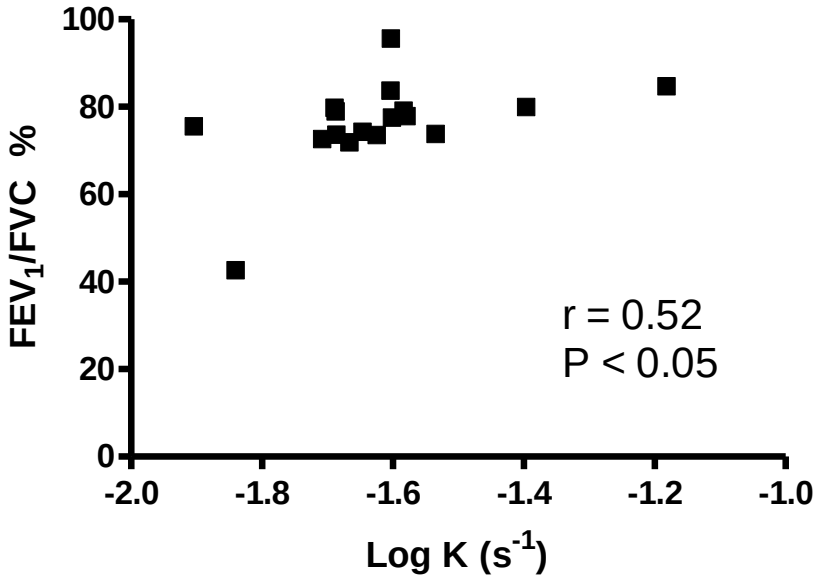

b) Asthma only

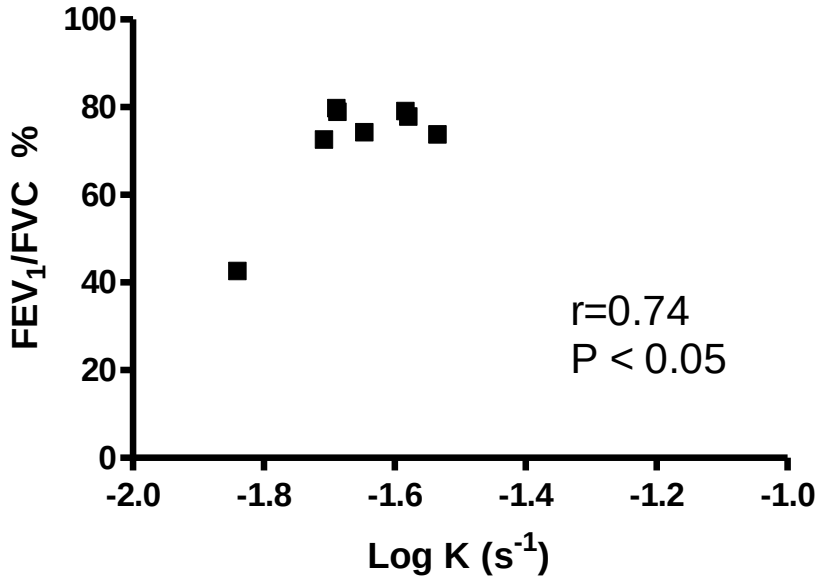

Figure 4.26 a) Pearson correlation between FEV_1/FVC as a function of log K is significant for, (a) asthma and normal donors (n=17, r=0.52, P<0.05), and also significant for, (b) asthma donors (n=8, r=0.74, P<0.05) only.

Table 4.3 **Clinical characteristics** (A = asthma, N = Normal)				
Age	**Sex**	**FEV_1 (% predicted)**	**Diagnosis**	**K (s^{-1})**
23	Male	92	A	0.0226
32	Male	82	A	0.0205
66	Male	59	A	0.0144
73	Female	129	A	0.0196
34	Male	89	A	0.0261
33	Female	100	A	0.0205
		124	A	0.0292
63	Male	100	A	0.0263
19	Male	100	A	0.0658
63	Male	108	N	0.0237
27	Female	96	N	0.0249
52	Male	105	N	0.0125
57	Female	89	N	0.0401
57	Female	102	N	0.0216
36	Male	79	N	0.0249
54	Male	103	N	0.0250
77	Female	90	N	0.0206

4.2.5 Caffeine

Caffeine is a member of the methylxanthine family of compounds. Another methylxanthine, theophylline, is used as a bronchodilator in second-line treatment of asthma. Caffeine has various smooth muscle actions. It is a PDE inhibitor, an IP_3R and adenosine receptor antagonist and a RyR agonist. I found purely by chance that caffeine generates a rapid onset, significant decrease in baseline $[Ca^{2+}]_i$ in hASM cells (Figure 4.27a and b). Caffeine addition was initially considered as an inexpensive positive control, for its agonist-like properties at the end of $[Ca^{2+}]_i$ characterisation experiments. The observed effect is similar to removing extracellular Ca^{2+}, and caffeine treatment abolishes any baseline Ca^{2+} oscillatory activity (see Figure 4.27a). I have not exhaustively explored the mechanism(s) through which caffeine exerts this action, however, I have shown that there was no significant difference in the ability of caffeine to reduce basal $[Ca^{2+}]_i$ between asthma and normal donors (Figure 4.28).

One potential mechanism of action of caffeine is to inhibit the IP_3R, thus blocking Ca^{2+} efflux into the cytoplasm from the SR. This would suggest that Ca^{2+} release via IP_3Rs could be significant in hASM cells under basal conditions and might contribute to observed basal Ca^{2+} oscillatory activities. To test this hypothesis, various concentrations of $[Ca^{2+}]_i$ mobilising agonist bradykinin in the presence of a fixed concentration of caffeine (10mM) were applied to fura-2 loaded hASM cells. Figure 4.29 shows concentration-response curves for bradykinin alone and bradykinin in the presence of caffeine in hASM cells from normal and asthma subjects (n=3). Although small differences were observed at specific concentrations of bradykinin, the overall effect of caffeine was to cause only modest decreases in bradykinin-stimulated $[Ca^{2+}]_i$ responses (Figure 4.29). These data suggest that caffeine likely exerts its effect at a site other than the IP_3R, which I have been unable to define here.

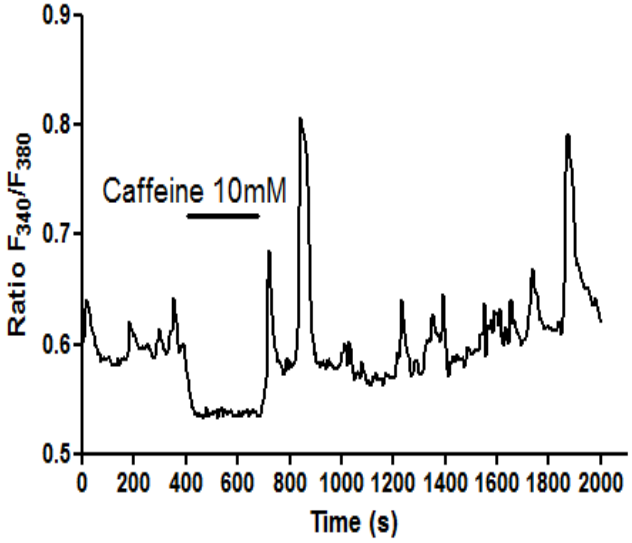

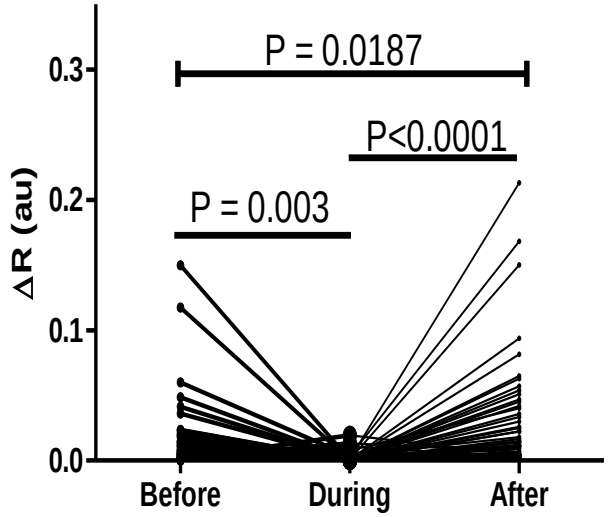

Figure 4.27 a) Representative trace showing effect of 10mM caffeine on the emission ratio following excitation at F_{340}/F_{380} of an asthmatic hASM cell. Notice that $[Ca^{2+}]_i$ oscillations cease and the basal $[Ca^{2+}]_i$ decreases during the application of caffeine.

b) Change in ratio F_{340}/F_{380}, ΔR, before during and after application of 10mM caffeine to asthmatic hASM cells (n=77 cells from 7 hASM cell donors) indicates that caffeine significantly and reversibly decreases $[Ca^{2+}]_i$.

a)

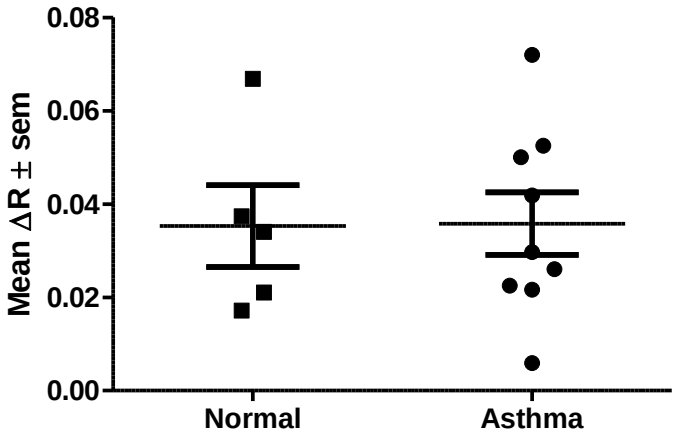

b)

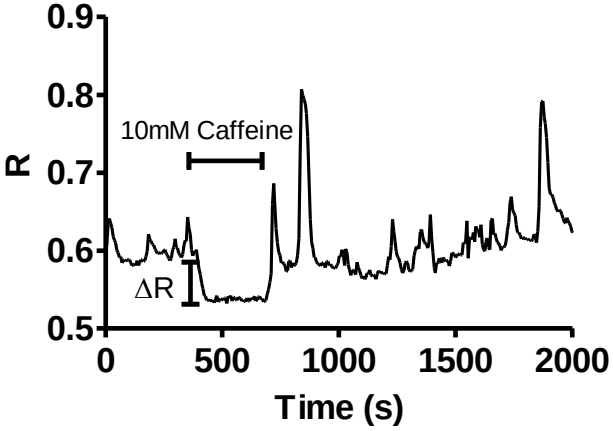

Figure 4.28 a) Effect of 10mM caffeine on basal $[Ca^{2+}]_i$ in hASM cells from asthma (n=9) and normal (n=5) donors. The decrease in $[Ca^{2+}]_i$, which is proportional to ΔR, showed no significant difference (Student's t-test) between asthma and health. b) Shows a representative Ca^{2+} waveform. The change in basal $[Ca^{2+}]_i$ fluorescence, ΔR = basal R – R during caffeine perfusion.

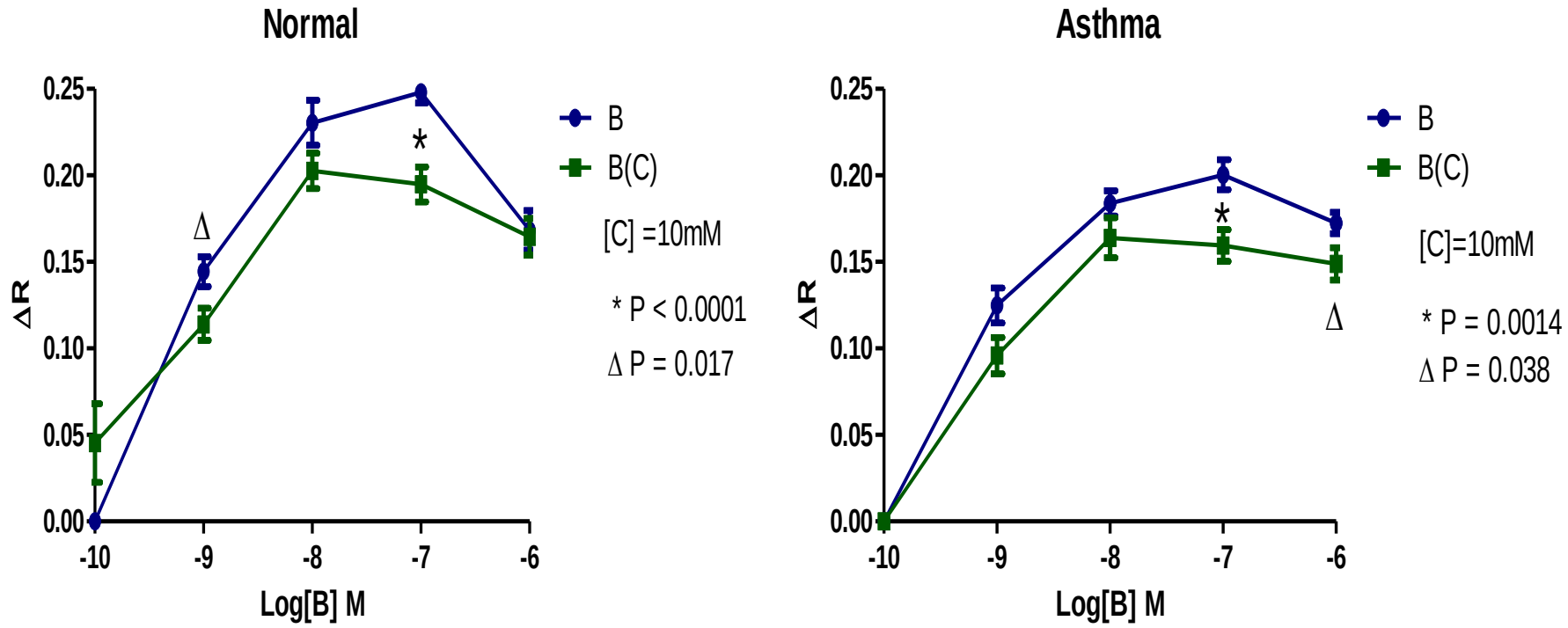

Figure 4.29 Concentration-response curves representing the change in R with bradykinin (B), or with bradykinin in the presence of 10mM caffeine (B(C)). Data are shown for asthma (n=3) and normal (n=3) donors; 5 cells per donor, Student's t-test used for P values.

4.2.6 Store operated Ca^{2+} entry (SOCE)

The protocol for measuring changes in fura-2 fluorescence ratio (R) during store emptying and store refilling is shown in Figure 4.30. Figure 4.31 shows the change in fluorescence (ΔR) associated with SR Ca^{2+} store depletion or emptying after SERCA inhibition by CPA under low extracellular Ca^{2+} conditions. Subsequent SR Ca^{2+} store refilling (ΔR) when normal (2mM) Ca^{2+} buffer was reperfused, inducing a SOCE response, is shown in Figure 4.32. There was not a statistically significant difference in Ca^{2+} store emptying or store refilling in asthma compared to normal donors.

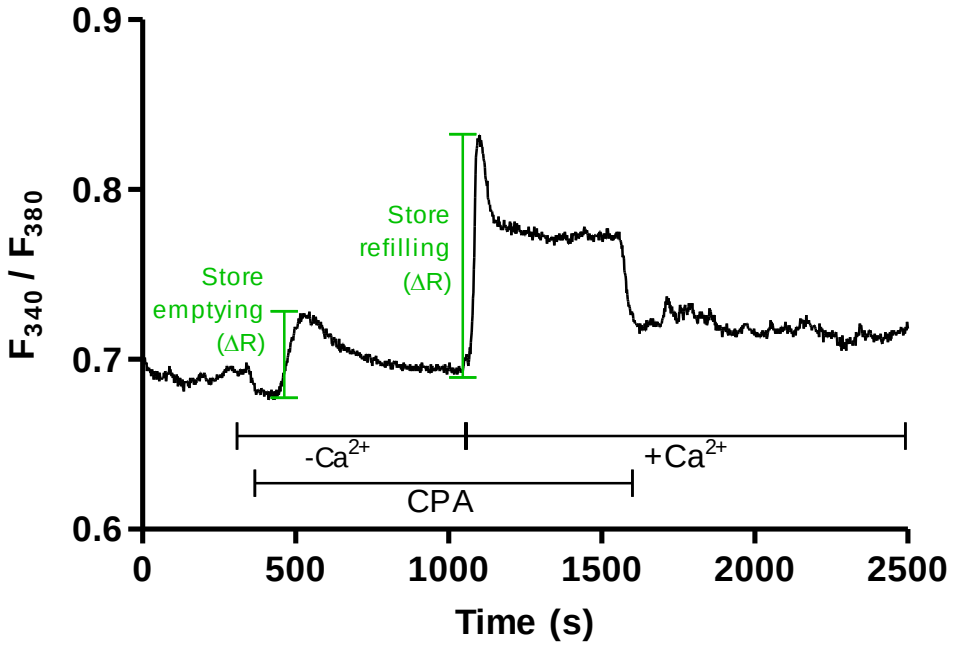

Figure 4.30 Store operated Ca^{2+} entry (SOCE) protocol. After 300s in normal (2mM) Ca^{2+}-containing buffer, low Ca^{2+} buffer was perfused for 60s to reduce $[Ca^{2+}]_i$ levels. At this point, CPA (10µM) was perfused to release Ca^{2+} stored in the SR by inhibiting SERCA. After 600s normal (2mM) Ca^{2+}-containing buffer was re-introduced ($+Ca^{2+}$) in the continued presence of CPA. This initially causes a maximum Ca^{2+} peak as maximum SOCE occurs to refill the SR Ca^{2+} store. This quickly falls to a constant plateau raised above the starting baseline as Ca^{2+} flux courses through the cell unopposed by SERCA. Removal of CPA from the perfusion buffer causes the $[Ca^{2+}]_i$ to decrease indicating that CPA rapidly dissociates from SERCA which regains function to remove excess $[Ca^{2+}]$ from the cytoplasm to the SR.

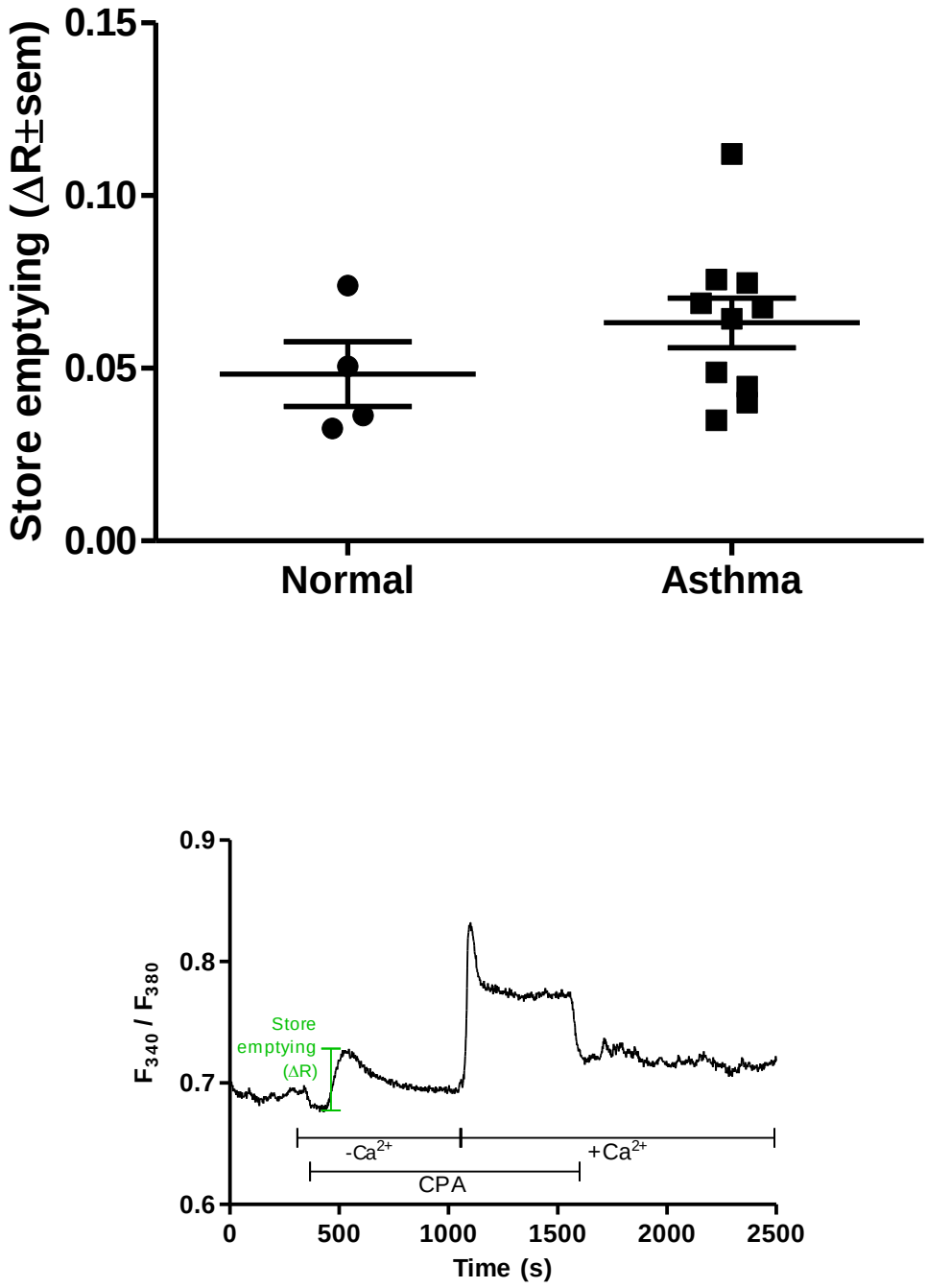

Figure 4.31 Mean store empting (ΔR ± sem) is not significantly different (Student's t-test) between hASM cell asthma (n=10) and normal (n=4) donors. The pane below indicates store emptying (in green) on a representative trace.

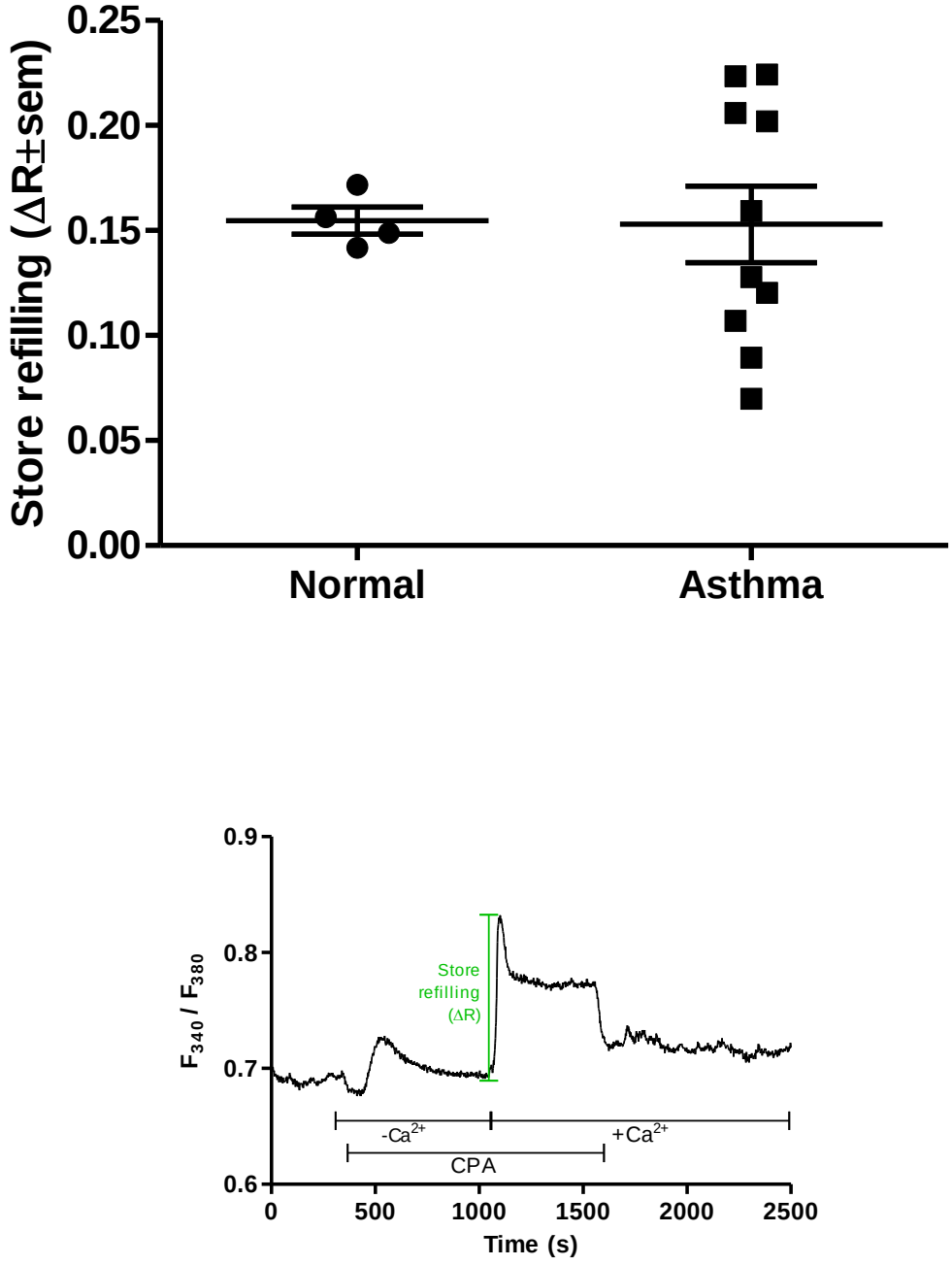

Figure 4.32 Mean Ca^{2+} store -refilling (ΔR ± sem) is not significantly different (Student's t-test) between hASM cell asthma (n=10) and normal (n=4) donors. The pane below indicates store refilling (in green) on a representative trace.

4.3 Discussion

4.3.1 Ca^{2+} uncaging

For various cell types, UV flash photolysis has been used to break down the molecular cage holding biologically active molecules; examples include Ca^{2+}, IP_3, cAMP and even caffeine. Uncaging of Ca^{2+} was used to examine the dynamics of intracellular Ca^{2+} handling, which is the focus of this chapter.

Previous studies utilising Ca^{2+} uncaging in smooth muscle have concentrated on the intracellular kinetics of CICR; for example, in isolated rabbit urinary bladder myocytes (Ji *et al.*, 2006; Wang *et al.*, 2006), and other cell types such as pancreatic acinar cells (Ashby *et al.*, 2002). Moreover, local Ca^{2+} uncaging has proved useful in CICR mechanistic studies, for example it has been shown that Ca^{2+} uncaging induces further Ca^{2+} release through RyRs and IP_3Rs (Wang *et al.*, 2006). But Ca^{2+} uncaging using UV flash photolysis is a versatile technique and has applications beyond dissecting CICR; for example in other cell systems it has been employed to analyse intercellular Ca^{2+} kinetics. Other notable examples include the analysis of interalveolar Ca^{2+} signaling in relation to lung surfactant secretion (Ichimura *et al.*, 2006) and intercellular Ca^{2+} waves propagated via gap junctions in HeLa cells (Nakano *et al.*, 2009).

However, the methodology presented here is most closely related to that of a group working on cystic fibrosis (CF) at Université de Poitiers, France (Antigny *et al.*, 2008). This group generated UV photo-activated intracellular Ca^{2+} transients in airway epithelial cells to compare Ca^{2+} handling kinetics in CF and non-CF donors. I have translated and modified their method of Ca^{2+} uncaging for use with hASM cells, but the method of analysis using an exponential decay rate parameter, K, is significantly

different. There are no published studies involving release of caged Ca^{2+} in single hASM cells.

I have shown that a local rapid increase in $[Ca^{2+}]_i$ can be generated in a direct and reproducible manner by UV flash photolysis of NP-EGTA caged Ca^{2+}. In my experiments, I have demonstrated that a locally directed burst of laser energy at 405nm into a region of hASM cell cytoplasm can induce a rapid increase in $[Ca^{2+}]_i$ that exponentially decays back to baseline without inducing a cell-wide CICR response. Although by increasing laser energy and/or duration of exposure I was able to produce CICR, this was not the aim of my study. The aim was to create a system whereby the response of the cell to a local increase in $[Ca^{2+}]_i$ could be monitored in real time to test the recently published postulate, (see Introduction), that $[Ca^{2+}]_i$ handling is dysfunctional in asthma hASM cells. Moreover, the exponential decay rate determined for the decrease in Ca^{2+} following uncaging is a direct measure of the ability of the cellular Ca^{2+} homeostatic system to handle an increase in $[Ca^{2+}]_i$. Using this experimental system I was able to derive exponential $[Ca^{2+}]_i$ decay rate constants, K, in hASM cells from asthma and normal donors. This approach to investigating the postulate that $[Ca^{2+}]_i$ handling is dysfunctional in asthma hASM cells is both comprehensive and efficient. It tests the dynamic Ca^{2+} reaction kinetics of the hASM cell, dispensing with the need to characterise the properties of each constituent protein of the Ca^{2+} homeostasis system, and their relative cellular locations. Furthermore, it also has the advantage over other methods of raising $[Ca^{2+}]_i$, for example through agonist-dependent mechanisms, of causing a rapid increase in $[Ca^{2+}]_i$ without the simultaneous activation of signal transduction elements that might contribute to the subsequent handling of the elevated $[Ca^{2+}]_i$. For example, a receptor-mediated increase in $[Ca^{2+}]_i$ might occur via both Ca^{2+} mobilisation and influx routes but might

additionally activate subsidiary pathways, for example, a PKC-dependent modulation of plasmalemmal Ca^{2+}-ATPase activity. This effect would contribute to any differences in pure $[Ca^{2+}]_i$ handling observed in asthma compared to normal hASM cell donors. However, no significant differences in $[Ca^{2+}]_i$ recovery rates, K, in hASM cells from normal and asthma donors were observed using the Ca^{2+} uncaging methodology.

Recent high profile papers, (see Introduction), reported that a diminished expression of the Ca^{2+} homeostatic protein SERCA was evident in asthma hASM cells. This prompted me to also investigate the effect of removing SERCA, by pharmacological inhibition, on cellular Ca^{2+} kinetics in hASM cells from normal and asthma donors. The SERCA inhibitor CPA was used and the UV flash photolysis Ca^{2+} uncaging method increased local $[Ca^{2+}]_i$.

My theoretical model suggested that if SERCA was diminished, then based on the Mahn postulate (Mahn *et al.*, 2009) of dysfunctional $[Ca^{2+}]_i$ handling, $\Delta K_{asthma} < \Delta K_{normal}$. Indeed, there was an expected decrease in K after application of CPA. This is because locally uncaged $[Ca^{2+}]_i$ is removed more slowly by the Ca^{2+} homeostasis system when SERCA activity is inhibited. However, the magnitude of ΔK, which is a measure of SERCA function, was not significantly different in hASM cells from asthma compared to normal donors. Therefore, my experimental data on the actions of CPA on Ca^{2+} uncaging recovery kinetics do not support the Mahn postulate. This demonstrates that the contribution made by SERCA to the hASM cell Ca^{2+} homeostasis system is unlikely to be dysfunctional in asthma compared to normal.

These functional studies on the kinetics of cellular recovery after a Ca^{2+} uncaging event have shown that at least in my hands there is no significant difference in the way hASM cells from asthma and normal donors handle a transient increase in $[Ca^{2+}]_i$ as defined by

ΔK. This finding was also supported by real time PCR and western blotting studies indicating that there was no significant change in SERCA2abc mRNA gene transcription or SERCA protein expression respectively.

The functional and structural results taken together demonstrate that there was not a significant difference in Ca^{2+} handling in asthma compared to normal hASM cells, as might be expected if SERCA expression were either diminished or dysfunctional in asthma.

There was also no significant correlation between FEV_1 as functions of K_{-CPA}, K_{+CPA} or ΔK for asthma or normal hASM cell donors. This indicates that the rate of recovery after an increase in $[Ca^{2+}]_i$ is not associated with airway physiology parameter, FEV_1, and this result persists even if SERCA activity is removed from the system for both normal and asthma hASM cell donors.

4.3.2 Bradykinin

In addition to the uncaging of Ca^{2+} by UV flash photolysis, I wanted to characterise the effect of an $[Ca^{2+}]_i$ mobilising agonist that is clinically relevant to asthma. Bradykinin was chosen because it produces an increase in $[Ca^{2+}]_i$ in the vast majority of hASM cells. Clinically, bradykinin is present in asthmatic airways and functions as a potent bronchoconstrictor causing cough and neurogenic inflammation (Barnes, 1992). It has been shown to release $[Ca^{2+}]_i$ in airway smooth muscle cells with EC_{50} value around 300nM and is maximally effective at around 10μM (Marsh *et al.*, 1993; Marsh *et al.*, 1994; Yang *et al.*, 1994). Cellular $[Ca^{2+}]_i$ release caused by bradykinin stimulation is mediated via a $G\alpha_q$-sensitive PLC pathway with IP_3 acting as second messenger (Marsh *et al.*, 1992). Furthermore, bradykinin has been shown to enhance $[Ca^{2+}]_i$ signaling in ASM from airway hyperresponsive rats (Tao *et al.*, 2003). However, there are no

published data comparing $[Ca^{2+}]_i$ responses in hASM cells from asthma and normal donors. Therefore, a sub-maximal concentration of 1μM bradykinin was used to generate a $[Ca^{2+}]_i$ increase which decayed exponentially back to basal levels in the epifluorescence video microscopy experimental system used, while higher concentrations of bradykinin could generate CICR.

My results showed that $[Ca^{2+}]_i$ handling, assessed in terms of basal-to-peak, ΔR, values or $AUC_{t=0\rightarrow60s}$, or rate of decline, K, following addition of bradykinin to hASM cells was not significantly different between cells from asthma or normal donors. These data indicate that the Ca^{2+} homeostatic system is not dysfunctional with respect to $[Ca^{2+}]_i$ handling following bradykinin stimulation. Clinically, there was no correlation between FEV_1 and K. Generally, variables were tested for correlations with FEV_1 and FEV_1/FVC and if there is no correlation only the FEV_1 data are shown as this is the most frequently quoted respiratory parameter in clinical practice. However, in this case, there was a significant correlation between FEV_1/FVC and K that was not disease specific. This correlation exists in normal and asthma donors analysed together, but also persists in the asthma only donor sub-group. The correlation r values of 0.52 and 0.74 respectively are based on a low number of donors, n, and hence confidence in this finding is presently low. For example r = 0.74 for the asthma correlation is heavily weighted by the result obtained for a single donor. Hence, if increasing n reinforces this emerging trend, then this will indicate that FEV_1 taken as a fraction of FVC is an important association variable rather than FEV_1 itself. But this correlation appears to be a general property of hASM cells, not disease related. In essence, Ca^{2+} kinetics are not different in hASM cells from asthma or normal donors and agonist-stimulated Ca^{2+} handling, or K, may be associated with a clinical lung function parameter FEV_1/FVC. It is not clear why this should be.

Since bradykinin did not lead to a significant difference in the amount of Ca^{2+} released in hASM cells from asthma and normal donors, it follows that the amount of IP_3 generated should also not have been different. Indeed this was the case, the EC_{50} for bradykinin mediated IP_3 accumulation and the basal-to-peak ΔIP_3, demonstrated that the amount of IP_3 generated in asthma compared to normal hASM cell donors was not significantly different.

4.3.3 Ca^{2+} handling is not significantly altered in asthma

My results also demonstrate that the dynamics of $[Ca^{2+}]_i$ handling is not significantly different in hASM cells from asthma compared to normal donors. On a local scale by Ca^{2+} uncaging or on a cell-wide scale by Ca^{2+} mobilising agonist bradykinin, cellular recovery rate or decline rate (K) is not different in asthma compared to normal. The equivalent outcomes of these two quite different methods increase confidence in this important result. That is Ca^{2+} handling, the rate at which dynamic Ca^{2+} equilibrium or homeostasis is restored after a deliberate disturbance in $[Ca^{2+}]_i$, is not intrinsically altered in asthma compared to normal hASM cell donors. There was no significant correlation between airway physiology, FEV_1, and Ca^{2+} handling, K, indicating that these two variables are not associated. But in the case of $[Ca^{2+}]_i$ liberation by bradykinin stimulation, there may be a non-disease specific correlation between FEV_1/FVC and K.

4.3.4 Caffeine, an anachronous case?

Caffeine (10mM) was found to exert a consistent decrease in basal $[Ca^{2+}]_i$ levels. Caffeine rapidly and reversibly inhibited $[Ca^{2+}]_i$ oscillations in those hASM cells in which baseline $[Ca^{2+}]_i$ oscillations were observed before and after caffeine application. $[Ca^{2+}]_i$ oscillations in rat hepatocytes induced by noradrenaline and vasopressin are

similarly known to be inhibited by 5-10mM caffeine (Combettes *et al.*, 1994). Therefore, I tested the hypothesis that in hASM cells the mechanism of $[Ca^{2+}]_i$ oscillation generation involves opening and closing of IP_3Rs. It has been proposed that this inhibition of $[Ca^{2+}]_i$ oscillations is mediated by caffeine inhibiting IP_3Rs (Missiaen *et al.*, 1994), this is certainly the case in the rat cerebellum (Brown *et al.*, 1992).

However, for hASM cells this explanation is unlikely, since the brakykinin/caffeine concentration-response curve (Figure 4.29) does not show a convincing effect on bradykinin mediated $[Ca^{2+}]_i$ release. At some bradykinin concentrations the effect of caffeine was significant, but this may be due to the high concentration of caffeine used and the fact that it is known to have pleiotropic effects.

However, these data have been included here because caffeine is ingested by millions of people each day in products such as tea and coffee. However, I have found that it consistently and rapidly decreases basal hASM cell $[Ca^{2+}]_i$ levels and baseline $[Ca^{2+}]_i$ oscillations. Moreover, one of its chemical relatives, theophylline, is established in clinical respiratory practice. Hence, maybe caffeine's time is belated and the $[Ca^{2+}]_i$ modifying effect discovered here may become useful clinically for treatment of bronchospasm, if administered by inhalation for example.

4.3.5 SOCE

Both STIM1 and ORAI1 have been shown to play key roles in hASM cell SOCE (Peel *et al.*, 2006; Peel *et al.*, 2008). However, other hASM plasma membrane Ca^{2+} ion channels are also involved, such as TRPC homologues (Corteling *et al.*, 2004) and more recently, a STIM1-mediated reverse mode of NCX has been shown to contribute to Ca^{2+} influx after agonist stimulation (Liu *et al.*, 2010). I investigated whether there is a difference in SOCE in hASM cells from asthma compared to normal donors. This is an

important aspect of Ca^{2+} homeostasis because if differences are found at the single hASM cell level, then this could have important clinical ramifications for asthma. Indeed, a recent paper has shown that STIM1/ORAI mediated SOCE in hASM cells is involved in asthma hASM cell proliferation (Zou *et al.*, 2011).

Once again, the method of assessing SOCE adopted a functional approach. The results showed that there were no significant differences in the key parameters of SOCE function in asthma and normal hASM cells. Hence, I have determined that, in hASM cells from asthma and normal donors, the mechanisms of Ca^{2+} store repletion after a Ca^{2+} store depletion event are not significantly different in asthma compared to normal donors.

4.4 Conclusion

It was found that when $[Ca^{2+}]_i$ homeostasis is deliberately disturbed, dynamic $[Ca^{2+}]_i$ handling in hASM cells is not significantly different in asthma compared to normal donors. I also demonstrated that SERCA function is not different in asthma compared to normal donors. These results were obtained through experiments using Ca^{2+} uncaging or agonist stimulation. This was supported by the finding that SERCA2abc mRNA gene transcription and SERCA2 protein expression were also not significantly different in asthma compared to normal donors. Another important property of Ca^{2+} homeostasis, SOCE function, also was not significantly different in asthma compared to normal donors. These results are important because they do not support the prevailing postulate that $[Ca^{2+}]_i$ handling is dysregulated in asthma hASM cells (Mahn *et al.*, 2009; Prakash *et al.*, 2009; Sathish *et al.*, 2009; Mahn *et al.*, 2010). Generally, there was no correlation of airway physiology with Ca^{2+} handling rate kinetics. However, there may be an emergent correlation of FEV_1/FVC with K for bradykinin stimulated $[Ca^{2+}]_i$ release. Finally, caffeine was serendipitously found to reduce basal $[Ca^{2+}]_i$ and inhibit $[Ca^{2+}]_i$ oscillations.

CHAPTER 5

DISCUSSION, CONCLUSION AND FUTURE

5.1 Summary of $[Ca^{2+}]_i$ homeostasis

Intracellular calcium ion concentration $[Ca^{2+}]_i$ is homeostatically regulated within mammalian cells. Typically, $[Ca^{2+}]_i$ is around 100nM and extracellular $[Ca^{2+}]$ is around 2mM, hence there is a 10,000 fold maintained inward concentration gradient. To achieve this, several proteins function in either 'on' or 'off' reactions to facilitate the movement of Ca^{2+} ions into or out of the cell cytoplasm (Figure 5.1) creating a dynamic equilibrium. The controlled cellular influx and efflux of Ca^{2+} to and from the cytoplasm, called Ca^{2+} handling, is an efficient and ancient method of cell signaling conserved throughout evolution (Case *et al.*, 2007).

Extracellular signal transduction can lead to an increase in $[Ca^{2+}]_i$ which in turn leads to a physiological effect. Such externally induced changes in $[Ca^{2+}]_i$ may give rise to Ca^{2+} oscillations, either discontinuous transient spikes of $[Ca^{2+}]_i$ or global waves of $[Ca^{2+}]_i$ propagated throughout the cell. Sometimes Ca^{2+} oscillations can occur spontaneously as part of normal physiology (Gordienko *et al.*, 2002) and sometimes they can lead to pathology (Sui *et al.*, 2009).

Indeed, Ca^{2+} oscillations are a more efficient and diverse mode of signaling than a simple bulk change in $[Ca^{2+}]_i$ level (Thomas *et al.*, 1996). The former involves fewer Ca^{2+} ions and greater information transfer efficiency (Dolmetsch *et al.*, 1998) than the latter. Moreover, frequent whole cell increases in $[Ca^{2+}]$ can be toxic perhaps generating an apoptotic response (Berridge, 1997b).

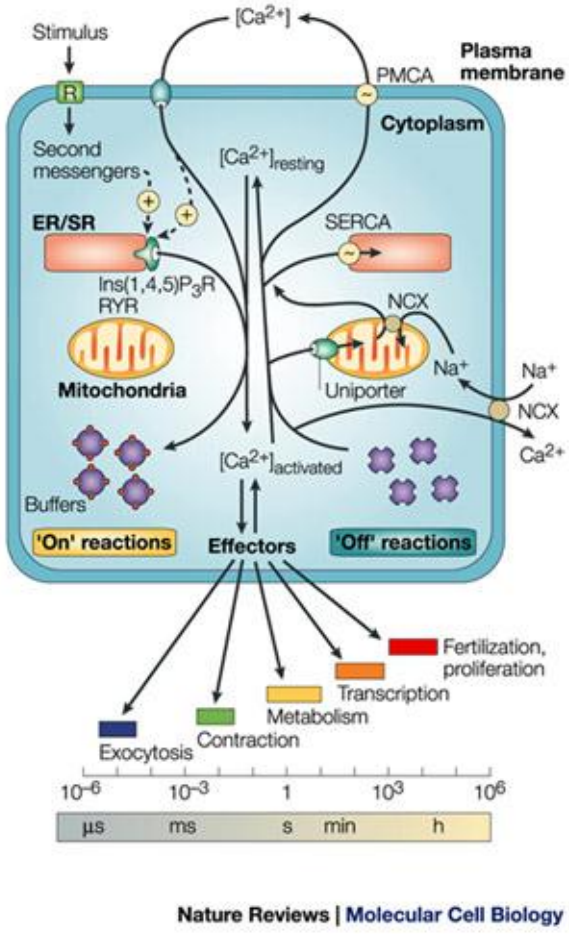

Figure 5.1 The maintenance of Ca^{2+} homeostasis. Regulation of intracellular Ca^{2+} can be thought of as a balance of 'on' and 'off' reactions, whereby calcium ions are released into or removed from the cytoplasm. Once disturbed the system tends back to equilibrium by the various mechanisms indicated. The results of $[Ca^{2+}]_i$ changes effect a raft of biological process on several timescales.

Reprinted with permission,

Berridge M.J., Bootman M.D., Roderick H.L. (2003) Calcium signaling: dynamics, homeostasis and remodelling, Nature Reviews Molecular Cell Biology 4, pp. 517-529

Hence, it is the frequency and amplitude characteristics of Ca^{2+} oscillations (Thomas *et al.*, 1996; Berridge, 1997a) that are of particular interest in cellular Ca^{2+} signaling.

This project investigated the hypothesis that $[Ca^{2+}]_i$ homeostasis and handling in hASM cells is intrinsically dysregulated in asthma compared to normal donors. Therefore, the aim of the project was to provide evidence, primarily from a single cell functional perspective, detailing the properties of passaged hASM cell Ca^{2+} homeostasis and handling at quiescence and after a deliberate disturbance respectively.

5.2 Characterisation of hASM cell $[Ca^{2+}]_i$ at homeostasis

Baseline or basal $[Ca^{2+}]_i$ in asthma and normal hASM cells was measured using wide field epifluorescence video microscopy with the ratiometric Ca^{2+}-sensitive fluorophore fura-2. There was no difference between the baseline $[Ca^{2+}]_i$ in either cell phenotype. Hence, at a holistic cellular level, the position of the $[Ca^{2+}]_i$ equilibrium is the same in both. That is, the sum of the rates of 'on' reactions equals that of the 'off' reactions in both asthma and normal hASM cells. This is a powerful result because it immediately suggests that there is no underlying net structural abnormality in the Ca^{2+} homeostasis system. Since the relative level of basal $[Ca^{2+}]_i$ was not different in asthmatic or normal hASM cells, investigation of the way in which $[Ca^{2+}]_i$ varies over time was assessed by quantifying the oscillatory behaviour of basal $[Ca^{2+}]_i$ waveforms. This is important because the aggregate pattern of temporal stochastic Ca^{2+} ion release, or basal Ca^{2+} oscillations, may reveal periodic patterns that are different in asthma compared to normal (Skupin *et al.*, 2010).

The calcium oscillation dominant frequency (CODF) obtained by FFT spectral analysis and the amplitude of $[Ca^{2+}]_i$ oscillations in hASM cells from asthma donors were found to be not significantly different to that of normal donors. Hence, the set of frequencies

and amplitudes that hASM cells normally use to maintain $[Ca^{2+}]_i$ signaling is unchanged in asthma compared to normal donors. However, there was a significant correlation between CODF and FEV_1 that was not reflected in FEV_1/FVC for normal and asthma hASM cell donors. Similarly, CODF and FEV_1, but not FEV_1/FVC, was significantly correlated in asthma hASM cell donors only. Moreover, a significant difference was found when AFO (FEV_1/FVC<70%) was compared to non-AFO hASM cell donors, which was considerably strengthened when AFO and airflow impairment (FEV_1/FVC<70%, FEV_1<80%) were compared to the remaining non-AFO group. Moreover, a ROC confirmed that CODF is an excellent predictor of AFO. Thus, CODF represents a distinct cellular signaling mode in AFO donors that is correlated with FEV_1. The origin of the increased CODF must have a structural basis, possibly mediated via microdomains. Thus, CODF, which is clearly enhanced in AFO, will be detected and transduced by $[Ca^{2+}]_i$ oscillation sensitive proteins (Parekh, 2011). Hence, CODF could represent the variable that describes the dynamic Ca^{2+} basis of bronchoconstriction and AHR in asthma hASM cells.

5.2.1 hASM cell Ca^{2+} handling after a disturbance to homeostasis

UV flash photolytic uncaging of Ca^{2+} ions into a small defined region in the cytoplasm enables assessment of cellular $[Ca^{2+}]_i$ recovery kinetics in a receptor independent manner. Comparison of the rate constant (K) for the Ca^{2+} recovery process was not significantly different for asthma or normal hASM cell donors.

The second, receptor dependent, mechanism by which $[Ca^{2+}]_i$ was raised involved application of bradykinin. This activates the $G\alpha_q$, PLC, IP_3 coupled signaling cascade, culminating in $[Ca^{2+}]_i$ release from IP_3Rs in the SR. The results showed that there is no significant difference in the way asthma and normal hASM cells return to $[Ca^{2+}]_i$

baseline equilibrium, in line with the outcome of the Ca^{2+} uncaging investigation. Also, there was no significant difference in the amount of second messenger IP_3 generated.

These findings demonstrate that there is no intrinsic functional abnormality in $[Ca^{2+}]_i$ handling in passaged hASM cells from asthmatic donors over normal controls. Because there is no functional difference to $[Ca^{2+}]_i$ handling, then it can be inferred that there is no underlying structural component of the Ca^{2+} homeostasis dynamic equilibrium that is changed in asthma. The Ca^{2+} uncaging and bradykinin stimulated $[Ca^{2+}]_i$ release data clearly demonstrate this.

Ca^{2+} ion uncaging in the presence and absence of a functional SERCA pump showed that there is no significant difference in SERCA function in hASM cells from asthma compared to normal donors. Further, structural studies supported this. Neither gene transcription of SERCA2abc nor protein expression of SERCA2 was different in asthma compared to normal hASM cell donors. This forces us to take a contrarian stance to the prevailing literature which suggests that SERCA is diminished in asthma hASM cells, having structural and functional consequences.

It has been shown that $[Ca^{2+}]_i$ at rest and after a deliberately induced increase are not disordered in asthma compared to normal hASM cells, the remaining function to test was the SOCE. The protocol used allows measurements of hASM cell Ca^{2+} store depletion and subsequent refilling to be made. The reason for doing this was to determine whether SOCE is disordered in asthma compared to normal hASM cells. If so, this would affect hASM cell tone and hence AHR. It is perfectly reasonable to test this hypothesis since SOCE is also implicated in a host of other diseases. For example, cell apoptosis and proliferation giving rise to a role in cancer, enhanced calcium influx of Duchenne's dystrophy, TCR receptor stimulation unable to activate T-cells in

primary immunodeficiency due to a lack of SOCE and involvement in neurodegeneration.

It was found that there was no difference in either the $[Ca^{2+}]_i$ initially released after store-depletion or the SOCE into the cell during refilling, for asthma and normal donors.

5.2.2 $[Ca^{2+}]_i$ homeostasis and handling conclusion

These data lead to the conclusion that the dynamics of $[Ca^{2+}]_i$ homeostasis and handling are not intrinsically altered under quiescent or disturbed homeostatic conditions in asthma or normal passaged hASM cells.

5.3 Clinical aspects

Overall, there was no significant difference between CODF or K between asthma and normal donors. This is strong evidence that there is no functional alteration in $[Ca^{2+}]_i$ handling, either at quiescence or after a deliberate disturbance, between asthma and normal hASM cell donors. However, even though asthma presents clinically with heterogeneous signs and symptoms, there are in fact non-disease specific underlying correlations between CODF and K with airway physiology. Furthermore, CODF is significantly different when an AFO asthma phenotype is considered.

CODF derived from hASM cell quiescent temporal $[Ca^{2+}]_i$ waveforms showed a significant non-disease specific inverse correlation with FEV_1 ($P=0.0036$, $r = -0.42$) but not with FEV_1/FVC ($P=0.064$, $r = -0.27$). Moreover, the inverse correlation persists for FEV_1 in asthma donors only ($P=0.016$, $r =-0.48$) but not for FEV_1/FVC ($P=0.11$, $r=-0.32$).

Furthermore, CODF is significantly different between AFO ($FEV_1/FVC<70\%$) and non-AFO donors ($P<0.032$). The significance persists and is strengthened when AFO and airflow impairment, $FEV_1/FVC<70\%$ and $FEV_1<80\%$, are compared to CODF ($P<0.0001$).

These results indicate that there is a non-disease specific link between airway physiology (FEV_1) and CODF. That the relationship holds for both asthma and normal hASM cell donors suggests that the subsets which define asthma and normal populations in terms of airway physiology are not fundamentally disparate. This contrasts with other published findings, introduced in section 1.6, where asthma phenotypes are multidimensional and therefore heterogeneous (Haldar *et al.*, 2008). That is, the severity of the disease in terms of airway physiology, symptoms and inflammation can all be very different; in fact they can be independent of each other. But the link between CODF and FEV_1 is important because it demonstrates that CODF can unify the heterogeneity of normal and asthmatic phenotypes in terms of a commonly measured lung function parameter, FEV_1. Therefore, CODF is demonstrably a strong link between macroscopic airflow physiology and the underlying pattern of $[Ca^{2+}]_i$ events at the molecular level in hASM cells; CODF increases as FEV_1 lung function deteriorates. Moreover, CODF is an important indicator of asthmatic airflow obstruction. For the AFO asthma phenotype, CODF was significantly different to the non-AFO group. Indeed a Receiver-Operator Curve (ROC) shows that CODF is an excellent prognostic predictor of AFO ($P<0.001$, $AUC=0.91$), exceeding any other current indicator including CT X-ray. This is not an isolated case because dominant frequency analysis is already being used as a prognostic indicator of cardiac pathology and the method is being seriously considered to analyse EMG waveforms taken from

parasternal muscles of lung disease patients (*pers. comm.* Prof. Moxham, King's College Hospital, London).

When the hASM cell $[Ca^{2+}]_i$ equilibrium is disturbed by a Ca^{2+} uncaging event, the rate of recovery (K) is not significantly different when FEV_1 is plotted as a function of K in asthma compared to normal donors. Similarly, when $[Ca^{2+}]_i$ is disturbed by bradykinin there is no correlation of FEV_1 plotted as a function of K, but there is a significant correlation with FEV_1/FVC and K for asthma and normal donors. It was found that there was no correlation between second messenger IP_3 generation and airway physiology.

To conclude, FEV_1 in quiescent hASM cells correlates with CODF for both asthma and normal hASM cell donors. CODF is a strong predictor of disordered asthmatic airway physiology, in particular AFO. Since passaged hASM cells were used, then this effect in the AFO asthma phenotype must be genetic or epigenetic. In the case where $[Ca^{2+}]_i$ is deliberately disturbed, K values present a rather more mixed bag, generally not correlating with FEV_1 or FEV_1/FVC, but bradykinin FEV_1/FVC does show an emergent correlation with K values. The latter is not yet a strong correlation and requires further data, it cannot be readily explained, it may be fortuitous, but certainly warrants further investigation.

It is probable that asthmatic bronchospasm is a hASM cell mediated reaction to being in an agonist-rich inflammatory *in vivo* environment, and that this is the biggest stakeholder in terms of altered $[Ca^{2+}]_i$ dynamics. Clearly, this constraint is absent in a stable non-inflammatory *in vitro* sub-culture environment. Indeed, asthma hASM cells have increased synthetic abilities that affect other lung structural cells and attract immune system cells (Damera *et al.*, 2011). This is therefore an important argument

that supports the idea that bronchoconstriction and AHR is an *in situ* immunopathology with respect to Ca^{2+} dynamics. Probably potentiated by altered genomic and/or epigenomic factors because of the change in CODF with AFO in cultured hASM cells.

So how do CODF and K add to our understanding of Ca^{2+} dynamics in asthma? A possible explanation of these phenomena comes from thinking of function-structure relationships: CODF is to microdomains what K-values are to $[Ca^{2+}]_i$ handling proteins. Hence, a CODF correlation with airway physiology is quite different to a correlation of K-values with airway physiology because they are separate processes. One is a property of Ca^{2+} homeostasis, the other a property of Ca^{2+} handling.

Quiescent CODF analysis suggests that there is an increase in organisation of 'on reactions' and hence generation of $[Ca^{2+}]_i$ oscillations as lung function, FEV_1, decreases. And that this effect is intrinsic to passaged hASM cells. Structurally, this effect may be explained by the presence of microdomains holding $[Ca^{2+}]_i$ release channels closer together and creating a more 'excitable medium' for the generation of $[Ca^{2+}]_i$ oscillations. In order to test this in the live cell, it can be hypothesised that the presence of a cholesterol-rich lipid raft microdomain type ultrastructure in hASM asthma cells can be detected as a change to intracellular viscosity. It is known that diseased or dying cells have increased intracellular 'stickiness' or viscosity and this too might be the case in asthma. A live cell method has been developed at Imperial College, London, whereby spectrally resolved fluorescence changes of a porphyrin dimer based molecular rotor can be used to detect intracellular viscosity changes (Kuimova *et al.*, 2009).

Thus a microdomain hypothesis could explain Ca^{2+} oscillations and CODF observed while the cell is in homeostasis. But when monitoring the after effects of an induced

$[Ca^{2+}]_i$ release, rate kinetics describe the Ca^{2+} handling process, composed of on and off reactions, that brings the cell back to homeostasis. Altered Ca^{2+} handling *in vivo* would most likely be a product of the inflammatory environment. In the laboratory, Ca^{2+} uncaging generated a local increase in $[Ca^{2+}]_i$ whereas bradykinin caused a cell-wide global change in $[Ca^{2+}]_i$. Moreover, Ca^{2+} handling for a local Ca^{2+} increase is probably biased toward the kinetics of off reactions, whereas the global increase in Ca^{2+} probably involves kinetics of both off reactions and on reactions, the latter in the form of SOCE and is more likely to lead to contraction. Therefore, since local Ca^{2+} increases are more usually used for Ca^{2+} signaling, and are cleared quickly, it is noteworthy that global Ca^{2+} changes perhaps leading to contraction, which are cleared more slowly (K is low), should show an emerging correlation with airway physiology, FEV_1/FVC. Even though for example no change in SERCA expression was found here, the effect of an inflammatory environment of course does not preclude an alteration to hASM cell Ca^{2+} handling proteins. Hence, with further phenotypic data, it might be the case that the rate at which $[Ca^{2+}]_i$ is cleared from the hASM cell cytoplasm is important in asthma.

5.4 Limitations of using fluorophores to monitor live cell $[Ca^{2+}]_i$

The ability to view the dynamic $[Ca^{2+}]_i$ changes that take place within a living cell using modern fluorescent dyes has certainly revolutionised the science of Ca^{2+} signaling. However, it must be appreciated that this is an invasive method, since a foreign compound, a fluorescent ester, is being introduced into the cell. In particular Ca^{2+} sensitive fluorophores are Ca^{2+} buffers, they setup their own Ca^{2+} equilibrium, they have a K_d value. Of course, without these properties they would not function as indicators. It is therefore reasonable to assume that they modify the cellular Ca^{2+} equilibrium system that they are introduced into (Molecular-Probes, 2011). It follows

that data derived from the use of such dyes as fura-2 and fluo-4 do not represent a true and faithful representation of Ca^{2+} phenomena going on inside the cell. It is of course an approximation, since the act of measuring $[Ca^{2+}]_i$ changes $[Ca^{2+}]_i$, 'but to what extent?' For example, throughout this project application of agonist bradykinin has never once led to a contractile response in asthma or normal hASM cells. Even high K^+(aq) did not induce contraction. Yet when hASM cells are transfected with GFP localised to the plasma membrane in order to delineate the cell boundaries, and then bradykinin or high K^+(aq) is applied, a very clear and reversible contractile response can be demonstrated. These facts should be borne in mind because they represent limitations that may indeed lead to artefactual results. But because relative differences are sought, this effect is threshold dependent.

However, given these constraints imposed by the fluorescence monitoring system I have been able to detect an expected rise in $[Ca^{2+}]_i$ in response to an agonist. Similarly, after Ca^{2+} uncaging, a definite increase in $[Ca^{2+}]_i$ was detected. That the increase in $[Ca^{2+}]_i$ is affected by the fluorophore is indeed somewhat cancelled when one considers that relative measurements between asthma and normal hASM cells are being taken, not absolute measures. Since the fluorophore loading protocol is always the same, then, all other things being equal, it can be said that the artefactual component of the subsequent $[Ca^{2+}]_i$ measurement will be some constant value. Hence any statistically significant results will reflect genuine differences between $[Ca^{2+}]_i$ homeostasis or handling in asthma compared to normal hASM cells. There have been reports that confocal microscopes can actually induce Ca^{2+} oscillations (Knight *et al.*, 2003). In my experiments epifluorescence microscopy was used to look for Ca^{2+} oscillations rather than confocal microscopy, but the principle of a scanning laser and on-off epifluorescence illumination both have a switching aspect in common that may induce

Ca^{2+} oscillations in hASM cells. This would have been a concern if $[Ca^{2+}]_i$ oscillations were found to be a feature of hASM cell signaling, and different exposure times would then have been tried.

The fact that fluorophore loading does actually change the mobility of $[Ca^{2+}]_i$ ions suggests that this method of monitoring places a threshold on observable $[Ca^{2+}]_i$ phenomena. For example, relatively low signal to noise ratio fast changes in $[Ca^{2+}]_i$ are more likely to be damped or attenuated by the fluorophore, or are beyond the capability of the fluorophore to react fast enough to those changes, probably because of a slow dissociation rate.

It may also be the case that the fluorophore actually inhibits some of the usual functions of the cell. For example the actinomyosin contractile apparatus does not function in the fura-2 monitoring system. Also, during loading the cell is exposed to anion transport blocker probenecid, and a non-ionic detergent pluronic F127 that creates fluorophore filled micelles, and dimethyl sulphoxide (DMSO) to dissolve the organic AM fluorophore, all of which assist fluorophore loading and accumulation into the cell. Again, these are foreign compounds that may affect a cell's biochemistry or biophysics that are simply not normally encountered by the cell.

The esterase mediated hydrolysis of the fluorophore-acetoxymethyl ester leads to the liberation of ionised carboxylic acid functional groups attached to the fluorophore, i.e. $fluorophore - (ethanoate)_5^-$. By design, these anions cannot easily pass through the hydrophobic plasma membrane. However, there are five AM groups per fura-2 molecule, all of which are ionised at physiological pH, liberating $5H^+(aq)$ per fura-2 molecule, hence causing a decrease in intracellular pH. Also, 5 molecules of methanol per fura-2 molecule are generated by this ester hydrolysis reaction. Additionally, the

same principle applies to fluo-4 AM and NP-EGTA AM in the Ca^{2+} uncaging methodology. 'Is the cell able to cope with these changes without suffering organellar damage'? Or, 'Does the cell suffer changes to the way it normally functions'? The answers to these questions are unknown. Clearly, the cell might be able to buffer the H^{+}(aq) internally, or after extrusion into the extracellular HEPES buffer, but maybe the damage has already been done. A decrease in pH or exposure to methanol may put the cell into a stressed state that is not normal.

Hence, there are many fairly concerning caveats to this method of $[Ca^{2+}]_i$ measurement. But to date this is the best technique available, and most experiments that seek to provide data about live cell $[Ca^{2+}]_i$ dynamics use loaded AM fluorophores.

Furthermore, the cells are passaged and cultured in an artificial general growth medium. There is no published recipe for FBS, one must assume that the constituents are different in every batch. Indeed, it could be that the bovine cytokines contained in the FBS change $[Ca^{2+}]_i$ to a greater extent than the uncertainty associated with the fluorophore AM methodology.

The epifluorescence Perkin Elmer software was set to an exposure time of 200ms. Hence, if the spectrometer switch over time between 340 and 380nm wavelengths is assumed to be negligible, then the maximum uncertainty in the measurements is the exposure time which is 200ms, this is the maximum time resolution of the data. This is more than adequate since it is not expected to see a biologically controlled $[Ca^{2+}]_i$ oscillator that is so fast ($\leq$200ms). Indeed, in hASM cells that did display high signal to noise ratio trains of $[Ca^{2+}]_i$ transients or oscillations the period was typically between 100 to 300s. 200ms also exceeds the time resolution required to perform the FFT for a CODF measurement. Since the minimum time domain trace duration was 600s, and the

number of samples taken to form the FFT was 1024, then the minimum time step required for the FFT is around 586ms, which is of course greater than 200ms raw data resolution.

For Ca^{2+} uncaging, the Olympus FV1000 confocal microscope used had only one scan head. Hence, the period between photoactivation of the Ca^{2+} cage and subsequent monitoring of the $[Ca^{2+}]_i$ pulse is not instantaneous. Therefore, there is uncertainty in the time it takes to perform the 405nm uncaging pulse and to then switch to the 488nm monitoring of the reaction to the generated $[Ca^{2+}]_i$ pulse. The photoactivation takes 300ms, therefore the switch-over takes at least this time plus that required to mechanically switch between the two lasers and then any signal digitisation and software capture delay. Therefore, there is no way of knowing how far the actual peak of the $[Ca^{2+}]_i$ transient extended. However, because the exponential decay follows a defined mathematical law, then the part of the reaction that was captured was more than adequate to calculate the K value. The parameter that cannot be reliably measured is the peak uncaging response ($\Delta F/F_0$), but for the reason given I do not have any truck with this.

5.5 Reliability of results

My results have overwhelmingly led us to the conclusion that $[Ca^{2+}]_i$ homeostasis and handling are not significantly different in hASM cells from asthma and normal donors. That is, the null hypothesis has been consistently accepted. So what is the probability that $[Ca^{2+}]_i$ metrics such as CODF and K have been misclassified as not different when actually they are different? This kind of consideration, when a researcher decides that the null hypothesis is true when it is actually false, leads to a type II error in statistics. In this scenario, failure to reject the null hypothesis may be because the test distribution

closely overlaps the control distribution. Hence, in the results data there was not a big enough difference such that the possibility of a difference occurring by chance could be rejected. Therefore the reason why a significant difference was not found may be because, a) there genuinely is no difference or b) there is actually a difference but it is not being detected. The latter leads to a type II error, and the probability of not committing a type II error is called the power of the test or experiment. In order to be confident that the experimental design is capable of detecting a significant difference it needs to have sufficient power. The area that the test distribution overlaps the control distribution is called β, it is this parameter that should be minimised in order to minimise the probability of a type II error.

Hence the power of an experiment is defined by, power = 1-β. The greater the power the smaller the area of β, and the greater is the probability that experimental test data will fall into the test distribution and not the control distribution. Typically, for a given level of significance (α=0.05 is usual) power can be increased by increasing the number of data points, n. Also to reduce variability or spread of data points one should seek to measure sub-maximal rather than threshold effects. For example, the greater the therapeutic effect of a drug the smaller is the required sample size, n, to achieve sufficient power to detect a significant difference. Clearly, with very small therapeutic effects n must be larger to achieve the required power to detect a significant difference.

In terms of CODF Figure 3.7 shows that the asthma (i.e. test) and control populations almost completely overlap and there is sufficient data to adequately define each distribution, so the data are not under powered. Therefore, there is confidence in not failing to detect two different sample populations. That is, CODF is not different in asthma compared to normal hASM cells. But when one considers individual donors, maybe a representative crossectional sample of the asthma population was not selected.

However, this is unlikely to be the case since all asthma hASM cells were derived from patients attending hospital clinics requiring specialist treatment and hence are unlikely to be threshold asthma.

As a rule of thumb, n = 3 control and n=3 test values are a minimum requirement for any measurement. For asthma donors because of the inherent heterogeneity of the disease and the consequent variability, n was chosen to be greater than 3 for each population in order that any significant difference could be detected. Hence, it is unlikely that the results parameters CODF or K are under powered and lead to a false negative result because the disease is well established in these patients. And if there were a true difference, the probability of detecting it would be high using these experimental designs. However, one issue is that donors might have been selected from different phenotypes, disease subtypes classified as asthma that have different molecular pathologies with respect to Ca^{2+} homeostasis and handling. This confounds the design because there are currently no clear rules to define asthma phenotypes at the molecular level. Thus there may be some phenotypes where dysregulated Ca^{2+} homeostasis is not a feature. This is reflected in the low Pearson correlation coefficient, r, values for the correlations. r = -1 is a perfect inverse correlation, rarely seen in biology. But since the experimental r-values are low, it maybe that there are mixed asthma phenotypes that should be considered separately.

Conversely, rejecting the null hypothesis, that there is no difference between test and control populations, when it is actually true is called a type I error in statistics. It leads to a false positive result. Student's t-test is used to determine the probability of there being a significant difference between two sample populations. In order to avoid a type I error the area of overlap that the control distribution has with the test distribution, called α, must be minimised. It is usual to reduce this error rate α to 0.05 or less,

indicating that there is at most a 5% probability of a significant difference occurring simply by chance. Hence significant results are often quoted with a probability, P ≤0.05. The error rate for any experiment cannot be completely eradicated, it can only be minimised. Hence, in my results a significant difference is taken when P≤0.05 or better.

Overall, and given the limitations of primary hASM cell culture discussed later in section 5.8, a conclusion can be reached by summarising the major factors that could affect the reliability of the results. I have discussed how the statistical analysis of the data presented here has been designed to avoid type I and type II errors. The data can be broadly separated into two parts in terms of biology. Analysis of a) quiescent $[Ca^{2+}]_i$, the undisturbed homeostatic state or b) dynamic $[Ca^{2+}]_i$ handling, the drive to restore homeostasis after a deliberate disturbance of $[Ca^{2+}]_i$ by Ca^{2+} uncaging or agonist action.

For a) CODF was derived from temporal $[Ca^{2+}]_i$ waveforms and the biggest uncertainty here was the effect of fura-2 and its loading upon the hASM cell $[Ca^{2+}]_i$ homeostasis. The uncertainty in CODF was minimised when the signal to noise ratio of Ca^{2+} oscillations was high. But as the waveforms displayed lower signal to noise ratio oscillations, then the Ca^{2+} buffering effect of the fura-2 would be expected to attenuate the signal to a threshold. And the aim of the experiments was to determine if Ca^{2+} oscillations occurred more frequently in asthma compared to normal hASM cell donors. But in practice, the FFT algorithm was still able to report a distinct CODF in all cases where oscillation was monitored. For b) the situation is more straightforward because I was able to deliberately generate high signal to noise ratio changes in $[Ca^{2+}]_i$. Hence, the uncertainty in the measurement is once again expected to be mainly composed of the buffering effect of the fluorophore. The effect will be the same for both asthma and

normal hASM cell donors. Hence, the essential characteristics of homeostatic drive acting to oppose the disturbance and restore $[Ca^{2+}]_i$ equilibrium will become evident, and any significant difference in asthma compared to normal will be revealed. Moreover, the overall results story is consistent for at least one $[Ca^{2+}]_i$ homeostasis protein, SERCA, which does not significantly vary in mRNA transcription or protein expression between asthma and normal hASM cell donors.

5.6 Overall conclusion

The consensual picture that emerges is that there is no difference in a) quiescent CODF, b) rate kinetics, K, after deliberate $[Ca^{2+}]_i$ increase, or c) SOCE, in asthma compared to normal hASM cells *in vitro*. Thus, overall hASM cell $[Ca^{2+}]_i$ homeostasis is not significantly different in asthma compared to normal. However, there is an important exception when an AFO asthma sub-group or phenotype is considered. It is also true that at the level of asthma clinical phenotypes parameters such as CODF and perhaps agonist K-values reveal correlations with airway physiology for both asthma and normal donors. Since these effects were observed in passaged hASM cells, the effect probably involves genetic or epigenetic changes. There is a clinical urgency to identify and categorise asthma phenotypes and, although it is not an easily measured biomarker, it is clear that COFD is important as it links quiescent $[Ca^{2+}]_i$ changes with AFO. This is not an isolated case because dominant frequency analysis is already being used as a prognostic indicator of real time cardiac pathology in hospitals and there is ongoing research into EMG waveform pattern analysis from parasternal muscles of hospitalised lung disease patients.

5.7 Critique

Recently, two groups have reported that hASM cell $[Ca^{2+}]_i$ homeostasis and handling is altered in asthma (Chapter 4, Introduction). The basis of this viewpoint is that there is a significant difference in the recovery of hASM cells from asthma and normal donors after an agonist challenge. But as I describe in Chapter 4, AUC and time to return to basal $[Ca^{2+}]_i$ can lead to large subjective errors. However, I have consistently shown throughout this project that in hASM cells taken from asthma and normal donors, $[Ca^{2+}]_i$ homeostasis and handling is not different. So, 'How can this apparent contradiction be explained?'

The first consideration stems from the inherently broad remit of the term 'asthma,' even though patients present with similar clinical signs and symptoms. I have shown that, with respect to Ca^{2+}, asthma hASM cell phenotypes are heterogeneous or graded in a non-disease specific correlation between lung function, FEV_1, and CODF. Hence, the most likely explanation lies in the fact that asthma covers a large spectrum of lung diseases. And it follows that the distribution of $[Ca^{2+}]_i$ phenomena too has a wide spread. It is therefore entirely consistent to suggest that actually a much larger data set should be analysed in order to arrive at a definitive answer about $[Ca^{2+}]_i$ homeostasis that reflects the true *in vivo* $[Ca^{2+}]_i$ properties of distinct asthma phenotypes in non-passaged hASM cells.

Therefore, despite contrarian published data, which postulates that $[Ca^{2+}]_i$ homeostasis and handling are dysregulated in asthma hASM cells, the results obtained here must be objectively considered. My results show that overall, there is no difference in $[Ca^{2+}]_i$ homeostasis or handling in asthma or normal hASM cells. This leads to two separate inferences.

Firstly, $[Ca^{2+}]_i$ homeostasis and handling are not altered in passaged asthma hASM cells and *ergo* are not an intrinsic disease of the genome, simply because a heritable change leading to pathology would most likely be detected through early passage.

Secondly, the true state of $[Ca^{2+}]_i$ homeostasis and handling in the *in vivo* inflammatory condition cannot necessarily be extrapolated from this *in vitro* work. This is because the inflammatory environment, including the action of hASM cell secreted mediators on the behaviour of immune system cells (Damera *et al.*, 2011), will affect hASM cell Ca^{2+} dynamics.

The first inference forms the basis for the conclusion of this project. But with the important exception that if asthma phenotypes are considered, such as AFO, there does appear to be a significant difference in comparison to a non-AFO group, which indicates that CODF *is* sensitive to heritable change in asthma hASM cells. This nicely illustrates the heterogeneity and complexity of the term 'asthma': most asthmatics do not have an altered CODF with respect to normal hASM cell donors, but some hASM cell donors, those with disordered airway physiology, do have altered CODF. The second inference, to which I shall now turn, means that issues associated with *in vitro* data and *in vivo* reality must be considered.

The key issue to consider is, 'How close are these results to the true *in vivo* condition?' Hence, attention must be focussed upon the hASM cells and how they were prepared. Looked at in this manner, and to be absolutely precise, it can only be said that $[Ca^{2+}]_i$ homeostasis and handling is not different in the passaged hASM cells that were available to me. Therefore, the cell culture system is potentially a significant source of variation preventing observation of the *in vivo* state. Moreover, normal or control cells are not necessarily true normal hASM cells. They are derived from 'normal' tissue

resected from lung cancer patients at post mortem, which may or may not have been smokers. Or, explants from bronchoscopy tissue samples from living volunteers that again, may or may not have been smokers.

It has been shown that the expression of ion channels and receptors in freshly dissociated, compared to sub-cultured proliferating hASM cells, is considerably different, with differing functional consequences (Snetkov *et al.*, 1996). And hASM cells demonstrate a high degree of phenotypic plasticity, depending upon the local chemical environment (Hirota *et al.*, 2009).

It is known that genes control an organism's response to its environment. And asthma can be considered to be, in large part, the product of an immunological failure to tolerate certain triggers. Then chronic airway inflammation, changing the cellular and chemical environment of the lungs, profoundly effects airway structural cells, including hASM cells, and inevitably acts as an *in vivo* constraint to their normal functioning, in addition to any intrinsic genomic lesions that might be present.

Therefore, it is reasonable to assume that there will be a substantially different set of genomic responses established in those *ex vivo* hASM cells grown in bovine cytokine based cell culture medium, containing anti-microbial agents, and taken through several passages over several months before and during use. This of course leads to the suggestion that sub-culturing significantly distorts *in vivo* changes that existed in asthma hASM cell $[Ca^{2+}]_i$ homeostasis and handling, because the inflammatory environment constraint has been removed. It follows that the *in vitro* laboratory method of preparation has in effect sanitised the cells, to such an extent that asthma and normal hASM cells have been made to behave in the same, artefactual, way with respect to Ca^{2+} homeostasis and handling.

However, caution has to be exercised even when using non-passaged primary cells. The term hASM cell cannot be precisely defined. Airway wall smooth muscle cell bundles, from which the cell cultures are derived, may contain a mixture of fibroblasts, myofibroblasts and myocytes. Myofibrobalsts and their fibrocyte progenitors are known to migrate into lung tissue in response to inflammation or tissue injury, as is the case in asthma. Therefore, one cannot be absolutely sure that the cell cultures contain exclusively myocytes or hASM cells. They most likely also contain fibroblasts and myofibroblasts as well. These cells may be a significant source of error, for example when reporting the enhanced synthetic, migratory and other properties attributed to hASM cells (Singh *et al.*, 2008). And of course, sub-culturing selects for those cells that proliferate the fastest, further changing the original *in vivo* cell type make up. Therefore, a useful first approximation would be gained by determining whether $[Ca^{2+}]_i$ homeostasis and handling is different in freshly dispersed cells from hASM bundles from asthma and normal donors.

There are examples of work using non-passaged smooth muscle cells that are producing useful data with clinical relevance. It is instructive to consider a recent publication from a collaborative group of British researchers from University College, London and the University of Surrey (I have abbreviated this to UCLS). Their work essentially investigated the mechanistic basis of spontaneous $[Ca^{2+}]_i$ oscillations in human bladder smooth muscle cells (Sui *et al.*, 2009). They compared bladder smooth muscle cells from the pathological state, overactive bladder (OAB) syndrome, to bladder smooth muscle cells from normal donors. They found a significant difference and concluded that spontaneous aberrant Ca^{2+} oscillations contribute to the up-regulated contractile activity seen clinically in OAB syndrome. The group have essentially made steps toward understanding the basic sub-cellular dysfunctional regulation of $[Ca^{2+}]_i$ in these

cells. Surely the next steps will be toward clinical trials of drugs that modify $[Ca^{2+}]_i$ activity.

The parallels between this OAB study and the hypothesis that I have proposed in this project to investigate dysfunctional $[Ca^{2+}]_i$ homeostasis in hASM cells from asthmatics is striking. The fundamental difference between the approach taken by UCLS and my approach was that UCLS used *ex vivo* bladder smooth muscle cells that were in the lab within 60 minutes, and crucially the cells were not passaged. They were used freshly dispersed. Admittedly, OAB may turn out to be a more straightforward disease than asthma in that it may not have the added complication of the diverse molecular phenotypes that are still being grappled with by asthma researchers.

But at the end of the day, bronchoconstriction is a common feature of all asthmatics. And indeed, both OAB and asthma are termed syndromes. In my opinion, the UCLS method of preparing freshly dispersed non-passaged smooth muscle cells should be tried in asthma. Simply because it is not known how hASM cell $[Ca^{2+}]_i$ dynamics behave *in vivo*, the zero sub-culture route is the best method currently available to answer the question. In this way, the probability of success is stacked on our side because, if asthma $[Ca^{2+}]_i$ homeostasis and handling is dysfunctional *in vivo*, then this method gives the very best chance to quantify this phenomenon and to compare it with normal hASM cells.

5.8 Future research rationale

Everyone takes the limits of his own vision for the limits of the world.

Arthur Schopenhauer (1788-1860), Philosopher

5.8.1 Respiratory drugs industry

Estimated to be worth £20.1bn in 2008, industry analysts predict that the global respiratory therapeutics market will rise to £24.5bn by 2015 (GBIResearch, 2009). That being so, it is certain that from a business perspective any novel new chemical entity that taps an hitherto overlooked niche in respiratory medicine will be profitable. Since the mid twentieth century the focus of drug research has been inflammation and hASM driven bronchoconstriction. The results have generated a reasonable set of compounds that have come through rational pharmacology. Asthma can now be controlled more successfully and with fewer side effects than at any other time in history. The pharmaceutical industry has produced theophylline, SABAs, LABAs, muscarinic antagonists for bronchoconstriction and cromones, theophylline, corticosteroids, anti-leukotrienes and anti-IgE to tackle inflammation. This two pronged approach is reflected in the current gold standard for treating anything more than mild acute asthma; a combined LABA and corticosteroid inhaler. However, in some severe asthma patients, or more correctly the corresponding clinical phenotype, these symptomatic fixes are only a temporary respite from an underlying inflammatory process that is currently not adequately addressed by pharmacotherapy. Such patients are described as having asthma which is 'steroid-resistant'. Hence, the future will be composed of more work on bronchoconstriction and inflammation with a personalised

medicine emphasis, because a significant marketable breakthrough is long overdue (Barnes, 2004).

5.8.2 $[Ca^{2+}]_i$, the elephant in the room

Treatment of inflammation with glucocorticosteroids particularly for many severe asthmatics often fails to adequately control asthma exacerbations. Evidence is starting to emerge which suggests that airway remodelling is induced by compressive forces exerted on the airways during bronchoconstriction, independent of the remodelling changes induced by inflammation (Grainge *et al.*, 2011). Hence, this brings into sharp focus the need to address bronchoconstriction at an early stage of the asthma timeline, on an equal footing with inflammation, to stave off airway remodelling. To this end, the need for a wider set of drug choices, apart from those based on physiological antagonism *viz.* β_2-adrenoceptor agonists and anti-muscarinics, to treat aberrant hASM cell contraction is long overdue. It is clear that the kinetics of hASM cell Ca^{2+} handling is different depending upon how much $[Ca^{2+}]_i$ is released. Therefore, it is a no-brainer that pharmacological tools designed to directly manipulate hASM cell $[Ca^{2+}]_i$ should be investigated to satisfy this unmet niche for empirically defined asthma phenotypes.

As a start, serendipitously, a potential 'new' $[Ca^{2+}]_i$ modifier came to my attention during this project when I was looking for an inexpensive positive control agonist. Caffeine acted to consistently lower hASM cell $[Ca^{2+}]_i$. So confirmation of effect in freshly dispersed hASM cells could lead to an effective inhaled bronchodilator, if it passes safety pharmacology testing. The same chemical class of compound, theophylline, systemically administered is currently in established clinical use. Furthermore, it is also known that Ca^{2+} is required for membrane fusion and exocytosis of inflammatory mediators from mast cells (Nishida *et al.*, 2005). Hence, if caffeine is

also found to inhibit mast cell Ca^{2+} entry then it may turn out to be a very useful bronchodilator or even anti-inflammatory agent.

I have shown that airway physiology correlates with CODF and that there is probably a heritable basis for increased CODF in AFO asthma phenotypes. However, there is clearly potential for this work to be expounded using freshly dispersed hASM cells to, a) confirm that the effect occurs in non-passaged cells and to what extent, and b) to help define clinical phenotypes of asthma based on CODF.

Indeed, the question of whether consequences of the asthma inflammatory environment affect $[Ca^{2+}]_i$ homeostasis and handling should be investigated in its own right in non-passaged hASM cells. For example, 'Does the quiescent state of freshly dispersed *ex-vivo* hASM cells show a greater probability of displaying high signal/noise ratio $[Ca^{2+}]_i$ oscillations as in OAB syndrome?' Or, 'Is basal $[Ca^{2+}]_i$ different in asthma compared to normal?' Or, 'Are $[Ca^{2+}]_i$ rate kinetics different after a Ca^{2+} uncaging event and after agonist stimulation?' Or, 'Is SOCE affected in hASM cells from asthma compared to normal donors?' It might be that the same results are obtained as for passaged hASM cells. But the fact is I simply cannot reasonably make a definitive judgment. However, balance of probability suggests that freshly dispersed hASM cells will behave very differently to passaged cells.

Indeed, the correlation between airway physiology and CODF suggests an important role for $[Ca^{2+}]_i$ in asthma pathogenesis. This finding should certainly be followed up by a comprehensive study using freshly dispersed hASM cells from asthmatics and controls. $[Ca^{2+}]_i$ has of course been shown to have an important intracellular signaling function, not necessarily in terms of bulk changes, but certainly in terms of frequency and correlations with amplitude or even phase may follow. Conceptually, there is an

unmet niche here because currently there is no drug that directly modulates $[Ca^{2+}]_i$ in asthma. Given the centrality of this ion in the events leading up to hASM cell contraction the void is noteworthy. It is conceivable that extension of the work presented here could very easily leverage new drug discovery for more efficient management of bronchoconstriction. In particular, the next logical stage is to collect data not just of CODF but of complete frequency spectra to fingerprint $[Ca^{2+}]_i$ phenomena and map this onto airway physiology (Figure 5.2). If strong data mined correlations begin to emerge, the mechanistic basis of this effect should be investigated.

A good starting point would be to investigate to what extend the microdomain compartmentalisation of $[Ca^{2+}]_i$ release is different in asthma compared to control. If this is found to be important, the goal then of course would be a $[Ca^{2+}]_i$ modulator. Perhaps based upon the lipid raft disrupter methyl-β-cyclodextrin. The hypothesis is that formation of $[Ca^{2+}]_i$ release microdomains is a model candidate to explain increased CODF in AFO. Microdomain formation could be based upon the increased presence of reactive oxygen species (Davidson *et al.*, 2006). The Brightling lab will show later this year that hASM cells from asthma donors have increased ROS compared to normal donors. But also increased dietary cholesterol can enhance the formation of microdomains *in vivo* because it is the main constituent of lipid rafts. Cholesterol has also been shown to enhance eosinophilic inflammation in a mouse model of asthma (Yeh *et al.*, 2001).

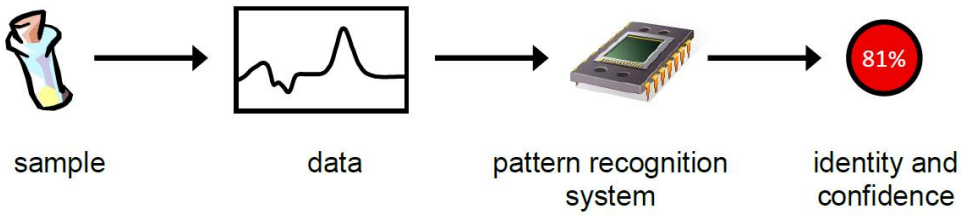

Figure 5.2 Pattern recognition services are now well established, with academic institutions offering high performance applied bioinformatics solutions to find patterns in complex data from diverse sources. It is not hard to see how CODF FFT spectra, or proteomics data, from hASM cells could be easily translated into this analytical framework.

Reproduced with kind permission of Dr Conrad Bessant, Cranfield University, UK:

http://www.cranfield.ac.uk/health/researchareas/bioinformatics/cranfield%20pattern%20recognition%20flyer.pdf

Then, development of a knowledge discovery algorithm would define specific asthma phenotypes by relating airway physiology to patterns in these FFT spectra or 'respiratory fingerprints'. This could also be linked to work on FFT spectra derived from parasternal EMG waveforms being pioneered at King's College Hospital. In this way, a move toward personalised medicine for asthma patients could be established, because the phenotyping algorithm would allow clinicians to treat with $[Ca^{2+}]_i$ modulators those clusters of patients that have altered $[Ca^{2+}]_i$ homeostasis, based on an empirically predetermined threshold. 'Biological String Theory' if you will. Further, this work should be carried out in non-passaged cells because the inflammatory environment affects hASM cell $[Ca^{2+}]_i$ dynamics. Hence, cytokine/agonist or sheer force driven contraction could be predicted by the algorithm.

It is entirely possible that proteomics data, from 2DGE and protein chips for example, can be integrated to produce an accurate model of the complex interactions of the asthma inflammasome (Crameri, 2005; Houtman *et al.*, 2005). In fact, this is probably the most efficient way of gaining a global understanding of asthma. The alternative is a jumble of haphazard cytokine effects that inevitably lead to a distorted and restricted viewpoint. To the hypothesised model, an AI algorithm can be applied that will predict when the systems biology becomes chaotic or non-linear and falls into pathology. This would be very useful in a hospital ICU setting when respiratory arrest occurs, particularly overnight when the patient is sleeping. The future is for the convergence of high-throughput experimental data and computer modelling. A synthetic approach. It is at once exciting and promises to deliver the holy grail of any inflammation based disease, true understanding of an inherently complex design.

Within Professor Brightling's group, cDNA microarray experiments have not revealed any altered gene expression in asthma related to Ca^{2+} homeostasis proteins in *passaged*

hASM cells. This supports the inference made here that there is no intrinsic dysregulation of Ca^{2+} homeostasis and handling in asthma compared to normal hASM cell donors. However, this situation may change when the data are analysed in terms of asthma phenotypes or when non-passaged hASM cells are used, because gene expression is most likely altered in an inflammatory environment and epigenetic effects are likely to be preserved in severe asthma phenotypes through passage.

Certainly, it is possible that there may be epigenetic changes associated with the progression of asthma *in vivo* and there is momentum to perform these studies (Rakyan *et al.*, 2011; Yang *et al.*, 2011). Epigenetic changes, such as DNA methylation, histone or chromatin modification are environmentally acquired changes which are not detected by cDNA microarrays, and may affect gene expression in asthma. Changes to the epigenome may or may not be heritable. However, in the passaged hASM cells, *overall* no significant change in $[Ca^{2+}]_i$ homeostasis or handling was observed, therefore heritable changes to the genome, including epigenetic change, cannot be a significant factor for asthma donors *en masse*. But in the case of CODF in AFO a significant difference was established that is most likely to be a product of a genetic or epigenetic change. If the genomics of AFO in passaged hASM cell donors reveals no significant differences compared to passaged hASM cells from non-AFO donors, then this lends more weight to an epigenetic explanation.

However, at the end of the day, it is changes to the proteome that will direct whether there is pathology or not (Muers, 2011). This is a post-genomic era but progress has been surprisingly slow to date (Houtman *et al.*, 2005). Of interest is a recent proteomics study in a rat model of asthma that has identified differences in the expression of certain Ca^{2+} binding proteins linked with changes to metabolism and mitochondrial activity (Xu *et al.*, 2010). This is an excellent pro-forma for human

studies. And it nicely links in with the hypothesis that altered Ca^{2+} homeostasis is associated with increased mitochondrial biogenesis in human asthma (Trian *et al.*, 2007).

In my opinion a top-down approach to disease knowledge discovery should be adopted, simply because a bottom up approach is akin to pinning a tail on the donkey or finding a needle in a haystack. The blindfold needs to be removed; we need information about the whole haystack. In short, we need to load the odds in our favour. Because genuine breakthroughs in asthma research that translate to step-change therapies are currently nowhere to be seen (Barnes, 2010). To this end, a comprehensive program of proteomics studies is now essential in non-passaged hASM cells from asthmatics compared to normals. This would allow associations to be made at a systems biology level, giving us access to the wider viewpoint, and saving us from chasing after every new 'hot lead' published in the literature. Moreover, a proteomics approach allows targets to be chosen both rationally and efficiently. Only then can directed genomic and single cell functional studies, such as the investigation of Ca^{2+} dynamics as in this project, be performed to work out the fine detail.

5.8.3 Inflammation

A shift in traditional thinking about asthma is required maybe even revisiting old ideas of cell biology in a new way. Indeed, this line of reasoning suggests that a fundamental question in asthma is, 'What causes such intolerance to inhaled allergens in one person that leaves another quite unaffected?' In essence the question now being addressed is, 'What agent 'lights the blue touch paper' and sets into motion the complex set of immunological reactions seen in asthma that manages to make pharmacological control so challenging?'

A radical paradigm shift in thinking needs to be adopted whereby researchers look to the fundamental, turning their sights to understanding the primary immunological lesion that manifests as breathlessness. The 'effect of a cause' variously described as asthma, COPD, emphysema, chronic bronchitis, productive cough, atopic rhinitis, hypersensitivity pneumonitis and so on. Here I have shown in a functional manner that dysfunctional $[Ca^{2+}]_i$ handling in asthma is not an intrinsically heritable disease of hASM cells *per se*. Hence, there is a more fundamental prime mover. I have already conjectured that hASM cells' function may be disturbed as a consequence of a changed *in vivo* chemical environment because of a property or sensitivity of the immune system that some people have and others do not. For example, studies of isometric contraction of hASM cells show an increase in the rate of contraction of allergic sensitised cells, reviewed in (Crimi *et al.*, 2001), and proteomic analysis of sensitised lung tissue from rat models showed disturbances in mitochondrial activity, glycolysis and calcium binding proteins (Xu *et al.*, 2010). Indeed, I have shown that airway physiology and CODF are correlated, which maybe an ancestral throw back to microdomain re-organisation of $[Ca^{2+}]_i$ release channels that exists *in vivo*. 'So what might be the nature of this asthmatic immunological reaction?'

5.8.3.1 Adaptive immune response

In chronic inflammatory diseases such as asthma, specific or adaptive immunity plays a central role. It is known that in atopic asthma the immunological reaction to allergens is for B-cells to produce IgE type antibodies, whereas this does not happen in non-asthmatic individuals. They tend to produce IgG antibodies that do not give rise to an inflammatory response, rather tolerance is induced – there is no threat. However, in asthmatics the immune system does perceive a threat from allergens and produces an

IgE response that is more sensibly seen in the gut as reaction to parasites such as intestinal helminths. In the latter case the immune response is in the gut, directed against parasites and does not disable the host. Whereas in asthma the response is in the lungs and it certainly does disable the host. So antibody isotype switching mechanisms are an obvious starting point.

Similarly, asthma has long been characterised as a Th2 cell skewed disease. One might fundamentally ask, 'Why do APCs such as DCs or monocytes lead to signal one and signal two to be given to activate T-cells in response to allergens, thus generating an unnecessary inflammatory response in the first place?' 'Could it be that respiratory tissue structural cells gain the ability to present self peptide fragments on local APCs, thereby provoking a T-cell mediated inflammatory response, which is exacerbated by the presence of formerly innocuous inhaled antigens?' And of course the reaction is attenuated somewhat when the patient breathes cleaner air. Interestingly, the paradigm of tissue transplantation has highlighted the property of DC tolerance in a therapeutic context which I suspect could also be translated to asthma (Morelli *et al.*, 2007).

Furthermore, as children are being raised in cleaner and cleaner environments, the early stages of immune system development are not being trained on the environment, and development of tolerance to common antigens in food for example (Cohn, 2001). This increasingly means that in adulthood there is a trend toward living in cleaner and cleaner environments, even wearing face masks to avoid environmental pollution. However, there is no clear epidemiological link between hygiene and asthma (Ramsey *et al.*, 2005). Of course, good hygiene should not be discouraged, and to this end there has been a proposal that emphasis should move away from the term hygiene, in favour of a hypothesis favouring terms like 'microbial exposure' or 'microbial deprivation'

(Bloomfield *et al.*, 2006). But however the hypothesis is termed, of greater concern is the potential for immunological intolerance to be turned on self.

This autoimmune type of phenomenon is not unprecedented and may be simply explained via the Danger Model (Tveita, 2010). Indeed cases of autoimmune urticaria and non-atopic asthma are known (Tedeschi *et al.*, 2009). For example eosinophilia and the presence of antibodies such as IgE also occur in some neuropathies such as diabetic neuropathy and reflex sympathetic dystrophy (RSD), the common result being the incidence of inflammation. Moreover, it is known that patients with atopic dermatitis have IgE autoantibodies (Mittermann *et al.*, 2004). Logically, symptoms worsen during exacerbations when exogenous allergens are present, as does the IgE titre. Notice that this could be a parallel model for respiratory hypersensitivity. That is, I have described a paradigm whereby tissue sensitivity is increased by a pre-existing chronic inflammation that is further aggravated by cross-reaction of IgE autoantibodies to otherwise innocuous allergens. Interestingly, it is possible to reduce allergic sensitivity of the adaptive immune system by treating patients with peptides containing a particular epitope. This results in tolerance to other linked epitopes of the same allergen, and is called linked epitope suppression (Campbell *et al.*, 2009).

5.8.3.2 Innate immune response

However, 'igniting the blue touch paper' may also be initiated by innate immunity, which commonly precedes and provokes an adaptive immune response. It is known that those foot soldiers of innate immunity, mast cells and eosinophils, infiltrate the lungs of asthmatics. But these cells have evolved to defend against parasites. So the question again arises, 'Why should some individuals mount such an attack on allergens as if they were parasites?' 'What are the different mechanisms of antigen peptide

presentation in asthmatics provoked by innate factors?' The answers to these questions are not clear.

However, recent advances have identified key cytokines that are thought to play a primary role in the initiation of innate inflammation. Allergen proteases have been found to stimulate respiratory epithelium cells to secrete several key innate immune system cytokines. Of current interest are IL-18, IL-33 (both part of the IL-1 family) and TSLP (thymic stromal lymphopoietin). It is thought that these 'master' cytokines play a fundamental role in initiating Th2 mediated asthma. These chemicals have the potential to be the long sought after 'lighters of the blue touch paper,' that come right at the beginning of the story of asthma pathogenesis. A genome wide association study has identified IL-33 as a protease mediated activator of innate airway inflammation nicely reviewed in (Oboki 2010), quite independent of the genes that control the adaptive Th2 / IgE mediated atopy. Hence, IL-33 is seen as an exciting new drug target to attenuate innate immune system inflammation. Similarly, in an overlap with the adaptive immune system, TSLP is also being actively investigated as a drug target to attenuate IgE mediated atopy. Moreover, such an anti-TSLP strategy could increase allergen tolerance by dis-inhibiting T_{reg} cells. IL-18 is a proinflammatory cytokine that has the ability to cause secretion of Th1 cytokine, IFNγ, and Th2 cytokines, IL-4 and IL-13. IL-18R are found on several cells including epithelial cells, macrophages and DCs, and IFNγ promotes IL-18R production on monocyte derived DCs. Hence, in terms of drug discovery, an IL-18R antagonist be would potentially useful because IL-18 is a chemoattractant for DCs where it can also activate an IL-18R mediated innate immune response which again attracts Th2 cells. Currently, therapeutic vaccines are being investigated for these targets.

Of course the innate and adaptive immune systems functionally overlap mainly via biochemical communication mechanisms. Hence, it could be that there is a fault with the most ancient and non-specific part of the immune system. Therefore, these three cytokines, IL-18, IL-33 and TSLP, are currently the subject of intensive research. If proved true, this primary lesion would generate a chain reaction of immune responses, resulting in the incredibly complex and robustly persistent hypersensitivity pathologies such as asthma.

5.8.3.3 So what are the fundamental considerations?

What I am really asking here is, 'What is the set of criteria that has to be forefilled in order to give the 'commit signal' to attack a perceived respiratory threat?' Not just a dangerous threat that the immune system can efficiently protect the host from as a matter of normal immune physiology. But the launch of a sustained pathological attack signal. Taking the immune system from a benign sub-clinical state right through to fully blown clinical signs and symptoms of asthma. 'What is the chain of molecular decisions that constitutes an attack signal in diseases such as asthma?' For asthmatics the attack sequence is initiated by a phantom attacker, allergens that normal individuals tolerate. So, 'What makes a phantom attack look like a real attack to an asthmatic's immune system?' Simply, no one knows for sure. The field is still wide open. 'What are the trigger activated signaling pathways?' Certainly not just epithelial protease activated receptors. 'How do multiple cell types move and interact?' And 'What is the precise role of 'master' cytokines such as IL-18, IL-33 and TSLP?'

Whatever the answers turn out to be, it is known that therapeutic intervention in the initial stages of an innate immune response is simpler than having to deal with the adaptive response that follows. Simply because the adaptive response comes with

memory and increased specificity to antigens, increasing as the chronicity component of inflammation progresses.

These questions will lead to a new fundamental rationale, yielding mechanisms that are simple fundamental truths of the immune system. With the assistance of software the complex chemically orchestrated cellular interactions can be mapped and understood. Incontrovertibly, the immune system is justifiably complex and mounts a formidably dynamic defence on many fronts. It fights with a diverse arsenal which all too often is the reason why respiratory pharmacy is found lacking. This is because current understanding of asthma fundamentals is lacking. Answers to the questions posed by myself and others, although hard won, will no doubt lead to understanding of novel immunological mechanisms that lead to disease. Inevitably suggesting therapies that are not just symptomatic patches, but that truly address and modify the perceived threat to the immune system of foreign triggers at the root.

REFERENCES

Aikawa T, Shimura S, Sasaki H, Ebina M, Takishima T (1992). Marked goblet cell hyperplasia with mucus accumulation in the airways of patients who died of severe acute asthma attack. *Chest* **101**(4)**:** 916-921.

Amrani Y, Da Silva A, Kassel O, Bronner C (1994). Biphasic increase in cytosolic free calcium induced by bradykinin and histamine in cultured tracheal smooth muscle cells: is the sustained phase artifactual? *Naunyn Schmiedebergs Arch Pharmacol* **350**(6)**:** 662-669.

Amrani Y, Panettieri RA, Jr. (2002). Modulation of calcium homeostasis as a mechanism for altering smooth muscle responsiveness in asthma. *Curr Opin Allergy Clin Immunol* **2**(1)**:** 39-45.

Antigny F, Norez C, Cantereau A, Becq F, Vandebrouck C (2008). Abnormal spatial diffusion of Ca2+ in F508del-CFTR airway epithelial cells. *Respir Res* **9:** 70.

Ashby MC, Craske M, Park MK, Gerasimenko OV, Burgoyne RD, Petersen OH, *et al.* (2002). Localized Ca2+ uncaging reveals polarized distribution of Ca2+-sensitive Ca2+ release sites: mechanism of unidirectional Ca2+ waves. *J Cell Biol* **158**(2)**:** 283-292.

AsthmaUK (2008). For Journalists: Key facts and statistics. *[Online] http://www.asthma.org.uk/news_media/media_resources/for_journalists_key.html, Last accessed: 12 September 2008.*

Bai Y, Sanderson MJ (2006). Airway smooth muscle relaxation results from a reduction in the frequency of Ca2+ oscillations induced by a cAMP-mediated inhibition of the IP3 receptor. *Respir Res* **7:** 34.

Barnes PJ (1992). Effect of bradykinin on airway function. *Agents Actions Suppl* **38 (Pt 3):** 432-438.

Barnes PJ (2004). New drugs for asthma. *Nat Rev Drug Discov* **3**(10)**:** 831-844.

Barnes PJ (2008a). Immunology of asthma and chronic obstructive pulmonary disease. *Nat Rev Immunol* **8**(3)**:** 183-192.

Barnes PJ (2008b). Role of GATA-3 in allergic diseases. *Curr Mol Med* **8**(5)**:** 330-334.

Barnes PJ (2010). New therapies for asthma: is there any progress? *Trends Pharmacol Sci* **31**(7)**:** 335-343.

Barnes PJ, Chung KF, Page CP (1998). Inflammatory mediators of asthma: an update. *Pharmacol Rev* **50**(4)**:** 515-596.

Berridge MJ (1990). Calcium oscillations. *J Biol Chem* **265**(17)**:** 9583-9586.

Berridge MJ (1993). Inositol trisphosphate and calcium signaling. *Nature* **361**(6410)**:** 315-325.

Berridge MJ (1997a). The AM and FM of calcium signaling. *Nature* **386**(6627)**:** 759-760.

Berridge MJ (1997b). Elementary and global aspects of calcium signaling. *J Physiol* **499 (Pt 2):** 291-306.

Berridge MJ (2006). Calcium microdomains: organization and function. *Cell Calcium* **40**(5-6)**:** 405-412.

Berridge MJ, Bootman MD, Roderick HL (2003). Calcium signaling: dynamics, homeostasis and remodelling. *Nat Rev Mol Cell Biol* **4**(7)**:** 517-529.

Berridge MJ, Dupont G (1994). Spatial and temporal signaling by calcium. *Curr Opin Cell Biol* **6**(2)**:** 267-274.

Berridge MJ, Galione A (1988). Cytosolic calcium oscillators. *FASEB J* **2**(15)**:** 3074-3082.

Bezprozvanny I, Watras J, Ehrlich BE (1991). Bell-shaped calcium-response curves of Ins(1,4,5)P3- and calcium-gated channels from endoplasmic reticulum of cerebellum. *Nature* **351**(6329)**:** 751-754.

Bird GS, DeHaven WI, Smyth JT, Putney JW, Jr. (2008). Methods for studying store-operated calcium entry. *Methods* **46**(3)**:** 204-212.

Black JL, Marthan R, Armour CL, Johnson PR (1989). Sensitization alters contractile responses and calcium influx in human airway smooth muscle. *J Allergy Clin Immunol* **84**(4 Pt 1)**:** 440-447.

Bloomfield SF, Stanwell-Smith R, Crevel RW, Pickup J (2006). Too clean, or not too clean: the hygiene hypothesis and home hygiene. *Clin Exp Allergy* **36**(4)**:** 402-425.

Borger P, Tamm M, Black JL, Roth M (2006). Asthma: is it due to an abnormal airway smooth muscle cell? *Am J Respir Crit Care Med* **174**(4)**:** 367-372.

Bradley E, Hollywood MA, McHale NG, Thornbury KD, Sergeant GP (2005). Pacemaker activity in urethral interstitial cells is not dependent on capacitative calcium entry. *Am J Physiol Cell Physiol* **289**(3)**:** C625-632.

Brandman O, Meyer T (2008). Feedback loops shape cellular signals in space and time. *Science* **322**(5900)**:** 390-395.

Brasen JC, Olsen LF, Hallett MB (2010). Cell surface topology creates high Ca2+ signaling microdomains. *Cell Calcium* **47**(4)**:** 339-349.

Brightling CE, Bradding P, Symon FA, Holgate ST, Wardlaw AJ, Pavord ID (2002). Mast-cell infiltration of airway smooth muscle in asthma. *N Engl J Med* **346**(22)**:** 1699-1705.

Brown GR, Sayers LG, Kirk CJ, Michell RH, Michelangeli F (1992). The opening of the inositol 1,4,5-trisphosphate-sensitive Ca2+ channel in rat cerebellum is inhibited by caffeine. *Biochem J* **282 (Pt 2):** 309-312.

Campbell JD, Buckland KF, McMillan SJ, Kearley J, Oldfield WL, Stern LJ, *et al.* (2009). Peptide immunotherapy in allergic asthma generates IL-10-dependent immunological tolerance associated with linked epitope suppression. *J Exp Med* **206**(7)**:** 1535-1547.

Cantero-Recasens G, Fandos C, Rubio-Moscardo F, Valverde MA, Vicente R (2010). The asthma-associated ORMDL3 gene product regulates endoplasmic reticulum-mediated calcium signaling and cellular stress. *Hum Mol Genet* **19**(1)**:** 111-121.

Carroll NG, Cooke C, James AL (1997). Bronchial blood vessel dimensions in asthma. *Am J Respir Crit Care Med* **155**(2)**:** 689-695.

Carroll NG, Perry S, Karkhanis A, Harji S, Butt J, James AL, *et al.* (2000). The airway longitudinal elastic fiber network and mucosal folding in patients with asthma. *Am J Respir Crit Care Med* **161**(1)**:** 244-248.

Case RM, Eisner D, Gurney A, Jones O, Muallem S, Verkhratsky A (2007). Evolution of calcium homeostasis: from birth of the first cell to an omnipresent signaling system. *Cell Calcium* **42**(4-5)**:** 345-350.

Chakir J, Loubaki L, Laviolette M, Milot J, Biardel S, Jayaram L, *et al.* (2010). Monitoring sputum eosinophils in mucosal inflammation and remodelling: a pilot study. *Eur Respir J* **35**(1)**:** 48-53.

Challiss RA, Batty IH, Nahorski SR (1988). Mass measurements of inositol(1,4,5)trisphosphate in rat cerebral cortex slices using a radioreceptor assay: effects of neurotransmitters and depolarization. *Biochem Biophys Res Commun* **157**(2)**:** 684-691.

Chanez P, Wenzel SE, Anderson GP, Anto JM, Bel EH, Boulet LP, *et al.* (2007). Severe asthma in adults: what are the important questions? *J Allergy Clin Immunol* **119**(6)**:** 1337-1348.

Choe CU, Ehrlich BE (2006). The inositol 1,4,5-trisphosphate receptor (IP3R) and its regulators: sometimes good and sometimes bad teamwork. *Sci STKE* **2006**(363)**:** re15.

Cohn L (2001). Food for thought: can immunological tolerance be induced to treat asthma? *Am J Respir Cell Mol Biol* **24**(5)**:** 509-512.

Coleman NE, Dalton HJ (2009). Extracorporeal life support for status asthmaticus: the breath of life that's often forgotten. *Crit Care* **13**(2)**:** 136.

Combettes L, Berthon B, Claret M (1994). Caffeine inhibits cytosolic calcium oscillations induced by noradrenaline and vasopressin in rat hepatocytes. *Biochem J* **301 (Pt 3):** 737-744.

Conchello JA, Lichtman JW (2005). Optical sectioning microscopy. *Nat Methods* **2**(12)**:** 920-931.

Corren J, Busse W, Meltzer EO, Mansfield L, Bensch G, Fahrenholz J, *et al.* (2010). A randomized, controlled, phase 2 study of AMG 317, an IL-4Ralpha antagonist, in patients with asthma. *Am J Respir Crit Care Med* **181**(8)**:** 788-796.

Corteling RL, Li S, Giddings J, Westwick J, Poll C, Hall IP (2004). Expression of transient receptor potential C6 and related transient receptor potential family members in human airway smooth muscle and lung tissue. *Am J Respir Cell Mol Biol* **30**(2)**:** 145-154.

Crameri R (2005). The potential of proteomics and peptidomics for allergy and asthma research. *Allergy* **60**(10)**:** 1227-1237.

Crimi E, Milanese M, Pingfang S, Brusasco V (2001). Allergic inflammation and airway smooth muscle function. *Sci Total Environ* **270**(1-3)**:** 57-61.

Dabertrand F, Mironneau J, Macrez N, Morel JL (2008). Full length ryanodine receptor subtype 3 encodes spontaneous calcium oscillations in native duodenal smooth muscle cells. *Cell Calcium* **44**(2)**:** 180-189.

Dai JM, Kuo KH, Leo JM, van Breemen C, Lee CH (2006). Mechanism of ACh-induced asynchronous calcium waves and tonic contraction in porcine tracheal muscle bundle. *Am J Physiol Lung Cell Mol Physiol* **290**(3)**:** L459-469.

Damera G, Panettieri RA, Jr. (2011). Does airway smooth muscle express an inflammatory phenotype in asthma? *Br J Pharmacol* **163**(1)**:** 68-80.

Darby PJ, Kwan CY, Daniel EE (2000). Caveolae from canine airway smooth muscle contain the necessary components for a role in Ca(2+) handling. *Am J Physiol Lung Cell Mol Physiol* **279**(6)**:** L1226-1235.

Davidson SM, Duchen MR (2006). Calcium microdomains and oxidative stress. *Cell Calcium* **40**(5-6)**:** 561-574.

Deshpande DA, Wang WC, McIlmoyle EL, Robinett KS, Schillinger RM, An SS, *et al.* Bitter taste receptors on airway smooth muscle bronchodilate by localized calcium signaling and reverse obstruction. *Nat Med* **16**(11)**:** 1299-1304.

Deshpande DA, White TA, Dogan S, Walseth TF, Panettieri RA, Kannan MS (2005). CD38/cyclic ADP-ribose signaling: role in the regulation of calcium homeostasis in airway smooth muscle. *Am J Physiol Lung Cell Mol Physiol* **288**(5)**:** L773-788.

Dolmetsch RE, Lewis RS, Goodnow CC, Healy JI (1997). Differential activation of transcription factors induced by Ca2+ response amplitude and duration. *Nature* **386**(6627)**:** 855-858.

Dolmetsch RE, Xu K, Lewis RS (1998). Calcium oscillations increase the efficiency and specificity of gene expression. *Nature* **392**(6679)**:** 933-936.

Dolovich J, Hargreave F (1981). The asthma syndrome: inciters, inducers, and host characteristics. *Thorax* **36**(9)**:** 614-644.

Du W, Stiber JA, Rosenberg PB, Meissner G, Eu JP (2005). Ryanodine receptors in muscarinic receptor-mediated bronchoconstriction. *J Biol Chem* **280**(28)**:** 26287-26294.

Ebina M, Takahashi T, Chiba T, Motomiya M (1993). Cellular hypertrophy and hyperplasia of airway smooth muscles underlying bronchial asthma. A 3-D morphometric study. *Am Rev Respir Dis* **148**(3)**:** 720-726.

Einstein R, Jordan H, Zhou W, Brenner M, Moses EG, Liggett SB (2008). Alternative splicing of the G protein-coupled receptor superfamily in human airway smooth muscle diversifies the complement of receptors. *Proc Natl Acad Sci U S A* **105**(13)**:** 5230-5235.

Endo M, Tanaka M, Ogawa Y (1970). Calcium induced release of calcium from the sarcoplasmic reticulum of skinned skeletal muscle fibres. *Nature* **228**(5266)**:** 34-36.

Floyd R, Wray S (2007). Calcium transporters and signaling in smooth muscles. *Cell Calcium* **42**(4-5)**:** 467-476.

Galanter J, Choudhry S, Eng C, Nazario S, Rodriguez-Santana JR, Casal J, *et al.* (2008). ORMDL3 gene is associated with asthma in three ethnically diverse populations. *Am J Respir Crit Care Med* **177**(11)**:** 1194-1200.

GBIResearch (2009). The Future of Respiratory Diseases Therapeutics - Market Forecasts to 2015, Competitive Benchmarking, Product Pipeline and Deals Analysis, . *[Online] http://www.docstoc.com/docs/64933497/The-Future-of-Respiratory-Diseases-Therapeutics---Market-Forecasts-to-2015-Competitive-Benchmarking-Product-Pipeline-and-Deals-Analysis*.

Giepmans BN, Adams SR, Ellisman MH, Tsien RY (2006). The fluorescent toolbox for assessing protein location and function. *Science* **312**(5771)**:** 217-224.

Global Initiative for Asthma G (2010). GINA Report, Global Strategy for Asthma Management and Prevention: http://www.ginasthma.com/GuidelinesResources.asp.

Gomez E, Powell ML, Bevington A, Herbert TP (2008). A decrease in cellular energy status stimulates PERK-dependent eIF2alpha phosphorylation and regulates protein synthesis in pancreatic beta-cells. *Biochem J* **410**(3)**:** 485-493.

Gordienko DV, Bolton TB (2002). Crosstalk between ryanodine receptors and IP(3) receptors as a factor shaping spontaneous Ca(2+)-release events in rabbit portal vein myocytes. *J Physiol* **542**(Pt 3)**:** 743-762.

Gosens R, Stelmack GL, Dueck G, Mutawe MM, Hinton M, McNeill KD, *et al.* (2007). Caveolae facilitate muscarinic receptor-mediated intracellular Ca2+ mobilization and contraction in airway smooth muscle. *Am J Physiol Lung Cell Mol Physiol* **293**(6)**:** L1406-1418.

Grainge CL, Lau LC, Ward JA, Dulay V, Lahiff G, Wilson S, *et al.* (2011). Effect of bronchoconstriction on airway remodeling in asthma. *N Engl J Med* **364**(21)**:** 2006-2015.

Grynkiewicz G, Poenie M, Tsien RY (1985). A new generation of Ca2+ indicators with greatly improved fluorescence properties. *J Biol Chem* **260**(6)**:** 3440-3450.

Haldar P, Pavord ID, Shaw DE, Berry MA, Thomas M, Brightling CE, *et al.* (2008). Cluster analysis and clinical asthma phenotypes. *Am J Respir Crit Care Med* **178**(3)**:** 218-224.

Hart PH (2001). Regulation of the inflammatory response in asthma by mast cell products. *Immunol Cell Biol* **79**(2)**:** 149-153.

Hassan M, Jo T, Risse PA, Tolloczko B, Lemiere C, Olivenstein R, *et al.* (2010). Airway smooth muscle remodeling is a dynamic process in severe long-standing asthma. *J Allergy Clin Immunol* **125**(5)**:** 1037-1045 e1033.

Hirota JA, Nguyen TT, Schaafsma D, Sharma P, Tran T (2009). Airway smooth muscle in asthma: phenotype plasticity and function. *Pulm Pharmacol Ther* **22**(5)**:** 370-378.

Hirota S, Helli P, Janssen LJ (2007). Ionic mechanisms and Ca2+ handling in airway smooth muscle. *Eur Respir J* **30**(1)**:** 114-133.

Hofer AM, Brown EM (2003). Extracellular calcium sensing and signaling. *Nat Rev Mol Cell Biol* **4**(7)**:** 530-538.

Holgate ST, Polosa R (2006). The mechanisms, diagnosis, and management of severe asthma in adults. *Lancet* **368**(9537)**:** 780-793.

Hollins F, Kaur D, Yang W, Cruse G, Saunders R, Sutcliffe A, *et al.* (2008). Human airway smooth muscle promotes human lung mast cell survival, proliferation, and constitutive activation: cooperative roles for CADM1, stem cell factor, and IL-6. *J Immunol* **181**(4)**:** 2772-2780.

Houtman R, van den Worm E (2005). Asthma, the ugly duckling of lung disease proteomics? *J Chromatogr B Analyt Technol Biomed Life Sci* **815**(1-2)**:** 285-294.

Ichimura H, Parthasarathi K, Lindert J, Bhattacharya J (2006). Lung surfactant secretion by interalveolar Ca2+ signaling. *Am J Physiol Lung Cell Mol Physiol* **291**(4)**:** L596-601.

Isenberg G (2004). Ca2+ control of transcription: can we extrapolate signaling cascades from neurons to vascular smooth muscle cells? *Circ Res* **94**(10)**:** 1276-1278.

Jeffery PK (2001). Remodeling in asthma and chronic obstructive lung disease. *Am J Respir Crit Care Med* **164**(10 Pt 2)**:** S28-38.

Jeffery PK, Wardlaw AJ, Nelson FC, Collins JV, Kay AB (1989). Bronchial biopsies in asthma. An ultrastructural, quantitative study and correlation with hyperreactivity. *Am Rev Respir Dis* **140**(6)**:** 1745-1753.

Ji G, Feldman M, Doran R, Zipfel W, Kotlikoff MI (2006). Ca2+ -induced Ca2+ release through localized Ca2+ uncaging in smooth muscle. *J Gen Physiol* **127**(3)**:** 225-235.

Kao JP (2006). Caged molecules: principles and practical considerations. *Curr Protoc Neurosci* **Chapter 6:** Unit 6 20.

Kellner J, Tantzscher J, Oelmez H, Edelmann M, Fischer R, Huber RM, *et al.* (2008). Mechanisms altering airway smooth muscle cell Ca+ homeostasis in two asthma models. *Respiration* **76**(2)**:** 205-215.

Knight MM, Roberts SR, Lee DA, Bader DL (2003). Live cell imaging using confocal microscopy induces intracellular calcium transients and cell death. *Am J Physiol Cell Physiol* **284**(4)**:** C1083-1089.

Knot HJ, Laher I, Sobie EA, Guatimosim S, Gomez-Viquez L, Hartmann H, *et al.* (2005). Twenty years of calcium imaging: cell physiology to dye for. *Mol Interv* **5**(2)**:** 112-127.

Kraneveld AD, James DE, de Vries A, Nijkamp FP (2000). Excitatory non-adrenergic-non-cholinergic neuropeptides: key players in asthma. *Eur J Pharmacol* **405**(1-3)**:** 113-129.

Kuba K, Nishi S (1976). Rhythmic hyperpolarizations and depolarization of sympathetic ganglion cells induced by caffeine. *J Neurophysiol* **39**(3)**:** 547-563.

Kuimova MK, Botchway SW, Parker AW, Balaz M, Collins HA, Anderson HL, *et al.* (2009). Imaging intracellular viscosity of a single cell during photoinduced cell death. *Nat Chem* **1**(1)**:** 69-73.

Kumar A, Ghosh B (2009). Genetics of asthma: a molecular biologist perspective. *Clin Mol Allergy* **7:** 7.

Kumar RK, Thomas PS, Seetoo DQ, Herbert C, McKenzie AN, Foster PS, *et al.* (2002). Eotaxin expression by epithelial cells and plasma cells in chronic asthma. *Lab Invest* **82**(4)**:** 495-504.

Lamche HR, Silberstein PT, Knabe AC, Thomas DD, Jacob HS, Hammerschmidt DE (1990). Steroids decrease granulocyte membrane fluidity, while phorbol ester increases

membrane fluidity. Studies using electron paramagnetic resonance. *Inflammation* **14**(1)**:** 61-70.

Lichtman JW, Conchello JA (2005). Fluorescence microscopy. *Nat Methods* **2**(12)**:** 910-919.

Limpert E, Stahel WA, Abbt M (2001). Log-normal Distributions across the Sciences: Keys and clues. *BioScience* **51**(5)**:** 341-352.

Lipworth BJ, Struthers AD, McDevitt DG (1989). Tachyphylaxis to systemic but not to airway responses during prolonged therapy with high dose inhaled salbutamol in asthmatics. *Am Rev Respir Dis* **140**(3)**:** 586-592.

Liu B, Peel SE, Fox J, Hall IP (2010). Reverse mode Na+/Ca2+ exchange mediated by STIM1 contributes to Ca2+ influx in airway smooth muscle following agonist stimulation. *Respir Res* **11:** 168.

Liu YJ (2006). Thymic stromal lymphopoietin: master switch for allergic inflammation. *J Exp Med* **203**(2)**:** 269-273.

Lotvall J, Inman M, O'Byrne P (1998). Measurement of airway hyperresponsiveness: new considerations. *Thorax* **53**(5)**:** 419-424.

Low RB, White SL (1998). Lung smooth muscle differentiation. *Int J Biochem Cell Biol* **30**(8)**:** 869-883.

Ma X, Cheng Z, Kong H, Wang Y, Unruh H, Stephens NL, *et al.* (2002). Changes in biophysical and biochemical properties of single bronchial smooth muscle cells from asthmatic subjects. *Am J Physiol Lung Cell Mol Physiol* **283**(6)**:** L1181-1189.

Mahn K, Hirst SJ, Ying S, Holt MR, Lavender P, Ojo OO, *et al.* (2009). Diminished sarco/endoplasmic reticulum Ca2+ ATPase (SERCA) expression contributes to airway remodelling in bronchial asthma. *Proc Natl Acad Sci U S A* **106**(26)**:** 10775-10780.

Mahn K, Ojo OO, Chadwick G, Aaronson PI, Ward JP, Lee TH Ca(2+) homeostasis and structural and functional remodelling of airway smooth muscle in asthma. *Thorax* **65**(6)**:** 547-552.

Mahn K, Ojo OO, Chadwick G, Aaronson PI, Ward JP, Lee TH (2010). Ca(2+) homeostasis and structural and functional remodelling of airway smooth muscle in asthma. *Thorax* **65**(6)**:** 547-552.

Marsh KA, Hill SJ (1992). Bradykinin B2 receptor-mediated phosphoinositide hydrolysis in bovine cultured tracheal smooth muscle cells. *Br J Pharmacol* **107**(2)**:** 443-447.

Marsh KA, Hill SJ (1993). Characteristics of the bradykinin-induced changes in intracellular calcium ion concentration of single bovine tracheal smooth muscle cells. *Br J Pharmacol* **110**(1)**:** 29-35.

Marsh KA, Hill SJ (1994). Des-Arg9-bradykinin-induced increases in intracellular calcium ion concentration in single bovine tracheal smooth muscle cells. *Br J Pharmacol* **112**(3)**:** 934-938.

Marthan R (2004). Store-operated calcium entry and intracellular calcium release channels in airway smooth muscle. *Am J Physiol Lung Cell Mol Physiol* **286**(5)**:** L907-908.

Matzinger P (2002). The danger model: a renewed sense of self. *Science* **296**(5566)**:** 301-305.

Mauad T, Silva LF, Santos MA, Grinberg L, Bernardi FD, Martins MA, *et al.* (2004). Abnormal alveolar attachments with decreased elastic fiber content in distal lung in fatal asthma. *Am J Respir Crit Care Med* **170**(8)**:** 857-862.

Middleton E, Jr. (1984). Airway smooth muscle, asthma, and calcium ions. *J Allergy Clin Immunol* **73**(5 Pt 2)**:** 643-650.

Missiaen L, Parys JB, De Smedt H, Himpens B, Casteels R (1994). Inhibition of inositol trisphosphate-induced calcium release by caffeine is prevented by ATP. *Biochem J* **300 (Pt 1):** 81-84.

Mittermann I, Aichberger KJ, Bunder R, Mothes N, Renz H, Valenta R (2004). Autoimmunity and atopic dermatitis. *Curr Opin Allergy Clin Immunol* **4**(5)**:** 367-371.

Miyakawa T, Maeda A, Yamazawa T, Hirose K, Kurosaki T, Iino M (1999). Encoding of Ca2+ signals by differential expression of IP3 receptor subtypes. *EMBO J* **18**(5)**:** 1303-1308.

Molecular-Probes (2011). Fura and Indo Ratiometric Calcium Indicators. *Product Information* **http://probes.invitrogen.com/media/pis/mp01200.pdf**.

Morales S, Diez A, Puyet A, Camello PJ, Camello-Almaraz C, Bautista JM, *et al.* (2007). Calcium controls smooth muscle TRPC gene transcription via the CaMK/calcineurin-dependent pathways. *Am J Physiol Cell Physiol* **292**(1)**:** C553-563.

Morelli AE, Thomson AW (2007). Tolerogenic dendritic cells and the quest for transplant tolerance. *Nat Rev Immunol* **7**(8)**:** 610-621.

Muers M (2011). Gene expression: Transcriptome to proteome and back to genome. *Nat Rev Genet*.

Nakano T, Koujin T, Suda T, Hiraoka Y, Haraguchi T (2009). A locally-induced increase in intracellular Ca2+ propagates cell-to-cell in the presence of plasma membrane Ca2+ ATPase inhibitors in non-excitable cells. *FEBS Lett* **583**(22)**:** 3593-3599.

Ng J, Goldberger JJ (2007). Understanding and interpreting dominant frequency analysis of AF electrograms. *J Cardiovasc Electrophysiol* **18**(6)**:** 680-685.

Nguyen KD, Vanichsarn C, Nadeau KC (2010). TSLP directly impairs pulmonary Treg function: association with aberrant tolerogenic immunity in asthmatic airway. *Allergy Asthma Clin Immunol* **6**(1)**:** 4.

Nishida K, Yamasaki S, Ito Y, Kabu K, Hattori K, Tezuka T, *et al.* (2005). Fc{epsilon}RI-mediated mast cell degranulation requires calcium-independent microtubule-dependent translocation of granules to the plasma membrane. *J Cell Biol* **170**(1)**:** 115-126.

O'Haver T (2009). Peak Finding and Measurement, Version 2. *[Online] http://www.wam.umd.edu/~toh/spectrum/PeakFindingandMeasurement.htm*.

Pani B, Singh BB (2009). Lipid rafts/caveolae as microdomains of calcium signaling. *Cell Calcium* **45**(6)**:** 625-633.

Parameswaran K, Janssen LJ, O'Byrne PM (2002). Airway hyperresponsiveness and calcium handling by smooth muscle: a "deeper look". *Chest* **121**(2)**:** 621-624.

Parekh AB (2011). Decoding cytosolic Ca2+ oscillations. *Trends Biochem Sci* **36**(2)**:** 78-87.

Peel SE, Liu B, Hall IP (2006). A key role for STIM1 in store operated calcium channel activation in airway smooth muscle. *Respir Res* **7:** 119.

Peel SE, Liu B, Hall IP (2008). ORAI and store-operated calcium influx in human airway smooth muscle cells. *Am J Respir Cell Mol Biol* **38**(6)**:** 744-749.

Perez-Zoghbi JF, Karner C, Ito S, Shepherd M, Alrashdan Y, Sanderson MJ (2009). Ion channel regulation of intracellular calcium and airway smooth muscle function. *Pulm Pharmacol Ther* **22**(5)**:** 388-397.

Perez JF, Sanderson MJ (2005). The frequency of calcium oscillations induced by 5-HT, ACH, and KCl determine the contraction of smooth muscle cells of intrapulmonary bronchioles. *J Gen Physiol* **125**(6)**:** 535-553.

Poburko D, Kuo KH, Dai J, Lee CH, van Breemen C (2004). Organellar junctions promote targeted Ca2+ signaling in smooth muscle: why two membranes are better than one. *Trends Pharmacol Sci* **25**(1)**:** 8-15.

Prakash YS, Kannan MS, Sieck GC (1997). Regulation of intracellular calcium oscillations in porcine tracheal smooth muscle cells. *Am J Physiol* **272**(3 Pt 1)**:** C966-975.

Prakash YS, Sathish V, Thompson MA, Pabelick CM, Sieck GC (2009). Asthma and sarcoplasmic reticulum Ca2+ reuptake in airway smooth muscle. *Am J Physiol Lung Cell Mol Physiol* **297**(4)**:** L794.

Prakash YS, Thompson MA, Vaa B, Matabdin I, Peterson TE, He T, *et al.* (2007). Caveolins and intracellular calcium regulation in human airway smooth muscle. *Am J Physiol Lung Cell Mol Physiol* **293**(5)**:** L1118-1126.

Pucovsky V, Bolton TB (2006). Localisation, function and composition of primary Ca(2+) spark discharge region in isolated smooth muscle cells from guinea-pig mesenteric arteries. *Cell Calcium* **39**(2)**:** 113-129.

Putney JW, Bird GS (2008). Cytoplasmic calcium oscillations and store-operated calcium influx. *J Physiol* **586**(13)**:** 3055-3059.

Rakyan VK, Down TA, Balding DJ, Beck S (2011). Epigenome-wide association studies for common human diseases. *Nat Rev Genet*.

Ramos-Franco J, Fill M, Mignery GA (1998). Isoform-specific function of single inositol 1,4,5-trisphosphate receptor channels. *Biophys J* **75**(2)**:** 834-839.

Ramsey CD, Celedon JC (2005). The hygiene hypothesis and asthma. *Curr Opin Pulm Med* **11**(1)**:** 14-20.

Ribatti D, Puxeddu I, Crivellato E, Nico B, Vacca A, Levi-Schaffer F (2009). Angiogenesis in asthma. *Clin Exp Allergy* **39**(12)**:** 1815-1821.

Ridgway EB, Durham AC (1976). Oscillations of calcium ion concentrations in Physarum polycephalum. *J Cell Biol* **69**(1)**:** 223-226.

Ringer S (1883). A further Contribution regarding the influence of the different Constituents of the Blood on the Contraction of the Heart. *J Physiol* **4**(1)**:** 29-42 23.

Roche WR, Beasley R, Williams JH, Holgate ST (1989). Subepithelial fibrosis in the bronchi of asthmatics. *Lancet* **1**(8637)**:** 520-524.

Sakai Y, Kwan CY (1993). Calcium regulation and contractile dysfunction of smooth muscle. *Biol Signals* **2**(5)**:** 305-312.

Salazar C, Politi AZ, Hofer T (2008). Decoding of calcium oscillations by phosphorylation cycles: analytic results. *Biophys J* **94**(4)**:** 1203-1215.

Sanderson MJ, Delmotte P, Bai Y, Perez-Zogbhi JF (2008). Regulation of airway smooth muscle cell contractility by Ca2+ signaling and sensitivity. *Proc Am Thorac Soc* **5**(1)**:** 23-31.

Sathish V, Thompson MA, Bailey JP, Pabelick CM, Prakash YS, Sieck GC (2009). Effect of proinflammatory cytokines on regulation of sarcoplasmic reticulum Ca2+ reuptake in human airway smooth muscle. *Am J Physiol Lung Cell Mol Physiol* **297**(1)**:** L26-34.

Savineau JP, Marthan R (2000). Cytosolic Calcium Oscillations in Smooth Muscle Cells. *News Physiol Sci* **15:** 50-55.

Siddiqui S, Gupta S, Cruse G, Haldar P, Entwisle J, McDonald S, *et al.* (2009). Airway wall geometry in asthma and nonasthmatic eosinophilic bronchitis. *Allergy* **64**(6)**:** 951-958.

Singh SR, Hall IP (2008). Airway myofibroblasts and their relationship with airway myocytes and fibroblasts. *Proc Am Thorac Soc* **5**(1)**:** 127-132.

Skupin A, Kettenmann H, Falcke M (2010). Calcium signals driven by single channel noise. *PLoS Comput Biol* **6**(8).

Snetkov VA, Hirst SJ, Ward JP (1996). Ion channels in freshly isolated and cultured human bronchial smooth muscle cells. *Exp Physiol* **81**(5)**:** 791-804.

Sneyd J, Tsaneva-Atanasova K, Yule DI, Thompson JL, Shuttleworth TJ (2004). Control of calcium oscillations by membrane fluxes. *Proc Natl Acad Sci U S A* **101**(5)**:** 1392-1396.

Streb H, Irvine RF, Berridge MJ, Schulz I (1983). Release of Ca2+ from a nonmitochondrial intracellular store in pancreatic acinar cells by inositol-1,4,5-trisphosphate. *Nature* **306**(5938)**:** 67-69.

Sui G, Fry CH, Malone-Lee J, Wu C (2009). Aberrant Ca2+ oscillations in smooth muscle cells from overactive human bladders. *Cell Calcium* **45**(5)**:** 456-464.

Suissa S, Ernst P, Benayoun S, Baltzan M, Cai B (2000). Low-dose inhaled corticosteroids and the prevention of death from asthma. *N Engl J Med* **343**(5)**:** 332-336.

Takeda N, Sumi Y, Prefontaine D, Al Abri J, Al Heialy N, Al-Ramli W, *et al.* (2009). Epithelium-derived chemokines induce airway smooth muscle cell migration. *Clin Exp Allergy* **39**(7)**:** 1018-1026.

Tao FC, Shah S, Pradhan AA, Tolloczko B, Martin JG (2003). Enhanced calcium signaling to bradykinin in airway smooth muscle from hyperresponsive inbred rats. *Am J Physiol Lung Cell Mol Physiol* **284**(1)**:** L90-99.

Tedeschi A, Cottini M, Asero R (2009). Simultaneous occurrence of chronic autoimmune urticaria and non-allergic asthma: a common mechanism? *Eur Ann Allergy Clin Immunol* **41**(2)**:** 56-59.

Teerlink CC, Hegewald MJ, Cannon-Albright LA (2007). A genealogical assessment of heritable predisposition to asthma mortality. *Am J Respir Crit Care Med* **176**(9)**:** 865-870.

Thomas AP, Bird GS, Hajnoczky G, Robb-Gaspers LD, Putney JW, Jr. (1996). Spatial and temporal aspects of cellular calcium signaling. *FASEB J* **10**(13)**:** 1505-1517.

Trepat X, Deng L, An SS, Navajas D, Tschumperlin DJ, Gerthoffer WT, *et al.* (2007). Universal physical responses to stretch in the living cell. *Nature* **447**(7144)**:** 592-595.

Trian T, Benard G, Begueret H, Rossignol R, Girodet PO, Ghosh D, *et al.* (2007). Bronchial smooth muscle remodeling involves calcium-dependent enhanced mitochondrial biogenesis in asthma. *J Exp Med* **204**(13)**:** 3173-3181.

Triggle DJ (1983). Calcium, the control of smooth muscle function and bronchial hyperreactivity. *Allergy* **38**(1)**:** 1-9.

Tveita AA (2010). The danger model in deciphering autoimmunity. *Rheumatology (Oxford)* **49**(4)**:** 632-639.

Uhlen P (2004). Spectral analysis of calcium oscillations. *Sci STKE* **2004**(258)**:** pl15.

Van Eerdewegh P, Little RD, Dupuis J, Del Mastro RG, Falls K, Simon J, *et al.* (2002). Association of the ADAM33 gene with asthma and bronchial hyperresponsiveness. *Nature* **418**(6896)**:** 426-430.

Vorndran C, Minta A, Poenie M (1995). New fluorescent calcium indicators designed for cytosolic retention or measuring calcium near membranes. *Biophys J* **69**(5)**:** 2112-2124.

Wang M, Chen Z, Xing Y, Zhang X, Dong XZ, Ji GJ (2006). Localized Ca2+ uncaging induces Ca2+ release through IP3R in smooth muscle. *Acta Pharmacol Sin* **27**(7)**:** 939-944.

Weiss EB (1985). Toxic oxygen products alter calcium homeostasis in an asthma model. *J Allergy Clin Immunol* **75**(6)**:** 692-697.

Wenzel S, Wilbraham D, Fuller R, Getz EB, Longphre M (2007). Effect of an interleukin-4 variant on late phase asthmatic response to allergen challenge in asthmatic patients: results of two phase 2a studies. *Lancet* **370**(9596)**:** 1422-1431.

WHO Global surveillance, prevention and control of chronic respiratory diseases: a comprehensive approach. *http://www.who.int/gard/publications/GARD_Manual/en/index.html* **Chronic Respiratory Diseases**.

Woodruff PG, Dolganov GM, Ferrando RE, Donnelly S, Hays SR, Solberg OD, *et al.* (2004). Hyperplasia of smooth muscle in mild to moderate asthma without changes in cell size or gene expression. *Am J Respir Crit Care Med* **169**(9)**:** 1001-1006.

Woods NM, Cuthbertson KS, Cobbold PH (1986). Repetitive transient rises in cytoplasmic free calcium in hormone-stimulated hepatocytes. *Nature* **319**(6054)**:** 600-602.

Xing J, Yan X, Estevez A, Strange K (2008). Highly Ca2+-selective TRPM channels regulate IP3-dependent oscillatory Ca2+ signaling in the C. elegans intestine. *J Gen Physiol* **131**(3)**:** 245-255.

Xu YD, Cui JM, Wang Y, Yin LM, Gao CK, Liu YY, *et al.* (2010). The early asthmatic response is associated with glycolysis, calcium binding and mitochondria activity as revealed by proteomic analysis in rats. *Respir Res* **11:** 107.

Yang CM, Hsia HC, Hsieh JT, Ong R, Luo SF (1994). Bradykinin-stimulated calcium mobilization in cultured canine tracheal smooth muscle cells. *Cell Calcium* **16**(2)**:** 59-70.

Yang IV, Schwartz DA (2011). Epigenetic control of gene expression in the lung. *Am J Respir Crit Care Med* **183**(10)**:** 1295-1301.

Yazid S, Solito E, Christian H, McArthur S, Goulding N, Flower R (2009). Cromoglycate drugs suppress eicosanoid generation in U937 cells by promoting the release of Anx-A1. *Biochem Pharmacol* **77**(12)**:** 1814-1826.

Yeh YF, Huang SL (2001). Dietary cholesterol enhances pulmonary eosinophilic inflammation in a murine model of asthma. *Int Arch Allergy Immunol* **125**(4)**:** 329-334.

Zou JJ, Gao YD, Geng S, Yang J (2011). Role of STIM1/Orai1-mediated store-operated Ca2+ entry in airway smooth muscle cell proliferation. *J Appl Physiol* **110**(5)**:** 1256-1263.